Workshop on Quantifying the Value of Structural Health Monitoring

Proceedings of the 1st Workshop, 04.-05.05.2015, DTU, Denmark

COST Action TU1402: Quantifying the Value of Structural Health Monitoring
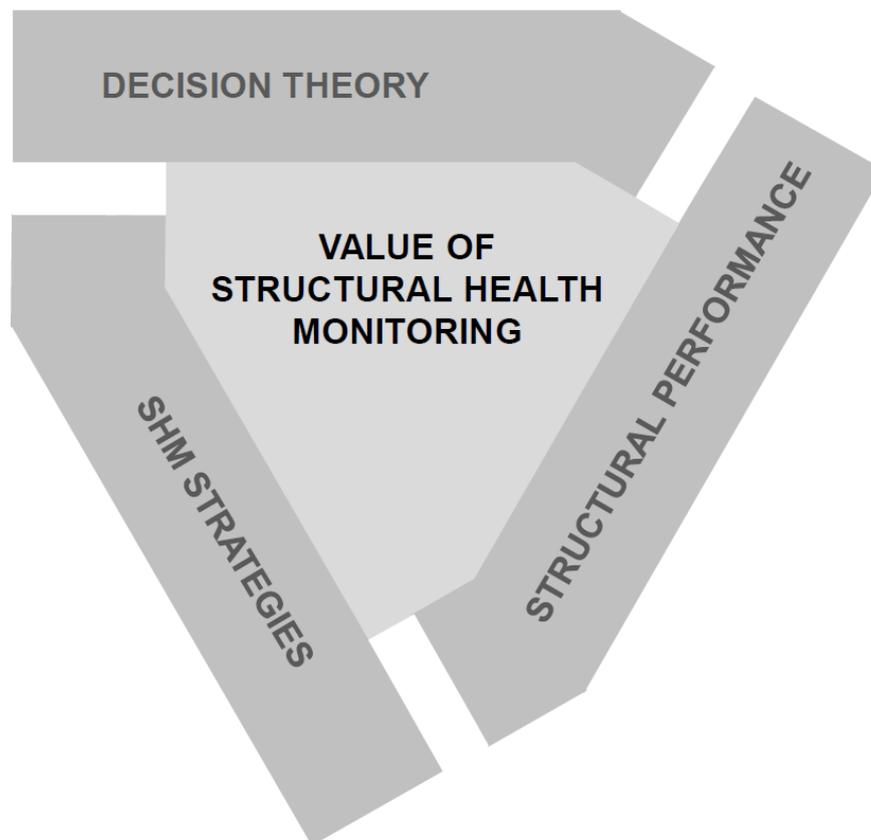
Editor: Sebastian Thöns, September 2015

cost
EUROPEAN COOPERATION
IN SCIENCE AND TECHNOLOGY

1 Summary

The Workshop on Quantifying the Value of Structural Health Monitoring constitutes the major event throughout the starting phase of the COST Action TU1402 in the early months of 2015. The Action has already received a tremendous interest throughout European industry and research resulting in a substantial growth of the Action in the starting phase.

The COST Action TU1402 enhances the benefit of Structural Health Monitoring (SHM) by novel utilization of applied decision analysis on how to assess the value of SHM – even before it is implemented. This improves decision basis for design, operation and life-cycle integrity management of structures and facilitates more cost efficient, reliable and safe strategies for maintaining and developing the built environment to the benefit of society.

The objectives of the 1st Workshop are to disseminate the aims and ideas of the COST Action TU1402 and to progress in building a common understanding within the Action network. Further aims according to the Scientific Work Plan are to progress in (1) the clarification of the theory on quantifying the value of SHM, (2) the formulation of the theory for applications and (3) a categorisation of SHM strategies and structural performance models. For these aims, consecutive plenary sessions involving all working groups (WGs) are organised which are followed by parallel Working Group sessions.

65 participants from 23 countries representing researchers, structural engineers, SHM engineers and infrastructure operators and owners took part in the workshop. The aims and the ideas of the Action were discussed and connected to the individual challenges of the Working Groups (WGs) and to the expertise of the Action network. This workshop contributed substantially to the progress according to the Scientific Work Plan, facilitated the individual detailed WG planning and initiated a number of working and networking activities.

The proceedings of the 1st Workshop contain paper contributions for WG1, WG2 and WG4 covering the theoretical framework, SHM strategies and structural performance modelling both in research and in application. Further contributions in the form of presentations and posters as well as the session videos can be accessed via the Action website: http://www.cost-tu1402.eu/.

WG 1 Session: Theoretical Framework
Chairs: M.H. Faber, D. Val

WG 2 Session: SHM Strategies and Structural Performance
Chairs: M. Chryssanthopoulos, G. Lombaert and M. Döhler

WG 4 Session: Case Study Portfolio
Chairs: H. Wenzel and J. Köhler

Value of Information in SHM – Considerations on the Theoretical Framework

M. H. Faber, Department of Civil Engineering, Technical University of Denmark, Denmark
D. Val, Institute for Infrastructure and Environment, Heriot-Watt University, UK
S. Thöns, Department of Civil Engineering, Technical University of Denmark, Denmark

Objectives, abstract and conclusions

The present paper aims to identify and describe the framework for quantifying the value of Structural Health Monitoring (SHM). Starting point is taken in a presentation of the problem of structural integrity management from an information theoretical viewpoint. This perspective is then set in relation to the utilization of Bayesian decision theory and methods of structural reliability theory as basis for decision making with respect to integrity management of structures. Following this an account of previous applications of value of information (VoI) analysis in general as well as more directly related to the field of civil engineering is given and finally more recent developments directly related to VoI analysis in structural health monitoring are summarized. Structural health monitoring has been increasingly applied over the last 2-3 decades in the context of assets integrity management, i.e. for collecting information on loads and aggressive environments acting on structures, structural performances, deterioration processes and changes in the use of structures. The pre-posterior analysis from the Bayesian decision theory and the associated VoI analysis provide a formal and transparent theoretical basis for the quantification of the value of SHM prior to its implementation. Though the concept of VoI analysis had been progressively formulated and applied throughout the scientific community for a long time only a few years ago this concept was fully appreciated in the field of SHM and there are still significant methodical and practical challenges to overcome before its potential benefits can be fully achieved in this field. Finally, based on a simple illustration the core theoretical elements of VoI analysis in the context of SHM are presented and discussed, challenges associated with the successful utilization of VoI in this context are summarized and potential strategies for overcoming them are outlined.

2 Introduction

2.1 Objectives and challenges of Structural Health Monitoring (SHM)

The ultimate goal of SHM is to provide information about the performance of structures in order to facilitate rational decision making with respect to their integrity management. In doing so SHM comprises a very wide range of activities which, through different technologies, collect knowledge about the performance of structures over their life-cycle. On this basis efficient remedial actions to counter deterioration, damage, extreme loads and unintended use may be timely identified and implemented so that an appropriate level of safety for personnel and qualities of the environment may be secured and life-cycle costs minimized.

In present practice it is implicitly assumed that SHM provides a benefit when implemented, either in terms of improved safety and serviceability, or reduced life-cycle costs, or both. However, this is not always the case and this is an issue which needs to be carefully addressed to ensure safe and efficient life-cycle management of structures in the future. Inappropriate SHM strategies may at best lead to economical losses and at worst easily trigger unnecessary or inappropriate remedial activities, which may jeopardize the safety of the structures or cause unnecessary disruption of the functionalities they provide.

For structures forming parts of infrastructure and building systems, past experience can be very valuable and it has been often utilized, with some success, as a basis for identifying efficient strategies for their performance management. However, there are two important drawbacks associated with experience based strategies in this context, namely that (i) many structures include

innovations (e.g., new materials, technologies) or unique so that there is little or no relevant experience to take basis on and (ii) an experience basis does not lend itself to a framework that enables new monitoring technologies to be qualified with respect to their performance prior to their implementation. This calls for the formulation and utilization of a robust theoretical framework and corresponding consistent analytical approaches for both the assessment and the optimisation of SHM strategies.

Thus, the present paper aims to identify a theoretical framework for the quantification of the value of SHM. Starting point is taken in a presentation of the problem of structural integrity management from an information theoretical viewpoint. This perspective is then set in relation to the utilization of Bayesian decision theory and methods of structural reliability theory as basis for decision making with respect to integrity management of structures. Thereafter, an account of previous applications of VoI analysis more directly related to the field of civil engineering is provided and more recent developments directly related to structural health monitoring are summarized. Finally, the core theoretical elements of VoI analysis in the context of SHM are presented and discussed, challenges associated with the successful utilization of VoI in this context are summarized and potential strategies for overcoming them are outlined.

3   Structural integrity management and SHM

3.1   Structural integrity management as an information management problem

Following the Joint Committee on Structual Safety (JCSS) (2008) and the principles of ISO 2394 (2015) decision making with respect to structural integrity management can be seen as a 'game' where moves (i.e., decisions) made by the player (i.e., decision maker) aim to optimize the utility (benefit) of the structural system in accordance to certain preferences. The main opponent in the game is nature but also individuals of the society which by lack of knowledge, by accident or by malevolence may cause damage to the system, for which the society will be accounted for. Figure 1 illustrates risk informed decision making in a societal context from an intergenerational perspective. Within each generation decisions have to be made which will not only affect the concerned generation but all subsequent generations as well. It should be emphasized that the definition of the system must include, in principle, a full inventory of all potentially occurring consequences as well as all possible scenarios of events which could lead to the consequences. At an intra-generational level the constituents of the game include the knowledge about the system and the surrounding world, available decision alternatives with respect to possible physical interventions and criteria (preferences) for assessing the utility associated with the different decision alternatives.

Knowing the rules (constituents) of the game, i.e. the assets, the possible consequences and how all these factors interrelate with the world outside the assets and into the future is essential for winning the game. For this reason, in practice a very significant part of risk based decision making is concerned with the system identification/definition as well as the identification of acceptance criteria, possible consequences and their probabilities of occurrence. Playing the game is done by "buying" physical changes in the system or "buying" knowledge about the system such that the utility (benefit) of the system may be optimized.
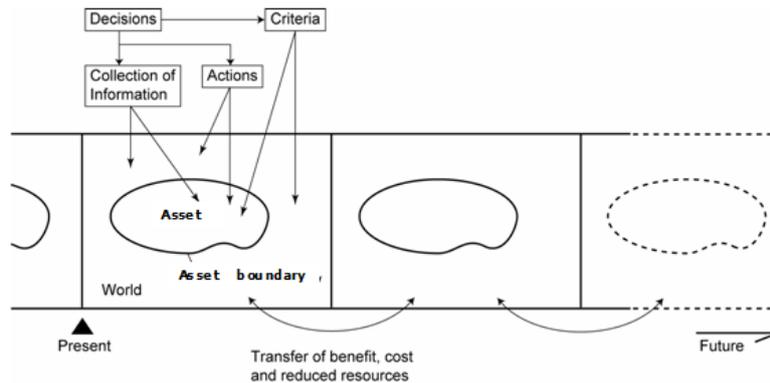
Figure 1:   Illustration of the constituents of the "game" of structural integrity management (JCSS, 2008).

Knowledge about the considered decision context is the main factor for successful optimal decision making. In real world, a lack of knowledge (or uncertainty) is associated with a normal decision making situation and it is thus necessary to be able to represent and deal with this uncertainty in a consistent rational manner.

From the foregoing it becomes apparent that integrity management, in essence, is a problem of managing information. In principle, the knowledge which is decisive for the management of the integrity of structures may be achieved by buying information in two ways, either indirectly through choises which affect the physics of the structural system or directly by sampling observations from the constituents. By choises affecting the physics reference is made to choises concerning e.g. materials and cross sections; choosing a particular construction material implies knowledge through experience with respect to the performance characteristics of the material. By sampling, reference is made to tests, inspections and monitoring. A particular choise with respect to sampling concerns which performance characteristics are sampled as well as the procedures and techniques applied for the sampling, which in turn are decisive for the precision associated with the aquired knowledge. Whatever choices are made with respect to acquiring knowledge about the constituents they serve in principle one purpose only, namely to win the game, i.e., to optimize the structural integrity management.

The possibilities for making choises affecting the available knowledge about the performance of a system involving structures may be realized through an appropriate systems representation as proposed in JCSS(2008), see also Figure 2.
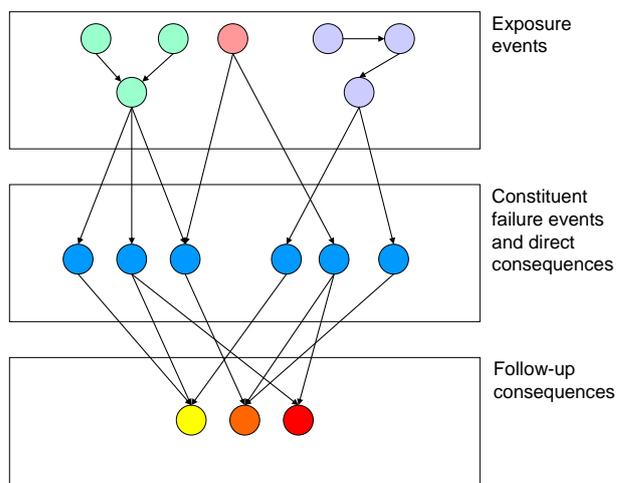
Figure 2:   Illustration of a systems representation which points to the various possibilities of improving knowledge about the system of interest (JCSS, 2008).

The main issue in the representation of systems is to facilitate and enhance the identification of scenarios of events which start with exposures such as loads and attacks by chemical substances, continue be induced damages and failures and end up by consequences. The exposure of the system illustrated in Figure 2 is represented as different exposure events acting on the constituents of the system. The damages of the system caused by failures of the constituents are considered to be associated with direct consequences. Direct consequences may comprise different attributes of the system such as monetary losses, loss of lives, damages to the qualities of the environment or just changed characteristics of the constituents. Direct consequences are thus defined as all consequences directly associated with damages or failures of the constituents of the system. Based on the combination of events of constituent failures and the corresponding consequences indirect consequences may occur. Indirect consequences could include e.g. the sum of monetary losses associated with physical changes of the system as a whole caused by combined effect of the constituent failures. Indirect consequences may thus be defined as any consequences associated with the loss of the functionalities of the system and by any specific characteristic of the joint state of the constituents and the direct consequences themselves. The indirect consequences play a major role in the systems risk assessment, and special attention should be given to their modeling. It should be noted that any constituent in a system can be modeled as a system itself.

A large number of propositions exist for the characterization of knowledge or equivalently uncertainty. It has become standard to differentiate between uncertainties due to inherent natural variability, model uncertainties and statistical uncertainties. Whereas the first mentioned type of uncertainty is often denoted as aleatory (or Type 1) uncertainty, the two latter are referred to as epistemic (or Type 2) uncertainties. However this differentiation is introduced for the purpose of setting focus on how uncertainty may be reduced rather than calling for a differentiated treatment in the decision analysis. In reality the differentiation into aleatory uncertainties and epistemic uncertainties depends on the model definition of a system under consideration.

The relative contribution of the two components of uncertainty depends on the spatial and temporal scale applied in the model. For the purpose of decision support the differentiation is irrelevant; a formal decision analysis necessitates that all uncertainties are considered and treated in the same manner.

More than a half century ago the foresighted work of Freudenthal (1947) pointed to the need of establishing a rationale for the integrity management of structures by consistently accounting for the knowledge available about the structure performance. This was the initiation point of what is now known as modern structural reliability theory. A fundamental feature of this theory is that uncertainties associated with the available knowledge are represented and treated in a way consistent with probability theory. In particular Bayesian probability theory has proven its merits in this context as it allows for a seamless and consistent combination of subjective experience-based knowledge with frequentistic information acquired through sampling.

3.2   Structural health monitoring in structural integrity management

SHM activities may be understood as the portfolio of possible ways by which information of relevance for the management of structural performance can be acquired. It is useful, however, to categorize the different decision support contexts to which the information contributes. The following list shall be seen as an attempt to summarize engineering decision making contexts in which SHM has a potential to provide value as a means of reducing costs or/and saving human lives:

1. Prototype development.
2. Code making and code calibration for the design and assessment of structures.
3. Devising warning measures to allow for loss reduction in situations where structures or systems involving structures perform unreliably due to accumulated damage or extreme load events.
4. Optimization of inspection and maintenance strategies.

Regarding 1): SHM of new structural concepts facilitates the concept optimization with respect to their life-cycle benefits before the initiation of their larger production. By instrumentation and subsequent monitoring and analysis of monitoring results it is possible to gather knowledge on important (model) uncertainties associated with the response and performance of the prototype. Such information may be utilized for the purpose of optimizing design decisions which in turn can be related to the life cycle.

Regarding 2): Systematic and strategically undertaken monitoring of structures may indicate that the design basis for the considered category/type of structure needs to be modified or adapted in accordance with the information collected. The monitoring could e.g. focus on information concerning the model uncertainties associated with codified design equations, reflecting uncertainty in relevant load-response transfer functions. The value of monitoring in this application may be realized through an improved design rationale facilitating the minimization of materials and costs and the control of risk, safety and reliability at adequately acceptable and affordable levels.

Regarding 3): Monitoring may facilitate the detection of possible adverse performances or damages of structures in operation, which then may be utilized as trigger for remediate actions. Adverse performances could be related to damages from extreme load effects, accumulated damages or other changes of the assumptions underlying the design of the structure. For example, information obtained by monitoring could be related to changes in stiffness properties monitored in terms of dynamic and/or static responses. In this application the value of monitoring is related to the loss reduction due to shutting down the function or reducing load on the structure, before human lives, environment and the structure are lost and/or damaged further.

Regarding 4): Collection of information concerning the performance of a structure may facilitate improved decision basis for optimizing inspection and maintenance activities. As for 1) monitoring may provide information of relevance for improving the understanding of the performance and response of the structure and this improved understanding may in turn be utilized during the life of the structure to adapt inspection and maintenance activities accordingly.

Disregarding the specific context of SHM the fundamental logic is the following:
- Monitoring may provide information concerning variables which have a significant influence on the service life performance of a structure.
- The information can be collected at a cost and with a given precision which depends on the technique and thereby also depends on the costs.
- The information collected through monitoring facilitates decisions regarding adaptive actions that are to be taken to reduce life cycle costs or increase life cycle benefits.
- Of course, if the collected information is incorrect and/or biased the actions will not be optimal and may even increase the service life costs.
- When assessing the benefit or value of different monitoring schemes and corresponding optimal strategies for adaptive actions the only basis for modeling of the not yet collected information is the a priori available data and models concerning the variables of interest. The benefit of SHM cannot be assessed through one or a few anticipated monitoring results.

The latter bullet point directs the attention towards the search for a formal framework to quantify the VoI before it has been actually acquired.

4   On the theoretical basis for quantification of the value of new information

4.1   The pre-posterior analysis and the VoI analysis based on Bayesian decision analysis

As recognized in the field of civil engineering half a century ago (Benjamin and Cornell 1970), a framework for the consistent quantification of the value of new knowledge, before it has become

available, can be based on the pre-posterior Bayesian decision analysis as described in Raiffa and Schlaifer (1961). Since then, especially in the context of inspection and maintenance planning of offshore facilities, see e.g. Straub (2004) for an overview, but also in the context of experiment planning, see e.g. Sorensen and Faber (2000), the pre-posterior decision analysis has been applied extensively as a means of supporting decisions on how collection of new knowledge may facilitate the optimization of structural integrity management. In the last decade the term Value of Information analysis (VoI) which is a property directly related to pre-posterior analysis, has been introduced explicitly in civil engineering and is now applied more frequently when pre-posterior decision analysis are utilized as a means of quantifying the benefit of acquiring new knowledge in a given decision support context, see e.g. Bayraktarli (2009) and Straub (2004). In the context of SHM VoI is utilized in among others by Pozzi and Kiureghian (2011), Zonta et al. (2013), Straub (2014), Thoens and Faber (2013), Konakli and Faber (2014) and Roldsgaard et al. (2015). A short appraisal of these works is given in Chapter 4.

Following closely Roldsgaard et al (2015) the idea underlying the concept of pre-posterior analysis and value of information analysis (VoI), might be illustrated by considering the simple decision event tree illustrated in Figure 3. In Figure 3 it is assumed that the true state of nature X is random with possible outcomes $x \in \{\mathbf{X}\}$ and given a-priori probability assignment $f_X'(x)$. Moreover, it is assumed that actions $a \in \{\mathbf{A}\}$ may be taken which affect the probability assignment of the possible states of the true state of nature, why more generally this may be given as $f_X'(x,a)$. Two cases are considered, namely the case in which it is decided to collect information and the case where it is decided not to collect information, corresponding to the branches 1 and 0 in the left end of the figure, respectively. Considering first the part of the decision event tree corresponding to decision 0, i.e. not to collect information, the optimal decision with respect to the choice of a may be identified by maximizing the expected value of the benefit $b_0(x,a)$, i.e.:

$$\arg\max_a (E_X' \left[b_0(a,x) \right]) = \arg\max_a (\int_{-\infty}^{\infty} f_X'(x) b_0(a,x) dx) \tag{1}$$

with corresponding expected value of benefit:

$$B_0(a^*) = E_X' \left[b_0(a^*, X) \right] \tag{2}$$
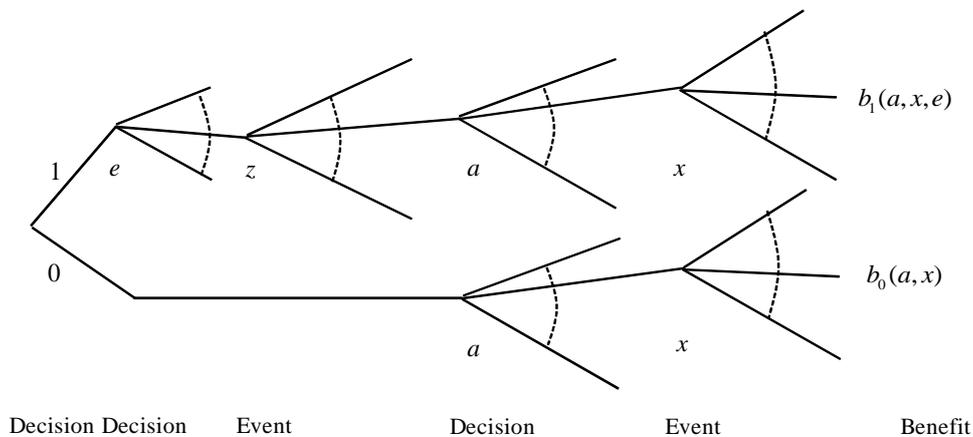
Figure 3: Illustration of a decision event tree for the assessment of the value of information in the framework of Bayesian pre-posterior decision analysis, Roldsgaard et al. (2015).

For the upper branch in Figure 3, corresponding to decision alternative 1 one additional choice and one additional realization of an uncertain phenomenon are included in comparison to the lower branch. The choice concerns the characteristics of the monitoring, i.e. the performance characteristics to be monitored, the accuracy of the applied technique(s), the extent (number of monitored locations) and the resolution of the monitoring over time. The realization concerns the outcome of the monitoring. In the following, for the purpose of illustration we will refer to these as the experiment $e \in \{\mathbf{E}\}$ and the experiment outcome $z \in \{\mathbf{Z}\}$, respectively and assume that z is an outcome of a scalar valued random variable Z with probability density function $f_Z(z)$. The outcome of the experiment z may be related to the probability assignment of the random true state of nature X by application of Bayes rule:

$$f_X''(x|z) = \frac{L(x|z)f_X'(x)}{\int_{-\infty}^{\infty} L(x|z)f_X'(x)dx} \tag{3}$$

where $L(x|z)$ is the likelihood of the true state of nature x given the observation z. This likelihood is the link between the observation and the condition of the structure which may affect the benefit and depends on two aspects, namely whether the observed quantity has a strong relation to the true state of nature of interest and whether the observation is precise (measurement uncertainty). Given the experiment outcome z the optimal action $a^*_{|z}$ is thus determined from:

$$\arg\max_a (E_X'' [b_1(a, X, e)]) = \arg\max_a (\int_{-\infty}^{\infty} f_X''(x)b_1(a, x, e)dx) \tag{4}$$

with corresponding expected value of benefit:

$$B_1(a^*, e) = E_X'' [b_1(a^*, X, e)] \tag{5}$$

where a benefit function $b_1(a, X, e)$ has now been introduced which also depends on the choice of experiment e since different experiments will introduce different costs.

However, since the experiment outcome z is not known with certainty the expected value of conducting the experiment with subsequent optimization of actions a must be evaluated over the possible different realizations of z, i.e.:

$$B_1(e) = E_Z [B_1(a^*, e)] = E_Z [E_X'' [b_1(a^*, X, e)]] \tag{6}$$

and finally the optimal experiment e^* may be determined from:

$$\arg\max_e (E_Z [B_1(a^*, e)]) = \arg\max_e (E_Z [E_X'' [b_1(a^*, X, e)]])$$
$$= \arg\max_e (E_Z [\arg\max_a \int_{-\infty}^{\infty} f_X''(x)b_1(a_{|z}, x, e)dx]) \tag{7}$$

with corresponding expected value of benefit:

$$B_1(e^*) = E_Z [E_X'' [b_1(a^*, X, e^*)]] \tag{8}$$

The expected values of benefits for branch 0 and branch 1 in the decision event tree are thus given in Equation (2) and Equation (8) why the expected VoI associated with conducting an experiment can be quantified through:

$$VoI = B_1(e^*) - B_0 \qquad (9)$$

The foregoing presentation of the VoI analysis follows the extensive form of the Bayesian pre-posterior decision analysis which is rather convenient whenever it is possible to formulate the likelihood of the true state of nature in terms of the observations using Bayes's Rule as provided in Equation (3). In other cases this might not be straight forwardly achieved and in such cases the normal form pre-posterior decision analysis might be more applicable. In the normal form of the pre-posterior decision analysis the equivalent to Equation (8) yields:

$$B_1(e^*) = E_X \left[E_{Z|x} \left[b_1(Z, d^*(Z), X, e^*) \right] \right] \qquad (10)$$

where $d^*(Z)$ is a decision rule specifying the (optimal) action to take given the experiment outcome z. The decision rule is often formulated in terms of parameters which may be subject to optimization themselves. The normal form formulation is very adequate in the context of risk based or reliability based inspection and maintenance planning as demonstrated in e.g. Faber (1997). In the context of VoI for structural health monitoring a main purpose of the structural health monitoring is to facilitate adaptation of inspection and maintenance strategies during the service life of the structures. In such applications the assessment of the VoI of a structural health monitoring strategy might appropriately be formulated in the extensive form but in which the benefit function in Equation (8) is assessed through an optimization of the service life, inspection and maintenance strategy utilizing a normal form pre-posterior decision analysis; i.e. a normal form decision analysis within an extensive form decision analysis.

5   Appraisal of selected previous works on VoI in structural health monitoring

5.1   Contributions on VoI in structural health monitoring

Pozzi and Kiureghian (2011) outline the framework for assessing the VoI, as applicable to the ranking of competitive measuring systems. The concept is derived and described, issues related to monitoring of civil structures are highlighted, the problem of non-linearity of the cost-to-utility mapping are addressed and an approximate Monte Carlo approach suitable for the implementation of time-consuming predictive models is introduced. The value of long term structural health monitoring information is calculated as the difference between the lowest expected loss and the expected loss in case an experiment is free. Given this definition, an experiment should be performed if the expected cost of the experiment is below the value of information assessed for the specific situation.

Zonta et al. (2013) present a methodology for economic evaluation of the impact of monitoring on bridge management using the VoI. A generalized modelling framework is developed to facilitate the consideration of various damage scenarios and remedial actions for evaluating the life-cycle value of monitoring. Monitoring is here defined as any information about the structure including visual inspection, consultants, archive research, and any other investment producing. The methodology is partly applied to the simplified case of the Streicker Bridge. It is shown that three to four measurements provided by the monitoring system following a hazardous event can justify the implementation of monitoring and it is exemplified how the economic benefit of a monitoring system can be estimated for any detectable event, which requires damage assessment.

Straub (2014) presents the modelling and computation framework of VoI for structural health monitoring systems based on structural reliability methods. It is described that the challenges for application of VoI regard the:

- probabilistic modelling of the monitoring and the monitored process,
- assessment and modelling of actions triggered by the monitoring information and
- computational efforts.

The computational challenges are addressed with an approach which builds upon a Monte Carlo Importance Sampling Scheme defining the Importance Sampling densities as the most likely failure points assuming perfect (structural health monitoring) information (of the equality type). The sampling density of the monitoring outcome is evaluated by coupling to the structural performance model given the monitoring outcomes which further reduces the computational efforts. The framework and the algorithm are applied in an example considering the monitoring of a structure subject to fatigue deterioration validating the algorithm and quantifying the value of measurements in conjunction with perfect information. The example application showed that a simplified modelling of action alternatives may be sufficient which facilitates that the VoI analysis may provide useful insights even when there is a large complexity of the involved models. It is concluded that the Value of information (VoI) is a powerful theory to assess the usefulness of monitoring or any other means of obtaining information.

The paper of Konakli and Faber (2014) describes an approach for pre-posterior analysis for support of decisions related to maintenance of structural systems given inspections or structural health monitoring. The Value of Information concept is applied for determining whether the experimental cost is justified by the expected benefit and for identifying the optimal among different possible experimental schemes for structural system models. Parameter studies are performed to investigate how the Value of Information is influenced by the uncertainty of the structural properties, the amount and quality of inspection and monitoring information and the dependencies between components of a system. As the main limitation of VoI analyses, the computational demand is identified.

Roldsgaard et al. (2015) address the risk management of cable structures with respect to icing events, which may lead to safety issues related to human life, functional disruptions and the associated economic consequences. The paper focusses on quantifying the value of early warning of icing events based on probabilistic models, which relate environmental conditions to the events of icing in terms of occurrence, and the monitoring of environmental conditions and short-term forecasting. With the help of a Bayesian Probabilistic Network model, the ice occurrence probability is updated facilitating in conjunction with the consequence model for ice falls the quantification sensitivities of model parameters to structural and human risks. The cable-supported Øresund bridge subject to the risk of falling ice from the cables is investigated as an example and it is shown how the expected value of SHM and forecasting can be assessed. It is shown that the costs of bridge closure and of false alarms have a significant influence on the value of SHM.

Thöns et al. (2015) address the quantification of the value of structural health monitoring (SHM) before its implementation for structural systems on the basis of its Value of Information (VoI). The value of SHM is calculated utilizing the Bayesian pre-posterior decision analysis modelling the structural life cycle performance, the integrity management and the structural risks. The relevance and precision of SHM information for the reduction of the structural system risks and the expected cost of the structural integrity management throughout the life cycle constitutes the value of SHM and is quantified with this framework. The approach is focused on fatigue deteriorating structural steel systems for which a continuous resistance deterioration formulation is introduced. In a case study, the value of SHM for load monitoring is calculated for a Daniels system subjected to fatigue deterioration. The influence of the structural system risks and the integrity management on the value of SHM is explicated and explained. The results are pointing to the importance of the consideration of the structural system risks for the quantification of the value of SHM due to high consequences usually associated to system failure.

Qin et al. (2015) address the quantification of the value of SHM with a service life cost assessment and generic structural performance model in conjunction with the observation, i.e. monitoring, of deterioration increments. The structural performance is described with a generic deterioration model to be calibrated to the relevant structural deterioration mechanism, such as e.g. fatigue and

corrosion. The generic deterioration model allows for the incorporation of the monitoring of the damage increments and accounts for the precision of the data by considering the statistical uncertainties, i.e. the amount of monitoring data due to the monitoring period, and by considering the measurement uncertainty. The value of structural health monitoring is then quantified in the framework of the Bayesian pre-posterior decision theory as the difference between the expected service-life costs considering an optimal structural integrity management and the service life costs utilizing an optimal SHM system and structural integrity management. With an example the application of the approach is shown and the value of the monitoring period optimized SHM information is determined.

5.2   Challenges for future consideration

To summarize, it is observed that several formulations and studies concerning the quantification of the Value of SHM have been developed in the last half decade. Most of the considered formulations and applications address the problem types 3) and 4) from Chapter 2, i.e. SHM in the context of operation and maintenance of structures.

In principle, it appears that the formulation of the decision problems through which the VoI can be determined is relatively straightforward but can be somewhat specific for specific contexts of applications. The prevailing formulation of the decision problem applied for the quantification of the value of SHM is the extensive form of the pre-posterior decision analysis whereas much earlier works relating to risk based optimization of inspections and maintenance strategies see e.g. Straub (2004) were based on the normal form of the pre-posterior decision analysis.

As outlined in Straub (2014) the computational efforts associated with the VoI analysis is a real challenging issue. The decision–event trees which need to be analysed may easily become prohibitively large for numerical analysis. This was also the case in earlier developments relating to risk based inspection and maintenance planning leading to the development of a range of assumptions and approximations – whereby the decision analysis supporting the identification of optimal strategies were shifted from formal to informal. Such approximations are doubtlessly also necessary when pre-posterior decision analysis and VoI assessments are undertaken in the broader context of SHM. For some problems Straub (2014) points to possible solutions in this respect. However, there is a need to better understand how to best represent the decision problems (extensive/normal form) and which approximations are more appropriate then. To this end a broader and also deeper assessment of available techniques utilized in sequential decision making problems such as specifically addressed under problems of type 2) (Chapter 4). The stochastic meshing techniques considered in Anders (2013) is one example where methodical developments from economic options analysis have found application in real time decision making in the context of risk management for engineered facilities subject to emerging hazards.

6   Summary and conclusions

The present paper introduces the problem of structural integrity management from an information theoretical viewpoint. This perspective is then set in relation to the utilization of Bayesian decision theory and methods of structural reliability theory as basis for decision making with respect to integrity management of structures. Taking basis in a simple illustration the core theoretical elements of Value of Information analysis in the context of Structural Health Monitoring are then presented. Following this an account of previous applications of VoI analysis in general as well as more directly related to the field of civil engineering is given and finally more recent developments directly related to value of information analysis in structural health monitoring are summarized.

Structural health monitoring has over the last 2-3 decades been increasingly applied in the context of assets integrity management, i.e. for collecting information on loads and aggressive environments acting on structures, structural performances, deterioration processes and changes

in the use of structures. The pre-posterior analysis from the Bayesian decision theory and the associated value of information analysis (VoI) provides a formal and transparent theoretical basis for the quantification of the value of SHM prior to its implementation. Though VoI analyses are progressively being formulated and applied throughout the scientific community it was only very recently the concept of VoI analysis was fully appreciated in the field of SHM and there are still significant methodical and practical challenges to overcome before the potential benefits of this concept can be fully achieved.

In principle it appears that the formulation of the decision problems through which the VoI can be determined is relatively straightforward but can be somewhat specific for specific contexts of applications. The prevailing formulation of the decision problem applied for the quantification of the value of SHM is the extensive form of the pre-posterior decision analysis whereas much earlier works relating to risk based optimization of inspections and maintenance strategies see e.g. Straub (2004) were based on the normal form of the pre-posterior decision analysis.

It appears that the computational efforts associated with the VoI analysis is the real challenging issue. The decision–event trees which need to be analysed may easily become prohibitively large for numerical analysis and idealizations and approximations are deemed necessary. Some proposals for this are already available in the literature, however, there is a pressing need to better understand how to best represent the decision problems (extensive/normal form) and which approximations are more appropriate when. To this end a broader and also deeper assessment of available techniques utilized across different fields of science are needed.

Contact information

M. H. Faber
Professor Risk and Safety, Chair of Department of Civil Engineering
Brovej, Building 118, DK-2800, Kgs. Lyngby, Denmark
Phone: +4551537677
Email: mihf@byg.dtu.dk

References

Benjamin, J R and Cornell, C A (1970). Probability, statistics, and decision for civil engineers New York: McGraw-Hill. 684 pp.

Faber, M.H. (1997), Risk Based Structural Maintenance Planning, In: Probabilistic Methods for Structural Design, ed. C. Guedes Soares, the Netherlands, Kluwer Academic Press, ISBN 0-7923-4670-X, Vol. 56, June 1997, pp. 377-402.

Faber, M.H. and S. Thöns (2013). On the Value of Structural Health Monitoring. ESREL 2013. Amsterdam, The Netherlands.

Freudenthal, A M (1947). The Safety of Structures, Transactions of ASCE, Vol. 121, Proc. Paper 2843, 1956, pp. 137-197.

Konakli, K. and M. H. Faber (2014). Value of Information Analysis in Structural Safety. Vulnerability, Uncertainty, and Risk: Quantification, Mitigation, and Management: 1605-1614.

Pozzi, M. and A. D. Kiureghian (2011). Assessing the Value of Information for Long-Term Structural Health Monitoring. Health monitoring of structural and biological systems 2011. San Diego, California, United States.

Qin, J., S. Thöns and M. H. Faber (2015). On the Value of SHM in the Context of Service Life Integrity Management. 12th International Conference on Applications of Statistics and Probability in Civil Engineering (ICASP12), . Vancouver, Canada.

Raiffa, H. and R. Schlaifer (1961). Applied statistical decision theory. New York, Wiley (2000).

Roldsgaard, J. H., Georgakis C. T. and M. H. Faber (2015). On the Value of Forecasting in Cable Ice Risk Management. Structural Engineering International 1(2015).

Sørensen, J. D., D. Straub and M. H. Faber (2005). Generic Reliability-Based Inspection Planning for Fatigue Sensitive Details – with Modifications of Fatigue Load. 9th International Conference on Structural Safety and Reliability (ICOSSAR), Rom.

Straub, D. (2004). Generic Approaches to Risk Based Inspection Planning for Steel Structures. PhD. thesis. Chair of Risk and Safety, Institute of Structural Engineering. ETH Zürich.

Straub, D. (2014). Value of information analysis with structural reliability methods. Structural Safety 49(0): 75-85.

Straub, D. and M. H. Faber (2005). Risk based inspection planning for structural systems. Structural Safety 27(4): 335-355.

Sørensen, J D; Engelund, S.; Faber, M. H. (2000) Reliability Analysis and Test Planning using CAPO-Test for Existing Structures. Applications of Statistics and Probability - Civil Engineering Reliability and Risk Analysis: Proceedings of the 8th international conference on applications of statistics and probability in civil engineering. ed. Robert E. Melchers; Mark G. Stewart. Vol. 2 2000. p. 723-730.

Thöns, S. and M. H. Faber (2013). Assessing the Value of Structural Health Monitoring. 11th International Conference on Structural Safety & Reliability (ICOSSAR 2013). New York, USA.

Thöns, S., R. Schneider and M. H. Faber (2015). Quantification of the Value of Structural Health Monitoring Information for Fatigue Deteriorating Structural Systems. 12th International Conference on Applications of Statistics and Probability in Civil Engineering (ICASP12), . Vancouver, Canada.

Yokota, F. and K. M. Thompson (2004). Value of Information Literature Analysis: A Review of Applications in Health Risk Management. Medical Decision Making 24(3): 287-298.

Zonta, D., B. Glisic and S. Adriaenssens (2013). Value of information: impact of monitoring on decision-making. Structural Control and Health Monitoring: n/a-n/a.

Structural health monitoring, a tool for improving critical infrastructure resilience

Dániel Honfi, SP Technical Research Institute of Sweden
David Lange, SP Technical Research Institute of Sweden

Objectives, abstract and conclusions

Critical infrastructure (CI) needs to be able to provide a certain level of functionality before, during, and after a crisis, and should be able to return to this level of functionality as soon as possible following an incident. Structural Health Monitoring (SHM), among many others, is a key concept to enable quick and efficient response and restoration following a major incident. Nevertheless, SHM can significantly contribute to the resilience of CI during non-crisis times. A review of related concepts is given in the current paper.

Technical information

1   Introduction

Critical Infrastructures are assets, systems or parts thereof, which are essential for the maintenance of vital societal functions, such as e.g. health, safety, security, economic or social well-being of people, and the disruption or destruction of which would have a significant impact as a result of the failure to maintain those functions (Council Directive, 2008). Examples of CI include critical components of transportation, energy distribution and communication networks, etc. Even single assets of CI usually represent complex systems, which consist of several components. A possible classification of these components after Catbas et al. (2006) is given here with some examples referring to a bridge as a part of a transportation network:

- Natural components (e.g. river the bridge is crossing over, soil the bridge is built upon);
- Engineered components (structure of a bridge, road and railway crossing the bridge, etc.);
- Operational/organizational components (infrastructure operators and owners, law enforcement units, fire department, etc.).
- Administrative components (e.g. local, regional, national or even international authorities and agencies);

Due to their complexity, CIs may be exposed to several types of hazards resulting in unfavourable events with serious consequences; therefore, protection of CIs is extremely important for society to maintain a sustainable development. Further, CIs often are subject to interdependencies with other types of infrastructure, for example a bridge or tunnel might provide a transportation link for road and railway traffic and can also carry elements of telecommunications infrastructure and power distribution networks.

Safety of assets cannot be ensured by all means, i.e. they cannot be fully protected against all incidents and accidents regardless the scale of the event. Therefore new policies and research initiatives shift the focus from protection towards resilience. Critical infrastructure resilience refers to the ability of CIs to mitigate hazards, contain the effects of disasters when they occur, and carry out recovery activities in ways that minimize disruption and mitigate the effect of future disasters.

Structural health monitoring comprises strategies for identifying, locating and quantifying damage in infrastructure assets. This is usually done by comparing the current state of the system, based on current or recent sensor output, with previous (assumed undamaged) states, based on historical records of sensor output (Farrar and Worden, 2007). SHM has growing applications in the aerospace industry as well as civil infrastructure such as bridges and buildings including CI assets (Sohn et al., 2004). CIs often have to be functional during response and recovery after disasters (e.g. bridges, hospitals), therefore (Catbas et al., 2006):

- Emergency teams and engineers should have access to time-sensitive data to determine the type and amount of damage to bridges.
- Rapid evaluation methods for emergency response operations specifically for critical vehicles (fire trucks, ambulances, and evacuation buses) are needed.
- Communication, coordination, and integration of information from different sources is needed to improve the capacity of first responders.

It is obvious that information gained from SHM systems is extremely valuable for the above purposes, and can be used for safety, security and emergency management of CI assets and thus improve their resilience.

To gain a better understanding about how different methods and measures, such as SHM among many others, contribute to CI resilience, a research project has been recently initiated to operationalise existing resilient concepts entitled: Improved risk evaluation and implementation of resilience concepts to critical infrastructure, IMPROVER (www.improverproject.eu). The project builds on the assumption that several mechanisms based on different resilience concepts contribute to the overall resilience of CI. Some relevant aspects related to CI downtime at large scale incidents have been investigated in the ongoing project: Modelling of dependencies and cascading effects for emergency management in crisis situations, CascEff (www.casceff.eu).

The relationship between critical infrastructure resilience and the various resilience concepts may be described as follows. In an undamaged state the system is fully functional, possibly capable of delivering services above the minimum level expected of it, and in any event functioning at normal capacity. In the event of an incident, normal functionality is not available and the resilience concepts, applied by means of technological and organisational measures and tools, 'patch' the system to ensure that it is capable of providing the minimum function required of it and to return to the normal level of performance as soon as possible. In such an event the minimum level expected of the infrastructure may also readjust as society responds to the situation. These resilience concepts may overlap in the way in which they ensure resilience. In order to evaluate resilience, it is therefore necessary not only to evaluate the overall resilience of infrastructure to threats but also to evaluate the performance and impact of the individual resilience concepts. In the light of this idea SHM could be seen as one of the concepts contributing to CI resilience.

Based on an improved understanding of the impact and functionality of the individual resilience concepts it is even possible that the overall resilience of a system could be streamlined by removing any overlaps or redundancies in resilience concepts whilst providing the same overall level of resilience. More insight about the above mentioned issues will be presented in the current paper.

2 Resilience concepts

2.1 General concept

Resilience refers to the ability of a system, community or society exposed to hazards to resist, absorb, accommodate and recover from the effects of a hazard in a timely and efficient manner, including through the preservation and restoration of essential basic structures and functions.. According to Holling (1996) resilience of a system has usually been defined in two very different ways. These differences reflect two fundamentally different types of resilience. Engineering resilience focuses on stability of an equilibrium state. In this case therefore, resilience refers to the ability of the system to resist disturbances and quickly return to the equilibrium state. In contrast, ecological resilience emphasizes conditions far from equilibrium, where large disturbances can flip the system to another equilibrium state. Resilience then is defined as the magnitude of disturbance that can be absorbed before the system changes state. The first definition, engineering resilience, could be characterized by efficiency, constancy and predictability aiming at a controlled, fail-safe

design and optimized performance. On the other hand, ecological resilience is described by persistence, change and unpredictability. These attributes are necessary for the adaptation and survival in a dynamically changing environment.

It should be noted that the contrasting aspects of engineering and ecological resilience require different management actions. Focusing on optimizing a system for a single objective function or a set of known objective functions might increase the vulnerability of the system to unforeseen events and lead to catastrophic failures. On the other hand, without effective use of materials, advanced construction techniques and maintenance strategies, the current spans of bridges and height of skyscrapers could have never been achieved. In structural engineering, especially of CIs due to their complex nature and close relation to non-structural systems, an advised strategy might be to find a balance between the two concepts.

2.2   CI resilience

CI resilience concepts encompass four interrelated dimensions; technical, organizational, social, and economic (Tierney and Bruneau, 2007):

- The technological dimension refers primarily to the physical properties of systems, including the ability to resist damage and loss of function and to fail in a safe way. The technical domain also includes the physical components that add redundancy.
- Organizational resilience relates to the organizations and institutions that manage the physical components of the systems. This domain encompasses measures of organizational capacity, planning, training, leadership, experience, and information management that improve disaster-related organizational performance and problem solving.
- The social dimension encompasses population and community characteristics that render social groups either more vulnerable or more adaptable to hazards and disasters. Social vulnerability indicators include poverty, low levels of education, linguistic isolation, and a lack of access to resources for protective action, such as evacuation.
- Economic resilience refers to the capacity to reduce both direct and indirect economic losses resulting from disasters.

Figure 1 shows how these four dimensions link to interconnected critical infrastructure systems and community (Bruneau et al., 2003). For each CI asset, technical and organizational performance measures can be defined that contribute to the ability of the physical system and the organization that manages it to withstand disasters and recover quickly from their impacts. However these performance measures are not common between the different systems or sectors and the different interrelated dimensions contribute in different ways to the overall resilience of the different systems, and the community which is reliant upon the infrastructure. Societal and economic resilience is strongly linked to the community, whereas organisational and technological resilience concepts are strongly related to the infrastructures themselves. These may broadly be seen to relate to the ability of society to adapt to the consequences of an event, and to how an event affects the performance of CI, respectively.
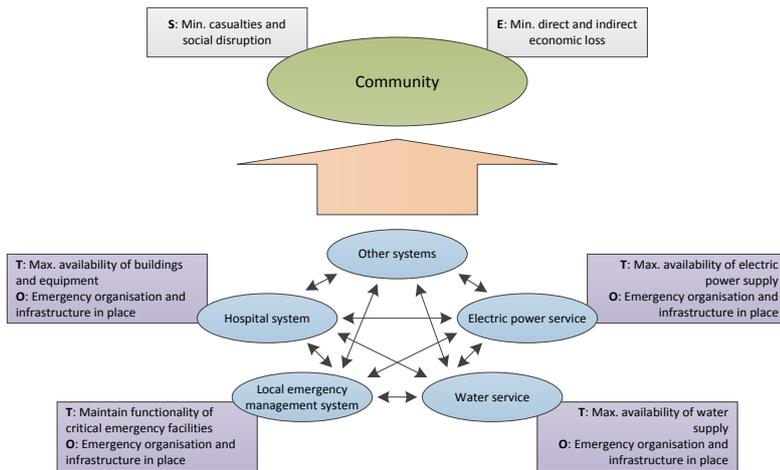
Figure 2: System and community performance measures (T: Technical; O: Organisational; S: Social; E: Economic) (Bruneau et al., 2003).

Extensions of these dimensions exist, such as in the PEOPLES framework identifying seven dimensions of community/urban resilience, namely: Population and demographics, Environmental/ecosystem services, Organized governmental services, Physical infrastructure, Lifestyle and community competence, Economic development and Social-cultural capital (Renschler et al., 2010).

2.3   Resilience triangle and attributes of resilience

Bruneau et al. (2003) define the so called "resilience triangle" which shows the loss of functionality from damage and disruption, as well as the pattern of restoration and recovery over time after a certain loss (see Figure 2).
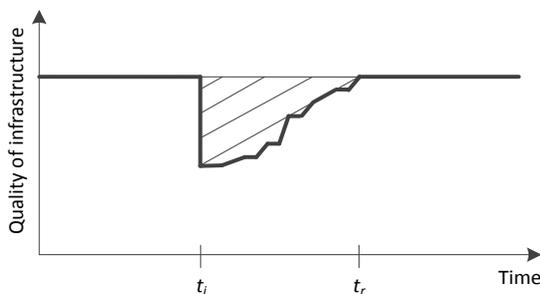
Figure 3: The resilience triangle (Bruneau et al., 2003).

Measures for improving resilience aim to reduce the size of the resilience triangle. This can be achieved through increasing functionality and performance and by decreasing the time to full recovery. The leads to the "four Rs" of resilience, namely: robustness, redundancy, resourcefulness and rapidity:

- Robustness: the inherent ability of a system to withstand external demands without suffering degradation or loss of function, such as e.g. damage avoidance and continued service provision of a physical asset.
- Redundancy: the extent to which the system could be replaced by alternative solutions under stress. Examples include backup/duplicate systems, equipment and supplies, for instance the proximity of assets providing the same function and their capacity to deal with the increased capacity.

- Resourcefulness: the capacity to identify problems, establish priorities and mobilize resources in emergency situations including diagnostic and damage detection technologies, availability of equipment and materials for restoration and repair.
- Rapidity: the speed to meet priorities and achieve goals in order to reduce losses, overcome disruption and restore services. This could for example refer to optimization of the time to return to pre-event functional levels.

The robustness and rapidity attributes can be directly associated to the resilience triangle by its vertical and horizontal axes. Robustness is associated with the drop of the functionality/performance function after the incident occurs, whereas rapidity could be quantified as the slope or duration of the recovery branch and is mainly characterised by the time needed for return to pre incident state. To visualise the resourcefulness a third axis might be used, whereas representation of redundancy requires a collection of functions as suggested by Bruneau and Reinhorn (2007).

The main focus of the original reference triangle is resilience towards earthquakes, thus it is assumed that loss of functionality happens immediately, when the incidents occur. It is not considered that structures might have sufficient robustness to tolerate certain damage and lose their performance gradually. This assumption could be justified, given that the time between the incident and structural failure is usually negligible compared to the time of reconstruction.

More generalized representations of the triangle are given e.g. in McDaniels et al. (2008) including effects the changing nature of external environment and effects of decision making on resilience, i.e. influence of *ex ante* mitigation and *ex post* adaptation. Another extension of the model is the RISE framework (Resilient Infrastructures and Structures against Emergencies) including deterioration of structures i.e. the assumption that at the time of the incident the structural performance is already reduced as a result of normal wear and tear (Ortenzi et al., 2013).

More sophisticated methods enable a probabilistic assessment of resilience due to earthquakes (Cimellaro et al., 2010) and in a multi-hazard environment (Ayyub, 2014). The latter framework is adapted in this paper and presented in Figure 3, which provides a schematic representation of a system performance Q, including effects of deterioration. An incident occurs with a rate λ according to a Poisson process. The figure illustrates three different system failure characteristics: sudden drop of performance after incident occurs, f_1, gradual loss of functionality f_2, and slow initial failure propagation followed by sudden system collapse f_3. Furthermore three recovery options are presented: recovery to better than new r_1, recovery to as good as new r_2, and recovery to as good as old r_3. The figure also shows the original performance path and the paths after the various recovery options. The different scenarios represent various rates of change in system performance and have an obvious effect on the "resilience triangle". In the referred paper a measure of resilience is calculated using the time to incident T_i, the time to failure T_f, the time to recovery T_r, the failure function f, the recovery function r and the performance function Q treated as random variables. The proposed method is useful for the analysis of the effects of SHM on resilience as will be shown in Section 3.
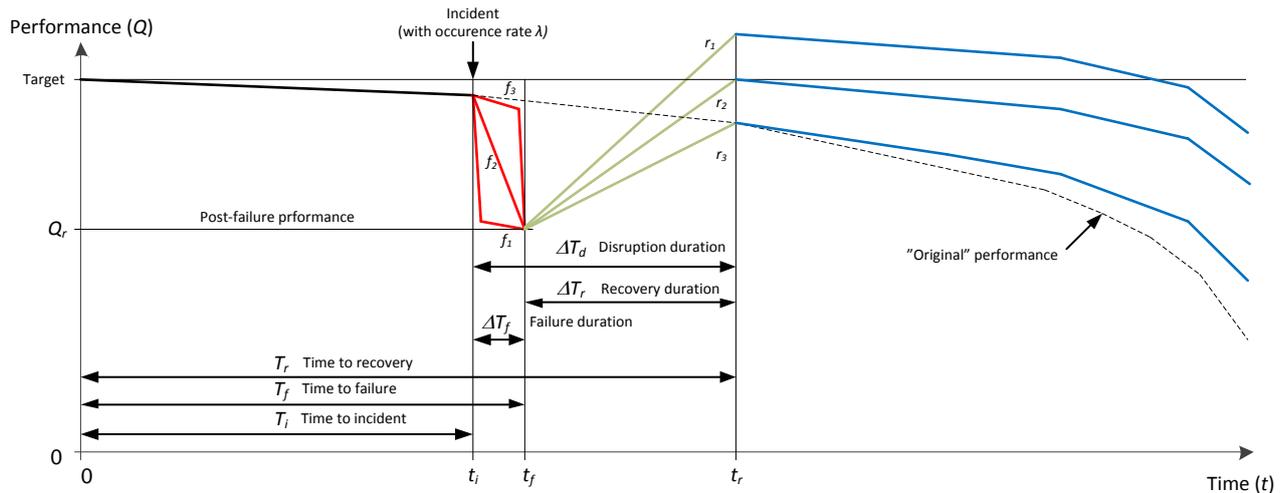
Figure 4: Definitions of resilience metrics (Ayyub, 2014).

2.4 Resilience vs structural robustness

CI resilience is usually considered in a wider context than the design of the physical asset itself. Therefore it is essential to link existing methods of structural reliability with resilience. An attempt for this linking is illustrated in Figure 4. Based on (Starossek and Haberland, 2010) a probabilistic representation of vulnerability and robustness of single assets is possible, where vulnerability and robustness are linked to conditional probabilities of damage given exposure $P(D|E)$ and failure given damage $P(F|D)$. This representation is consistent with the risk-based approach proposed by Baker et al. (2008) and accepted by JCSS (2008).

Robustness is sometimes defined as the attitude of a system to survive to a given set of exposures (Sørensen, 2010). Thus robustness is a property of the structural system, which depends on both local and global characteristics and is associated with the probability-product $P(F|D) \cdot P(D|E)$. Hence this definition of robustness considers vulnerability as a part of robustness and more consistent with the 4Rs of resilience described previously.

Consequences related to damage D, and linked with vulnerability are called direct consequences, whereas consequences related to asset failure F, i.e. linked to robustness are considered as indirect consequences. To be able to assess consequences beyond the failure of the single asset the probability of such consequences, i.e. the probability of cascading effects $P(C)$ is calculated based on the conditional probability $P(C|F)$. This might be affected by the redundancy of the asset, i.e. the availability of possible alternative solutions considering the community/urban context. Furthermore this is influenced by the (physical and functional) interdependencies between the different assets.

The conditional probabilities influenced by the physical characteristics at three different levels, i.e. components of the asset, the asset seen as system of components and system of assets in the urban context, referring to vulnerability, robustness and redundancy respectively are related to the technological (T) resilience dimension of resilience, as indicated with the blue color in Figure 5. These aspects are mainly reflected in the robustness and redundancy attributes of the 4R concept. As discussed in the previous sections resilience of single assets is closely related to the organizational dimension of resilience (O). The organizational counterparts of vulnerability, robustness and redundancy might be seen as recognition capacity, response capacity and recovery capacity. These properties usually contribute to the reduction of the associated consequences rather than the above mentioned conditional probabilities. Within the 4R concepts

these are expressed as resourcefulness and rapidity. The blue and orange triangles in Figure 4 reflect the possibilities and effectiveness of current methods to influence the different properties. Traditional structural design is primarily focused on the limit state design of elements, therefore has a greater impact on influencing vulnerability, than robustness and very little impact on redundancy (as used in this context). Similarly, the main focus of emergency organizations is on how to respond and recover during and after an incident.

Figure 4 also attempts to illustrate the time aspects of damage propagation, by placing the "resilience triangle" above the conditional probability boxes from time to incident t_i, through time to damage t_d and time to failure t_f until time to recovery t_r.
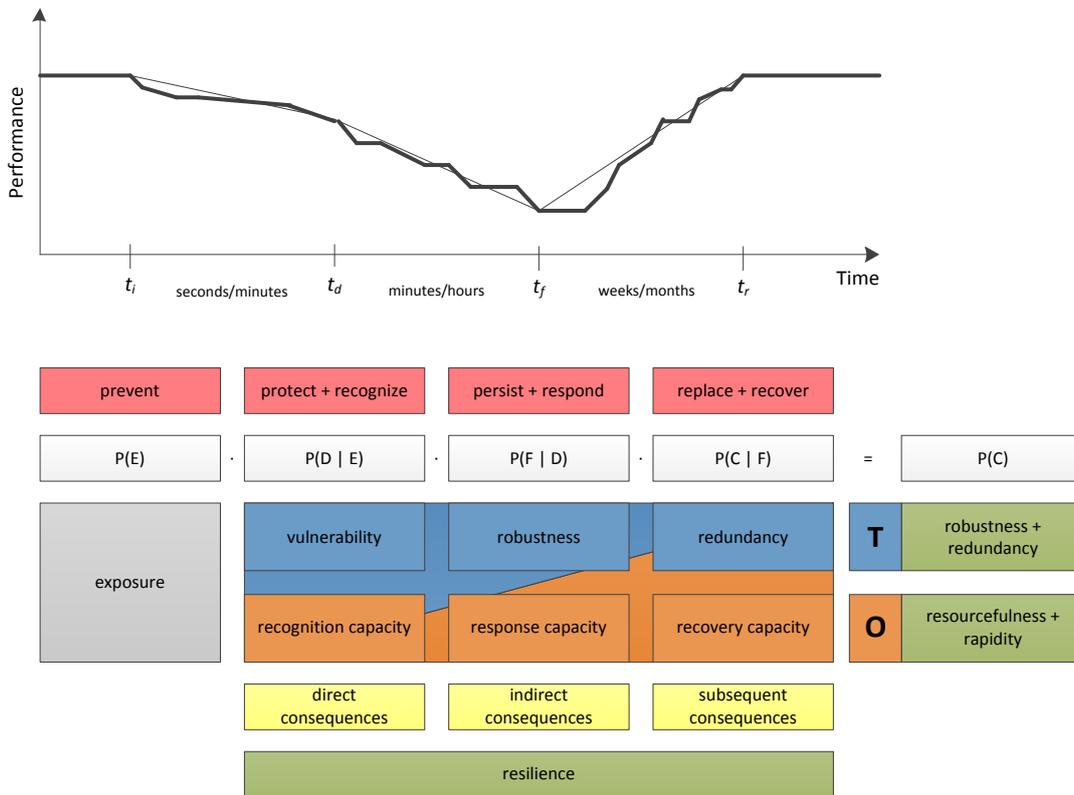
Figure 5: Linking of structural robustness and resilience

3   SHM and resilience

If SHM is not designed and implemented properly then resources might be wasted and the time to recovery might be prolonged causing unnecessary disruption to infrastructure network users or it might even trigger cascading effects impacting other vital societal functions through interdependencies. However, proper use of SHM can significantly contribute to the different dimensions of resilience through e.g.:

- Developing condition-based maintenance strategies (*robustness*),
- Provide information on alternative possibilities (*redundancy*),
- Prioritizing maintenance and emergency actions for better use of resources (*resourcefulness*),
- Alerting first responders in case of emergency (*rapidity*).

This could especially be achieved through the integration of SHM with other systems, such as (traffic) surveillance, security control systems, weather stations, asset management systems, decision support tools etc. However the integration of such systems is difficult due to various reasons e.g. (Catbas et al.):

- Resilience of CI should be assessed for different types of hazards (natural and man-made disasters), which require different types of data;
- To develop and maintain resilience, adaptable SHM is needed that can respond to changing requirements and possibilities, as well as opportunities;
- Protection of the system itself and the data collected should be ensured;
- Management of a large amount of data might be demanding;
- Administrative issues might arise, due to the different organizations and/or authorities involved.

An illustration of how the resilience triangle could be reduced utilizing SHM is illustrated in Figure 5 and 6. Figure 5, inspired by Ayyub and Zhang (2014) shows how SHM system could generate an alarm signal if the strain exceeds the pre-specified limit state (e.g., yielding, fracture or buckling) and thus initiate a response action. This might include mobilizing resources for repair, evacuation or increasing capacity at alternative assets, therefore reducing the consequences of loss of functionality at damaged asset. A better emergency management, due to the utilisation of SHM alarm signal might increase the adaptive capacity of the system when the incident occurs, leading to an increased residual performance Q_{r2}. Hence, either: a faster recovery could be achieved with the same resources used for recovery (option r_{2a}), or the same recovery time could be obtained by utilising fewer resources (option r_{2b}).
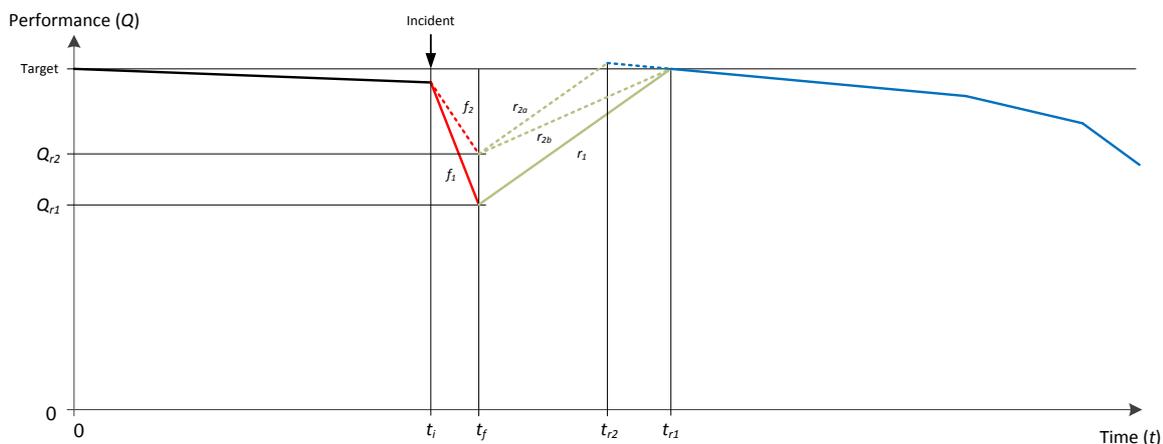
Figure 6: SHM contributing to adaptive resilience.

Figure 6 illustrates a situation where two different maintenance strategies are applied characterised by repair threshold RT_1 and RT_2. A stricter threshold RT2 might lead to an inherent increase in robustness and thus resilience leading to a similar situation as before, but without utilising additional resources at emergency.

The above examples illustrate that SHM is an important part of improving disaster resilience, thus this aspect should be considered when quantifying the value of structural health monitoring. This requires a better understanding of resilience concepts, which is a main objective of the IMPROVER project.
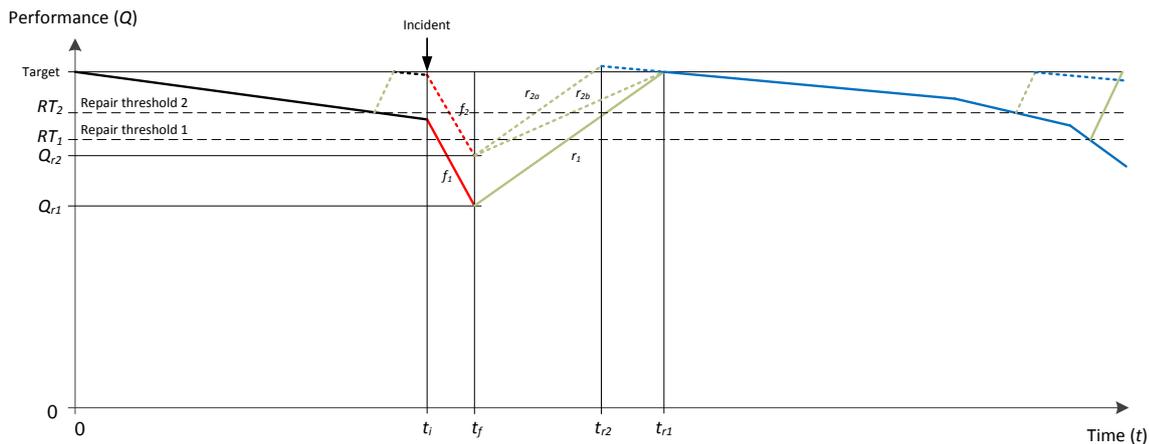
Figure 7: SHM contributing to inherent resilience.

4   Conclusions

The paper attempted to place structural health monitoring in the urban resilience concept and link it to the generally accepted concepts of structural reliability and risk assessment characterised by vulnerability and robustness. However, further studies and refinement of the presented ideas are needed for better quantification of the value of SHM. These steps will be carried out within a recently initiated European research project IMPROVER.

Some of the main conclusions of the paper could briefly be summarized as follows:

- SHM should focus on monitoring the performance of structures in a way that the available resources could be optimized and recovery actions after deterioration or damage could be effectively and rapidly undertaken, i.e. to improve resilience taking into account all 4 attributes (robustness, redundancy, resourcefulness and rapidity).
- Integrated SHM systems should not consider resilience in isolation, but together with external services and assets.
- SHM should be flexible for adaptation, thus adaptability should be incorporated in the quantification of the value of SHM.
- Protection of the data and the SHM system should be ensured. Furthermore the robustness (or even resilience) of the SHM system should assessed.

Contact information

Dániel Honfi
Researcher, SP, Box 24036, SE-400 22 Gothenburg, Sweden
+46 (0)10 516 50 00
daniel.honfi@sp.se

References

Ayyub, B. M. (2014). Systems Resilience for Multihazard Environments: Definition, Metrics, and Valuation for Decision Making. Risk Analysis 34(2): 340-55.

Ayyub, B. M. and Y. Zhang (2014). Monitoring the Health of Structures for Quantifying and Achieving Resilience for Natural Hazards, Mpact – Engineering Innovations that Improve Millions of Lives. University of Maryland, College Park, 22 October, 2014.

Baker, J. W., M. Schubert and M. H. Faber (2008). On the assessment of robustness, Structural Safety 30(3): 253-267.

Bruneau, M., S. E. Chang, R. T. Eguchi, G. C. Lee, T. D. O'Rourke, A. M. Reinhorn, M. Shinozuka, K. Tierney, W. A. Wallace, and D. von Winterfeldt (2003). A framework to quantitatively assess and enhance the seismic resilience of communities. Earthquake Spectra 19(4): 733-752.

Bruneau M. and A. Reinhorn (2007). Exploring the Concept of Seismic Resilience for Acute Care Facilities. Earthquake Spectra 23(1): 41-62.

Catbas, F.N., M. Susoy, and N. Kapucu (2006). Structural Health Monitoring for Improving Transportation Security: Case Study for Bridges. Journal of Homeland Security and Emergency Management 3(4).

Cimellaro, G.P., A.M. Reinhorn, and M. Bruneau (2010). Framework for analytical quantification of disaster resilience. Engineering Structures 32(11): 3639–3649.

Council Directive 2008/114/EC of 8 December 2008 on the identification and designation of European critical infrastructures and the assessment of the need to improve their protection. Offical Journal of the European Union, 23 December 2008.

Farrar, C.R. and K. Worden (2007). An introduction to structural health monitoring. Phil. Trans. R. Soc. A 365, doi: 10.1098/rsta.2006.1928.

Holling, C. S. (1996). Engineering Resilience versus Ecological Resilience, in Schulze P.C. (ed.), Engineering Within Ecological Constraints, Washington, D.C., National Academy Press, 31-43.

JCSS (2008). Risk Assessment in Engineering - Principles, System Representation & Risk Criteria, Joint Committee on Structural Safety, ISBN 978-3-909386-78-9.

McDaniels, T., S. Chang, D. Cole, J. Mikawoz, and H. Longstaff (2008). Fostering resilience to extreme events within infrastructure systems: Characterizing decision contexts for mitigation and adaptation. Global Environmental Change 18(2), 310-318.

Ortenzi, M., F. Petrini, F. Bontempi, and L. Giuliani (2013). RISE: a method for the design of resilient infrastructures and structures against emergencies. In Proceedings of the 11th Int. Conf. on Structural Safety & Reliability Conference (ICOSSAR 2013). New York, USA.

Starossek, U. and M. Haberland (2010) Disproportionate collapse: terminology and procedures. Journal of Performance of Constructed Facilities 24(6): 519–528.

Sohn, H., C. R. Farrar, F. M. Hemez, D.D. Shunk, D. W. Stinemates, B. R. Nadler and J. J. Czarnecki (2004). A Review of Structural Health Monitoring Literature: 1996–2001; Los Alamos National Laboratory LA-13976-MS.

Sørensen, J.D. (2011). Theoretical framework on structural robustness. In Faber. M.H. (ed.), Robustness of Structures: Final Report of COST Action TU0601. Czech Technical University, Prague, Czech Republic, Klokner Institute, Prague, B.1-B.42.

Tierney, K. and M. Bruneau (2007). Conceptualizing and Measuring Resilience: A Key to Disaster Loss Reduction, TR News 250, Transportation Research Board, 14-15, 17.

Renschler, C., A. Frazier, L. Arendt, G. P. Cimellaro, A. M. Reinhorn, and M. Bruneau, M. (2010). Framework for Defining and Measuring Resilience at the Community Scale: The PEOPLES Resilience Framework. MCEER Technical Report, MCEER-10-006, University at Buffalo (SUNY), The State University of New York, Buffalo, New York.

Evaluating the value of structural heath monitoring with longitudinal performance indicators and hazard functions using Bayesian dynamic predictions

C. Xing, R. Caspeele, L. Taerwe

Ghent University, Department of Structural Engineering, Ghent, Belgium

Objectives, abstract and conclusions

The objective of this paper is to illustrate the evaluation of the value of Structural Health Monitoring (SHM) in the framework of pre-posterior analysis, elaborating the joint modeling of the time-varying structural performance and hazard function in inspection/repair planning and expected total life cycle cost calculation. The hazard function in the joint model is updated by the assumed monitoring outcome, which results in a change of inspection/repair plan and expected Total Life Cycle Cost (TLCC). The difference of expected TLCC is defined as the value of SHM which changes as decision parameter $h(t)^T$ related to the inspection time changes within the maximum acceptable value h_{max}.

Technical information

The joint modeling of the time-varying structural performance and hazard function is introduced in the framework of Bayesian decision making. This framework is taken as basis to update the inspection/repair planning, expected TLCC and correspondingly the value of SHM.

Abstract: In this article, we present a framework for evaluating the value of structural heath monitoring (SHM) in order to optimize the SHM implementation and to estimate the inspection/repair investment. A joint model consisting of a time-varying structural Performance Indicator (PI) prediction and a hazard function is proposed. Structural condition data used to estimate and update predictions of PI can be obtained from monitoring and a Bayesian dynamic model is proposed to forecast structural performance. For the survival process the time-dependent PI values and their changing rates are incorporated in the hazard function, in which the risk of structural failure depends on both the current value of PI and the slope of its trajectory at time t. A Bayesian approach using the Markov-chain Monte Carlo method can be adopted for the parameter estimation. The advantageous feature of these predictions is that they are dynamically updated as extra monitoring data are collected, providing real time risk assessment using all recorded information. Furthermore, inspections, with a probability of detecting damage followed by a probability of repair action, are planned when the hazard function at time *t* crosses a threshold value. Subsequently, the problem of optimizing the strategy of monitoring and maintenance can be solved by minimizing the expected total cost during the expected service life of the structure. Finally, the Value of SHM (VoSHM) is obtained by calculating the difference between the expected Total Life Cycle Costs (TLCC) of the inspection/repair plans with and without SHM implemented.

5 Introduction

Civil engineering structures are subjected to time-dependent degradation processes which require considerations of a wide range of uncertainties. When it is required to forecast or make decisions under uncertainty and risk, gathering further information prior to making the decision is often crucial. Such information reduces the uncertainty and thus facilitates improved decision making. As Structural Health Monitoring (SHM) provides a way for collecting information and reducing uncertainty, it has received a lot of attention and is also widely implemented in practice. Since monitoring systems and inspection methods are due to costs limited in time, the decisions should be based on the evaluation of its benefit, which should be done prior to its installation. The general decision can be characterized by whether or not to apply SHM, which strategy to apply, and when

to apply it if it's a short term monitoring strategy. Among these decisions, whether or not to apply SHM plays a fundamental role, based on which also decisions related to which kind of SHM and when to apply it can be investigated as well as their characteristics (e.g. precision, time intervals). The value of a certain SHM strategy is quantified by the value of information it provides, in monetary form. This can be calculated in the framework of decision theory introduced in Raiffa and Schlaifer (1961) as the difference between the expected life-cycle cost, or expected benefits, of performing SHM or not, as also presented by Faber and Thöns (2014). In order to calculate the expected TLCC, a threshold-based inspection/repair planning should be decided prior to further analysis of e.g. inspection times, repair rules and related costs. It requires a decision tree describing all possible events and the calculation of probabilities for each event. To do that, a joint modeling of the time-varying structural Performance Indicator (PI) and the hazard function is proposed first to calculate the failure rate (cf. infra). A threshold approach, as described in Straub and Faber (2006), is then adopted for planning the inspection time based on maximum failure rate and pre-posterior analysis for calculating the expected total life-cycle cost. The effect of SHM is accounted for by incorporating the monitoring outcome, including its uncertainty, to update the probability distribution of parameters related to the time-varying PIs, which in turn results in a change of inspection planning and expected total life-cycle cost. The VoSHM is then evaluated as the difference between the expected TLCC with and without SHM implemented. In the next parts, the process of this joint modeling and the parameter estimation methodology are first introduced. Then a framework for hazard based maintenance planning and determination of the VoSHM is elaborated.

6 Joint model of longitudinal data and hazard function

The joint modeling of longitudinal data, or in other words time sequent performance data, and the time to the occurrence of a particular event is an active area of research in statistics, mainly applied in medical related research, where two types of outcomes are recorded: (1) time sequent response measurements and (2) the time to an event of interest, such as time to death. These two types of outcomes are often analyzed using joint modeling of time sequent and time-to-event data, facilitating a prognostic tool for estimation and evaluation of risk rate for patients subjected to a certain disease, see Baghfalaki et al. (2014). Statistical methods for estimating and evaluating risk scores using reference data have been extensively studied in this field. It is clear that a similar procedure might be of interest for civil engineering structures. The joint modeling procedure and parameter estimation method are presented in the following section. Figure 1 shows an illustrative example of the joint modeling.

6.1   Process for modeling the time dependent structural performance:

The time dependent PIs can be expressed as:

$$y(t) = m(t) + \epsilon(t) \tag{1}$$

where $y(t)$ denotes the value of the time dependent observation outcome at any particular time point t, $m(t)$ is the underlying structural state which is a function of t and random effects denoted by b_i, and $\epsilon(t)$ the error terms that are assumed independent of the random effects. We assume that $\epsilon(t) \sim N(0, \sigma_1^2)$ and Cov. $[\epsilon(t), \epsilon(t')] = 0$ for $t \neq t'$.

6.2   Survival process defining the hazard function:

$$h(t) = \lim_{s \to 0} \frac{Pr(t < T < t + s | T > t)}{s} = h_0(t) \exp\{\alpha_1 m(t) + \alpha_2 m'(t) + \alpha_3\} \tag{2}$$

Where $h_0(t)$ is the baseline hazard function. This formulation postulates that the risk for a failure event at time t is associated with parameters α_1 and α_2 which quantify the strength of connection between the value of $m(t)$, its derivative over time $m'(t)$ and the failure rate for an event (failure

according to a limit state function) at the same time point. There are several association structures between $m(t)$ and $h(t)$ for an event. For the functional forms one can refer to Rizopoulos et al. (2014). Here we formulate the joint model of the two process based on the assumption that the failure risk depends on both the current value of the $m(t)$ and its changing rate $m'(t)$, which is often the case for degrading structures. For purpose of illustration, see Figure 2. For a certain limit of PI, the curve with higher $m(t)$ value and lower decreasing rate $m'(t)$ at time t leads to a lower failure rate h(t), as for PI$_1$(t) (as indicated by the red curve in Figure 2). From comparing PI$_2$(t) and PI$_3$(t) with similar deceasing rate $m'(t)$ at time t, it is observed that higher $m(t)$ leads to a lower risk of failure. α_3 is a another regression coefficient. Under the assumption that the hazard of the failure event is mainly based on the value of $m(t)$ and its decreasing rate $m'(t)$, α_3 can be predefined to a certain value.

More specifically, for the survival process, we consider a parametric proportional hazard model with Weibull baseline hazard, as in equation (3). The use of the Weibull proportional hazard model has the advantage that it is the only one that is a hazard model proportional to the baseline hazard as well as an accelerated failure time model. This is suitable for modeling degrading structures, as the failure risk accelerates with time, especially in the end period of the service life.

$$h(t) = \sigma_2 t^{\sigma_2 - 1} \exp\{\alpha_1 m(t) + \alpha_2 m'(t) + \alpha_3\} \tag{3}$$
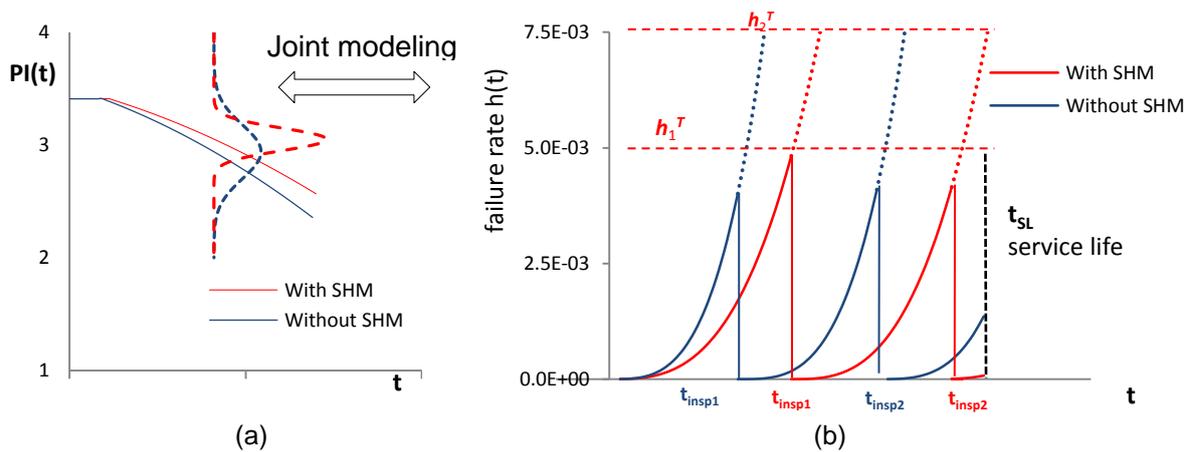
Figure 1. Joint modeling for (a) time-dependent structural performance and (b) hazard function

Details for the estimation of parameters in the two processes are provided in the Appendix. As soon as the evaluated value of the parameters are available, the failure rate h(t) at a time point and the failure probability during a period of time can be calculated and used for inspection time planning.

Under the Bayesian specification of the joint model, we can derive estimations and predictions for the hazard rate for a subject based on the observed time-dependent structural performance outcomes. Although the model fitting process can require considerable calculation and simulation work, it is very efficient for use once the joint model is formulated. Moreover, the hazard value h(t) can be updated when new monitoring information is recorded for updating the performance indicator, thus proceeding in a time-dynamic manner.
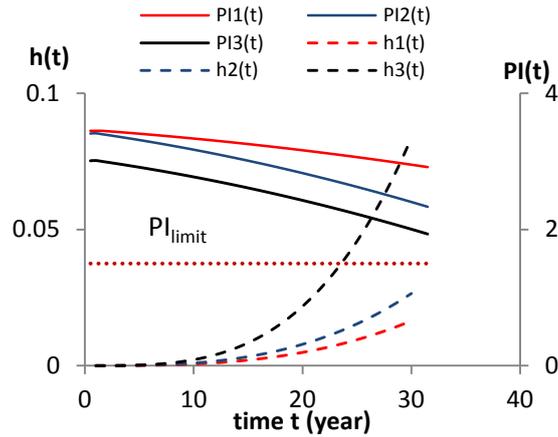
Figure 2 Illustration of interaction of PI(t) and PI'(t) with hazard function

One advantage of applying the joint modeling in civil engineering is that the functional form of the time-dependent feature of the structural performance, i.e. PI(t), is often available. Simulations of reference datasets can be performed by using a prior pdf assumption, which afterwards can be implemented into the joint modeling of the time-dependent performance and survival process. In this paper, the simulation based parameter estimation is not treated in detail and focus is given to the quantification of value of SHM, which is presented in the following part.

7 Hazard based maintenance planning and value of SHM

7.1 Value of SHM

An event tree model of a structure (e.g. the beam of a bridge) with or without monitoring is presented in Figure 3. For the time being, it is assumed that the structure returns to its original state after repair. This assumption makes it convenient to calculate the probabilities of occurrence of each branch in the event tree; for details refer to section 3.2.

As illustrated previously in Figure 1, the implementation of SHM can provide more information of the structure which would lead to a significant change of inspection/maintenance planning and as a result, the TLCC. Before making the decision of whether or not to implementing a certain SHM system, a prior estimation of the value of information that can be provided by the SHM is essential. Since the structural state and monitoring results are both uncertain, the decision problem can be described in terms of the following notations and events in a pre-posterior framework for Bayesian decision theory as developed in Raiffa and Schlaifer (1961):

Θ: Time-dependent structural state with prior pdf $f'_{\Theta}(\theta)$. Its time-dependent evolution is described by the joint model introduction in section 2;

Z: The inspection outcome which has an influence on the probability of detection and repair;

e: The inspection decision (i.e. inspection date, type of inspection, etc.). Inspection decision e varies according to the value of threshold $h(t)^T$ which is applied;

a: The maintenance action determined by the decision rule d and as a function of the inspection outcome Z and inspection decision e, i.e. $a=d(e, z)$;

X: The monitoring result variable which leads to an updating of the probability distribution of Θ to $f_\Theta''(\theta)$. We denote M_0 for the case without taking SHM, and M_1 for undertaking a certain monitoring strategy, as in the first node illustrated in Figure 3.

Analysis is then carried out for determining the expected TLCC (cf. infra).
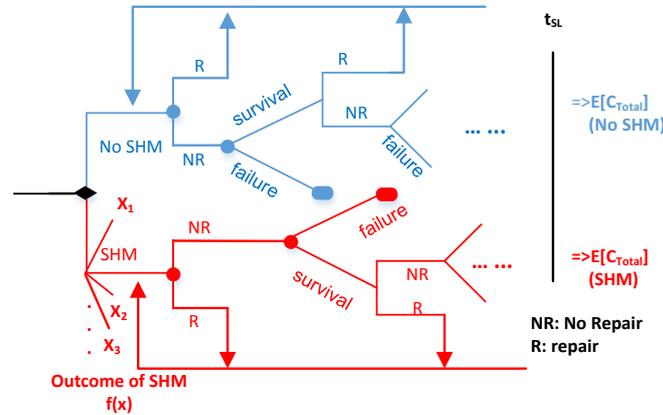
Figure 3 Decision tree model for inspection/repair planning with and without monitoring

For M_0, the true structural state Θ is described by a prior probability density function $f_\Theta'(\theta)$ and the expected TLCC is:

$$E_\Theta'[C_T(e,d,\theta)] = \int_\Theta C_T(e,d,\theta)f_\Theta'(\theta)d\theta \qquad (4)$$

For M_1, the analysis is in principle identical, except that new monitoring information is available and taken into account. Based on the additional monitoring information, the prior pdf $f_\Theta'(\theta)$ is updated to the posterior $f_\Theta''(\theta)$ leading to a change of the inspection and repair decisions. The expected TLCC is thus:

$$E_\Theta''[C_T(x,e,d,\theta)] = \int_\Theta C_T(x,e,d,\theta)f_\Theta''(\theta|x)d\theta \qquad (5)$$

In addition, based on the prior pdf of Θ and the monitoring strategy M, the probability of occurrence of the possible monitoring outcomes can be evaluated as:

$$f_X(x|M) = E_\Theta[f_X(x|M,\theta)] \qquad (6)$$

The monitoring data enable to determine the equivalent stress ranges, of course,
accounting for the measurement uncertainties.The value of information obtained by one monitoring outcome X, denoted as Condition Value of Sample Information (CVSI), has therefore the value

$$v(x) = CVSI(x) = E_\Theta'[C_T(e,d,\theta)] - E_\Theta''[C_T(x,e,d,\theta)] \qquad (7)$$

The expected value of this SHM strategies can, therefore, be determined by the Expected Value of Sample Information (EVSI) as

$$EVSI = E_X[CVSI(x)] = \int_X v(x)f_X(x)dx = E_\Theta'[C_T(e,d,\theta)] - \int_X E_\Theta''[C_T(x,e,d,\theta)]f_X(x)dx \qquad (8)$$

By assigning different pdfs for the monitoring result X, different monitoring strategies can be defined and the optimal decision on the monitoring strategy is the one with maximum value $\max_X EVSI(x)$.

In order to be able to evaluate the expected TLCC (see section 3.5), we need first to calculate the probabilities related to the decision tree based on a risk acceptance criterion h_{max} and decision rules.

7.2 Probabilities related to the decision tree

For a certain monitoring strategy (M_0 or M_1), calculation of the expected TLCC is needed based on the branches after the first node. This requires again pre-posterior analysis since the inspection results are also uncertain prior to being carried out. Hazard (failure rate) based inspection planning is applied in this contribution. The probability of occurrence of the branches after the first node in the decision tree is calculated based on the probabilities of detection of a certain deterioration state P_{det} and probabilities of taking repair action P_{rep} given a detected deterioration state with no repair before t as in equation (9) and (10) in accordance with Frangopol et al. (1997), Kim et al. (2011) and Barone (2013) .

$$P_{det} = \Phi\left(\frac{\delta(t) - \delta_{0.5}}{\sigma_{0.5}}\right) \tag{9}$$

$$P_{rep} = \left(\frac{\delta(t)}{\delta_{max}}\right)^{r_a} \qquad \delta(t) \leq \delta_{max} \tag{10}$$

in which Φ = standard Gaussian cumulative distribution function. $\delta(t)$ and δ_{max} are damage intensity at time t and maximum acceptable damage intensity; $\delta_{0.5}$ and $\sigma_{0.5}$ are parameters describing the quality of the inspection procedure, representing the damage intensity corresponding to a 50% probability of damage detection, and its standard deviation; r_a is a model parameter reflecting the attitude of the decision maker towards a repair action.

The branch of a failure event in the event tree requires the calculation of a failure probability $p_F(t)$ during time t given no repair before t. It can be calculated as soon as the hazard function is determined.

7.3 Risk acceptance criterion

The risk acceptance criterion used in this contribution is denoted by h_{max}, the maximum acceptable annual failure rate. It is related to the failure consequences of a structure and can be obtained from the Probabilistic Model Code, JCSS (2002), where the target reliability index as a function of the consequence of failure and the risk reduction cost is defined. For existing structures of which the relative cost for increasing the safety is generally large, the acceptance criterion can be lowered as also suggested in JCSS (2002), i.e. $\Delta p_f^{max} = 10^{-4}\ yr^{-1}$ for large consequences, $\Delta p_f^{max} = 5 \times 10^{-4}\ yr^{-1}$ for moderate consequences and $\Delta p_f^{max} = 10^{-3}\ yr^{-1}$ for minor consequences, where Δp_f^{max} is the maximum acceptable annual probability of failure, Straub (2004). Of course decision makers can decide to use other values than the latter ones. It can be noticed from the definition of the hazard function in section 2 that the value of hazard h(t) in this paper corresponds to the annual probability of failure Δp_f. Similarly, the maximum acceptable hazard value h_{max} can be specified in accordance with Δp_f^{max}.

7.4 Decision rule

As the probabilities of detecting a deterioration state and the corresponding repair are both function of the structural state which is a time dependent variable described by PI(t), the planning of inspection times will have a large influence on the probability of occurrences of each branch in the decision tree. The threshold approach introduced in Straub (2006) is thereby implemented in such a way that inspection is carried out in the year before the threshold of failure rate h(t)$^\top$ is crossed.

The h(t)^T is a decision parameter that can be changed as long as it remains lower than h_{max}. For decisions on repair, it requires the specification of the parameters used in equation (10) :

$$\begin{cases} h(t)^T \leq h_{max} & \text{for inspection} \\ \delta_{max} = \delta_0, r_a = r_0 & \text{for repair} \end{cases} \tag{11}$$

In which δ_0 and r_0 are values assigned by the decision makers. The decision for repair needs a direct indication of unacceptable defect sizes for a specific spot, (e.g. max pit depth of a rebar or maximum allowable crack depth). After an inspection was carried out, the repair decision is made based on the inpection result, detected structural states and repair attitude of the decision maker.

7.5 Expected TLCC

The expect TLCC for an inspection plan is calculated based on the occurrence of each branch in the decision tree as well as the cost of the basic events, i.e. the expected cost of failure, inspection, repair and monitoring if undertaken. The expected cost for each branch is calculated as the sum of all the events that happened in the branch. The expected TLCC for this inspection plan then takes weighted sums of the costs for all branches based on the occurrence probability of each branch introduced in section 3.2.

Specifically, the expected TLCC of a structural component during its design service life t_{SL} consists of the cost of failure, inspection, repair and monitoring (if undertaken):

$$E[C_T(e,d,t_{SL})] = E[C_F(e,d,t_{SL})] + E[C_I(e,d,t_{SL})] + E[C_R(e,d,t_{SL})] + E[C_M(e,d,t_{SL})] \tag{12}$$

Where $E[C_T(e,d,t_{SL})]$ is the expected TLCC, and $E[C_F(e,d,t_{SL})]$, $E[C_I(e,d,t_{SL})]$, $E[C_R(e,d,t_{SL})]$, $E[C_M(e,d,t_{SL})]$ are the expected cost of failure, inspection, repair and monitoring respectively, which can be calculated in accordance with Straub (2004) and Faber and Thöns (2014).

$$E[C_F(e,d,t_{SL})] =$$
$$\sum_{t=1}^{t_{SL}} \left[\left(1 - \sum_{i=1}^{t-1} p_R(e,d,i)\right) \frac{1}{(1+r)^t} \left(h(e,d,t)(1 - p_F(e,d,t-1))C_F + p_R(e,d,t)E[C_F(e,d,t_{SL}-t)]\right)\right] \tag{13}$$

$$E[C_I(e,d,t_{SL})]$$
$$= \sum_{t=t_1}^{t_{nInsp}} \left[(1 - p_F(e,d,t))\left(1 - \sum_{i=1}^{t-1} p_R(e,d,i)\right) \frac{1}{(1+r)^t} \cdot \left(C_{Insp} + p_R(e,d,t)E[C_I(e,d,t_{SL}-t)]\right)\right] \tag{14}$$

$$E[C_R(e,d,t_{SL})]$$
$$= \sum_{t=t_1}^{t_{nInsp}} \left[(1 - p_F(e,d,t))\left(1 - \sum_{i=1}^{t-1} p_R(e,d,i)\right) \frac{1}{(1+r)^t} \cdot p_R(e,d,t) \cdot \left(C_R + E[C_R(e,d,t_{SL}-t)]\right)\right] \tag{15}$$

$$E[C_M(e,d,t_{SL})] = C_{M_{Iv}} + C_{M_{Is}} + \left(1 - p_F(e,d,t)\right) \cdot C_{M_{Op}} \cdot \frac{1}{(1+r)^t} \tag{16}$$

Where t_{nInsp} is the time for the nth planned inspection, r is the discount rate. $C_F, C_{Insp}, C_R, \boldsymbol{C_M} = (C_{M_{Iv}}, C_{M_{Is}}, C_{M_{Op}})$ are the expected cost of failure, cost of inspection, cost of repair and cost of monitoring consisting of system investment $C_{M_{Iv}}$, installation $C_{M_{Is}}$ and operation $C_{M_{Op}}$ respectively, Faber and Thöns (2014). For details, we refer to Straub (2004) and Thöns (2012).

It should be mentioned that with a different value of $h(t)^T$, the planning of inspection times changes, leading to a change of the expect TLCC. Similarly, given a certain $h(t)^T$, the expected TLCC can also be different for M_0 and M_1, since the planned inspection times are likely to be different in case the monitoring outcome leads to a different joint model. Therefore, the maximum VoSHM can be found by changing $h(t)^T$, considering the risk acceptance criterion, to maximize the EVSI. The evaluation process is illustrated in the following flow chart in Figure 4:
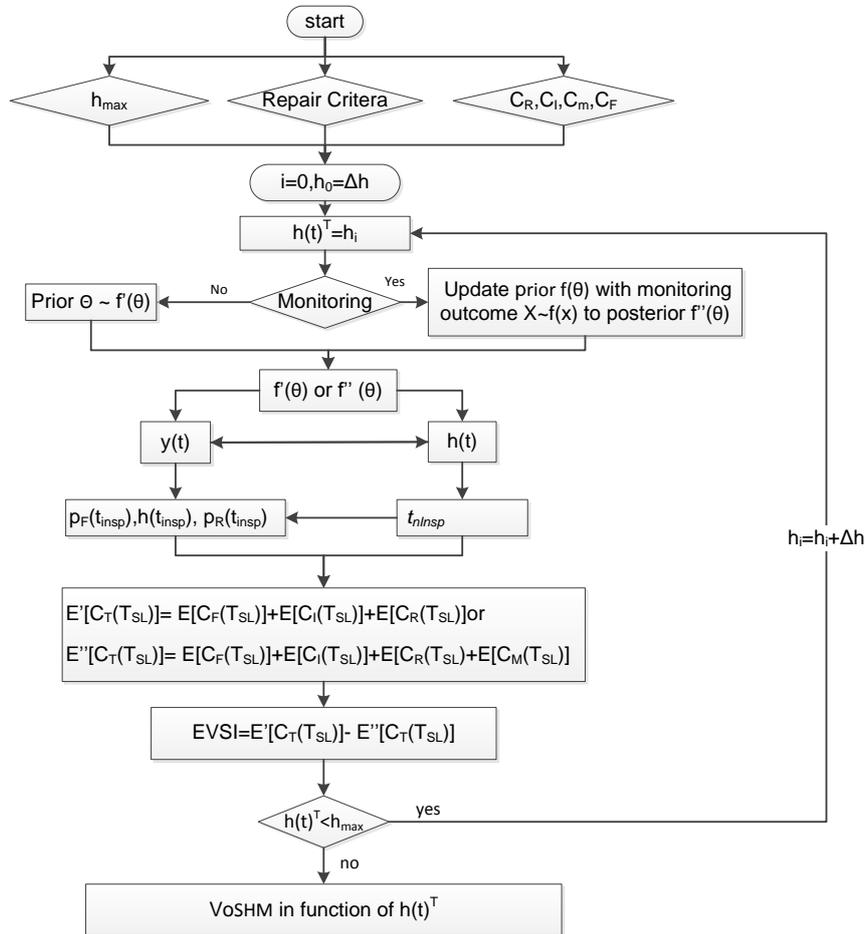
Figure 4. Flow chart for evaluating the value of SHM

8   Conclusive remarks

The paper proposes a framework for evaluating the VoSHM based on pre-posterior analysis incorporating Bayesian decision theory. A joint modeling of a time dependent structural performance function and a hazard function is first introduced and the derived hazard function is used as a tool for determining optimal inspection/repair plans for deteriorating structures. Consequently, also the expected TLCC is calculated. The effects of uncertainties related to the quality of monitoring outcomes are considered and incorporated in the joint model which leads to an updated the inspection/repair planning and expected TLCC. The difference between the prior and posterior expected TLCC is defined as the VoSHM and its dependency on the failure rate threshold is explained. Further research on the parameters estimation of joint modeling and identification of an optimal SHM strategy among others are needed.

9   Acknowledgements

10 References

Baghfalaki, T., Ganjali, M. and Hashemi, R. (2014). Bayesian Joint Modeling of Longitudinal Measurements and Time-to-Event Data Using Robust Distributions. Journal of Biopharmaceutical Statistics, 24, 834-855.

Barone, G. and Frangopol, D. M. (2013). Hazard-Based Optimum Lifetime Inspection and Repair Planning for Deteriorating Structures. Journal of Structural Engineering, 139.

Faber, M. H. and Thöns, S. (2014). On the value of structural health monitoring. Safety, Reliability and Risk Analysis: Beyond the Horizon, 2535-2544.

Frangopol, D. M., Lin, K. Y. and Estes, A. C. (1997). Life-cycle cost design of deteriorating structures. Journal of Structural Engineering-Asce, 123, 1390-1401.

JCSS (2002). Probabilistic Model Code. Joint Committee on the Structural Safety JCSS, internet publication.

Kim, S., Frangopol, D. M. and Zhu, B. J. (2011). Probabilistic Optimum Inspection/Repair Planning to Extend Lifetime of Deteriorating Structures. Journal of Performance of Constructed Facilities, 25, 534-544.

Raiffa, H. and Schlaifer, R. (1961). Applied statistical decision theory, Boston (Mass.), Harvard university press.

Rizopoulos, D., Hatfield, L. A., Carlin, B. P. and Takkenberg, J. J. M. (2014). Combining Dynamic Predictions From Joint Models for Longitudinal and Time-to-Event Data Using Bayesian Model Averaging. Journal of the American Statistical Association, 109, 1385-1397.

Straub, D. (2004). Generic Approaches to Risk Based Inspection Planning for Steel Structures. ETH Zürich, Institute of Structural Engineering.

Straub, D. and Faber, M. H. (2006). Computational aspects of risk-based inspection planning. Computer-Aided Civil and Infrastructure Engineering, 21, 179-192.

Thöns, S. (2012). Monitoring based condition assessment of offshore wind turbine support structures. ETH Zürich, Institute of Structural Engineering.

11 Appendix

For the joint model, we assume a reference dataset consisting of N samples each with its performance trajectory and time-to-event information available. The time-to-event (or time to failure) is defined by the structural performance crossing a limit value. Let T_i denote the observed lifetime for the ith individual, i =1, 2, ..., N, which is taken as the minimum of the true failure time T_i^* and the censoring time C_i (e.g. didn't fail up to the time when the experiment ends), that is, T_i =min(T_i^*, C_i). We define a censoring indicator, $\delta_i = I(T_i^* \leq C_i)$, which takes the value 1 when $T_i^* \leq C_i$, and 0 otherwise. Therefore, the time to failure dataset consists of the pairs $\{(T_i, \delta_i), i = 1, 2, ..., N\}$. Furthermore, we let $\boldsymbol{y_i}$ denotes the time dependent PI data for the ith subject, with element y_{il} denoting the value of the PI outcome observed at time point t_{il}, $l = 1, \ldots, n_i$.

One way to estimate the joint model's parameters is based on the Markov Chain Monte Carlo algorithm (MCMC). The likelihood of the model is derived under the assumption that the vector of time-independent random effects $\boldsymbol{b}$, included in m(t) accounts for all interdependencies between the observed outcomes. That is, given the random effects, the longitudinal and survival process are assumed independent, and in addition, the longitudinal responses of each subject are assumed independent. Formally we have:

$$p(y_i, T_i, \delta_i | b_i, \theta) = p(y_i | b_i, \theta) p(T_i, \delta_i | b_i, \theta) \tag{A(1)}$$

$$p(y_i | b_i, \theta) = \prod_l p(y_{il} | b_i, \theta) \tag{A(2)}$$

In which the parameters included in the two processes of the joint model is denoted by $\theta = [\alpha_1, \alpha_2, \alpha_3, \sigma_1, \sigma_2, D)$, where D is the parameter characterizing the random effects b. Thus, the likelihood contribution for the ith subject conditional on the parameters and random effects takes the form:

$$
\begin{aligned}
&p(y_i, T_i, \delta_i | b_i, \theta) \\
&= \prod_{l=1}^{n_i} p(y_{il} | b_i; \theta_y) \, p(T_i, \delta_i | b_i; \theta_t) \, p(b_i; \theta_b) \\
&\propto \left[\begin{array}{c} (\sigma_1^2)^{-\frac{n_i}{2}} \exp\{ -\sum_l (y_{il} - m_i(l))^2 / 2\sigma_1^2 \} \times [\sigma_2 t^{\sigma_2 - 1} \exp\{\alpha_1 m_i(T_i) + \alpha_2 m_i'(T_i) + \alpha_3\}]^{\delta_i} \\ \times \exp\left[-\int_0^{T_i} \sigma_2 t^{\sigma_2 - 1} \exp\{\alpha_1 m_i(s) + \alpha_2 m_i'(s) + \alpha_3\} ds \right] \\ \times p(b_i; \theta_b) \end{array} \right]
\end{aligned}
\tag{A(3)}
$$

The parameter vector $\boldsymbol{\theta}$ is divided into 3 parts, where θ_t denotes the parameters for the failure time outcome, θ_y the parameters for the longitudinal outcomes, and θ_b the unique parameters of the variance of the random effects, and p($\cdot$) denotes an appropriate probability density function, which is a normal distribution for $p(y_{il} | b_i; \theta_y)$, and for $p(T_i, \delta_i | b_i; \theta_t)$ derived from the hazard function.

Therefore, the likelihood function for the complete data $\boldsymbol{D_a} = (\boldsymbol{y}, \boldsymbol{T}, \boldsymbol{\delta})$ is given by:

$$L(\boldsymbol{D_a} | \theta) = \prod_{i=1}^{N} [p(y_i, T_i, \delta_i | b_i, \theta)] \tag{A(4)}$$

Bayesian specification of the model needs to consider prior distributions for all the unknown parameters $\boldsymbol{\theta}$. In the situation where no prior information is available, non-informative prior distributions for the parameters should be adopted. Assuming elements of the parameter vector to be independent, we can take some traditional prior distributions. In particular, for the regression parameters of the survival model α_1, α_2 and α_3 we use independent univariate normal priors. For σ_1, σ_2 and D we take inverse-Gamma priors. In general, we denote the prior distribution of the parameters as $\pi(\theta)$.

Based on the prior distribution and likelihood function, the joint posterior density of parameters $\boldsymbol{\theta}$, $\pi''(\theta)$, is given by combining A(4) and $\pi(\theta)$:

$$\pi''(\theta) \propto L(\boldsymbol{D_a} | \theta) \pi(\theta) = \prod_{i=1}^{N} [p(y_i, T_i, \delta_i | b_i, \theta)] \, \pi(\theta) \tag{A(5)}$$

MCMC methods such as the Gibbs sampler and Metropolis–Hastings algorithm can be used to draw samples, from which characteristics of the marginal posterior distribution of interest can be inferred. As a result of the simulation, the parameters of $\boldsymbol{\theta}$ are estimated and the hazard function is determined.

Contact information

Cheng Xing,
PhD student,
Ghent University, Department of Structural Engineering,
Technologiepark-Zwijnaarde 904, 9052 Gent, Belgium.
+32(0)9 264 55 35
Cheng.Xing@Ugent.be

Damage and resistance correlation influence on the value of Structural Health Monitoring

Sebastian Thöns, Dept. of Civil Engineering, Technical University of Denmark, Lyngby, Denmark
Michael H. Faber, Dept. of Civil Engineering, Technical University of Denmark, Lyngby, Denmark

Objectives, abstract and conclusions

This paper addresses the influence of deteriorating structural system characteristics on the value of structural health monitoring (SHM) information before implementation of the SHM strategy. The value of SHM is calculated utilizing the Bayesian pre-posterior decision analysis modelling the structural system life cycle performance, the integrity management, the structural risks and the SHM information.

The quantification of the value of SHM as recently introduced involves a probabilistic representation of the loads and environmental conditions acting on structural systems as well as their responses and performances over their life-cycle. In addition, the structural integrity management is modelled comprising decision rules, probabilistic models of the quality of monitoring and the performance of possible remedial actions triggered by monitoring results. The consequences include in principle all consequences associated with the performance of the structure over its life-cycle as well as the costs associated with monitoring and possible remedial actions. Building upon these models, the value of SHM takes basis in the relevance and precision of SHM information for the reduction of the structural system risks and the expected costs of the structural integrity management throughout the life cycle.

With the described approach, the value of SHM for structural systems subjected to fatigue deterioration is calculated. The structural system characteristics are modelled building upon Daniels systems and a coupled SN and fracture mechanics approach describing the deterioration state in conjunction with the structural resistance throughout the service life. The dependencies between the resistances and the deterioration states of the individual structural components are accounted for. The SHM strategies are modelled in the context of a pre-posterior decision analysis. The value of SHM is then quantified by calculating the difference of the service life benefits with SHM and without SHM for different levels of dependencies between the deterioration and the resistances of the individual components. The influence of the dependencies on the value of SHM is then analyzed and documented for ductile Daniels systems.

The value of SHM increases for ductile systems and decreases for brittle systems with increasing resistance correlation caused by the dominance of system risks, the ductile and brittle system characteristics and the approximately constant uncertainty reduction due to load monitoring. A similar behaviour can be observed for the deterioration state correlation given the deterioration is relevant for the system reliability.

Technical information

1   Introduction

The value of Structural Health Monitoring (SHM) is influenced by structural system characteristics such e.g. as the number of components, the type of the structural system and the dependencies of performance of the system components. This paper focusses thus on the system modelling and the explication of the influence of dependencies of the component performance on the value of SHM building upon Thöns, Schneider et al. (2015) and the framework for the quantification of the Value of SHM (Section 2) and taking basis in mechanical justified Daniels system formulations. The structural system deterioration and integrity management models are described in Section 3 containing a coupled ultimate performance model and a fatigue deterioration model formulation. The SHM information model including the influence on the structural system deterioration and integrity management model is formulated in Section 4. Section 5 summarizes the case study definition and describes the influence of the resistance dependencies and the deterioration state dependencies on the Value of SHM. The conclusions are documented in Section 5.

2   Quantification of the value of SHM for structural systems

The quantification of the value of SHM takes basis in the value of Information theory and the Bayesian pre-posterior decision theory as documented in Thöns, Schneider et al. (2015). The value of SHM can be calculated through the difference between the expected value of the life cycle benefits B_1 utilizing SHM and the expected value of the life cycle benefits B_0 without SHM (Equ. (1)).

$$V = B_1 - B_0 \tag{1}$$

The expected value of the life cycle benefit B_0 depends on the structural performance subjected to the uncertainties $\mathbf{Z}$ consisting of epistemic and aleatory uncertainties $\mathbf{Z}_E$ and $\mathbf{Z}_A$ respectively and the decision rules $\mathbf{d}$ for adaptive actions $\mathbf{a}$ for the structural integrity management throughout the life cycle (Equ. (2)).

$$B_0 = \max_{\mathbf{a},\mathbf{d}} E_{\mathbf{Z}_E} \left[E_{\mathbf{Z}_A} \left[B\big(\mathbf{d}(\mathbf{a},\mathbf{Z}_E,\mathbf{Z}_A),\mathbf{Z}_E,\mathbf{Z}_A\big) \right] \right] \tag{2}$$

Utilizing SHM, the expected value of the life cycle benefit B_1 depends additionally on the SHM strategies $\mathbf{s}$ which deliver the uncertain SHM information $\mathbf{X}$. The decision rules and adaptive actions for the structural integrity management ($\overline{\mathbf{a}}$ and $\overline{\mathbf{d}}$) are now modified to account for the SHM information. Further, the uncertainties in regard to the life cycle performance may have changed due to the observations collected through SHM and are thus denoted as $\overline{\mathbf{Z}}_E$ and $\overline{\mathbf{Z}}_A$ (Equ.(3)).

$$B_1 = \max_{\mathbf{s}} E_{\overline{\mathbf{Z}}_E} \left[E_{\overline{\mathbf{Z}}_A} \left[\max_{\mathbf{a},\mathbf{d}} E_{\mathbf{X}|\overline{\mathbf{Z}}_E,\overline{\mathbf{Z}}_A} \left[\overline{B}\big(\overline{\mathbf{d}}(\overline{\mathbf{a}},\mathbf{X},\overline{\mathbf{Z}}_E,\overline{\mathbf{Z}}_A),\mathbf{s},\mathbf{X},\overline{\mathbf{Z}}_E,\overline{\mathbf{Z}}_A\big) \right] \right] \right] \tag{3}$$

3   Structural system deterioration and integrity management model

The performance of the structural system accounting for fatigue deterioration throughout the life cycle is modelled with the structural system deterioration model. The expected costs of the structural integrity management and the structural risks are calculated with the structural system integrity management model.

3.1   Structural system deterioration model

Efficient means of calculating the system performance are Daniels systems (Figure 1) as they have a clear mechanical justification Gollwitzer and Rackwitz (1990).
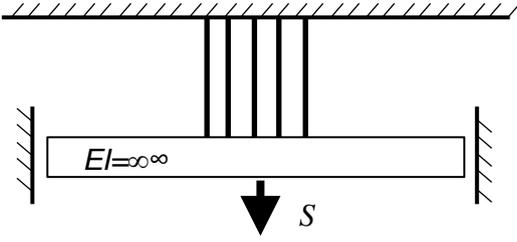
Figure 1: Daniels System

The probability of failure of a ductile Daniels system can be calculated with the limit state function $g_{FS,D}$ as the sum (over n components) of the deterioration and thus time dependent component resistances $R_i(t)$ including the model uncertainties $M_{R,i}$ minus the system loading S multiplied with the loading model uncertainty M_S (Equ. (4)).

$$P\left(g_{FS,D} \leq 0\right) = P\left(\sum_{i=1}^{n} M_{R,i} R_i(t) - M_S S \leq 0\right) \tag{4}$$

The probability of brittle system failure is defined with the limit state function $g_{FS,B}$. The system resistance is modelled with an ordered set of the component resistance including model uncertainties such that $\hat{M}_{R,1}\hat{R}_1 \leq \hat{M}_{R,2}\hat{R}_2 \leq \ldots \leq \hat{M}_{R,n}\hat{R}_n$ (Equ. (5)).

$$P\left(g_{FS,B} \leq 0\right) = \prod_{i=1}^{n} P\left((n-i+1)\hat{M}_{R,i}\hat{R}_i(t) - M_S S \leq 0\right) \tag{5}$$

The fatigue deterioration is modelled with a fracture mechanics (FM) model which is calibrated to an SN fatigue model. The SN limit state function g_i^{SN} (Equ. (6)) for the component i, i.e. hot spot is formulated in dependency of fatigue capacity Δ, the annual number of stress cycles ν, the stress ranges $\Delta\sigma_i$ and the SN curve constants m and K.

$$g_i^{SN} = \Delta - \nu \cdot t \frac{E\left[\Delta\sigma_i^m\right]}{K} \tag{6}$$

The expected value of the stress ranges $E\left[\Delta\sigma_i^m\right]$ (Equ. (7)) is calculated with the model uncertainty M, the cut-off stress range s_0 and the Weibull scale parameter λ as well as the Weibull location parameter k.

$$E\left[\Delta\sigma_i^m\right] = (Mk)^m \Gamma\left(1 + \frac{m}{\lambda}; \left(\frac{s_0}{k}\right)^\lambda\right) \tag{7}$$

The FM model is described with the limit state function g_i^{FM} (Equ. (8)) containing the critical crack depth $a_{i,c}$ and the crack depth distribution $a_i(t)$ at time t for the component i.

$$g_i^{FM} = a_{i,c} - a_i(t) \tag{8}$$

The quantification of the crack size distribution $a_i(t)$ facilitates a yearly discrete modelling of the deterioration state $D_i(t)$. This deterioration state is modelled with the reduction initial component

resistance $R_{i,0}$ in dependency of a resistance reduction factor r_R multiplied with the crack size $a_i(t)$ to wall thickness d_i ratio, see Equ. (9).

$$R_i(t) = R_{i,0}\left(1 - D_i(t)\right) = R_{i,0}\left(1 - r_R \frac{a_i(t)}{d_i}\right) \tag{9}$$

The crack depth at year t conditional on the inspection outcomes can be calculated with the approach recently proposed by Straub and Papaioannou (2014). The algorithm can be interpreted as an enhancement of the classical rejection sampling algorithm for Bayesian updating which can be based on subset simulation (Au and Beck (2001)).

3.2 Structural system integrity management model

The structural system integrity management model builds upon the reliability based inspection and repair planning decision rule (see Faber, Engelund et al. (2000), Straub (2004) and Schneider, Thöns et al. (2013)) with the adaptive actions inspection and repair. Additionally, the risks due to component fatigue failure and system failure are calculated.

The expected life cycle benefits B_0 are the sum of the expected costs (negative expected benefits) of the componential structural integrity management $E\left[C_{i,Insp}\right]$ and $E\left[C_{i,R}\right]$, the risk of component fatigue failure $R_{i,D}$ and the risk for structural system failure R_{F_S} (Equ. (10)). The expected costs of the componential structural integrity management consist of the expected value of the costs of inspection $E\left[C_{i,Insp}\right]$ and the expected value of the repair costs $E\left[C_{i,R}\right]$.

$$B_0\left(d(\mathbf{a},\mathbf{Z}),\mathbf{Z}\right) = -\left(\sum_{i=1}^{n}\left(E\left[C_{i,Insp}\right] + E\left[C_{i,R}\right] + R_{i,D}\right) + R_{F_S}\right) \tag{10}$$

4 Structural system deterioration and integrity management model with SHM

SHM concerns the loading, the structural and/or the structural response as well as the consequence characteristics. These characteristics can be represented with analytical, empirical or semi-empirical models which are subjected to model uncertainties. The model uncertainties may be determined by means of measurements (see e.g. JCSS (2006)) which implies that SHM data contain information about the model uncertainties. In this way, yet unknown SHM data can be modeled pre-posteriorly in the context of the Bayesian decision theory. This means that the expected stress ranges for fatigue are calculated in dependency of realizations of the model uncertainties $\hat{M}$ (Equ. (11)) accounting for the SHM uncertainty U.

$$E\left[\Delta\sigma_i / \hat{M}\right] = \left(\hat{M}Uk\right)^m \Gamma\left(1 + \frac{m}{\lambda};\left(\frac{s_0}{k}\right)^\lambda\right) \tag{11}$$

In the context of structural systems, the SHM system information can also be utilized for the calculation of system failure probability by utilizing the realizations of a vector of system model uncertainties $\hat{\mathbf{M}}$ and accounting for the measurement uncertainty (Equ. (12)).

$$P\left(F_S \mid \hat{\mathbf{M}}\right) = \int_{\Omega_{F_S}} f_{\mathbf{Z},U}\left(\mathbf{z},u \mid \hat{\mathbf{M}}\right) d\mathbf{z}du \tag{12}$$

The expected value of the life cycle benefit utilizing SHM B_1 is calculated with the expected value of the costs for the componential structural integrity management (see Equ. 12), the risk of component fatigue failure $R_{i,D}^{SHM}$ and the risk of system failure $R_{F_S}^{SHM}$ which are changing due to the

different probabilistic characteristics (see section 2.2) and the expected SHM costs $E\left[C_{i,SHM}\right]$ (Equ. (13)).

$$B_1\left(d\left(\mathbf{a},\mathbf{X},\mathbf{Z}\right),\mathbf{s},\mathbf{X},\mathbf{Z}\right)=-\left(\sum_{i=1}^{n}\left(E\left[C_{i,Insp}^{SHM}\right]+E\left[C_{i,R}^{SHM}\right]+E\left[C_{i,SHM}\right]+R_{i,D}^{SHM}\right)+R_{F_S}^{SHM}\right) \tag{13}$$

5   Case study

5.1   Structural system deterioration

A Daniels system consisting of $n=5$ hot spots which are designed with fatigue design factors of 2.0 (three hot spots) and 3.0 (two hot spots) is considered. The system loading S is resisted by the components with the initial resistance $R_{0,i}$ which is reduced due to the fatigue deterioration.

The mean of the initial resistance is calibrated to the component structural reliability. The loading of the Daniels system and the resistance of the components are Log-Normal and Weibull distributed with a standard deviation of 0.1, see Table 1. The probabilistic models for the model uncertainties M_R and M_S are determined in accordance with JCSS (2006).

Table 1: Probabilistic structural system model

Var.	Dim.	Dist.	Exp. value	Std. dev.
M_R	-	LN	1.0	0.05
$R_{0,i}$	-	LN	calibrated	0.1
M_S	-	LN	1.0	0.1
S	1/y	WBL	3.5	0.1
r_R	-	Det.	0.6	-

LN: Lognormal, WBL: Weibull

The SN fatigue resistance Δ and the model uncertainties M_L (load calculation), M_σ (nominal stress calculation), M_{HS} (hot spot stress calculation) and M_Q (weld quality) are modelled following Folsø, Otto et al. (2002), see Table 2. The location parameter k of the long-term stress distribution is scaled so that the accumulated fatigue damage after $t = FDF \cdot t_{SL}$ years equals one applying the characteristic value for *K*.

Table 2: Probabilistic SN fatigue deterioration model

Var.	Dim.	Dist.	Exp. value	Std. dev.
Δ	-	LN	1.0	0.3
lnK	-	N	28.995	0.572
m	-	Det.	3.0	
k	MPa	LN	Dep. on FDF	$0.2 \times \mu_k$
$1/\lambda$	-	Det.	1.2	
s_0	MPa	Det.	0.0	
ν	yr^{-1}	Det.	3.0×10^6	
t_{SL}	yr	Det.	20.0	
M_L		LN	0.89	0.27

M_σ		LN	1.01	0.12
M_{HS}		LN	1.02	0.20
M_Q		LN	1.02	0.20

LN: Lognormal, N: Normal

The FM model is based on a 2D-FM-model and a single slope Paris' law crack growth model, see BS 7910 (2005). For simplicity identical hot spots in terms of the wall thickness and the degree of bending are assumed (Table 3). The initial crack size is modelled exponentially distributed following Moan and Song (2000).

Table 3: Probabilistic FM model

Var.	Dim.	Dist.	Exp. value	Std. dev.
d	mm	Det.	16	
a_c		Det.	16	
DoB		Det.	0.5	
r_{aspect}		Det.	0.2	
a_0		EX	0.11	0.11
$\ln C$	N and mm	N	Cal.	0.77
M_{SIF}		LN	Cal.	0.1

LN: Lognormal, N: Normal, EX: Exponential

The expected values of the crack growth parameter and of the stress intensity factor model uncertainty are calibrated to the SN model.
A correlation of the fatigue deterioration of 0.6 is assumed following on Moan (1994). Further, the component resistances including their model uncertainties are assumed to be correlated with 0.5.

5.2   SHM strategy

The SHM strategy consists of monitoring the system loading and of hot spot stresses, i.e. the hot spot loading. The probability of ductile and brittle structural system failure utilizing SHM is calculated with the realizations of the system loading model uncertainty $\hat{M}_S$ by:

$$P\left(g_{FS,D}^{SHM} \leq 0\right) = P\left(\sum_{i=1}^{n} M_R R_i(t) - \hat{M}_S U_L S \leq 0\right) \tag{14}$$

$$P\left(g_{FS,B}^{SHM} \leq 0\right) = \prod_{i=1}^{n} P\left((n-i+1)\hat{M}_{R,i}\hat{R}_i(t) - \hat{M}_S U_L S \leq 0\right) \tag{15}$$

The expected values of the stress ranges for the individual hot spots are modeled conditional on the realizations of the hot spot loading model uncertainties, i.e.:

$$E\left[\Delta\sigma_i / \hat{M}_L\right] = \left(\hat{M}_L M_\sigma M_{HS} M_Q U_L k\right)^m \Gamma\left(1 + \frac{m}{\lambda}; \left(\frac{s_0}{k}\right)^\lambda\right) \tag{16}$$

In Equ. (14) to (16), the measurement uncertainty U_L is introduced to account for the uncertainties associated with the observations of the structural system and the hot spot loading. The probabilistic model builds upon the quantified measurement uncertainties in Thöns (2011), see Table 4. The costs of the considered 5 channels SHM system consisting of investment, installation and operation are chosen in accordance with Thöns, Faber et al. (2014).

Table 4: Probabilistic model and cost model for SHM

Var.	Dim.	Dist.	Exp. value	Std. dev.
U_L	-	N	1.0	0.05
$C_{i,\text{Inv}}$	1 /channel	Det.	1.33×10^{-4}	-
$C_{i,\text{Inst}}$	1 /channel	Det.	1.33×10^{-4}	-
$C_{i,\text{Op}}$	1/y	Det.	2.00×10^{-4}	-

N: Normal

5.3   Structural system integrity management model

The structural system integrity management model takes basis in the reliability based inspection and repair planning at component, i.e. hot spot, level. The inspection plans for the individual hot spots are determined such that a given maximum threshold for the annual probability of component fatigue failure Δp_D for each of the hot spots is maintained throughout the service life of 20 years. The inspection strategy is magnetic particle inspections (MPI) which are modelled with the parameters α and β following e.g. Straub (2004), see Equ. (17) and Table 5.

$$PoD(a) = \frac{\exp(\alpha + \beta \ln(\alpha))}{1 + \exp(\alpha + \beta \ln(\alpha))} \qquad (17)$$

Table 5: Probabilistic inspection model

Var.	Dim.	Dist.	Exp. value	Std. dev.
α	-	Det.	0.63	
β	-	Det.	1.16	

The cost model for the service life integrity management and the calculation of risks builds upon generic normalized values for the adaptive actions inspection and repair and the consequences in case of component, i.e. hot spot, fatigue failure and structural system failure (see Straub (2004) and Baker, Schubert et al. (2008)). The discounting rate is assumed to be equal to 0.05.

Table 6: Cost model for the service life integrity management and the calculation of risks

Var.	Exp. value
$C_{i,Insp}$	1.0×10^{-3}
$C_{i,R}$	1.0×10^{-2}
$C_{i,\text{D}}$	1.0
C_{F_S}	100
r	0.05

5.4   Value of load monitoring in dependency of the system characteristics

The value of load monitoring (Equ. (1)) is calculated by quantifying the service life benefits B_1 utilizing SHM (Equ. (13)) and B_0 without SHM (Equ. (10)). The structural integrity management is performed with four different probability of component fatigue failure thresholds Δp_D, namely 1.0×10^{-2}, 3.0×10^{-3}, 1.0×10^{-3} and 3.0×10^{-4}.

Figure 2 documents the value of SHM in dependency of the fatigue failure thresholds for a ductile and a brittle Daniels system with a resistance correlation $\rho\left(R_i, R_j\right) = 0.5$, a deterioration state correlation $\rho\left(D_i, D_j\right) = 0.6$ and probability of component deterioration failure of $P\left(F_{c,i}\right) = 1.0 \cdot 10^{-2}$.

For both the ductile and the brittle Daniels systems, the value of SHM is positive with a maximum for the maximum considered fatigue failure threshold and the minimum for a threshold of 1.0×10^{-3}. The largest part of the value of SHM is due to system risk reduction. For low fatigue failure thresholds, the value of SHM is additionally caused by the reduction of the component deterioration risks and the accumulated component inspection and repair costs.

Ductile Daniels System   Brittle Daniels System
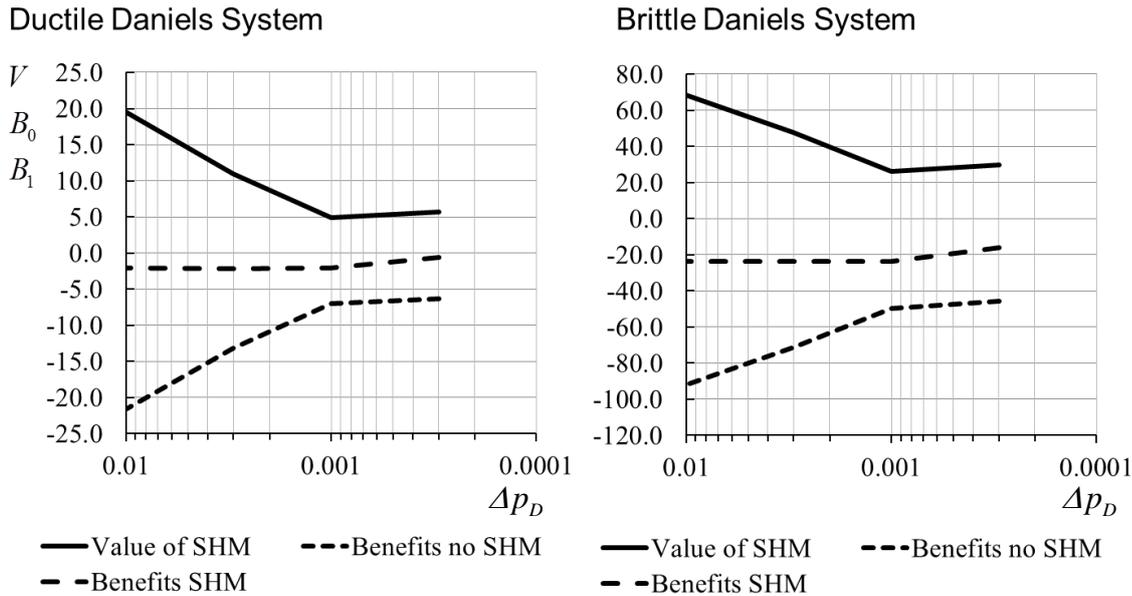
Figure 2: Value of SHM for a ductile and a brittle Daniels system with a resistance correlation $\rho\left(R_i, R_j\right) = 0.5$, a deterioration state correlation $\rho\left(D_i, D_j\right) = 0.6$ and probability of component deterioration failure of $P\left(F_{c,i}\right) = 1.0 \cdot 10^{-2}$.

The value of SHM increases for an increasing correlation of the resistances of a ductile system and decreases for a brittle system for all considered probability of component fatigue failure thresholds (Figure 3). This can be explained for a ductile system by the facts that (1) the system failure probability increases with increasing component resistance correlation caused by the reduction of the system resistance and that (2) the uncertainty reduction due load monitoring is approximately constant because it is primarily associated to the (resistance correlation independent) system loading. The uncertainty reduction due to load monitoring is thus more influential for a high correlation of the resistances which causes higher values of SHM caused primarily by system risk reduction.

A similar explanation is found for a brittle Daniels system. Here, the system failure probability decreases caused by an increasing system resistance when the component resistance correlation increases and the uncertainty reduction due load monitoring is approximately constant. The uncertainty reduction due to load monitoring is thus less influential for a high correlation of the resistances which causes lower values of SHM caused primarily by system risk reduction.

Ductile Daniels System
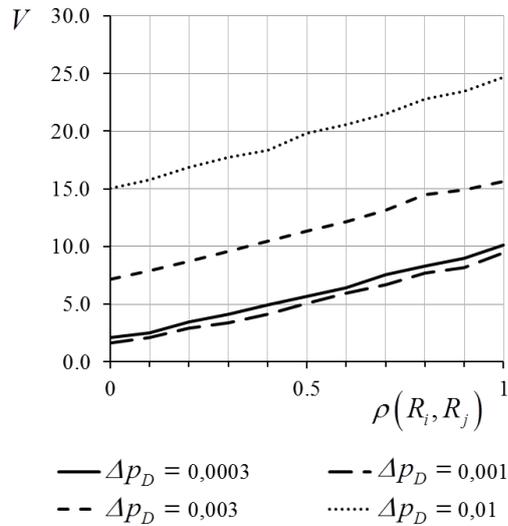
Brittle Daniels System
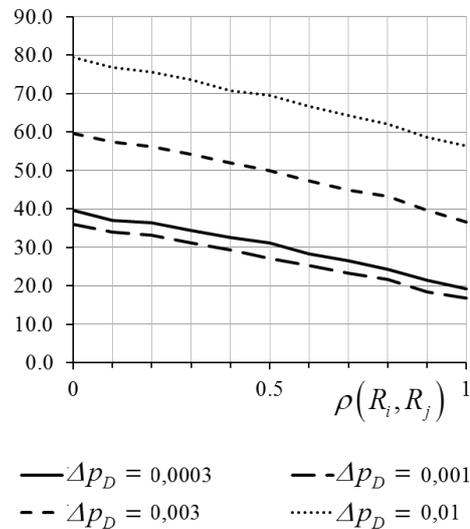
Figure 3: Value of SHM for a ductile and a brittle Daniels system in dependency of the resistance correlation $\rho(R_i, R_j)$ with a deterioration state correlation $\rho(D_i, D_j) = 0.6$ and probability of component deterioration failure of $P(F_{c,i}) = 1.0 \cdot 10^{-2}$.

Considering the deterioration state correlation, the value of SHM is approximately constant, i.e. independent of the deterioration state correlation, for low component deterioration failure thresholds (Figure 4). Here, the deterioration does not significantly influence the system probabilities of failure. For higher thresholds, the value of SHM increases for an increasing deterioration correlation for the ductile system and decreases for the brittle system. The explanation of this behaviour is found to be very similar to the resistance correlation (see above).

Ductile Daniels System
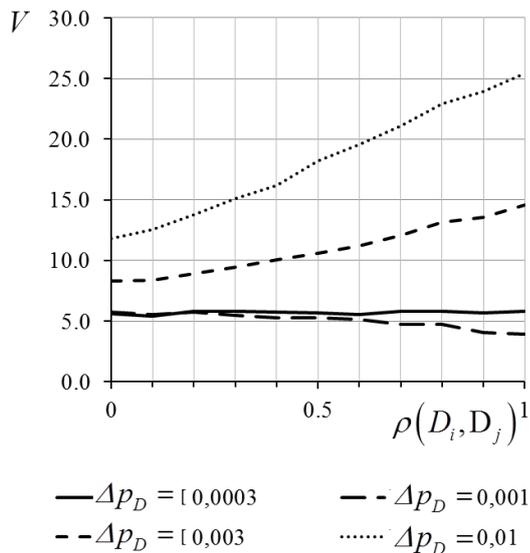
Brittle Daniels System
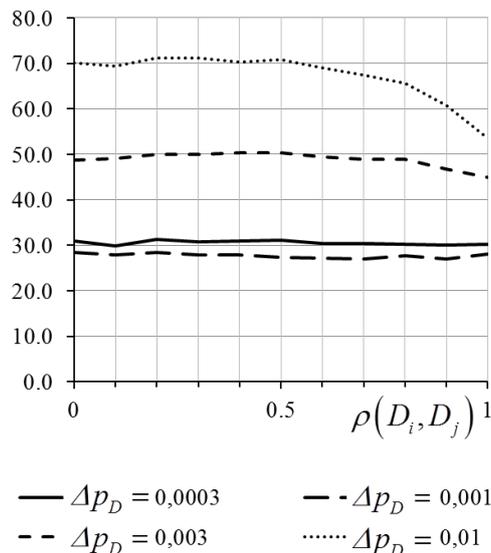
Figure 4: Value of SHM for a ductile and a brittle Daniels system in dependency of the deterioration state correlation $\rho(D_i, D_j)$ with a resistance correlation $\rho(R_i, R_j) = 0.5$ and probability of component deterioration failure of $P(F_{c,i}) = 1.0 \cdot 10^{-2}$.

6   Conclusions

This paper addresses the influence of deteriorating structural system characteristics on the value of structural health monitoring (SHM) information before implementation of the SHM strategy. The value of SHM is calculated utilizing the Bayesian pre-posterior decision analysis modelling the structural system life cycle performance, the integrity management, the structural risks and the SHM information.

The paper focusses on the influence of the resistance and the deterioration correlation on value of SHM for a fatigue deteriorating system with the SHM strategy load monitoring. The value of SHM for load monitoring is quantified with a generic structural system formulation utilizing ductile and brittle Daniels system formulations, with the decisions rule reliability based inspection and repair planning and the adaptive actions inspection and repair. The structural system performance is modeled by a yearly discrete structural resistance reduction due to fatigue deterioration.

The value of SHM increases for ductile systems and decreases for brittle systems with increasing resistance correlation caused by the dominance of system risks, the ductile and brittle system characteristics and the approximately constant uncertainty reduction due to load monitoring. A similar behaviour can be observed for the deterioration state correlation given the deterioration is relevant for the system reliability.

Contact information

Sebastian Thöns
Associate Professor of Engineering Decision Analysis
Technical University of Denmark, Department of Civil Engineering
Brovej, Building 118, Room 124
DK-2800 Kgs. Lyngby, Denmark
Phone: +45 4525 1714
Email: sebt@byg.dtu.dk

References

Au, S.-K. and J. L. Beck (2001). Estimation of small failure probabilities in high dimensions by subset simulation. Probabilistic Engineering Mechanics 16(4): 263-277.

Baker, J. W., M. Schubert and M. H. Faber (2008). On the assessment of robustness. Structural Safety 30(3): 253-267.

BS 7910 (2005). Guide to methods for assessing the acceptability of flaws in metallic structures. BSI. UK.

Faber, M. H., S. Engelund, J. D. Sørensen and A. Bloch (2000). Simplified and Generic Risk Based Inspection Planning. Proceedings OMAE2000, 19th Conference on Offshore Mechanics and Arctic Engineering, New Orleans, Louisiana, USA.

Folsø, R., S. Otto and G. Parmentier (2002). Reliability-based calibration of fatigue design guidelines for ship structures. Marine Structures 15(6): 627-651.

Gollwitzer, S. and R. Rackwitz (1990). On the Reliability of Daniels Systems. Structural Safety 7: 229-243.

JCSS (2006). Probabilistic Model Code, JCSS Joint Committee on Structural Safety.

Moan, T. (1994). Reliability and risk analysis for design and operations planning of offshore structures. Structural Safefy & Reliability, Rotterdam.

Moan, T. and R. Song (2000). Implications of Inspection Updating on System Fatigue Reliability of Offshore Structures. Journal of Offshore Mechanics and Arctic Engineering 122(3): 173-180.

Schneider, R., S. Thöns, W. Rücker and D. Straub (2013). Effect of different inspection strategies on the reliability of Daniels systems subjected to fatigue. 11th International Conference on Structural Safety & Reliability (ICOSSAR 2013). New York, USA.

Straub, D. (2004). Generic Approaches to Risk Based Inspection Planning for Steel Structures. PhD. thesis. Chair of Risk and Safety, Institute of Structural Engineering. ETH Zürich.

Straub, D. and I. Papaioannou (2014). Bayesian Updating with Structural Reliability Methods. Journal of Engineering Mechanics 141(3): 04014134.

Thöns, S. (2011). Monitoring Based Condition Assessment of Offshore Wind Turbine Structures. PhD thesis. Chair of Risk and Safety, Institute of Structural Engineering. ETH Zurich.

Thöns, S., M. H. Faber and W. Rücker (2014). Optimal Design of Monitoring Systems for Risk Reduction and Operation Benefits. SRESA's International Journal of Life Cycle Reliablity and Safety Engineering 3(1): 1-10.

Thöns, S., R. Schneider and M. H. Faber (2015). Quantification of the Value of Structural Health Monitoring Information for Fatigue Deteriorating Structural Systems. 12th International Conference on Applications of Statistics and Probability in Civil Engineering (ICASP12), . Vancouver, Canada.

Frameworks for structural reliability assessment and risk management incorporating structural health monitoring data

Piotr Omenzetter, The LRF Centre for Safety and Reliability Engineering, The University of Aberdeen, UK

Objectives, abstract and conclusions

This paper explores the challenges, opportunities, benefits, and limitations of reliability assessment of major and critical components of infrastructure using structural health monitoring (SHM) data. The focus is on bridges but the discussion is intentionally kept at a general level so that it is applicable to a wide range of infrastructural systems. This paper argues that holistic and strategic approaches are required to pave the way to the realization of the latent befits of SHM and maximising the value of information derived from SHM data. Firstly, it discusses these benefits and situations were implementing SHM can be considered to be potentially most useful. It later discusses two frameworks for seeing the SHM technologies in a broader context of asset management decision making. The first framework is underpinned by prioritisation of structures for monitoring, moves to guidelines for instrumentation and SHM data analysis, and ends with the integration of SHM results into asset management and disaster emergency plans and decisions. The second framework understands SHM as a starting point in a value chain of enabling technologies delivering information to infrastructure stakeholders. A separate section is devoted to deliberations on the emerging and important way of thinking of SHM outputs as 'big data' and associated challenges. One of the opportunities brought about by abundant SHM dig data is the prospect of creating better 'digital twins' – a high fidelity, multi-physics, multi-scale models of structural systems underpinned by and calibrated using SHM data to assess and forecast reliability.

Finally, an example of a recently constructed 12-span, 690 m long post-tensioned concrete viaduct equipped with a continuously operating SHM system comprising around 90 channels of strain, temperature, displacement and environmental data, and also subjected to one-off ambient dynamic testing campaigns is presented. The proposed framework for structural reliability assessment of the bridge integrates information on the mechanical properties of construction materials obtained via laboratory and in situ tests, the heterogeneous SHM and dynamic testing data from the full scale structure, and predictions from numerical models of the bridge. Several aspects of this information fusion will be discussed. Dynamic tests and static responses, including time dependent creep and shrinkage behaviour, enable system identification of the structure and creation, via model updating, of numerical (finite element) structural models, or 'digital twins', of the physical structure. These models can in turn be used for assessing quantitatively the bridge time dependent condition, health, safety and performance via more realistic numerical reliability evaluations. The collected temperature and strain and displacement data form the basis for generating realistic spatial and temporal load fields for reliability assessment utilizing calibrated numerical models of the structure. The monitoring of responses to traffic loads enables formulation of the dynamic live load demands actually acting on the bridge and response to these.

1   Introduction

The need to protect and maintain assets and their functionality and reliability has been growing quickly with the increasing number of infrastructures and their aging and associated risk of impaired condition and performance. This trend is apparent across any major sector of infrastructure, including energy, transport, housing, industrial and office buildings, to name just a few. Owners and operators are under intensifying pressure to manage their assets at tighter economic margins, while having to comply with increasing demands and often also legal obligations to ensure the needs of communities, economy, and the environmental sustainability are adequately met. Structural health monitoring (SHM) is a technology that, if used strategically and purposefully, can help to address these challenges. SHM can be defined as collecting data on full-

scale, in-situ structures and interpreting them using engineering knowledge so that structural condition and reliability can be quantified objectively (Aktan et al. 2002). While this paper focuses on SHM of bridges, it uses them as a convenient example of components of a complex (transportation) system, which themselves are intricate man-made systems, to present more general observations and discussions that will be applicable to a wider range of infrastructures.

Bridges are critical and expensive components within the transportation network providing essential services and interconnections within the various road networks that underpin the life of communities and their economic activities. However, bridges are subject to various natural hazards, e.g. earthquakes, floods and strong winds, long-term deterioration processes, such as corrosion, material creep and shrinkage and fatigue, and harmful anthropogenic effects, e.g. overloading from vehicles and collision impacts. Complex topography and constraints of built environment often produce transportation networks with limited or no redundancy and failure of a small number of bridges may have significant negative consequences when roads may be closed or their use restricted due to safety or performance concerns, and may only be re-opened for use once site investigations and necessary maintenance have been carried out. Due to the large number of bridges within any network and limited resources for inspections, this may lead to traffic delays and congestion. Furthermore, adequate functionality of the critical links within the transportation network is necessary immediately in the aftermath of an event such as earthquake to ensure access to such services as hospitals, evacuations centres and airports, and operation of search and rescue, fire and emergency services etc. To exacerbate the challenges brought about by usually limited resources, judging the soundness of a bridge is difficult because of the subjective and qualitative nature of visual inspections (Phares et al. 2007).

Research into strategies, tools and technologies that can assist in the assessment of bridge damage, condition and performance and overcome, or at least lessen, the aforementioned problems is urgently required. SHM systems can collect real time data and, with appropriate and careful data interpretation, provide information about the condition and performance of bridges. This will provide asset managers and emergency response centres with valuable information to assist decision making. While it is not expected, or necessary, or practical to completely replace visual inspections by monitoring systems, the latter can be a useful component in the whole spectrum of assessment methods. However, to achieve the maximum benefit from monitoring systems they need to be implemented in a strategic, planned and targeted way, and integrated well into the entire asset management plans and practices.

This paper advocates for such holistic and strategic ways of addressing the need to pave the way to the realization of befits of SHM. Firstly, it discusses these benefits and situations where implementing bridge SHM is likely to be most useful. It later discusses two frameworks for seeing the SHM technologies in a broader context of asset management and emergency response decision making. The first framework starts with prioritisation of structures for monitoring, moves to guidelines for instrumentation and SHM data analysis, and ends with the integration of SHM results into asset management and disaster emergency plans and decisions. Examples of prioritisation methodologies are given. The second framework posits SHM as an initial link in a value chain of enabling technologies delivering benefits to infrastructure stakeholders. These discussions are then followed by deliberations on the emerging, but increasingly important in future, theme of thinking of monitoring outputs as 'big data' and associated challenges. Finally, an example of a recently constructed 12-span, 690 m long post-tensioned concrete viaduct equipped with a continuously operating SHM system is discussed to share some practical insights into the challenges, opportunities, benefits, and limitations of reliability assessment of major and critical components of infrastructure using SHM. A summary and conclusions round up the paper.

2   Benefits of monitoring systems

Because traditional visual inspections with simple testing can be expensive and time consuming, are qualitative, subjective, and only capable of assessing conspicuous problems (Phares et al. 2007), it is desirable to supplement them with monitoring. Monitoring is often recommended in the following situations (Inaudi and Walder 2011):

- New structures with innovative design, construction techniques, or materials.
- New structures with poorly understood risks, including geological, seismic, meteorological, environment, construction, and quality risks.
- New or existing structures which are representative of a larger population, where information derived from monitoring can be extrapolated to the wider population.
- New or existing structures that are critical at a network/system level, such that their failure or deficiency would have a serious impact on the network functioning.
- Existing structures with known deficiencies, problems and/or very low rating.
- Candidate structures for replacement or refurbishment, where the real need for interventions can be assessed a priori and repair efficiency evaluated a posteriori.

Planned and proactive implementation of SHM already at the construction stage is gaining momentum in newly constructed innovative, landmark and/or record breaking structures (Abdelrazaq 2011), but it often remains 'blue sky' research driven by academic curiosity. The above list of SHM applications also envisages widespread monitoring of numerous existing structures better risk management. Despite existing examples of such SHM applications (Tozser et al. 2011), such projects tend to be undertaken in an ad hoc manner in reaction to identified problems, rather than being proactively planned and integrated into the overall asset management or disaster/emergency response, and their benefits may not always be immediately apparent.

Potential general benefits of using SHM can be summarised as follows (Abdelrazaq 2011):
- Reducing uncertainty about structural condition and performance.
- Discovering hidden structural reserves.
- Discovering deficiencies that may be missed by traditional assessment techniques.
- Increasing safety and reliability.
- Ensuring long term quality of aging infrastructure.
- Allowing better informed asset management.
- Increasing knowledge about in-situ structural performance.

This list of the potential benefits of SHM makes monitoring very useful for organisations responsible for efficient, undisturbed functioning of transportation networks, as the benefits address their key needs and challenges of developing advanced knowledge about bridge condition and performance via gathering reliable data for ensuring that bridges can keep performing to the expected level. Monitoring systems can collect data in real time and can help detect damage to the structure, which can be in the form of changes to the material and/or geometric properties of the system. They can aid both long term asset management and rapid decision making immediately after a natural disaster such as an earthquake or flood.

In spite of the promise for better asset management, SHM has only made limited transition from academic research into practical applications. In order to achieve a more widespread, planned and proactive integration of monitoring into practice and realise its potential benefits it is necessary to establish a sound philosophy guiding the practical implementation of monitoring systems to bridges and tools for quantifying the value of data gathered by SHM and the information derived from it. By doing so, monitoring systems can be strategically deployed where they can make the most positive difference in enhancing the asset management processes and helping to address its current limitations in a cost effective way. SHM systems will only become attractive for the practitioners if they are convinced by evidence from past applications or realistic assessment of the expected benefits from new deployments that SHM can contribute to their 'bottom line'. In-situ applications of SHM carry, often significant, cost and it is necessary to understand better the benefits they can bring about. It is thus necessary to quantify the value of information derived from SHM data and offset it against the costs of SHM hardware, software, installation, maintenance and data analysis (Straub 2014). In any SHM deployment project, it is also very important to have a clear understanding of how the SHM data will be used and linked to the assessment of condition and performance and beyond that to long term asset management or emergency response decisions. This will enable better-informed, realistic discussions to be had, and decisions to be made, about whether to use SHM in particular cases. It can also alleviate potential problems resulting from

unrealistic expectations of what SHM can deliver and backlash when those are not met (Moon et al. 2010).

3 Risk-based prioritisation of bridges for data collection and use of SHM

This section discusses a philosophy for integration of SHM into wider data collection and asset management based on considering the risk that failures of individual bridges present to the functioning of the entire transportation system. A natural consequence is a risk-based prioritisation of bridges for implementation of monitoring systems. A comprehensive vision of strategies for bridge SHM for damage, condition and performance assessment is necessary if SHM is to fulfil its potential. To realise such a vision, the following building blocks are required (Omenzetter et al. 2014):

- Methodologies for prioritisation of bridges for application of sensing technologies based on bridge importance in the network and a broad spectrum of risks affecting the bridge that need to be treated with an interdisciplinary approach.
- Guidelines for instrumentation to be installed on bridge structures and in their vicinity (e.g. surrounding soil or watercourse), or even monitoring entire transportation networks and hydrological systems, for measuring operational and environmental effects, loads and demands and responses. The focus should be on affordable hardware platforms and relatively simple measurements which can help in structural assessment, but there is need to better quantify statistically the methods' performance, e.g. minimum damage size detectability.
- Methodologies for reliable condition, damage and performance assessment based on information extracted from data collected by instrumentation for structural elements, foundation and soil.
- Developing guidelines for integration of monitoring and quick assessment results into the asset management and, where necessary, emergency planning and response practices of organisations responsible for functionality of transportation networks.

Items 2 and 3 in the above list, while very important, are more concerned with specialised areas of expertise for SHM, such as sensing and data processing. Furthermore, it was decided to not focus in this paper on item 4 either. The reminder of the section will thus be devoted to the challenge of bridge prioritisation for SHM taking examples from the author and his collaborators' previous work. The need for such prioritisation comes from the fact that, due to the cost of monitoring, it is realistic, and indeed highly advisable, to instrument only selected bridges on a network. Furthermore detailed and (near) real-time information on the condition is not required for all bridges but only for those whose failure is more likely to result in larger consequences to network functioning. Considering risk of each bridge at a network level provides a rational basis for bridge selection for SHM.

A strategy for bridge data collection and implementation of SHM for this end was proposed and elaborated in Bush et al. (2013), where interested readers will find the details. (The strategy was further specified for SHM of bridges in a region affected by earthquake disaster in Omenzetter et al. (2014).) Below a short synopsis only is provided to highlight the most important aspects. All the bridges in a given network are assigned to one of three categories of data collection: core, intermediate and advanced. This classification is based on considering both the risk profile and criticality of each structure in the network and a simple scoring scheme was proposed. Risk is understood in the usual manner as failure probability multiplied by its envisaged consequences. For each bridge, risks related to four broadly defined performance criteria, namely structural safety, hydraulic/geotechnical safety, serviceability, durability and maintenance, and functionality are assessed adapting the framework proposed by Moon et al. (2009). Bridge criticality is measured by the wider consequences or impacts on the network functionality and regional economy resulting from a failure. By separately reporting on criticality, it ensures that the bridge asset manager takes into account those bridges that have a significant impact on network functionality, but because of their low probability might not have the same recognition if only a risk based approach were used.

A simple illustration of the resulting risk and criticality based bridge classification is shown in Figure 1. Bridges #1-4 are real structures sourced from New Zealand stock which have been 'anonymised' to only keep the relevant high-level detail. Bridge #1 scores highly on both risk and criticality, Bridge #3 has both intermediate scores, and finally Bridge #4 presents only low risk and criticality, respectively. Based on this assessment, the three bridges were assigned to the appropriate core, intermediate and advanced data collection category. Bridge #2 is a structure with only intermediate risk, however, its strategic importance in the transportation network dictates its high criticality and so advanced data collection is recommended. The presence of structures like Bridge #2 highlights the need and advantage of considering both risk and criticality to decide the appropriate regime of data collection.
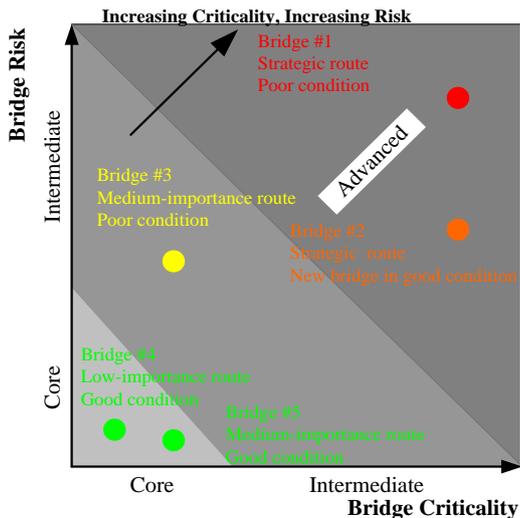
Figure 1: Risk and criticality based bridge classification for data collection and SHM implementation.

Table 1 outlines the approaches to data collection in each regime including the types of techniques and collection frequency. The core asset management process requires sufficient data to have a basic understanding of the asset and to manage, through prioritization, performance related risks. More information about the types of data required at each level of data collection is provided in Bush et al. (2011) and Omenzetter et al. (2015) and herein only general data categories are listed. For core bridges, data will be collected for key performance criteria, including basic traffic data, load carrying capability, bridge condition and defects, and, if required, scour or seismic susceptibility. Past work history data will also be stored, thereby allowing basic cost estimates to take place. For core bridges data quality can be lower and visual inspection will be the predominant form of data collection, with non-destructive evaluation (NDE) and SHM used sparingly and mostly reactively to understand identified performance weaknesses. Further, as the bridges are in good condition visual inspection can occur between 3 to 6 years allowing reallocation of resources to those assets with increased risks and criticality ratings.

Intermediate bridges will have an increased risk or criticality profile because they are subjected to increased levels of hazards, are in a poorer condition, operating close to performance capabilities or will have an increased impact on the functionality of the network if their performance is lost or reduced. To effectively carry out asset management of such structures, an improved level of information will be required, and therefore a broader range of data collected. Data resolution will also have to be at the bridge element level if an adequate risk assessment is to be achieved. Data will be collected for the full range of performance criteria including load carrying capability, bridge condition and defects, overhead strikes, overweight management data, barrier capacities, weigh in motion data, traffic data, scour data, seismic data and safety data, e.g., number of traffic accidents. To manage the increased risk and criticality, the visual inspection program will follow a 2 to 3 year

cycle, and NDE and SHM will have a greater level of integration into the data collection process. To improve decisions, NDE and SHM will be used to both carry out testing on bridge specific defects and undertaken for a number of typical bridges in the entire stock to improve the understanding of aspects such as deterioration models for a wider population of structures. Further, automatic data collection systems will also be used to collect network level data such as scour, hydrostatic and hydrodynamic, and vehicle loading.

It is envisaged that advanced data collection regime will be applied only to a limited number of structures that have the highest risk or criticality profile as they are central to the operation of the network. The advanced data collection regime is extended such that a component level understanding of the bridge performance and condition is developed. These bridges require very well defined reliability based performance assessments. It is considered that extensive and proactive use of NDE and SHM is required to achieve this level of data quality and is therefore highly recommended for the management of advanced bridges. SHM will be used either periodically to regularly update bridge risk status, or even continuously especially towards the end of the structure's useful life. These bridges will also have visual inspections on a 1 to 2 year cycle to be able to quickly identify problems as they develop. The high level of accuracy attained using NDE, SHM and the frequent visual inspections, linked with data collected at component level, will facilitate the development of high resolution long-term management plans, and will allow asset managers to more accurately understand the performance capabilities of their high risk and most critical infrastructure.

By providing the level of flexibility in data collection regime, the bridge asset manager can tailor the strategy to suit local network requirements, risk tolerance and budget, thereby ensuring cost efficiency of strategy implementation.

Table 1: Outline of risk and criticality based bridge data collection and monitoring strategy.

Data collection regime	Bridge risk and/or criticality band	Risk assessment resolution and reporting	Data collection techniques and frequency
Core	Low	Overall bridge performance risk and criticality	Visual inspections every 3-6 years Limited, usually reactive NDE and SHM
Intermediate	Intermediate	Individual element performance risk and criticality	Visual inspections every 2-3 years Some, reactive and proactive NDE and SHM
Advanced	High	Individual component performance risk and criticality	Visual inspections every 1-2 years Extensive, mostly proactive NDE and SHM

4   SHM in a value chain to deliver safe and reliable infrastructure at acceptable cost

To make a difference in the way bridge assets are managed, SHM needs to be put in a context of expectations and responsibilities of bridge owners, stewards and users so that its benefits can be critically examined and clearly articulated. A useful conceptual framework for seeing SHM this way was put forward by Wong and Yao (2001). They proposed understanding SHM as part of a *value chain*. Value chain is an end-to-end technological solution to a problem, comprising a series of so-called enabling technologies, and the user or beneficiary at the end of the chain. The value chain is shown in Figure 2. SHM, comprising data collection using sensing platforms, signal processing with various algorithms, and data analysis using damage detection and statistical tools, forms the beginning of the value chain. On its own, SHM presents only a latent potential. This potential can only be materialised if other enabling technologies are integrated into the value chain to link the SHM outputs to the stakeholders' objectives to generate value for them. These coupling technologies are reliability, safety and risk assessment methods and risk management decision making tools. It is within the decision making area where the value of information from SHM needs to be calculated to present quantitative options to the asset manager.

Seeing SHM as part the value chain enables a holistic view of its role and helps to appreciate other, often governing, aspects of the broad context SHM is used in. These aspects include risk management and financial considerations. While SHM researchers are often devoted to the SHM parts of the value chain (the boxes on the left hand side of Figure 2), in reality the top-down approach, driven by stakeholders needs will ultimately decide the fate of research achievements in the real world. Another important realisation from depicting the value chain is that the ultimate success of SHM technologies depends on unobstructed flow of data and information from left to right. This flow will only ever be as effective as the 'weakest link' as the value chain is clearly a serial system. Any future research efforts must thus be directed into the areas that represent the most severe bottle necks to create a balanced value chain. From that point of view, there is clear need to cross the gap between SHM and reliability, safety and risk assessment methods (indicated symbolically by the vertical dashed line in Figure 2) that should use SHM data more, so that they can underpin risk management decision making based on the observed deterioration symptoms (Cempel et al. 2000).
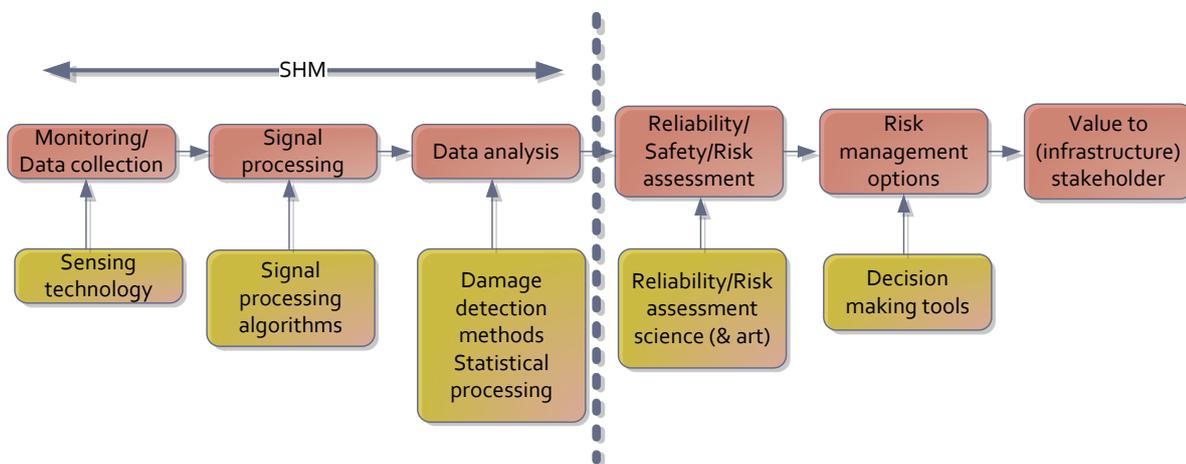
Figure 2: SHM as part of a value chain of enabling technologies delivering benefits to stakeholders.

5 'Big data' perspective on SHM

SHM researchers and practitioners have long realised that even modest monitoring systems can easily generate the types and volumes of data that are a challenge to handle and interrogate using traditional data analysis techniques. The term 'big data', that has recently been gaining increasing interest far beyond engineering context, captures the outputs from SHM systems well: big data is characterised by extraordinary volume, velocity, variety and/or veracity (Lloyd's Register Foundation 2014).

Modern large bridge structures can be monitored with the number of sensing channels of the order of 10^3 (Ni and Wong 2012). Knobbe et al. (2011) estimate that 145 sensors measuring at 100 Hz produce around 56 kB of data per second, or 5 GB per day, or over 1.7 TB per annum if represented in an efficient way. A video camera produces around 46 kB/s of compressed video data in a typical traffic monitoring situation. As can be seen from these estimates the transfer of data, their storage, and more importantly our ability to interrogate it in a timely and efficient way can quickly put pressure on the existing resources, capabilities and analytical techniques (Materazzo et al. 2015). Decisions must be made how much data should be collected and how much local vs. centralised data processing conducted.

An alternative to monitoring numerous structures which is worth exploring is to use specially selected 'indicator structures', representative of the wider stock that can be heavily instrumented. The condition of these structures can then be assessed locally and extrapolated to similar structures. For example, the Indicator Building procedure was formalized, albeit based on visual inspections after the devastating 2010 and 2011 Canterbury earthquakes in New Zealand (New Zealand Society for Earthquake Engineering 2011). The procedure entailed identifying a set

of buildings to specifically check following the main and significant aftershocks to gauge the extent of damage. Doing so helped with decision making whether to continue with the building assessment programme as planned, modify it or re-start. This proved invaluable for efficient use of limited inspection resources for re-assessing repeatedly a large building stock. However, this approach will suit some industries better than other sectors, notably civil structures are unique and extrapolating monitoring results will be especially challenging.

Another challenging aspect of SHM data is its unusual variety. A comprehensive bridge SHM system will have accelerometers, static and dynamic strain gauges, displacement sensors, inclinometers, weight-in-motion stations, global positioning system, anemometers, structural and ambient temperature sensors, barometers, and humidity sensors, corrosions cells and video cameras (Ni and Wong 2012). The variety of sensors will help to form a holistic view of bridge performance and condition, but the data will be sampled at different intervals, will relate to different actions and demands imposed on the structure and its responses to those demands, and will have different accuracy. The data sets may come from diverse technologies, e.g. legacy SHM systems installed during construction and new upgraded sensing platforms. Some data may be missing due to sensor or monitoring system malfunctioning or power supply problems, and accuracy may be dubious when sensors are misaligned or malfunctioning. Latent factors, e.g. influence of temperature (Sohn et al. 1999) or response magnitude (Chen et al. 2014), may not be directly measured but can influence the measurands considerably complicating extracting robust information from the data.

Further, SHM is only one source of data and information about the structure and its condition and performance. Visual inspections, based largely on inspector's judgement and experience (Phares et al. 2001), will likely remain the main source of knowledge for asset managers. Results of various tests on material samples taken during construction or in-service period are another source of structure specific data. Furthermore, very important bridge data is often stored in the form of drawings or descriptive and qualitative reports, rather than numbers. Thus, it becomes necessary to merge such diverse data sets and formats for enhanced understanding of assets to form the basis of management decisions. Various big data analytics algorithms, statistical techniques and machine learning for pattern recognition must be integrated with the human skills for deep insight to unveil meaning in the data.

Any interpretation of SHM data is immensely assisted by creating physics-based numerical models of the system being studied and assessed. The concept of 'digital twin' (Glaessgen and Stargel 2012) can come to fruition thanks to abundance of data. The digital twin will integrate high fidelity multi-physics and multi-scale simulations, such as from finite or boundary element models, with SHM data, maintenance history and all available historical data to mirror the life of its physical twin. The digital twin will be much more realistic than contemporary models, and will, e.g., include information on individual defects and loading and distress histories unveiled in extensive SHM data. This will enable achieving new and enhanced levels of safety and reliability without overdesigning infrastructure. The digital twin will continuously forecast and update the health and condition of the physical system, its reliability and the remaining useful life.

6   Example of SHM of a major bridge

Most existing systems are complex, their precise conditions may not be known completely, and direct measurements by nonintrusive means are difficult. Hence their conditions can only be inferred from response measurements under the actual loading, operational and environmental conditions. In addition, the future loads and environmental conditions cannot be predicted accurately. In this section, a comprehensive framework for systematic integration of SHM data into reliability assessment of a major bridge is discussed (Chen and Omenzetter 2013). The models for materials, structures, loads and other actions, and responses, calibrated and refined using the various types of monitoring data are used in structural reliability simulations, yielding more realistic results. The outline of the section is as follows. The proposed general framework for integration of SHM data into reliability assessment is first described. Then the case study bridge, the Newmarket Viaduct, is introduced. This part also provides a description of the bridge monitoring system, initial

numerical model and an overview of available data and results of dynamic testing and laboratory investigations on material properties. Based on these data, in the third section the framework for integration of testing results and SHM data into reliability assessment is described together with its constituent parts including probabilistic models for materials, structure, loads and other actions, and their effects. It is important to recognize that structural reliability assessment involves practically invariably forecasting and extrapolating the measured actions and responses, because the return periods are high and enough measured data are rarely, if ever, available, and so robust models must be formulated and calibrated using data that is available.

6.1   General framework for integration of SHM data into bridge reliability assessment

Figure 3 shows the framework for reliability assessment of an in-service bridge that can use various types of data, such as from long-term, continuous monitoring, one-off or periodic testing and monitoring, and laboratory tests. Also, finite element analysis and updating is included, which provide tools for building the digital twin of the bridge. For a given bridge structure, to perform its advanced reliability assessment, an initial finite element model, constructed using design drawings and specifications, is required. The various types of SHM data are used to calibrate, or update, the initial finite element model, or set of models as the case may be. Then based on the monitoring data and the updated model, the load effects of the various structural components can be assessed via numerical simulations. Furthermore, the load effects for structural components with sensors can be directly statistically evaluated using the monitoring data. Structural resistance models can be calibrated using material data. Bayesian updating framework will be used for incorporating information from SHM into analytical models. Finally, reliability assessment of main components or the bridge at any time will be conducted, which will aid the bridge maintenance decision-making process. This framework is further explained later using the case study.
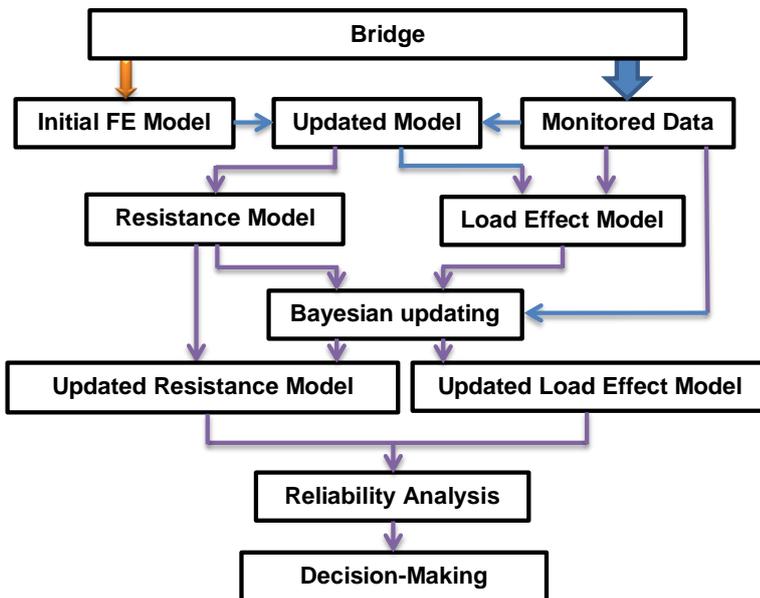
Figure 3: Framework for structural reliability assessment using SHM data (Chen and Omenzetter 2013).

6.2   The Newmarket Viaduct and its SHM

This sub-section provides a description the case study instrumented bridge, the Newmarket Viaduct, and the SHM programme implemented to assess its performance. While the general framework for SHM-assisted reliability assessment presented above is applicable to different types of loads, structures and limit states, the need for real-life data requires specifying the proposed framework further in that respect.

The Newmarket Viaduct, completed in 2012 in Auckland, New Zealand, is a major and most important bridge within the New Zealand road network. The structure comprises parallel, twin, horizontally and vertically curved, pre-cast, post-tensioned, box-cell girder concrete bridges joined at the deck level with an in-situ cast 'stitch'. The total length of the bridge is 690 m, with twelve different spans ranging in length between 38.67 m and 62.65 m, and an average length of approximately 60 m. Two views of the bridge, during construction and when completed, respectively, are shown in Figure 4.

a) b)

Figure 4: Newmarket Viaduct: a) during construction, and b) completed structure.

The SHM system is designed to continuously collect the following measurements:
- Strains and deflections in selected critical sections and spans.
- Accelerations of key sections.
- Environment data (temperature and humidity) and structural temperature.

Moreover, one-off in situ dynamic tests and laboratory material tests have been conducted to provide additional data.

The long term SHM system installed in the Newmarket Viaduct comprises 20 vibrating wire strain gauges that also measure temperature, 42 embedded temperature sensors, four baseline systems measuring deflections, and two external temperature and humidity sensors, one inside and another outwith the girder. Four strain gauges are embedded in concrete in each of the five cross-sections where sagging or hogging moments have the largest values, i.e. in the middle of two spans, close to their common pier and at both ends of the two spans. The 42 temperature sensors are located in the middle of a span and are spread evenly in both webs along their height; additional sensors are installed across the webs and in the top and bottom slab. In two spans, baseline systems (Stanton et al. 2003, Omenzetter and Ibrahim 2010) for measuring deflections are also installed. Data from all these sensors is sampled at 10 min intervals with the intention to measure static and slowly-varying responses due to creep, shrinkage and temperature variations. Communication with the data logger for data download is via a wireless modem over a cellular telephone network. Installation of six uniaxial accelerometers is planned to complement the aforementioned data with dynamic responses in the vertical and horizontal directions due to traffic.

6.3   Integration of the Newmarket SHM and testing data into reliability assessment

The integration of the various types of testing and monitoring data is schematically shown in Figure 5 and described below.

Figure 5: Integration of testing and monitoring data into reliability assessment.

In order to model the bridge and individual components to perform reliability studies, it is necessary to measure a number of mechanical properties of concrete. Twenty concrete 100×200 mm cylinders specimens were secured during construction. Six of these were used for measuring the compressive strength and elastic modulus but own results were supplemented by the analogous tests conducted by the contractor. Six concrete cylinders were made to evaluate shrinkage behaviour and additional four cylinders for a creep study under a constant load level of 40% of the ultimate compressive strength. Bayesian updating can be used to refine the estimates of the probability density functions for material properties, such as strength, Young's modulus, and creep and shrinkage coefficients, to be later used in numerical simulations of the digital twin of the bridge.

The measurements of the structural temperature at several points in the bridge (Omenzetter et al. 2012) will enable creating a stochastic field model for temperature loads with experimentally established properties, such as spatial and temporal correlations. Further, experimentally observed correlations between the temperature load and strains developing in the bridge will enable creating and calibrating both data driven and physics-based finite element digital twins for the simulations of reliability under the environmental demand. The availability of long term strain data, showing creep, shrinkage and possibly other long term deformations due to aging, will facilitate modelling and forecasting time dependent reliability. Likewise, dynamic response monitoring will enable creating stochastic models for the corresponding responses and, via solving inverse problems, the identification of the load models themselves.

An important step in the creation of the digital twin was a comprehensive ambient vibration testing and operational model analysis program (Chen et al. 2014). The second phase of the testing reported here was conducted on both twin bridges after casting of the 'stitch'. In order to identify as many modes of vibration as possible, including transverse, vertical and torsional, and map accurately mode shapes, acceleration measurements were taken at 288 points using several setups of roving sensors. Enhanced frequency domain decomposition (EFDD) and data driven stochastic subspace identification (SSI-DATA) methods allowed the identification of 9 transverse, 14 vertical and 12 torsional modes below 8 Hz.

The identified natural frequencies and mode shapes were compared with their numerical counterparts obtained from a finite element model constituting its digital twin for dynamic behaviour. The complexity of the viaduct and its geometry and the need for high-fidelity simulations necessitated the construction of a 3D model. Special attention was paid to the reproduction of the geometry, particularly the correct definition of the curvatures and variable cross sections, and the modelling of supports. The deck and the piers were represented in SAP2000 (Computers and Strictures 2009) using 3D eight node solid brick elements. Average size of finite elements adopted is of the order 0.80×1.00 m. The monolithic pier-girder connections were assumed to provide full restraint for all six translations and rotations, whereas pinned bearings to only restrict three translations. Sliding bearings were assumed to only allow translation in the longitudinal direction and rotation associated with vertical bending as their design prevented the other types of motions. Fixed boundary conditions were specified at the base of the piers, ignoring soil-structure interaction effects on the dynamics of the bridge system, which was not expected to be appreciable at the low levels of excitation and response encountered in the field under traffic loading.

The experimental and computed natural frequencies corresponding to the lowest five transverse, vertical and torsional modes are presented in Table 2. It can be seen that the identified frequencies and mode shapes (assessed using the modal assurance criterion (MAC) (Allemang (2003)) generally agree well with the numerical results. The vertical mode experimental frequencies and numerical natural frequencies are in very good agreement with all differences not exceeding 3.1%. The transverse natural frequencies differ by only up to 4.9% and the torsional natural frequencies agree to within 4.5%. The MAC values calculated between the numerical and experimental results typically exceed 0.80 and show that for most vibration modes, there is good to excellent agreement between the experimentally identified and numerical mode shapes. Damping ratios have also been identified and show values which are in line with those reported in the literature for similar class of structures. Nevertheless, full-scale testing and monitoring are required to confirm damping values as they cannot be derived from first principles. The lower MAC values obtained for a few modes are likely caused by system identification errors due to the low relative contributions of these modes to the measured bridge vibration and inaccuracies in the numerical model. The comparison constitutes a validation of the developed numerical model which has been proved to represent the bridge dynamics well, however, there is still scope for improvement via systematic model updating.

Table 2: Comparison of experimental and numerical natural frequencies, damping ratios and mode shapes (MACs).

Mode	Natural frequencies [Hz]			Damping ratios [%]	MAC with EFDD		
	EFDD	SSI	Numerical	SSI	SSI	Numerical	
Transverse modes							
T1	1.25	1.25	1.30	1.3	0.98	0.96	
T2	1.56	1.55	1.60	1.5	0.92	0.83	
T3	2.15	2.17	2.14	1.4	0.89	0.75	
T4	2.81	2.80	2.95	1.3	0.98	0.62	Table continues on next page
T5	3.94	3.91	3.87	1.1	0.98	0.69	
Vertical modes							
V1	2.03	2.04	2.10	1.4	1.00	0.96	

V2	2.15	2.15	2.19	1.4	0.95	0.97
V3	2.34	2.35	2.40	1.4	1.00	0.88
V4	2.55	2.55	2.61	1.5	0.96	0.85
V5	2.82	2.82	2.85	1.5	0.92	0.91
Torsional modes						
Tor1	3.17	3.14	3.16	1.5	0.90	0.86
Tor2	3.20	3.20	3.22	1.5	1.00	0.83
Tor3	3.34	3.33	3.37	1.5	0.84	0.90
Tor4	3.55	3.52	3.54	2.5	0.94	0.87
Tor5	3.71	3.74	3.69	1.6	0.88	0.69

Contact information

Dr Piotr Omenzetter
Senior Lecturer
The LRF Centre for Safety and Reliability Engineering
School of Engineering
The University of Aberdeen
Aberdeen AB24 3UE
UK
Phone: 44 1224 272529
Email: piotr.omenzetter@abdn.ac.uk

Acknowledgement

References

Abdelrazaq, A. (2011) Validating the Structural Behavior and Response of Burj Khalifa: Synopsis of the Full Scale Structural Health Monitoring Programs. Proceedings of the 1st Middle East Conference on Smart Monitoring, Assessment and Rehabilitation of Civil Structures SMAR 2011: 1-18.

Aktan, A. E., Catbas, F. N., Grimmelsman, K., Pervizpour, M., Curtis, J., Shen, K., Qin. X. and Cinar, O. A. (2002) Health Monitoring for Effective Management of Infrastructure. Proceedings of the 1st European Workshop on Structural Health Monitoring: 1245–1253.

Allemang, R. J. (2003). The Modal Assurance Criterion – Twenty Years of Use and Abuse. Journals of Sound and Vibration 37: 14-23.

Bush, S., Omenzetter, P., Henning, T and McCarten, P. (2013). A Risk and Criticality Based Approach to Bridge Performance Data Collection and Monitoring. Structure and Infrastructure Engineering 9(4): 329-339.

Cempel, C., Natke, H. G. and Yao, J. T. P. (2000). Symptom Reliability and Hazard for Systems Condition Monitoring. Mechanical Systems and Signal Processing 14(3): 495}505.

Chen, G.-W., Beskhyroun, S. and Omenzetter, P. (2014). Amplitude-dependent Modal Properties of an Eleven-span Continuous Concrete Bridge under Forced Vibration Testing. Proceedings of the 4th International Symposium on Life-Cycle Civil Engineering IALCCE2014: 1-7.

Chen, X. and Omenzetter, P. (2013). A Framework for Reliability Assessment of an In-service Bridge Using Structural Health Monitoring Data. Key Engineering Materials 558: 39-51.

Computers and Structures (2009). SAP2000, Structural Analysis Program.

Chen X., Omenzetter, P. and Beskhyroun (2014). Ambient Vibration Testing and Operational Modal Analysis of a Curved Multiple-span Viaduct: a Comparison of Four Modal Identification Techniques. Mechanical Systems and Signal Processing (in review).

Glaessgen, E. H. and Stargel, D. S. (2012). The Digital Twin Paradigm for Future NASA and U.S. Air Force Vehicles. Proceedings of the 53rd Structures, Structural Dynamics, and Materials Conference: 1-14.

Inaudi, D. and Walder, R. (2011) Integrated Structural Health Monitoring Systems for High-Rise Buildings. Proceedings of the 1st Middle East Conference on Smart Monitoring, Assessment and Rehabilitation of Civil Structures SMAR 2011: 1-8.

Knobbe, A. , Koopman, A., Kok, J., Obladen, B., Bosma, C. and Koenders, E. (2011). Large Data Stream Processing for Bridge Management Systems. Proceedings of the 1st Middle East Conference on Smart Monitoring, Assessment and Rehabilitation of Civil Structures SMAR 2011: 1-9.

Lloyd's Register Foundation (2014). Foresight Review of Big Data. Towards Data-centric Engineering, Report Series: No. 2014.2.

Materazzo, T., Shahidi, S., Chang, M., and Pakzad, S. (2015). Are Today's SHM Procedures Suitable for Tomorrow's Bigdata. Proceedings of the 33rd International Modal Analysis Conference IMAC XXXIIII, Volume 7 Structural Health Monitoring and Damage Detection: 58-66.

Moon, F. L., Laning, J., Lowdermilk, D. S., Chase, S., Hooks, J. and Aktan, A. E. (2009). A pragmatic, Risk-based Approach to Prioritizing Bridges. Proceedings of SPIE Conference on Nondestructive Characterization for Composite Materials, Aerospace Engineering, Civil Infrastructure, and Homeland Security 2009: 72940M-1 - 11.

Moon, F. L., Frangopol, D. M., Catbas, F. N. and Aktan, A. E. (2010). Infrastructure Decision-Making Based on Structural Identification. The 2010 ASCE Structures Congress.

New Zealand Society for Earthquake Engineering (2011). Building Safety Evaluation Following the Canterbury Earthquakes. Report to the Royal Commission of Inquiry into Building Failure Caused by the Canterbury Earthquakes.

Ni, Y. Q. and Wong, K. Y. (2012). Integrating Bridge Structural Health Monitoring and Condition-Based Maintenance Management. Proceedings of the 4th Civil Structural Health Monitoring Workshop: 1-10.

Omenzetter, P., Bush, S. and McCarten, P. (2015). Guidelines for Data Collection and Monitoring for Asset Management of New Zealand Road Bridges. Roading Infrastructure Management Support.

Omenzetter, P., Chua, P., Issa, A. and Sanders, B. (2012). Evaluation of Thermal Gradients and Their Effects in a Bridge Box Girder Using Monitoring Data. Proceedings of the 22nd Australasian Conference on the Mechanics of Structures and Materials: 921-926.

Omenzetter, P. and Ibrahim, N. (2010). Evaluation of Creep and Shrinkage in a Prestressed Bridge Using Data from Laboratory Experiments and In-situ Monitoring. Proceedings of the 21st Australasian Conference on the Mechanics of Structures and Materials: 185-190.

Omenzetter, P., Mangabhai, P., Singh, R. and Orense, R. (2014). Prioritisation Methodology for Application of Bridge Monitoring Systems for Quick Post-earthquake Assessment. Journal of Civil Structural Health Monitoring 4(4): 255-276.

Phares, B. M., Graybeal, B. A., Rolander, D. D., Moore, M. E. and Washer, G. A. (2007) Reliability and Accuracy of Routine Inspection of Highway Bridges. Transportation Research Record 1749: 82–92.

Sohn, H., Dzwonczyk, M., Straser, E.G., Kiremidjian, A. S., Law, K. H. and Meng, T. (1999) An Experimental Study of Temperature Effect on Modal Parameters of the Alamosa Canyon Bridge. Earthquake Engineering and Structural. Dynamic. 28: 879–97.

Stanton, J. F., Eberhard, M. O. and Barr, P. J. (2003) A Weighted-stretched-wire System for Monitoring Deflections. Engineering Structures 25: 347-357.

Straub, D. (2014). Value of Information Analysis with Structural Reliability Methods. Structural Safety 49: 75-85.

Tozser, O., Elliott, J. R. and Garcia, R. (2011) Acoustic Monitoring Used to Manage the Life of Cable Supported Bridges. Proceedings of the 1st Middle East Conference on Smart Monitoring, Assessment and Rehabilitation of Civil Structures SMAR 2011: 1-8.

Wong, F. S. and Yao, J. T. P. (2001) Health Monitoring and Structural Reliability as a Value Chain. Computer Aided Civil and Infrastructure Engineering 16(1): 71-78.

The interpolation method for the detection of localised stiffness losses

M.P. Limongelli, M. Domaneschi, L. Martinelli, M. Dilena, A. Morassi, A. Zambrano, A. Gecchelin

Abstract

In this paper is presented an approach to the detection of localized stiffness losses basing on Operational Deformed Shapes (ODS). The method uses as a damage feature the so called 'Interpolation Error' related to the use of a smooth cubic spline function in interpolating the operational deformed shapes of the structure. A localized reduction of smoothness in the operational deformed shapes detected between two consecutive inspections, points out a localized loss of stiffness. The ODS can be recovered from Frequency Response Functions calculated basing on responses measured at selected locations of the structure in terms of acceleration. In order to avoid false or missing indications of damage related to random variations of the damage feature, their effect should be properly taken into account. To this aim a threshold value of the damage feature is defined in terms of the values chosen for the tolerable probability of false alarm. This allows distinguish variations of the interpolation error due to damage from those due to random sources.
The IDDM has been successfully applied to bridges, multistorey buildings and, in its 2D formulation to plates. In this paper after a brief description of the method some examples of its application to different types of structures are reported.

1   Introduction

Existing methods for damage identification can be divided into those relying on the calibration and updating a finite element model of the structure, and feature-based methods, which perform damage identification checking the possible changes of a damage sensitive parameter. The last do not need a numerical model and rely on a procedure to extract the damage feature from the sole responses to vibrations recorded on the real structure. Due to the scarce human interaction they require, they are attractive for adoption within an automated monitoring system. Both modal parameters and non-modal parameters (e.g. Frequency Response Functions, Operational Deformed Shapes or their derivatives, Interpolation Errors) have been proposed in the literature as damage sensitive feature. The recently proposed Interpolation Damage Detecting method (IDDM) relies on a damage index defined in terms of the operational deformed shapes of the structure. The damage feature is the interpolation error related to the use of a spline function in modeling the operational deformed shapes: statistically significant variations of the interpolation error between two successive inspections of the structure indicate the onset of damage. The significance of the variation is defined in statistical terms on the base of exceedance of a certain threshold value defined in terms of the accepted probability of false alarm. In the following a brief outline of the method is reported together with some applications.

2   The interpolation damage detection method (iddm)

In the Interpolation Damage Detecting method the damage feature is the interpolation error related to the use of a spline function in modeling the Operational Deformed Shapes (ODSs) of the structure: statistically significant variations of the interpolation error between two successive inspections of the structure indicate the onset of damage. Specifically, at a given location of a structure the interpolation accuracy is defined as the difference between the measured ODS and the ODS calculated by interpolating the measured ODSs at all the other locations equipped with a sensor. An increase of the interpolation error in the inspection phase (after a potentially damaging event) with respect to the baseline phase, is an indication of the existence of damage at the location where the change has been recorded. The IDDM has been successfully applied for damage localization of multistory buildings [1], [2], supported bridges [3], [4], models of suspension and cable-stayed bridges [6] and recently extended to the case of two-dimensional structures [7]. Thanks to its formulation based on the detection of reduction stiffness through the detection of

reduction of smoothness in the Operational Deformed Shapes (ODS), the IDDM can be applied to any type of structure provided the ODSs can be estimated accurately in the original and in the damaged configurations and a proper continuous function is used to interpolate the ODS in order to detect possible reductions of smoothness.

2.1 The damage feature for beam-like structures

The basic idea of the IDDM for beam-like structures can be described with reference to Figure 1.
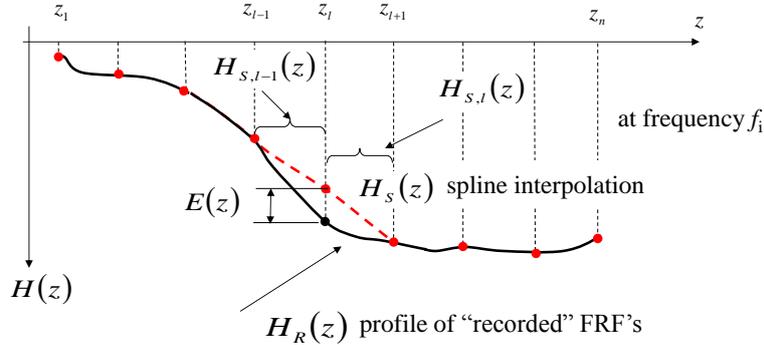
Figure 1: The interpolation error

The ODS can be determined through the Frequency Response Functions (FRFs) if the excitation giving rise to the available responses is known otherwise Power Spectra of the response can be used to this aim. In this latter case a normalization of the damage feature is required in order to remove the dependence from the amplitude of the external excitation. Let $z_1,\ldots z_n$, be instrumented location of the structure where responses in terms of acceleration have been recorded. At each frequency value, the set of frequency response functions $H_R(z)$ measured at the instrumented locations, give the operational deformed shape (ODS) at that frequency (red dots in Figure). At the l-th location z_l the ODS can be calculated through the spline interpolation using the following relationship:

$$ODS_S\left(z_l, f\right) = \sum_{j=0}^{3} c_{j,l}\left(f\right)\left(z_l - z_{l-1}\right)^j \qquad (1)$$

where the coefficients (c_{0l}, c_{1l} c_{2l} c_{3l}) are calculated from the values of the transfer functions "recorded" at the other locations:

$$c_{j,l}\left(f_i\right) = g\left(H_R\left(z_k, f_i\right)\right) \qquad\qquad k \neq l \qquad (2)$$

The explicit expressions of the coefficient of the spline function $c_{j,l}$ in terms of the ODS's are determined imposing continuity of the spline function and of its first and second derivative in the knots (that is at the ends of each subinterval). More details on the spline interpolation procedure to calculate acceleration responses can be found in reference [8]. In terms of ODS's the interpolation error at location z (in the following the index l will be dropped for clarity of notation) at the i-th frequency value f_i, is defined as the difference between the magnitudes of recorded and interpolated frequency response functions:

$$E\left(z, f_i\right) = \left|ODS_R\left(z, f_i\right) - ODS_S\left(z, f_i\right)\right| \qquad (3)$$

If the structure is subjected to a known input recorded, for example, during forced vibration tests or under a low seismic excitation the estimation of the ODS is quite straightforward basing on the well-known relationship between the auto and cross power spectra allowing the estimation of the Frequency Response Functions. If the input is not available, the ODS can be recovered from the power spectra of the responses but, being not scaled to the input, cannot be directly employed to estimate the interpolation error since its value is influenced by the magnitude of the ODS which is strictly dependent on the input if they are not scaled: in this case a normalization of the damage feature is required.

The interpolation error in this case can be defined as:

$$E(z, f_i) = \frac{\left| ODS_R(z, f_i) - ODS_S(z, f_i) \right|}{\left| ODS_R(z_{rif}, f_i) \right|} \tag{4}$$

being z_{rif} a reference sensor location arbitrarily chosen.

In order to characterize each location z with a single error parameter, the norm of the error on the significant frequency range (that is the frequency range with a signal to noise ratio sufficiently high to allow a correct definition of the ODS) is calculated:

$$E(z) = \sqrt{\sum_{i=1}^{N} E(z, f_i)^2} \tag{5}$$

The significant frequency range is selected limiting the summation in equation (5) to the frequency range of the fundamental modes of the structure. This frequency range can be tuned basing on vibration tests carried out on the undamaged structure. If a reduction of stiffness (damage) occurs at a certain location, the operational shapes change in the region close to that location and specifically their smoothness decreases due to the discontinuity of curvature induced by damage. If the estimation of the error function through Eq. (5) is repeated in the baseline (undamaged) and in the inspection (possibly damaged) configuration, the difference $\Delta E(z)$ between the two values, denoted respectively by $E_0(z)$ and $E_d(z)$, can provide an indication about the existence of degradation at location z. An increase $(\Delta E(z) > 0)$ of the interpolation error between the reference configuration and the current configuration at a station z, i.e., highlights a localized reduction of smoothness and therefore, it is assumed to be a symptom of a local decrease of stiffness at location z associated with the occurrence of damage. Basing on this assumption the following conditions will be assumed to define the damage index $IDI(z)$:

$$
\begin{aligned}
IDI(z) &= \Delta E & if & \quad \Delta E(z) \geq 0 \\
IDI(z) &= 0 & if & \quad \Delta E(z) < 0
\end{aligned}
\tag{6}
$$

2.2   Extension to plate-like structures

In this case a bi-cubic spline interpolation is used to interpolate the ODSs. Assuming that sensors lye on a rectangular grid n_{l+1} x n_{p+1}, (see Figure 3) for each value of frequency f_i, the actual value $ODS_R(x_l, y_p)$ of the ODS at a given location (x_l, y_p), and its spline interpolation $ODS_S(x_l, y_p)$ must be known in order to calculate the value of the interpolation error at that location: $E(x_l, y_p)$, as shown in Figure 2. To this aim the spline interpolation $ODS_S(x_l, y_p)$ is calculated basing on the ODSs at all the instrumented locations except $ODS_R(x_l, y_p)$.
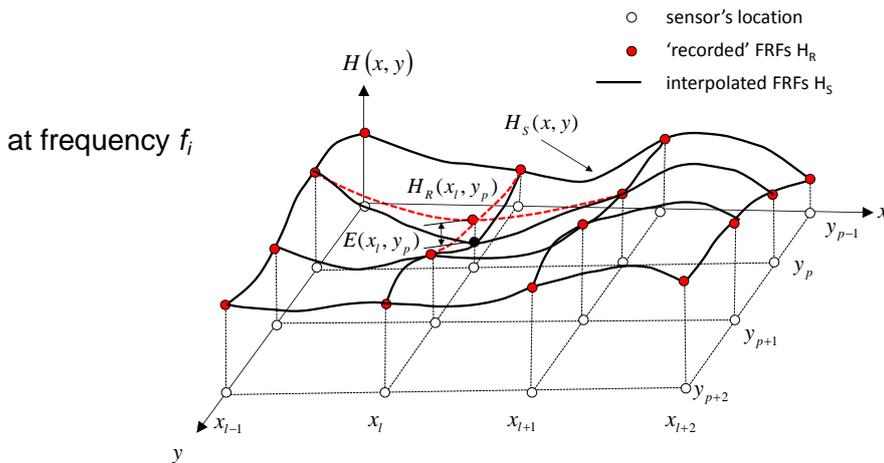
Figure 2. The interpolation error $E(x,y)$

At each instrumented location (x_l, y_p) and for each frequency value f_i, two values of the interpolation error E_x and E_y can be calculated basing on the difference between recorded and interpolated ODSs:

$$E_x(x_l, y_p, f_i) = \left| ODS_R(x_l, y_p,, f_i) - ODS_{S,x}(x_l, y_p, f_i) \right| \tag{7}$$

$$E_y(x_l, y_p, f_i) = \left| ODS_R(x_l, y_p,, f_i) - ODS_{S,y}(x_l, y_p, f_i) \right| \tag{8}$$

The total interpolation error at the given location can be calculated as the sum of the two latter values:

$$E(x_l, y_p, f_i) = E_x(x_l, y_p, f_i) + E_y(x_l, y_p, f_i) \tag{9}$$

In order to characterize each location $P(x, y)$ (in the following the suffix p and l will be dropped for clarity of notation) with a single error parameter, the norm of the error on the significant frequency range (that is the frequency range with a signal to noise ratio sufficiently high to allow a correct definition of the FRF) is calculated:

$$E(x, y) = \sum_{i=1}^{N} \sqrt{E(x, y, f_i)^2} \tag{10}$$

After the evaluation of the interpolation error in equation (10), which is the 2D version of equation (3), the calculation of the damage index for 2D structures follows the same procedures outlined for 1D structures.
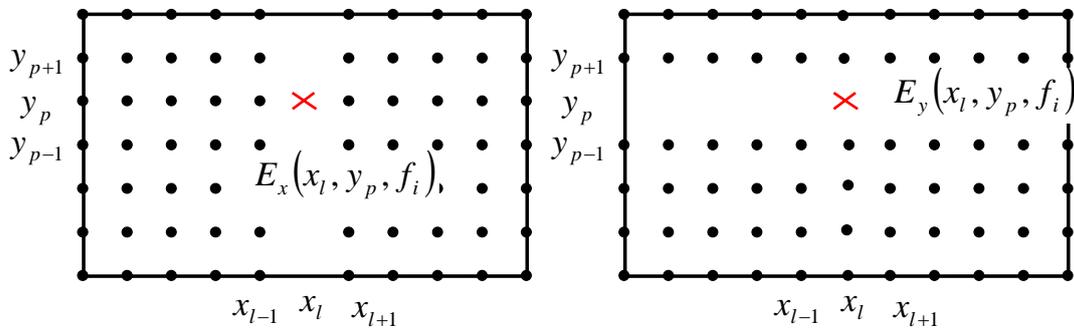
Figure 3. Regular grids for the evaluation of the interpolation error

2.3   Accounting for uncertainties

Several sources, such as temperature, nonlinear behavior, soil structure interaction and noise in recorded data, can induce variations of the interpolation error even if no damage occurs. To take into account their effect the statistical variability of the interpolation error $E(z_l)$ at each instrumented location z_i should be investigated. If enough samples of the damage feature are available both in the undamaged and in the inspection configurations the relevant probability distributions $p_{E,0}(z_l)$ and $p_{E,d}(z_l)$ can be estimated and compared. This is the case for structures permanently monitored and statistical methods are available for the comparison of the two distributions. A different situation occurs when a prompt alert is required, for example in the aftermath of an earthquake: the estimation of the damage feature should rely on a very small sample of values of E_d, possibly just one. In these cases the detection of possible damages should be carried out by comparing the value of E_d to the distribution $p_{E,0}$ in order to check if its value is 'likely to occur' in the undamaged configuration In this cases the definition of a threshold corresponding to an 'accepted probability of false alarm' is required.

The last situation is the very common one of structures that are periodically or occasionally inspected to check their 'health state': in this case the distribution of the damage feature is available neither in the inspection nor in the reference configurations hence the selection of the possibly damaged locations should be carried out basing on a very limited sample of data. In this case, the lack of experimental data requires some simplifying assumptions. For some of the applications reported in the following it was assumed that the sources of random variations equally affect all the instrumented locations the potentially damaged locations are identified among all the instrumented locations as the ones where the variation of the damage feature is

'significantly higher' with respect to the others. In order to select 'significantly higher' values of ΔE, a threshold value must is introduced in terms of its statistical parameters:

$$\Delta E = \mu_{\Delta E} + v\sigma_{\Delta E} \tag{11}$$

being μ and σ respectively mean and standard deviation of the statistical distribution of ΔE and v the value of the standard normal distribution corresponding to the threshold probability. More details will be given in the applications of the IDDM reported in the following.

3   Applications

3.1   The factor building under seismic excitation

The UCLA factor building (see Figure 4) is a 17-story moment-resisting steel frame structure consisting of two stories below grade and 15 above grade. The building houses laboratories, faculty offices, administrative offices, the School of Nursing, School of Medicine, auditoriums, and classrooms. More details on this application of the IDDM can be found in reference [2].
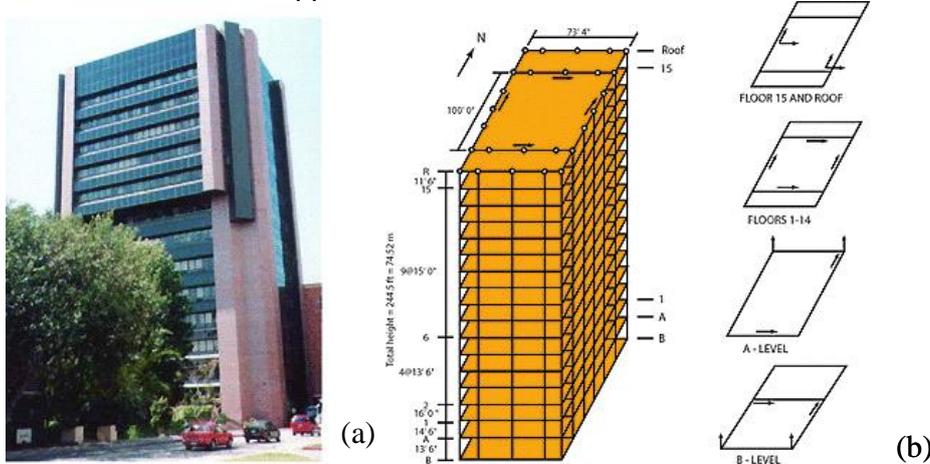
Figure 4: The Factor Building (a) East face; (b) Sensors location

The building is permanently instrumented with an embedded 72-channel accelerometer array recording both ambient vibrations of the building and motions from local earthquakes. The network of sensors deployed on the Factor building records responses in two directions as showed in Figure 4b.

(a) (b) (c)
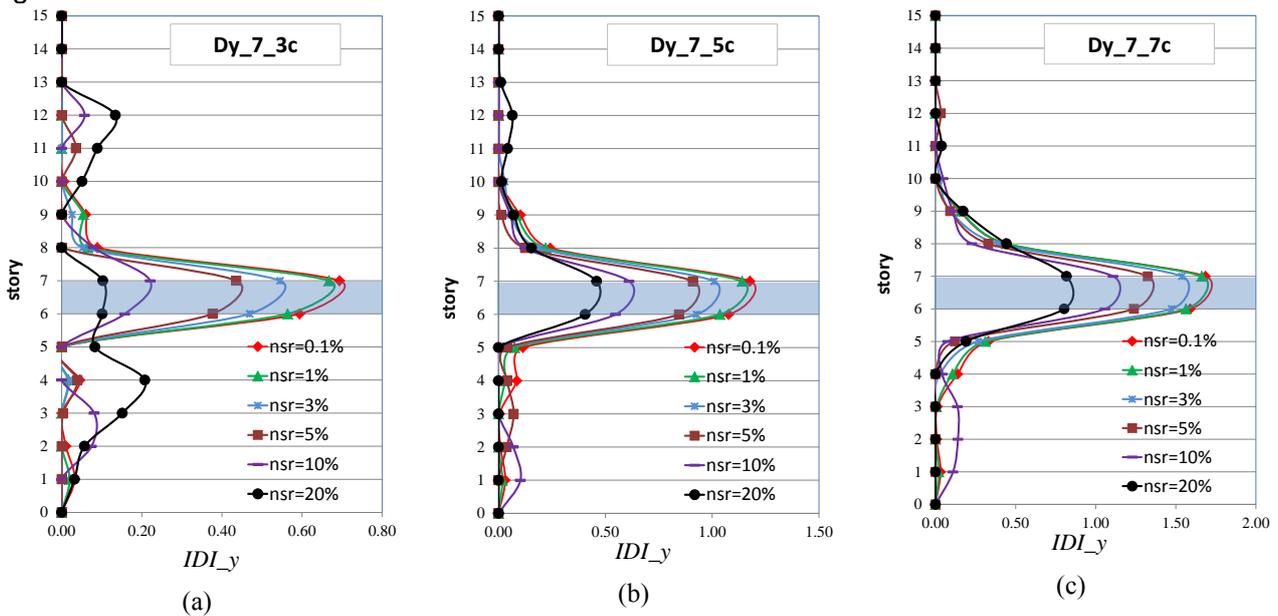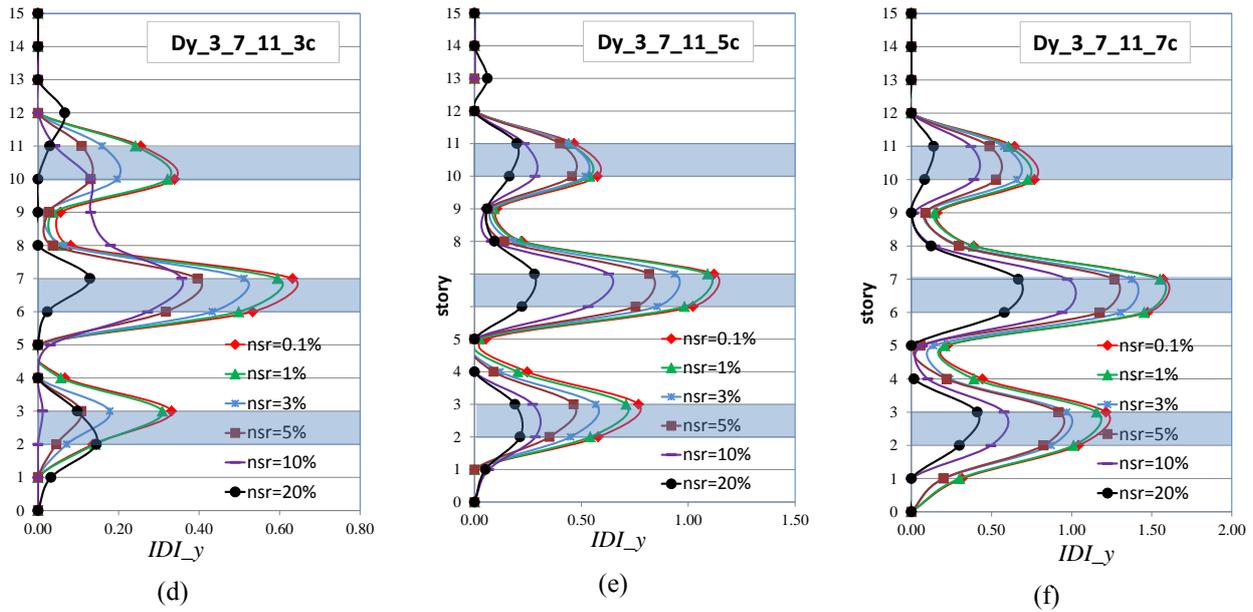
Figure5: Results for damage scenarios in *y*-direction.

Several damage scenarios have been modeled assuming damage to two column belonging to one frame in the *x* (or in the *y*) direction at one, two, three or four storeys. In order to study the influence of the quality of the available data on the reliability of the method, different levels of noise have been randomly added to the responses calculated by the numerical model.

Noise has been modelled as a Gaussian zero mean white noise vector: several different simulations were carried out considering values of noise increasing from 1% to 20%. The percentage represents the ratio between the root mean square of added noise and the root mean square of the amplitude of the absolute acceleration. Results show that the reliability of the method depends on the relationship between the severity of damage, on the intensity of noise and the value chosen for the threshold. Figure 5 reports results for different intensity of noise and for damage of increasing severity (3, 5 or 7 damaged columns)

A rough estimate of the reduction of stiffness per storey is given by the number of damaged columns with respect to the total number of columns at the storey (38 columns): one damaged column corresponds approximately to a reduction of stiffness of 2.5%, 7 damaged columns corresponds to about 18% storey stiffness reduction. At the increase of damage, the value of the IDI increases thus making easier the localization of the damaged storey also for high levels of noise. In the case of 7 damaged columns for both one damaged location (Figure 5c) and 3 damaged locations (Figure 5f) the identification of the damaged location is very clear. For damage of lower severity (3 damage columns, Figure 5a) the correct localization of damage is hampered by a number of false alarms that arise when the noise to signal ratio reaches values higher than 5%.

At the increase of the severity of damage that is at the increase in the number of the damaged elements per storey, also the damage index *IDI*(*z*) increases. In Figure the values of the damage index are reported for several scenarios corresponding to an increasing number of damaged columns in one frame along *y*, at the 7th story. At the moment a relationship between the amount of damage and the value of the Interpolation Damage Index has not yet been established hence it is not possible to recover the amount of damage from the value of the *IDI*.
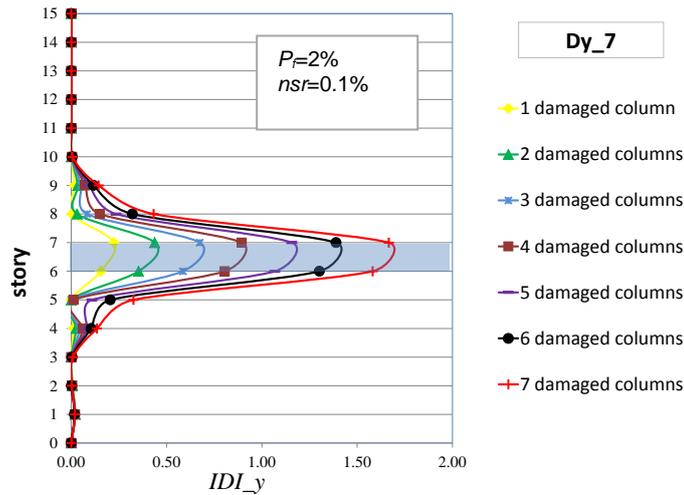
Figure 6: Increase of damage index with the severity of damage

3.2 The cable-stayed Bill Emerson Memorial Bridge under wind excitation

This bridge at the base of this study is a fan-type cable stayed bridge (Figure 7) which crosses the Mississippi River near Cape Girardeau (USA) with a composite concrete-steel deck stiffened by two longitudinal steel girders. For a more detailed description the reader is referred to reference [6]. In this case it has been assumed that a limited sample of responses is recorded both in the reference and in the inspection configurations hence the distributions of the interpolation error have been assumed unknown. This situation may occur if responses are recorded for a very limited period of time by a network of sensors temporarily installed on the structure. Damage to cables has been simulated by reducing the transversal section of 3 adjacent stays of 10%, 25% and 50% of the original section. Two different damage locations have been considered (see Figure 7b). The values of the damage parameters ΔE, calculated basing on ODS recovered from transversal responses are reported Figure 8a,b. The ODS have been estimated using the transmissibility functions of the responses at the nodes with respect to the response measured at the reference node assumed at location corresponding to Pier2. In the figures a blue vertical bar indicates the actual location of damage assumed at the node joining the deck with the damaged stay. The red dotted bar represents the threshold corresponding to the 98% percentile of the damage parameter distribution in equation (11). In all cases, even if damage is very low (10% reduction of transversal section) the damaged section is correctly identified.
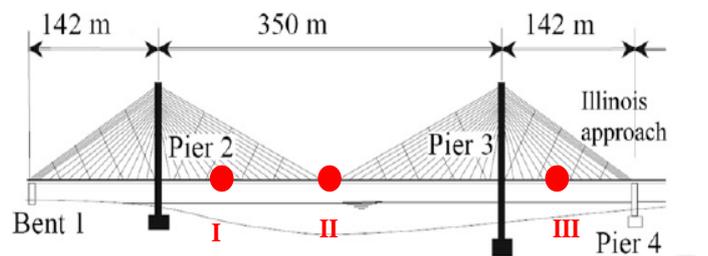
| (a) | (b) |

Figure 7: a) The Bill Emerson Memorial Bridge (Framerotblues, 2007; with permission); b) Damage scenarios

Of course the method is not able to indicate if the damage is located in the deck or in the cables, since only responses on the deck were considered in the procedure, but the damaged portion of the structure is correctly identified. The highest variation is found for the most severe scenario (C1_2_50) corresponding to a reduction of 50% of the stiffness in 6 cables of the bridge. In this case the maximum variation of modal frequencies was of 0.61% for the frequency of the 10th mode. Hence very low variations that would hardly allow the detection of damage, not to consider that in a real case noise would affect the estimation of modal parameters thus completely hampering the identification of damage through the estimated values of modal frequencies.
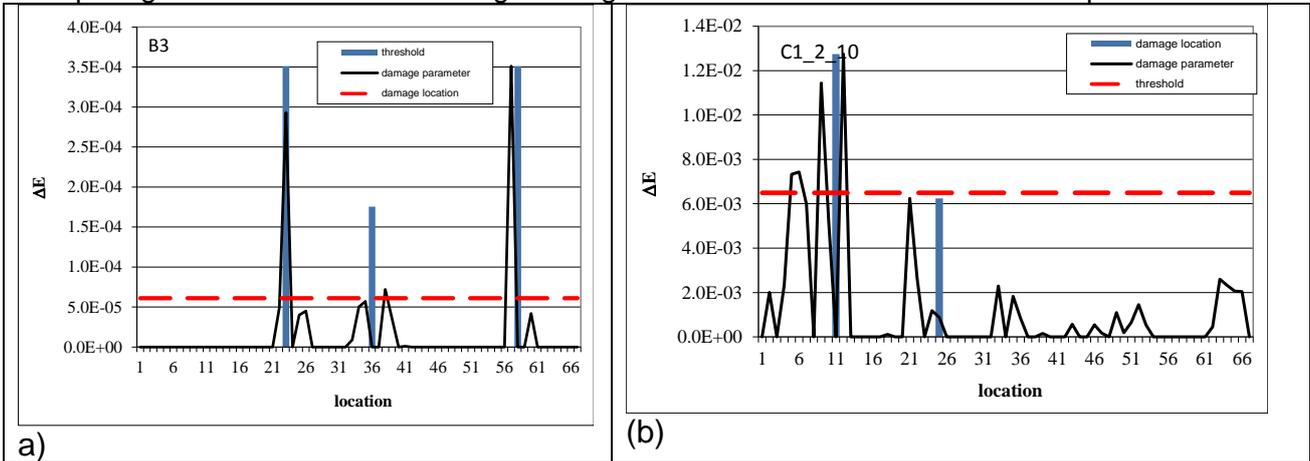
Figure 8: Damage parameter and threshold for the two damage scenarios a) B2: damage in the deck-beam at location 2; b) C1_2_10: damage in the cables at locations 1 and 2.

3.3 The Dogna Bridge under forced vibrations for inspection

Dogna Bridge is the four-span, one-lane reinforced concrete bridge shown in Figure 9. The bridge deck is formed by a reinforced concrete (RC) slab 0.18 m in thickness, supported by three longitudinal RC beams of rectangular cross-section 0.35×1.20 m. Beams are simply supported at the ends and are connected at the supports, at mid-span and at span-quarters by transverse RC diaphragms. Dynamic tests were performed from April 2 to April 11, 2008, and during the experiments the tested span was made independent of the adjacent span by removing the deck-joint in correspondence of the pier. Harmonically forced vibration tests were performed on the bridge in its original undamaged condition and in seven damaged configurations D1-D7, see The first six damage states were obtained by cutting the downstream lateral beam (see Figure 9right). Notches were produced by using a hydraulic saw fitted with a diamond disc. The seventh level of damage was obtained by removing the concrete near the mid-span cross-section of the same beam by means of a jackhammer. The vertical motions of the deck structure were produced by means of a vibration generator and deck's inertance of the bridge was measured by means of zoom analyses within narrow neighborhoods (approximately 3-5 Hz in size) of the natural frequencies. The above procedure has been applied for the characterization of all the damaged configurations D1-D7. Herein a very brief presentation of the main results is given; we refer to reference [4] for a more detailed description of this application of the IDDM.

Figure 9: General view of Dogna Bridge (left, tested span circled) and detail of damages D1-D6 (right).

The ODS in this case were easily calculated form the FRF recorded during the tests even if an interpolation of this functions was required in order to complete the experimental data, recorded only around small frequency ranges around the modal ones, with values calculated over the entire frequency range [4]. In almost all cases the values of the damage index, reported in Figure 10, exhibit the highest values at locations close to the actual position of damage. In order to check the capability of the IDDM to localize a new damage starting from a configuration already damaged (i.e., D6), the IDDM was applied to identify configuration D7 assuming configuration D6 as the reference one. Results show that the correct damaged section is always detected.
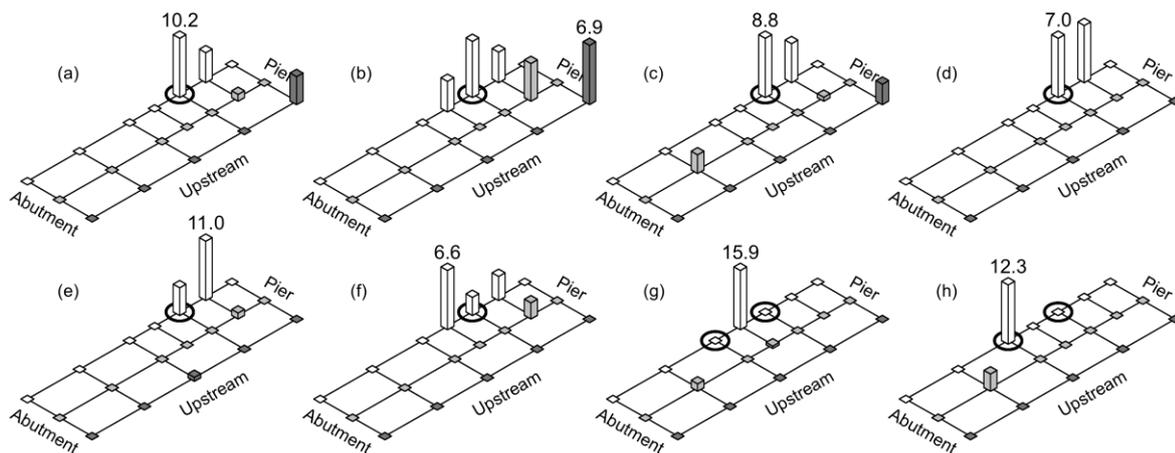
Figure 10. Damage index D calculated in the interval 8-50 Hz (first five vibrating modes) from the reference configuration (U) to actual damage configuration: (a) D1; (b) D2; (c) D3; (d) D4; (e) D5; (f) D6; (g) D7; (h) from D6 to D7. Threshold ν=1. Circles denote the actual damage locations.

3.4 The facade of the St Egidio church in old Bussana

The application of the 2D extension of the IDDM to plate like structures, has been successfully carried out for steel and composite plates [7] and [9]. Currently its application for damage localization in masonry structures is under investigation with reference to the case of the façade of the St Egidio Church in old Bussana (Italy) [10]. In the application is it assumed that the façade is permanently instrumented with a network of instruments arranged according the layout reported in the Figure 11. Numerical data recovered from a non linear time history seismic analysis will be used to check the capability of the method to give a prompt alarm allowing to detect almost in real time the location of possible damages to the façade, basing on the responses recorded from a quite dense network of the sensors permanently deployed on the structure Advances in sensors technology and miniaturized signal processing platforms allow exploring the possibility of using a large number of sensors widely distributed over the structure. This application is currently under development and the use of both accelerations, displacements and strains for the estimation of the interpolation error will be investigated.
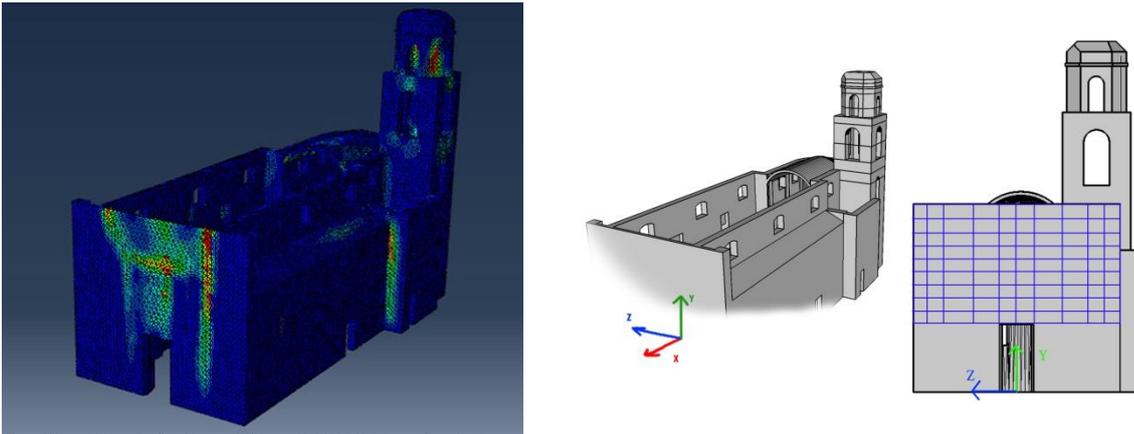
Figure 11. a) Damage pattern from numerical analysis; b) Locations of sensors

4   Conclusions and future developments

The results obtained so far by applying the IDDM in its 1D and 2D formulations are encouraging and several further developments are envisaged. First of all a correlation between the value of the damage index and the effective damage intensity would allow to quantify the severity of damage thus improving the knowledge about the structural condition. A second aspect which is worth investigations is the possible use of tri-cubic splines as interpolating shape functions for the ODS would allow to extend the method to 3D objects for particularly complex structures. Further investigations are also needed in order to define a 'reasonable' value for the threshold corresponding to the accepted probability of false alarm in the definition of the damage index. This should be carried out basing on an analysis cost-benefit carried out for the single monitored structure taking into account, together with the costs of a possible false alarm, the advantages related to a prompt intervention. These include both the direct cost savings deriving from a prompt remedial action that can reduce the costs of the interventions, both the increase the safety level and, in the case of historical structures and of structures hosting historically or culturally valuable objects (e.g. museums), the reduction of the risk related to the loss of invaluable objects.

References

[1]   Limongelli, M.P., (2011). The interpolation damage detection method for frames under seismic excitation. *Journal of Sound and Vibration*, 330. 5474–5489.

[2]   Limongelli, M.P., (2014). Seismic health monitoring of an instrumented multistorey building using the Interpolation Method. *Earthquake Engng. Struct. Dyn.* doi: 10.1002/eqe.2411.

[3]   Limongelli M.P. (2010). "Frequency response function interpolation for damage detection under changing environment". *Mechanical Systems and Signal Processing* doi:10.1016/j.ymssp.2010.03.004

[4]   Dilena M., Limongelli M.P. Morassi A. (2014). "Damage localization in bridges via FRF interpolation method". *Mechanical Systems and Signal Processing*, 52-53, pp 162-180.

[5]   M. Domaneschi, M.P. Limongelli, L. Martinelli (2013), "Vibration Based Damage Localization Using MEMS on a Suspension Bridge", *Smart Structures and Systems*, 12(6), 679-694.

[6]   Domaneschi M., Limongelli M.P., Martinelli L. (2014). Damage Identification in a Benchmark Cable-Stayed Bridge Using the Interpolation Method. Le Cam, Vincent and Mevel, Laurent and Schoefs, Franck. EWSHM - 7th EuropeanWorkshop on Structural Health Monitoring, Jul 2014, Nantes, France. <hal-01022077>

[7]   Limongelli M.P., (2013). "Two dimensional damage localization using the interpolation method". *10th International conference on damage assessment of structures. DAMAS 2013*. Dublin Ireland. July 8-10 2013.Key Engineering Materials. Vol. 569-570, 860-867.

[8]   Limongelli M.P., (2003),"Optimal location of sensors for reconstruction of seismic responses through spline function interpolation". Earthquake Engineering and Structural Dynamics, 32, pp. 1055-1074.

[9]   Limongelli M.P., Carvelli V. (2015). "Damage localization in a glass fiber reinforced composite plate via the surface interpolation method". *11th International conference on damage assessment of structures. DAMAS 2015*. Ghent Belgium, 24-26 August 2015. *Submitted*

[10] A. Gecchelin. (2014) Master thesis. 'Il tempo non si è fermato a... Bussana Vecchia. Valutazione della vulnerabilità sismica della Chiesa di Sant'Egidio'. Politecnico di Milano. Scuola di Architettura.

Subspace-based detection of fatigue damage on a steel frame laboratory structure for offshore applications

Falk Hille, BAM Federal Institute for Materials Research and Testing, Department for Safety of Structures, 12205 Berlin, Germany

Abstract

The contribution describes the application of a vibration utilizing statistical damage detection method on model structures for an utilization of this approach on offshore wind turbine structures. Aim of the study was therefore to analyze the usability and efficiency of the detection method as well as to determine an optimized set of parameter for realistic damage on support structures of wind energy turbines. Based on results of an experimental fatigue test on a steel frame laboratory structure a strategy for a numerical verification of the experimentally evolved damage detection was developed, utilizing a time integration approach to simulate the dynamic response. In a second step the identified modeling and computing methodology is used to numerically investigate the ability to detect damage in real size structural components of offshore wind turbines. The contribution outlines the basic necessity but also the difficulties and limitations associated with numerical simulations of the structural (dynamic) behavior of civil engineering structures to validate damage quantities within SHM strategies.

1 Introduction

The verification of the applicability of methods for damage diagnosis on real civil structures as well as their customization for an optimal operation is a difficult task. Simply their monetary value makes it almost impossible to test the performance and reliability of such methods on real structures. Besides the few possibilities of progressive damage tests on out of service structures being teared down, the only way for verification is the numerical simulation. But the reliability of the simulation result depends strongly on the quality of the model, accounting for all significant influences as i.e. operation and weather.

For that reason research activities have been performed at BAM to validate and verify the applicability of the Stochastic Subspace-based Damage Detection method (SSDD) on offshore wind turbines (OWT), especially to detect fatigue damage on framed OWT foundation structures. The work group enhanced the SSDD and optimized parameters for an effective and robust SHM application on offshore wind turbine structures. Unlike common vibration utilizing methods the SSDD methodology does not explicitly identify and assess modal properties. Instead a statistical χ^2-type test is used to analyze changes in the dynamic response of the system for their significance [1, 2]. Starting with analyzing a reference state of the undamaged structure a Gaussian type residuum is created. Within the subsequent observation of the structural state the residuum is recalculated and tested for significant changes by a statistical hypothesis testing. The method has been successfully applied to several laboratory and real application from different mechanical systems utilizing disciplines [3-5].

For adoption of the damage detection method on OWT structures a 2-step strategy including numerical simulations is adopted. In the first step a steel frame laboratory structure was used to test and verify the method in small scale as well as to validate a numerical model of the lab structure. With the so obtained modeling and computing parameters in a second step a numerical model of a real size structure is assembled and, using time integration analysis, a monitoring system based on the SSDD method was investigated.

In section 2 of the paper the theoretical basics of the stochastic subspace based damage detection method is briefly introduced. Section 3 describes the fatigue test on the laboratory structure and in section 4 the numerical analysis of the fatigue test is summarized. In section 5 the investigations of the SSDD on base of numerally simulated dynamics of an OWT are described.

2 Subspace-based damage detection method

The stochastic subspace-based damage detection algorithm as used in the here presented studies is generally based on the theory of system realization as described in [6]. But instead of extracting

modal system parameters the investigated approach exploits a residual, which uses the left null space of a Hankel matrix, describing the system. The theory has been widely used in the last years and some different approaches have been developed. The introduced work uses covariance-driven Hankel matrix estimates and a non-parametric χ^2-type test for damage detection [7, 8]. The mathematical model is based on a linear output-only dynamic system in the time-discrete state space description:

$$x_{k+1} = Ax_k + v_k$$
$$y_k = Cx_k + w_k .$$

To record the systems characteristic in the initial state, a block Hankel matrix H is filled with output covariance estimations $R_i = \mathbf{E}(y_k, y_{k-1})$ from the undamaged system. In this reference state S^T is the empirical left null-space (kernel) of the Hankel matrix $H^{(0)}$ and holds the property $S^T H^{(0)} = 0$. The kernel can be extracted by factorization of $H^{(0)}$, e.g. using singular value decomposition. For the damage detection algorithm the kernel is computed only once from the initial system. A residual vector ζ_N is defined as function of the reference matrix S^T and the Hankel matrix H of the actual system built from the covariance estimates of the measured output

$$\zeta_N = \sqrt{N} \, \text{vec}\left(S_0^T H_{p+1,q}\right)$$

It can be deduced that ζ_N has zero mean if changes of the system do not occur, and non-zero mean in the case of changes. Therefore, for the undamaged state the left null space of the Hankel matrix can be used as reference for future residual analysis.

Under convenient assumptions the residual function is asymptotically Gaussian. Then, it manifests itself to damage by a change in its mean value, also corresponding to an increase of the mean of the χ^2-test statistics

$$\chi^2 = \zeta_N^T \, \Sigma^{-1} \, \zeta_N$$

where $\Sigma = \mathbf{E}(\zeta_N, \zeta_N^T)$ is the residual covariance matrix. The monitoring of the system consists in calculating the χ^2-test value on the Hankel matrices determined from newly recorded output data and comparing it to a threshold. A significant increase in the χ^2-value indicates that the system is no more in the reference state.

3 Fatigue test on Laboratory Structure

Due to the deep sea waters in the German exclusive economic zone of the North Sea first choice for support structures are principally framework structures such as tripods or jackets. For this reason a jacket structure design is chosen as a model basis for studies on the applicability of the SSDD method. The laboratory steel structure represents a two-dimensional section of a jacket-type support structure of an offshore wind turbine with a scale of the general dimensions of approximately 1:10. Figure 1a shows the laboratory test structure with the loading unit in the testing facilities at BAM.

(a) Laboratory model structure   (b) SSDD result of fatigue test
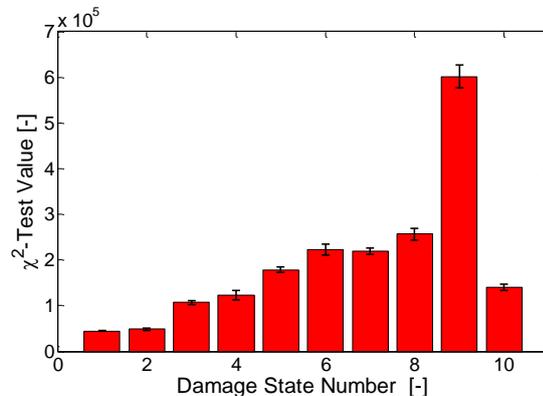
Figure 1 : Stochastic subspace-based damage detection during laboratory fatigue test.

After extensive studies with defined damage by successive opening of a flanged connection a fatigue test was accomplished to test the applicability of the SSDD-method to real damage. Principally, the test procedure consisted out of two general and alternating tasks, the inserting of the fatigue relevant load cycles and the measurement of dynamic response series for determination of the χ^2-value. The cyclic loading consisted of load series with a constant alternating horizontal force of 50 kN applied at the top girder of the structure with a frequency of 3 Hz. After completion of each load series a damage test was conducted. For the damage tests a broadband random signal with a frequency content between 10 Hz and 1000 Hz was produced by a shaker control unit and after amplification was induced via an electro-dynamic shaker at the top of the structure. For the vibration measurement, all in all 9 piezoelectric accelerometers were applied at the structure.

A total of 10 load series and therefore 10 damage states were implied. The result of the fatigue damage test is shown in Figure 1b. The bars represent the mean of 10 to 30 tests executed in one damage state and the error bar represents the related variance. The diagram shows a continuous increase of the χ^2-based damage indicator up the final load series, where a significant drop of the value is noticeable. The reason for this evolution is, that a first fatigue crack has evolved at one leg-footplate connection during load series 3 to 9. Due to stress redistribution in the last loading series a second fatigue crack developed at the other leg-footplate connection of the structure. While during progression of the first crack the modal system changed gradually with the effect of an continuous increase of the χ^2-value, the second crack resulted in a distinct switch back of the modal system and a decrease of the χ^2-value. A detailed description of the fatigue test and discussion of its result is given in [9].

4   Numerical Simulation of Fatigue Test

To transfer the experimentally obtained results from the laboratory structure to real size foundation structures, a numerical simulation strategy is employed. It implies, that first the dynamic response of the structure under observation is simulated by transient (time integration) numerical analysis in an optimized complexity and secondly the so generated time series of deflection parameter are analyzed by the SSDD algorithm. Intention of the numerical studies is to analyze, to which extent this methodology is able to reproduce the effects of real structural damage to the dynamic response of the system and therefore, to which extent the numerical simulation is able to test the reliability and the sensitivity of the SSDD. Based on a successful application of the described approach the final objective is to configure an optimal measurement setup for monitoring real offshore wind turbine structures. The idea within this task is to verify and validate the numerical model of the lab structure on the results of the laboratory fatigue test to use this information for modeling a real offshore wind turbine structure. The numerical analysis was carried out using the commercial FEM program system ANSYS in version 14.5. Accordingly, the modeling was conducted using the element types and meshing algorithms, available within ANSYS.

Based on preliminary studies for comparison of models with beam and shell elements hybrid modeling has been chosen utilizing beam as well as shell elements. The use of shell elements arose from the necessity for a high resolution modeling of the fatigue crack. All other parts and components of the laboratory structure as well as the entire support structure were modeled by beam elements. This approach ensures a corresponding limited number of degrees of freedom for a sufficiently accurate description of the global dynamic behavior of the structure. Concentrated masses (flanges, shaker) were modeled as lumped masses.

The fatigue crack is modeled by successive elimination of neighboring nodal couplings between the legs and the footplates. For reasons of computational efforts the non-linear crack opening/closing behavior was not included into the modeling. The introduced simplification is well-known to the authors, but appraised negligible for the structural dynamic response. Figure 2b shows the region of modeled damage with the coupling of the beam and shell elements of the leg (magenta) as well the coupling of the leg and footplate shell elements (green) which are successively eliminated for damage simulation.

The validation of the numerical model was done by modal analysis. The mode shapes of the numerical model were compared with those of an experimental modal analysis conducted on the laboratory structure. As comparative parameter the Modal Assurance Criteria (MAC) was used. First tests showed a general consistency in the modal values. A small necessary modification of the numerical model was conducted by the change in the support stiffness at the feet of the structure.

For obtaining the structural dynamic response of the system time series of accelerations were generated by a transient analysis using the described model as well as a time series of loading sequences on the base of Gaussian white noise. In each performed analysis 98304 calculation steps were executed. Since the used load step frequency was 2500 Hz, each response data set consisted of 39.32 s simulated output accelerations.

Within the post processing the acceleration directions were transformed into the axes of the real sensors and finally were used as input in the SSDD algorithm. Due to the high computational effort of the transient analysis only a limited number of χ^2-test values were calculated for each damage state, with the exception of the reference state where a considerable number of 30 tests were used for the residual covariance matrix.
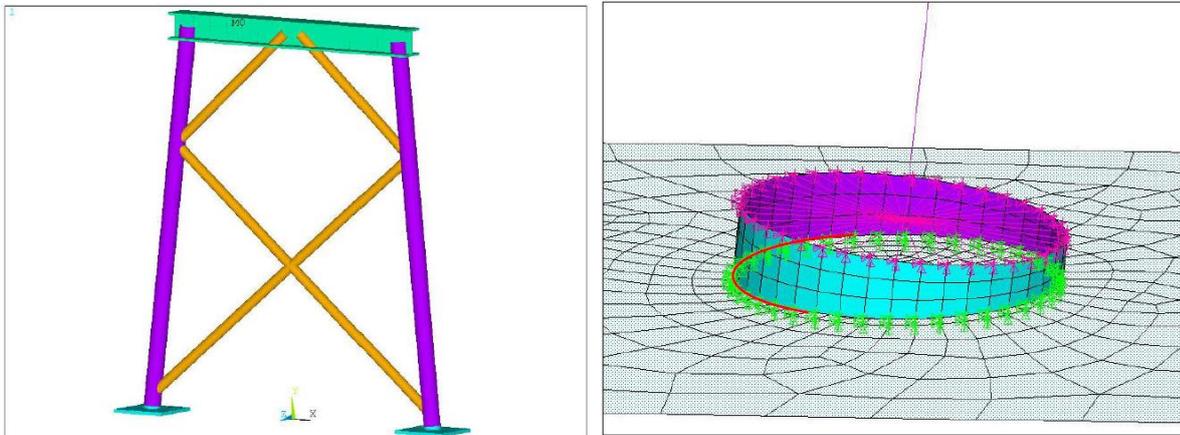
(a) ANSYS model of laboratory structure. (b) Model detail of damaged leg-footplate connection.

Figure 2 : Numerical model of laboratory structure.

The resulting sequence of χ^2-test values for the simulated fatigue damage propagation is shown in Figure 3. Compared with the results of the experimental fatigue test as displayed in Figure 1b} it can be shown, that the χ^2-values follow the same pattern. That applies also to the decrease of the damage indicator after appearance of the second fatigue crack, even though the decrease is not that distinctive than for the experimental obtained χ^2-values.
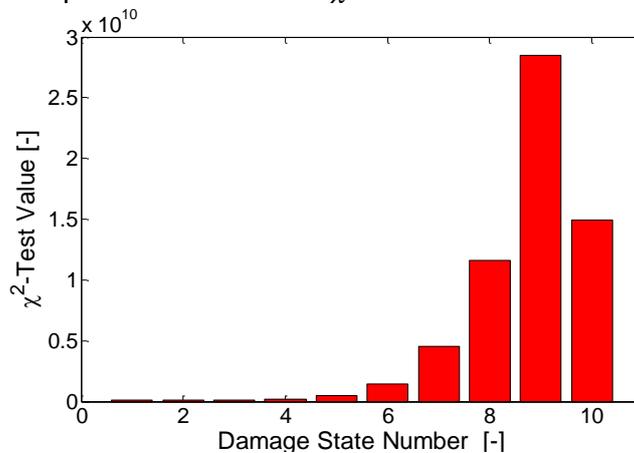
Figure 3. Simulated course of χ^2-test value for 10 damage states, partly comparable with those of the fatigue test.

So all in all it can be stated, that the numerical simulation is able to reproduce structural dynamic responses, comparable to those of the real fatigue test.

5   Numerical analysis of Jacket structure

In a second step the dynamic response of a real size jacket structure under progressive fatigue damage is simulated. Objective is to numerically analyze under which condition and to which extent a reliable detection of structural damage is possible under operational conditions at wind turbine structures.

Generally, the same modeling principles as for the lab structure model are applied. In particular this concerns the element types, where with the exception of the damaged area, beam elements were applied. For reasons of high resolution for the double-K-joint with the simulated fatigue crack shell elements are used (see Figure 4). The successive damage itself is modeled by elemination of nodal couplings between shell elements. The model consists out of the jacket itself, the transition piece to the tower and the tower. The rotor-nacelle system is modeled as lumped mass on the top of the tower. All used dimensions are close to real ones.
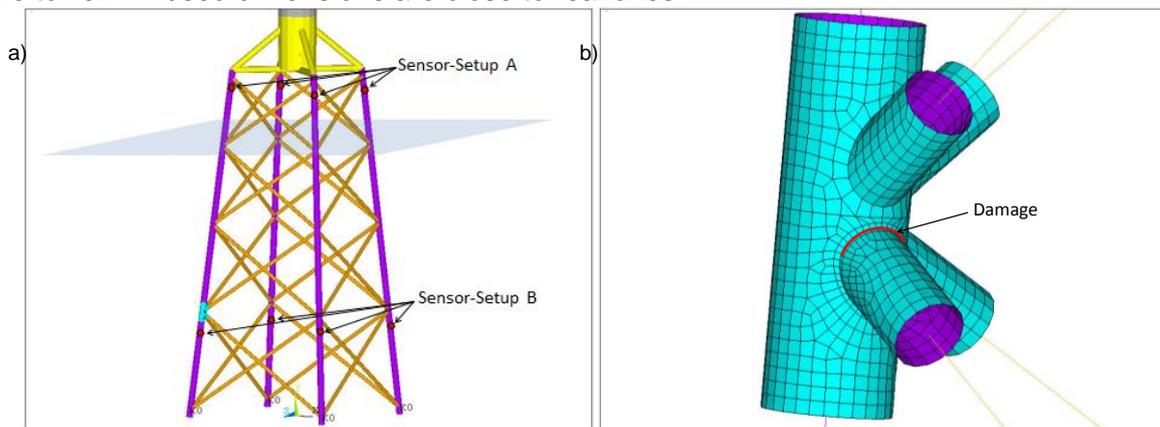
Figure4: Numerical model of jacket structure, (a) with additional information of the two analyzed sensor setups for the SSDD and (b) with additional indication of the damaged area.

Specific attention was directed into accounting for those boundary conditions which essentially influence the dynamic behavior of the wind turbine structure and therefore influence the damage detection result. This concerns mainly the loading process, the support conditions in the seabed as well as the damping characteristics of the dynamic systems. A major influence on the dynamic structural behavior and, thus, on the quality of the damage indication has the wind loading. To provide loading for the numerical simulation of the dynamic response, measured responses of a real onshore wind turbine are used. Strain-time signals were recorded on the top of the tower of the monitored wind turbine and processed to stress resultants which are used in the simulation as lateral and axial force input as well as bending moments acting on the top of the tower. In addition the so generated load time series are conditioned with white noise to emphasize the stochastic nature of wind. The described monitored time signals were also used to develop lateral load time series to apply on the tower structure, distributed over its length. Loading from waves and current as well as from turbine control operations are not considered.

Another considerable effect on the dynamic behavior results from damping. Besides the classic material and structural damping effects the damping from the bedded pile support and especially from the hydrodynamic and the aerodynamic damping have a major influence on the dynamic behavior of an offshore wind turbine structure. With the exception of aerodynamic damping the single parts of damping are taken into account as stiffness proportional damping, separately for the tower and the support structure. Due to the complexity of its modeling, aerodynamic damping was not accounted for. In succession it needs to be postulated, that the rotor is not moving during the damage detection tests and only load files measured at wind speed of less then 4 m/s were

considered in the analysis. For modeling the support conditions, the horizontal and vertical stiffness parameter are determined by integration of the pile bedding constants.

Similar to the analysis procedure of the lab model as described above the dynamic response of the system was computed and time series of output accelerations at defined locations were generated. For a later optimization of sensor number and location, output time series were produced for every element node of the model. To indicate the systems eigenstructure, a sampling frequency of 1000 Hz was applied for a time period of 60 s. So each record contained 60000 acceleration samples for each channel. For each computation lasting approximately 12 h only a limited number of damage states were investigated. All in all 55 data sets were generated, 41 for the reference state and 14 for the seven states of progressive damage.

Within the presented study two different sensor setups and at the same time two sampling frequencies were analyzed. In the sensor-setup A (see Figure 4a) four 3D accelerometer are installed near the upper end of the corner legs. This sensor layout is quite attractive for the operators of monitoring systems since the sensors lie above sea level which makes installation, maintenance and replacement significant easier. Of course, possible installations need to be protected against mechanical damaging from breaking waves. Secondly, the sensor-setup B as shown in Figure 4a contains four 3D accelerometer, which are installed on the four corner legs within the lowest jacket section, near the damage.

Regarding the sampling frequency, two different values were analyzed, first the "measured" $f_a = 1000$ Hz and secondly the down-sampled $f_a = 250$ Hz. The reason for the study is to examine the sensitivity of the χ^2-test with respect to the necessary data volume.

The results for two sensor locations are shown in Figure 5. Both figures show the χ^2-values of the same simulated damage process, but analyzed in terms of SSDD for the two different sensor setups and the two sampling frequencies. To compare the χ^2-values for both sampling frequencies, the result values are related to the mean of the reference state χ^2-values in each analysis. For each damage state two records are analyzed. The utilized damage states are described in the legend of the diagrams as the length of the fatigue crack. Additionally, it should be mentioned, that the smallest damage with a crack length of L=260 mm stays for a reduction of the bending stiffness of 2% and the largest included damage with a crack length of L=1299 mm stays for a reduction of the bending stiffness of 91%. The threshold (dashed line) is defined as 1.5-time magnification of the 98% fractile of χ^2-values in the reference state.
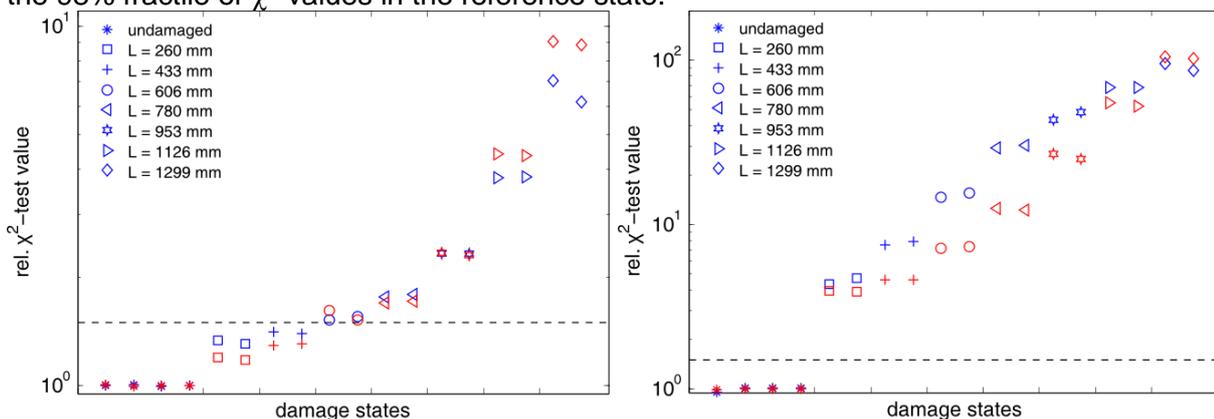
(a) c2-course for sensor-setup A (see Fig.4(a)).   (b) c2-course for sensor-setup B (see Fig.4(a)).

Figure 5: SSDD on numerically simulated dynamic response of a jacket structure for two different sensor setups and two sampling frequencies. Blue markers present the related c2-values of the data set, recorded with $f_a = 1000$ Hz and the red markers the ones with $f_a = 250$ Hz.

In terms of the sensor layout it can be shown that the detection of fatigue damage in early stage is possible with four 3D-accelerometer if the sensors are located in relative vicinity to the damage. For the sensors applied on the top of the jacket structure, a significant increase of the damage indicating χ^2-value can be detected for a crack length of L=606 mm, which is equivalent to a loss of

bending stiffness of 22%. Regarding the sampling frequency it is shown that a reduction of the amount of data to a fourth did not has any consequence to the quality of the damage indication. Our additional investigationss showed, that a further downsampling does have a significant influence to the damage indicator.

6   Conclusion

With the overall objective to test the applicability and functionality of the stochastic subspace-based damage detection method on offshore wind turbine structures numerical analysis is used to simulate the dynamic response of the structure. On the base of experimentally achieved detection results from a laboratory structure numerical modeling and computing approaches were developed and tested. In a second step the optimized numerical analysis methodology is applied on a "virtual" real size jacket structure of an offshore wind turbine. With the simulated responses of a structure in undamaged and damaged states the SSDD algorithm is utilized for investigations about several sensor location setups as well as on the influence of the sampling frequency.

Taking into account some simplifying assumptions the application of SSDD methods on numerically produced response data sets showed a respectable sensitivity of the χ^2-value-based damage indicator. Though not detectable in early stage, typical fatigue cracks in welded joints of support structures have a significant impact to the indicator for a remaining bending stiffness of the damaged component of app. 80%.

Future activity in this field should focus on a realistic modeling of the dynamic response influencing time-variant processes like wind and wave loading as well as the aerodynamic damping.

References

[1]   Basseville, M., M. Abdelghani, and A. Benveniste, *Subspace-Based Fault Detection Algorithms for Vibration Monitoring.* Automatica, 2000. **36**: p. 101-109.

[2]   Basseville, M., L. Mevel, and M. Goursat, *Statistical model-based damage detection and localization: subspace-based residuals and damage-to-noise sensitivity ratios.* Journal of Sound and Vibration, 2004. **275**(3-5): p. 769-794.

[3]   Mevel, L., L. Hermans, and H. Van Der Auweraer, *Application of a Subspace-baced Fault Detection Method to Industrial Structures* Mechanical Systems and Signal Processing, 1999. **13**(6): p. 823-838.

[4]   Mevel, L., M. Basseville, and M. Goursat, *Stochastic Subspace-Based Structural Identification and Damage Detection - Application the Steel-Quake Benchmark* Mechanical Systems and Signal Processing, 2003. **17**(1): p. 91-101.

[5]   Döhler, M., et al., *Structural health monitoring with statistical methods during progressive damage test of S101 Bridge.* Engineering Structures, 2014. **69**: p. 183--193.

[6]   Juang, J.-N., *Applied System Identification*1994, Englewood Cliffs: PTR Prentice Hall.

[7]   Balmès, É., et al., *Merging Sensor Data from Multiple Temperature Scenarios for Vibration Monitoring of Civil Structures* Structural Health Monitoring, 2008. **7**(2): p. 129-142.

[8]   Döhler, M., L. Mevel, and F. Hille, *Subspace-based damage detection under changes in the ambient excitation statistics.* Mechanical Systems and Signal Processing, 2014. **45**(1): p. 207-224.

[9]   Hille, F., Y.S. Petryna, and W. Rücker. *Subspace-based detection of fatigue damage on a steel frame laboratory structure for offshore applications.* in *9th International Conference on Structural Dynamics, EURODYN 2014.* 2014. Porto, Portugal, July 2014

Probability-based durability prediction for corroded shell of steel cylindrical tank for liquid fuel storage

Mariusz Maslak – Cracow University of Technology, Cracow, Poland
Michal Pazdanowski - Cracow University of Technology, Cracow, Poland
Janusz Siudut – Polish Oil Concern ORLEN Company, Cracow, Poland
Krzysztof Tarsa - Cracow University of Technology, Cracow, Poland

Objectives of the analysis

Evaluation of the forecasted durability of the corroded steel tank used to store liquid petroleum products is counted as one of the basic duties of technical supervising personnel in fuel tank farms. Estimation of this type allows for a more efficient management of resources at the base through a more rational planning of possible repairs or other modernization or maintenance works of lesser importance. In general durability is understood here as the safe service time of considered object, determined under the assumption that no preventive actions or actions just slowing down the destruction progress are undertaken. This time should not be referred directly to the moment of the tank failure, resulting from the loss of capacity to bear the external loads applied to it, but to such point in its service life in which the failure probability will become unacceptably high. Under the conditions of standard operational regime, assuming full service load, durability of the tank shell is determined by the corrosion state of the steel sheets of which the tank shell is made. Tank shell durability determination algorithm may be reliable only when the durability will be treated as a random variable, for which probability distribution parameters shall be determined based on fully probabilistic analytical procedures. Thus, first of all, maximum user accepted failure probability should be set, and in the second step compared with the values of analogous probability resulting from the appraisals of the technical condition of the tank under consideration. These appraisals should be performed after certain, predetermined, service time periods. If the person performing the appraisal has at least two statistical data sets, corresponding to two independent evaluations of the same steel sheet in two different times at his disposal, then under the assumption of constant service conditions, this person may attempt to model the statistical trend of corrosion changes for corresponding steel sheet. Knowledge of this trend, through extrapolation for coming service years, will allow for scientifically justified forecast of corrosion progress in the future. The randomness of the corrosion process, in association with the randomness due to the statistical distribution of yield limit for structural steel, of which the shell is made, allows for the estimation of random, decreasing in time, bearing capacity of the considered steel sheet. This bearing capacity should be compared with random effect of authoritative external loads combination. Such a comparison will allow for the determination of failure probability with reference to subsequent service periods of the considered tank. The time, after which such probability, ever increasing with corrosion progressing during service, will reach the threshold value acceptable to the operator of the fuel tank farm, will constitute the sought for measure of durability.

1   Structural health monitoring

According to Polish regulations (Law Journal (2001)) all the overground steel tanks must undergo detailed examination of technical condition at least every 10 years. However, if service life of those tanks exceeds 30 years, the maximum allowable time span between inspections is shortened to 6 years. Inspection of the sheathing against possible corrosion damage and evaluation of its advancement state is counted among the basic duties of the evaluator. Potential discovery of local pitting, generating the risk of bearing capacity loss or tightness loss for the tank shell, results in the need for immediate corrective action by, for instance, pad welding. Because of this fact, pitting repaired immediately after discovery during inspection, does not constitute the critical factor in estimating the corrosion durability of the tank shell. Instead, the uneven corrosion, existing on large surfaces of the tank shell, should be considered as authoritative. According to the recommendations, the development of such corrosion is recorded for each sheet of the shell in five

characteristic points, i.e. in its geometrical center and four corners. An example of such inspection record, for an overground steel tank equipped with a floating roof, located in a petroleum products depot in Poland is shown in Fig. 1. As may be observed, due to multiple interventions by the depot personnel, resulting in local pad welding of sheathing plates, the thickness of those plates after 30 years of service frequently exceeds the nominal thickness determined in the technical design.
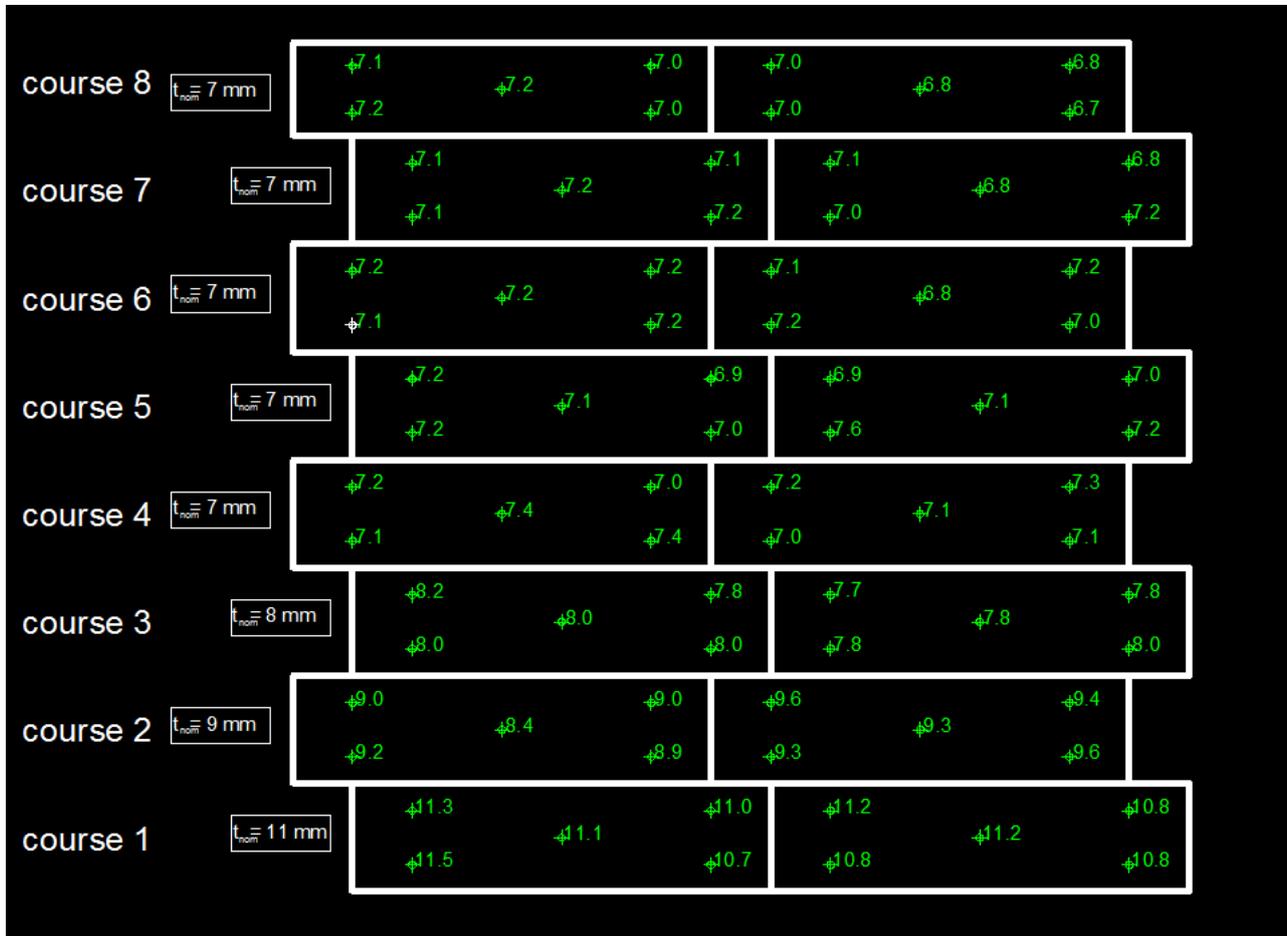
Figure 1: A part of the sheating of the tank under consideration with measured thickness of corroded sheating plates. Nominal sheet thickness indicated at left.

Due to cyclic repetition of such inspections every 6 years one may gather a formally uniform population of statistical data monitoring the random changes in sheathing plate thickness, related to the same spots located on the same sheathing plates of the same tank. Thus one may, for each considered spot, determine the statistical trend describing the previous corrosion progress, and in the next step extrapolate this trend for the future, under the assumption, that mode of use and the conditions influencing the aggressiveness of environment in the nearest vicinity of considered structure will remain unchanged. Based on observations and measurements performed by the authors one may conclude, that the linear trend will yield sufficient accuracy, though formally more complex nonlinear trends may be modelled as well, especially the exponential trend widespread in the professional literature.

2 Simplified approach – durability analysis of single tank shell plate, ideal geometry and bending moment free stress state in the shell

2.1 Random resistance of the tank shell and random authoritative load effect

Let time τ_0 denote the beginning of service life for the considered tank, and the time $\tau^* > \tau_0$ the technical condition evaluation moment. Specification of the time period $\tau_d - \tau^*$, counted from the moment τ^*, during which the analyzed tank shell plate will safely resist the loads applied to it, is the objective of this research. This is an equivalent to the constatation, that the tank shell destruction probability Ω_{ult} acceptable to the user will not be exceeded. In such an approach the tank sheathing is treated as a thin cylindrical shell of random thickness $t(\tau)$, decreasing in time due to the progressing corrosion, and constant radius r, in further considerations treated as a fully deterministic parameter. At the first approximation perfect geometry of the tank is assumed, thus all the geometrical imperfections resulting in ovalization of the tank shell are disregarded. Also bending moment free stress state in the shell is considered, while the boundary effects, important in the case of the plates adjacent to the tank bottom are disregarded. The case of the tank filled to full capacity is authoritative for analysis. This means that the computational situation associated with the empty tank, which may result in the stability type destruction, in general due to the local or global denting is not considered. As a result of such assumptions the global tensioning hoop force N_φ becomes the determining factor in the evaluation of tank shell bearing capacity. This force is generated in the tank shell as a result of random hydrostatic internal pressure ρ_c and/or random overpressure ρ_n (Fig. 2). The value of this force is found by the following formula:

$$N_\varphi = (\rho_c z + \rho_n) r \qquad (1)$$
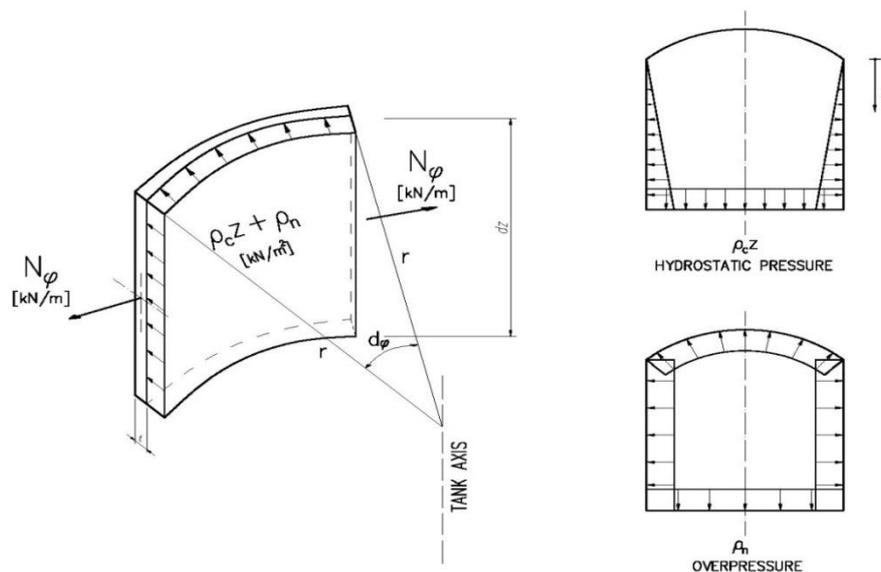
Figure 2: Internal load acting on the considered sheathing plate and generating the tensile hoop force N_φ.

On the other hand, the random resistance of the tank shell plate N_R is limited by the bearing capacity of the weld between connecting plates. Let the coefficient $\alpha_\perp < 1$ constitute the deterministic multiplier specifying the strength ratio of the considered weld to the welded plate. If

the random yield limit f_y, related to the steel of which it was made, is a measure of a plate strength, then the following formula holds:

$$N_R = \alpha_\perp f_y t \tag{2}$$

As one can see, the random resistance of the considered shell plate constitutes a product of two random variables, plate thickness and steel yield limit for the steel of which this plate was made, respectively. Let us assume for simplicity, that those random variables are statistically independent (in reality the yield limit for the considered steel decreases with increasing plate thickness). Besides that, both those variables are in general described by the log-normal probability distribution with the following parameters $LN(\breve{t}, \upsilon_t)$ and $LN(\breve{f}_y, \upsilon_f)$, respectively. By the theorem on stability of the log-normal probability distribution with respect to the product, it follows that random resistance N_R conforms to the log-normal distribution as well, with the parameters $LN(\breve{N}_R, \upsilon_{NR})$. Finally, for the time τ^*, one gets:

$$\breve{N}_R^* = \alpha_\perp \breve{f}_y \breve{t}^* \text{ and } \upsilon_{NR}^* = \sqrt{\upsilon_f^2 + \left(\upsilon_t^*\right)^2} \tag{3}$$

Statistical random plate thickness t distribution parameters, the mean value and the logaritmic coefficient of variation, respectively, are usually estimated based on the data measured during the tank shell technical state inspection, and thus:

$$\ln \breve{t}^* = \frac{1}{N} \sum_{i=1}^{N} \ln t_i^* \rightarrow \breve{t}^* \text{ and } \upsilon_t^* = \sqrt{\frac{1}{N-1} \sum_{i=1}^{N} \ln^2\left(\frac{t_i^*}{\breve{t}^*}\right)} \tag{4}$$

The median yield limit value for the steel $\breve{f}_y$, in the case of missing empirical data gathered during statical tension test, may be easily calculated based on the known a priori characteristic value f_{yk}. This value in turn, for the given structural steel grade, is listed in the code EN 1993-1-1. Subject to the assumption, that it constitutes the lower 2% quantile of a log-normal probability distribution, the following occurs:

$$\breve{f}_y = f_{y,k} \exp\left(2{,}05\sqrt{\upsilon_f^2 + \upsilon_A^2}\right) \tag{5}$$

In the above formula υ_A^2 is the variance covering the variation of geometrical dimensions of the plate cross-section. Let us note, that the variation of this type is usually specified with respect to the nominal thickness of the applied plate. Such nominal value is usually interpreted as the initial average value $\bar{t}(\tau_0)$. In practice this variation tends to increase with the service life, as it covers not only the initial variation in thickness, due to imperfections in steel plate manufacturing process, but also an additional variation due to the random progress of corrosion in individual zones of the plate. This means that $\upsilon_A(\tau_0) < \upsilon_A^*(\tau^*)$. Although this difference is considered in the computational model proposed in this paper at the stage of statistical trend description of the plate thickness loss due to corrosion, it does not find a simple transformation into the correction of the mean yield limit for the steel of which this plate was made. For Polish conditions, based on representative statistical research, it was estimated that $\upsilon_f = 0{,}08$ and $\upsilon_A = 0{,}06$, resulting in:

$$\upsilon_R = \sqrt{\upsilon_f^2 + \upsilon_A^2} = \sqrt{0{,}08^2 + 0{,}06^2} = 0{,}10 \tag{6}$$

In addition, during this analysis it is assumed that the statistical parameters of the steel yield limit do not change during the tank service life, meaning that $\breve{f}_y(\tau_0) = \breve{f}_y^*$ with respect to the mean, and $\upsilon_f(\tau_0) = \upsilon_f^*$ with respect to the logarithmic coefficient of variation. In reality both those parameters depend on the progress of the corrosion process, since this process tends to weaken the steel by the generation of new and amplification of existing microdefects in the crystalline structure. This was shown by the authors of this work in the paper (Maslak and Siudut (2008)). Those effects are so far not estimated quantitatively with sufficient certainty, and thus may not be considered in the formal model proposed here in a reliable manner.

The random parameters pertinent to the probability distributions of external loads applied to the tank, especially hydrostatic pressure ρ_c and overpressure ρ_n, may be taken directly from relevant design codes, provided that appropriate characteristic values, combination rules for the loads and unequivocally specified partial safety factors are listed there (Maslak and Siudut (2007)).

2.2 Failure probability forecasting

The additive convention was selected to illustrate the proposed computational algorithm. This results in the requirement to recalculate all the random parameters, specified for various probability distributions to their Gauss (normal) equivalents, by the classical probabilistic moments method. As a result of such conversion one obtains the normal distributions of the tensioning force $N\left(\overline{N_\varphi}, v_{N\varphi}\right)$ and of the shell plate resistance $N\left(\overline{N_R(\tau)}, v_{NR}(\tau)\right)$, respectively. Let us assume, to simplify the further considerations, that the loading process is stationary during the whole tank service life. This in the turn means that $\overline{N_\varphi(\tau)} = \overline{N_\varphi} = const$ and $\sigma_{N\varphi}(\tau) = \sigma_{N\varphi} = const$, resulting in $v_{N\varphi}(\tau) = v_{N\varphi} = const$ (see Fig. 3). Such an assumption does not mean that the local fluctuations in the load level are disregarded. It means only that the average value of the load level as well as the statistical measures of its scatter do not change during the tank service life. Especially the following holds (σ denotes the respective standard deviation here):

$$\overline{N_\varphi} = \left(\overline{\rho_c}z + \overline{\rho_n}\right)r \qquad \sigma_{N\varphi} = r\sqrt{(\sigma_c z)^2 + \sigma_n^2} \qquad v_{N\varphi} = \sqrt{v_c^2 + v_n^2} \tag{7}$$

$$\overline{f_y} = \breve{f}_y \exp\left(\frac{\upsilon_f^2}{2}\right) \approx \breve{f}_y \qquad v_f = \sqrt{\exp(\upsilon_f)^2 - 1} \approx \upsilon_f \qquad v_t(\tau) = \sqrt{\exp[\upsilon_t(\tau)]^2 - 1} \approx \upsilon_t(\tau) \tag{8}$$

On the other hand it comes out of equations (3) that:

$$\overline{N_R(\tau)} = \alpha_\perp \overline{f_y}\, \overline{t(\tau)} \quad \text{and} \quad v_{NR}(\tau) \approx \sqrt{v_f^2 + (v_t(\tau))^2} \tag{9}$$

Since both the random resistance and the random loading effect are the time dependent functions, the safety margin Δ is also time dependent:

$$\Delta(\tau) = N_R(\tau) - N_\varphi(\tau) \tag{10}$$

Thus:

$$\overline{\Delta(\tau)} = \overline{N_R(\tau)} - \overline{N_\varphi} \quad \text{and} \quad \sigma_\Delta(\tau) = \sqrt{(\sigma_{NR}(\tau))^2 + \sigma_{N\varphi}^2} \tag{11}$$

where $\sigma_{NR}(\tau) = \overline{N_R(\tau)}v_{NR}(\tau)$ and $\sigma_{N\varphi} = \overline{N_\varphi}v_{N\varphi}$. Standardization of the random variable $\Delta(\tau)$ results in:

$$u(\tau) = \frac{\Delta(\tau) - \overline{\Delta(\tau)}}{\sigma_\Delta(\tau)} \tag{12}$$

In general, for the standardized random variable $u(\tau)$ the failure probability $\Omega(\tau)$ may be estimated via the special cumulative distribution function (*cdf*) of this variable specified for the normal probability distribution. This is the well-known Laplace function $\Phi(u(\tau))$, tabulated in the classical statistical tables. Let us note, that the symbol $F(\Delta(\tau))$ denotes as well the cumulative distribution function characterizing the normal probability distribution, though specified for a random variable $\Delta(\tau)$, which in turn may not be standardized. As a result the failure probability is determined by the following formula:

$$\Omega(\tau) = P(N_R(\tau) \le N_\varphi(\tau)) = P(\Delta(\tau) \le 0) = F(\Delta(\tau)) = \Phi(u(\tau)) \tag{13}$$

The failure will occur for the specific value $u(\tau) = u_0(\tau)$, where the random resistance of the corroded plate $N_R(\tau)$, decreasing with the tank service time due to the corrosion progress, equates with the random loading effect $N_\varphi(\tau)$. In such situation $\Delta(\tau) = 0 < \overline{\Delta(\tau)}$ occurs, and thus at the same time $u_0(\tau) < 0$. In heneral it is assumed, however, that the $u_0(\tau)$ parameter is always positive. This means, that the formulation has to be rewritten as:

$$\Omega(u_0(\tau) < 0) = 1 - \Omega(u_0(\tau) > 0) = \Omega(-(u_0(\tau) > 0)) \tag{14}$$

As a result, the equation (13) should be written as:

$$\Omega(-u_0(\tau)) = \Phi(-u_0(\tau)) = \Phi(-\beta_\Delta(\tau)) \tag{15}$$

As on can easily observe, the parameter $u_0(\tau)$ is interpreted here as the global reliability index $\beta_\Delta(\tau)$. The value of this index may be calculated directly by the formula (12):

$$-u_0(\tau) = \frac{0 - \overline{\Delta(\tau)}}{\sigma_\Delta(\tau)} = -\frac{\overline{N_R(\tau)} - \overline{N_\varphi}}{\sqrt{(\sigma_{NR}(\tau))^2 + \sigma_{N\varphi}^2}} \tag{16}$$

The probability $\Phi(-u_0(\tau))$ is usually found using the statistical tables. In this paper an alternative approach is recommended, based on the formula prepared by Warszynski (Warszynski (1988)):

$$\Omega(-u_0(\tau)) = \Phi(-u_0(\tau)) \approx 0.5^{\left[\left(\frac{u_0(\tau)}{2}\right)+1\right]^{2,46}} \tag{17}$$

2.3 Limit state condition

The corroded steel sheet considered in this paper will be able to safely resist external loads applied to it as long as the prognosed failure probability of this sheet will be so low, as to be acceptable to the tank user. This means, that the value of this probability may not exceed the allowable value, which may be specified arbitrarily, but usually is adopted based on the appropriate design codes. The limiting value is usually set so as to correspond to the 50 years reference period of the service life. If the recommendations of the code EN1990 are to be accepted, then for standard safety requirements (reliability class RC2) one gets:

$$\Omega_{ult} = \Omega(-\beta_{\Delta,req} = -\beta_{50,req} = -3.8) \approx 7.2 \cdot 10^{-5} \tag{18}$$

As a result, the corroded plate considered here, will in the future safely resist the loads applied to it, until the following formula will cease to be true:

$$\Omega\left(-u_0(\tau)\right) \le \Omega_{ult} \tag{19}$$

Specification of the limit acceptable failure probability level $\Omega_{ult} = \Omega\left(-u_0(\tau) = -u_{ult}\right)$, yields the capability to determine the allowable value of the reliability index $u_{ult} = \beta_{\Delta,ult} > 0$, as well as the acceptable value of the safety margin $\Delta_{ult}(\tau) > 0$ (the symbol $inv\,\Phi$ denotes an inverse of the Laplace function here):

$$\Omega_{ult} = \Phi\left(-u_{ult}\right) \rightarrow u_{ult} = -inv\,\Phi\left(\Omega_{ult}\right) \tag{20}$$

$$-u_{ult} = \frac{\Delta_{ult}(\tau) - \overline{\Delta(\tau)}}{\sigma_\Delta(\tau)} \rightarrow \Delta_{ult}(\tau) = \overline{\Delta(\tau)} - u_{ult}\sigma_\Delta(\tau) \tag{21}$$

The formulae presented above let us to identify the limit values u_{ult} and Δ_{ult}, if only the maximum failure probability level was accepted by the tank user. In general, statistical tables are applied for this purpose, but the sought values may be directly computed after a transformation of the formula (17) and substitution $u_0(\tau) = u_{ult}$. This yields:

$$u_{ult} = 2\left[\left(-\frac{\ln \Omega_{ult}}{0,693}\right)^{\frac{1}{2,46}} - 1\right] \tag{22}$$

As a result of these findings the limit state condition constituting a replacement of the formula (19) may be written as:

$$u_0(\tau) = \beta_\Delta(\tau) > u_{ult} = \beta_{\Delta,req} \quad \text{or alternatively} \quad \Delta(\tau) > \Delta_{ult}(\tau) \tag{23}$$

The authors of this paper recommend the replacement of those conditions by the condition written in a different format, which seems to be more readable and easier for application by the tank user. Let the symbol $\overline{\gamma(\tau)}$ denote the global average safety coefficient defined as the ratio:

$$\overline{\gamma(\tau)} = \frac{\overline{N_R(\tau)}}{\overline{N_\varphi}} \tag{24}$$

Application of this coefficient to the equation (16) leads to the condition:

$$u_0(\tau) = \frac{\overline{\gamma(\tau)} - 1}{\sqrt{\left(\overline{\gamma(\tau)}\right)^2 \left(v_{NR}(\tau)\right)^2 + v_{N\varphi}^2}} \tag{25}$$

As a consequence, the limit state condition takes the form of:

$$\overline{\gamma(\tau)} > \overline{\gamma_{ult}(\tau)} \tag{26}$$

The minimum acceptable value $\overline{\gamma_{ult}(\tau)}$ may be determined directly from the equation (25), through a substitution $u_0(\tau) = u_{ult}$. This yields:

$$\overline{\gamma_{ult}(\tau)} = \frac{1 + \sqrt{1 - \overline{\left(1 - u_{ult}^2 \left(v_{NR}(\tau)\right)^2\right)\left(1 - u_{ult}^2 v_{N\varphi}^2\right)}}}{1 - u_{ult}^2 \left(v_{NR}(\tau)\right)^2} \tag{27}$$

In this paper it is proposed to denote the moment in service life of the considered tank, in which the ultimate limit state defined by the formulae (23) or alternatively by the inequality (26) is reached, with the symbol τ_d. Then of course the $\tau_d - \tau^*$ time span will constitute an objective measure of the forecast durability of the corroded plate. The methodology proposed by the authors is illustrated in detail in the Fig. 3.
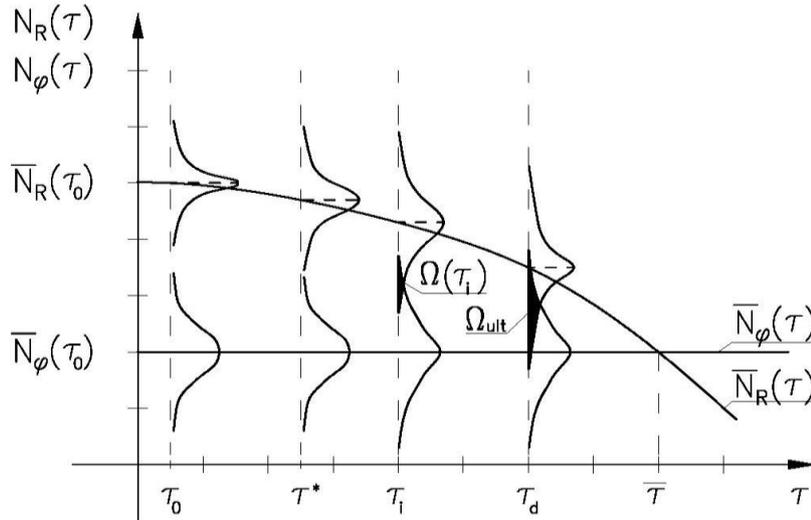
Figure 3:   Interpretation of the ultimate limit state for the corroded plate of a steel tank in service.

2.4 Forecasting the potential sheathing plate corrosion progress during the further tank service

Detailed measurements executed by the authors in situ, on tanks located in one of large fuel depots in southern Poland, allow for the conclusion, that the linear corrosion thickness-loss growth model during tank service sufficiently accurately describes the real corrosion progress in sheathing plates of typical tank shells. As a result the following formula was accepted to describe the previous corrosion process as well as to extrapolate this process for the future service life (Maslak and Siudut (2008)):

$$\overline{t(\tau)} = \overline{t(\tau_0)} - \overline{A}\tau \tag{28}$$

During the technical condition evaluation of the corroded tank shell performed at the time τ^* the evaluator determines the empirical average value of the measured random thickness t^* reduced with respect to the initial nominal thickness $t_{nom} = \overline{t(\tau_0)}$ due to the corrosion. Thus the directional coefficient of the trendline $\overline{A}$ may be determined:

$$\overline{A(\tau^*)} = \overline{A} = \frac{t_{nom} - \overline{t^*}}{\tau^* - \tau_0} \tag{29}$$

This results in:

$$\overline{t\left(\tau^*\right)} = \overline{t^*} = t_{nom} - \overline{A}\left(\tau^* - \tau_0\right) \tag{30}$$

The value of this directional coefficient is assumed to be constant during the whole future service of the tank. Of course, this value will be formally better justified, shall the evaluator have at his disposal the data gathered for the same plates during subsequent evaluations of the tank technical condition, for instance at the times τ^* and later on τ^{**}. Substitution of the value specified by the formula (29) to the formula (28) and consideration of the time $\tau > \tau^*$ leads to:

$$\overline{t(\tau)} = \overline{t^*}\frac{\tau}{\tau^* - \tau_0} + t_{nom}\left(1 - \frac{\tau}{\tau^* - \tau_0}\right) \quad \text{and} \quad \sigma_t(\tau) \approx \sigma_t^*\left(\frac{\tau}{\tau^* - \tau_0}\right) \tag{31}$$

resulting in:

$$v_t(\tau) = \frac{\sigma_t(\tau)}{\overline{t(\tau)}} = \frac{v_t^*}{1 + \dfrac{t_{nom}}{\overline{t^*}}\left(\dfrac{\tau^* - \tau_0}{\tau} - 1\right)} \tag{32}$$

Let us note, that the standard deviation of the random corroded sheathing plate thickness $\sigma_t(\tau)$ is computed in the simplified form here, as the influence of variations in initial plate thickness $t(\tau_0)$ on the final value $\sigma_t\left(\tau > \tau^*\right)$ is disregarded. This variation is an unavoidable result of the commonly accepted mill tolerances allowed during manufacture. This influence is taken into account, however, when the parameter σ_t^* is determined, but only for the time $\tau \leq \tau^*$. During a more detailed analysis the coefficient of variation $v_{t0} = v_t(\tau = 0)$ should be estimated, and quantitative relationship between the random thicknesses t^* and $t_0 = t(\tau_0)$ should be identified as well. However, in general in engineering practice such data is impossible to obtain in case of the steel tanks in service, especially with respect to the time τ^*.

3 Advanced approach – durability analysis for the whole tank sheathing, replication of real tank shell geometry and geometrically nonlinear stress analysis

3.1 Description of the numerical tank model

Simplicity constitutes the basic advantage of the approach proposed above. The durability of each separate tank sheathing plate is determined and out of estimates obtained for all the plates one selects the one yielding the minimum value as authoritative for the whole tank. In such an approach the tank shell is treated as the reliability system working in series, and the plate whose durability determined the global durability of the sheathing constitutes the weakest link in this system. Assumption of the ideal tank geometry in the computational algorithm presented above may raise serious objections. In order to estimate the quantitative and qualitative influence of this simplification on the forecast tank shell durability, the real tank shell geometry was measured on the fully filled tank with geodetic method during the technical inspection performed at the time τ^*. Results of the measurements taken are presented in the Fig. 4, for the levels +1.50 m, +6.00 m and +11.80 m counting from the tank bottom. One may easily observe, that the radial differences between the perfect and the real geometry reached 30 mm, thus exceeding the shell thickness by a factor of four. Knowledge of the real tank geometry was used to create the precise geometrical model of the tank in Abaqus. This model was subjected to analysis, with the resulting von Mises

equivalent stresses and displacements at selected nodes presented in Figs. 5 and 6, respectively. The results calculated using geometrically linear and geometrically nonlinear analysis were compared. The von Mises equivalent stress distributions in the tank shell are presented in Fig. 5 in the following sequence, beginning from the top: a) perfect shell geometry and geometrically linear analysis, b) real shell geometry and geometrically linear analysis, c) real shell geometry and geometrically nonlinear analysis. In addition, the differences in von Mises stresses measured along the selected meridian of deformed shell are presented in Fig. 6. This meridian was selected based on the largest von Mises equivalent stress gradients.

a)   b)

c)   d)
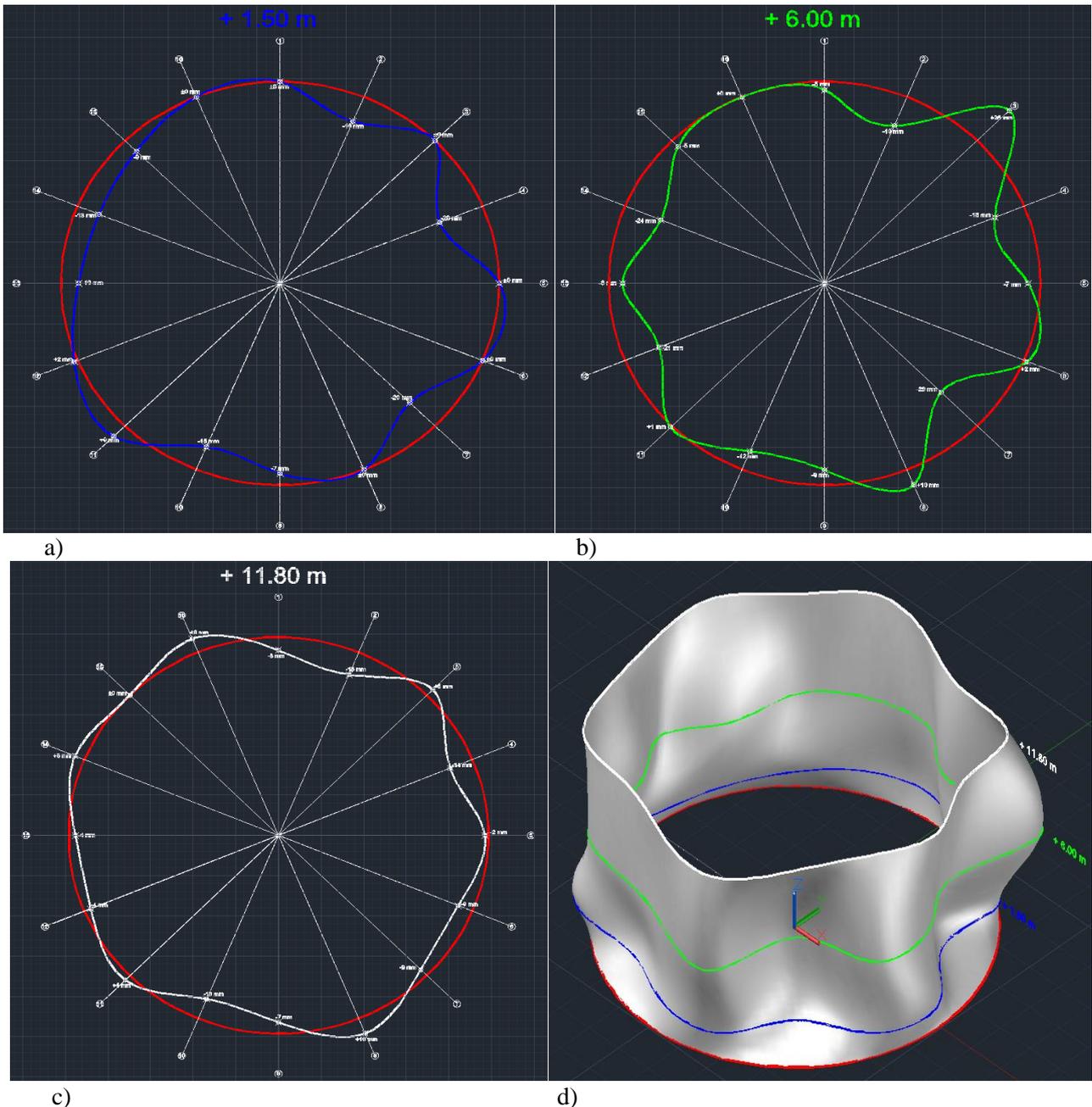
Figure 4:   Shell geometry of the filled tank as measured with geodetic methods, and its image in the numerical model applied. Radial displacements exaggerated 100 times. Levels with respect to the tank bottom: a) +1.50 m, b) +6.00 m, c) +11.80 m, d) deformed tank shell modelled in 3D.
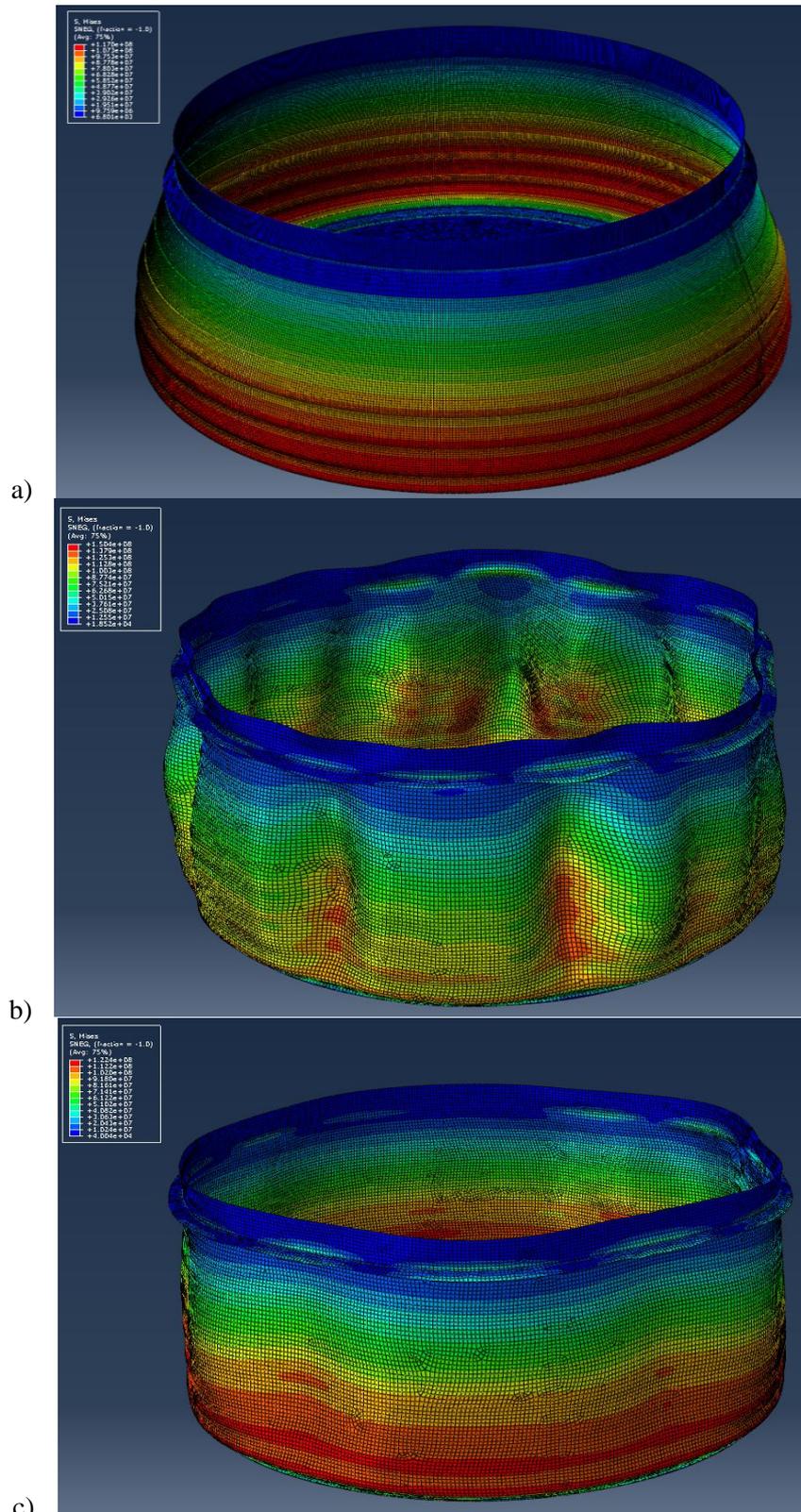
Figure 5: Distribution of von Mises equivalent stresses in the shell of fully filled tank, a) obtained for the perfect tank geometry and geometrically linear analysis, b) obtained for the real tank geometry and geometrically linear analysis, c) obtained for the real tank geometry and geometrically nonlinear analysis.
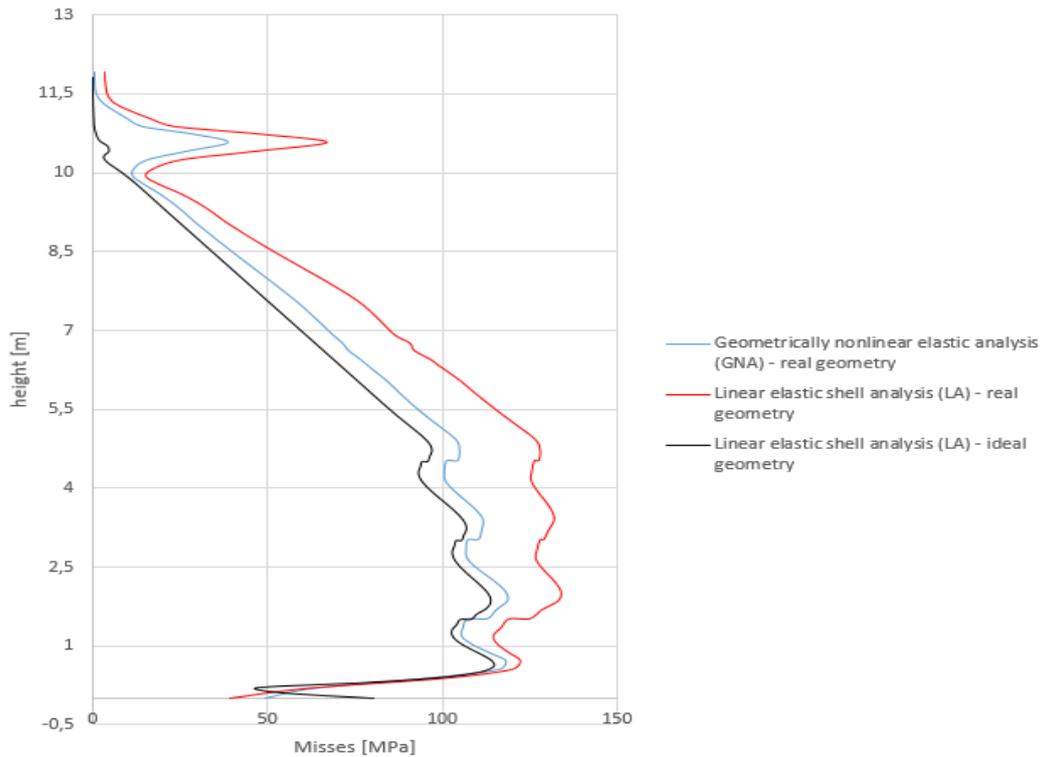
Figure 6: Von Mises equivalent stresses along the selected meridian. The jump in stresses at the top of the shell is due to the influence of the stiffening ring.

3.2 Representation of the shell corrosion state

The corroded shell thickness measurements were performed each time the tank technical condition was inspected, at five points located on each steel plate as shown in Fig. 1. Based on these measurements the corroded plate thicknesses were interpolated over the whole plates, to get the simulated thickness values at the centroids of all the finite elements defined for the purpose of numerical simulation. Results of such interpolation performed for one sheathing plate are shown in Fig. 7. Since the technical staff of the fuel depot does have the data files with corroded sheathing plate thickness measurements executerd during each tank inspection at the same locations, one may calculate the corrosion changes trendline for each of these locations. These trends may be nonlinear. Such trends may be extrapolated for the future service time in the numerical model prepared by the authors. This should allow for a more reliable forecast of the tank durability. At the current stage of analysis the authors are striving to extend the numerical model of the tank, already including the real geometry and nonlinear reaction of the tank material to applied loads to cover the sheathing corrosion state changing during service life, measured during the technical inspections and projected to the future based on identified statistical trends.

Figure 7: Interpolation of the measured values of the thickness of corroded steel sheet selected from the shell of the tank under consideration which allows to adjust the experimental results to the numerical model adopted by the authors (compare to Fig. 1).

4   The concept of evaluating the prognosed durability of a tank in service, based on the bayesian approach combining the a'priori information with a'posteriori measurement data

An attempt will be made by the authors to apply the classical bayesian inference algorithm at the next stage, after the forecast durability estimate of a corroded steel tank will have been made with the methods described above and the results arrived at using both the simplified and advanced methods will have been compared. The state of knowledge available to the investigator at the beginning of the consecutive technical state inspection, including the available thickness measurements of the corroded plates, will be correlated to the a'priori structure state. The random variables used to describe this state, authoritative for the reliability estimates, will be characterized by the a'priori known probability distributions with identified average and scatter parameters. New empirical data will be gathered as the result of the technical inspection, and this data will change the current perception of the object's state. In this sense this will be the information gathered a'posteriori. Initial perception of the technical condition of the tank contains the information I. The a'priori distribution of an estimated parameter θ depends on this information, i.e. $g(\theta) = g_I(\theta)$. The data $\mathbf{x}$ obtained as a result of the new measurement become the argument of the so called credibility function $l(\mathbf{x}; \theta)$. The value of this function denotes the probability (or probability density) of an observation $\mathbf{x}$, when the value of this parameter is equal to θ. It is important, that in order to find the character of the function $l(\mathbf{x}; \theta)$ one must know the probabilistic model describing the random properties of the analyzed object, which are of interest to the investigator. Knowledge of the methods applied to gather the information during research is also required. As a result of these assumptions the Bayes theorem can be applied for inference with the thesis written as follows:

$$h(\theta / x) = \frac{g(\theta) l(\mathbf{x}; \theta)}{\int_{\Theta} g(\theta) l(\mathbf{x}; \theta) d\mu(\theta)} \qquad (33)$$

Application of this theorem will allow the researcher to determine the a'posteriori distribution of the parameter θ. During gathering of the additional information the so obtained a'posteriori distribution may be treated as an a'priori distribution for new observations. The density of the final a'posteriori distribution, after a sufficiently long series of observations will be close to the true distribution density of the parameter θ. Even if two inspectors, due to the different initial information, began with different a'priori distributions, the final a'posteriori distributions obtained by both of them will be similar.

5   Concluding remarks

A simplified and an advanced approaches to estimating the forecast durability of the corroded overground petroleum products storage tank sheathing are proposed and discussed in this paper. The deterioration of the considered steel sheet due to corrosion is in general the continuous process with the intensity being constant, or sometimes even being monotonically increasing, during the tank use. The ratio of such deterioration can be expressed by the suitable reliability index $\beta_\Delta(\tau)$, or by the appropriate safety margin $\Delta(\tau)$. Alternatively, the partial safety factor $\overline{\gamma(\tau)}$ can be applied in this field. All of those measures are quantitatively decreasing when the corrosion is developing. However, an important difference between their ultimate acceptable values must be underlined. Regarding the required reliability index $\beta_{\Delta, req} = u_{ult}$, its value is constant during the

whole time of the tank use. Such conclusion is contrary to the other one, dealing with the values of minimum admissible safety margin $\Delta_{req}(\tau)$ as well as of the ultimate partial safety factor $\overline{\gamma_{ult}(\tau)}$.

Both of those values are changing during the tank use; however, the first of them is decreasing when the steel corrosion is expanding, whereas the second has to be increasing under such circumstances, to keep the constant level of the acceptable failure probability Ω_{ult}.

Contact information

Mariusz Maslak, Dr hab Eng., prof. CUT, Cracow University of Technology, Warszawska 24, Cracow, Poland, phone +48126415673, e-mail mmaslak@pk.edu.pl

References

Law Journal No 113, pos. 1211 (2001) – Rozporządzenie Ministra Gospodarki z dnia 18 września 2001 w sprawie warunków technicznych dozoru technicznego, jakim powinny odpowiadać zbiorniki ciśnieniowe i bezciśnieniowe przeznaczone do magazynowania materiałów ciekłych zapalnych (in Polish).

Maslak M. and Siudut J. (2007). Evaluation of deterioration ratio of randomly corroded side surface sheets in cylindrical steel tanks with vertical axis (in Polish). Ochrona przed Korozją (Corrosion Protection), 12/2007: 456-461.

Maslak M. and Siudut J. (2008). Deterioration of steel properties in corroded sheets applied to side surface of tanks for liquid fuels, Journal of Civil Engineering and Management, 14(3): 169-176.

Maslak M. and Siudut J. (2013). Durability prediction of randomly corroded side surface sheet in steel on the ground tank for liquid fuel storage, in: Silva Gomes J.R. and Meguid S.A. (Eds.). Proceedings of the 4th International Conference *Recent Advances in Integrity – Reliability – Failure, IRF 2013*, Funchal, Madeira, Portugal, June 23-27, 2013, Edições INEGI, Portugal, 2013: abstract 159-160 + CD 8 p.

Warszynski M. (1988). Reliability in structural calculations (in Polish), PWN, Warsaw, 1988.

Monitoring of bridges for calibration of load models

J. Markova, M. Holicky and M. Sykora, Czech Technical University in Prague, Klokner Institute, Czech Republic

Abstract

The Klokner Institute of the Czech Technical University in Prague has a long-term experience with the monitoring of buildings and historical monuments, bridges, cooling towers and industrial chimneys. Monitoring provides valuable information to be used for decision making about maintenance and rehabilitation of existing structures. Obtained data may also be applied for the calibration of partial factors and other reliability elements provided in National Annexes to Eurocodes.

Several road bridges have been monitored in the Czech Republic since the last decade of 20th century, focusing on temperatures and traffic loads. The results of temperature monitoring were statistically evaluated and used for the calibration of the characteristic and design values of uniform and temperature difference components. Long-term measurements of the traffic loads on selected road bridges were applied to specify the national adjustment factors for the load model LM1. Furthermore, special vehicles of the load model LM3 and requirements for their application were proposed in the Czech National Annex to EN 1991-2 (2003).

Several problems had to be solved during the monitoring including the selection of technique, suitable position of monitoring devices on a bridge, data transmission and backup, uncertainties in measurements and defects of hardware.

1   Introduction

After few years of application of Eurocodes for the design of bridges in the Czech Republic, the Nationally determined parameters (NDPs) of the traffic load models for road bridges were newly analysed and recalibrated. The first selection of NDPs for EN 1991-2 (2003) focused on traffic load models was mainly based on requirements of the Ministry of Transport to maintain costs for new bridges in comparison with those designed according to the previous Czech standards. There was no past experience with applications of partial factor method for bridge design (the method of permissible stresses was used only). That is why a value of 0,8 for all the adjustment factors was firstly accepted for highways, speedways and main roads in the Czech National Annex to EN 1991-2 (2003).

In the first period of the application of Eurocodes in the Czech Republic it was not obligatory to take into account the special vehicles of the Load Model 3 (LM3). This model was nationally applied for bridge design under specific requirement of a responsible public or regional authority. Therefore, it was not assured that all bridges on a given category of roads would have the same bearing capacity.

Considering the current needs and new experience with application of Eurocodes for the design of bridges, the adjustment factors of the Load Model 1 (LM1) and special vehicles of the model LM3 were analysed and proposed for the new Amendment of the Czech National Annex to EN 1991-2 (2003). The results of long-term monitoring of several bridges were taken into account to support the final decision. Selected results of comparative analyses are presented below.

2   Bridge monitoring

2.1 Selected bridges

The traffic intensity, weight of heavy vehicles and temperatures were monitored on two road bridges. The first bridge is a prestressed concrete box girder bridge in the highway across the river Ohre in West Bohemia with the periods of monitoring from 2005 to 2006 and from 2011 to 2013. The second bridge is a composite steel concrete bridge situated near the exit of the Lochkov tunnel in the Prague ring across the Slavici valley (period of monitoring 2011 to 2013), see Figure 1.

Figure 1: Trucks crossing the composite steel concrete bridge

2.2 Instrumentation

The bridge response was monitored by strain gauges installed on the bottom flanges of four longitudinal steel girders in the middle part of the abutment span of the bridge. A computer was installed on the bridge as a control unit. Obtained data were periodically transmitted to the Klokner Institute for further analysis.

2.3 Results of measurements

Basic outputs of the monitoring are the time histories of axial stresses at bottom flanges of steel beams, see an example in Figure 2. The attention was focused on passage of vehicles with total weight exceeding 100 kN. Time of the passage, the number of traffic lanes and the maximum axial load value were assigned to each vehicle. Total number of heavy vehicles passed over each traffic line in the period of monitoring from 01/2013 to 11/2013 is presented in Table 1.

Table 1 Relative and absolute number of heavy vehicles

Lane No.	Left (fast) lane (N5)	Middle (fast) lane (N6)	Right (slow) lane (N7)	Highway shoulder (N8)	Total number
No. of vehicles	941	52215	941915	2974	998045
Percentage	0,09	5,23	94,38	0,30	100

Averaged number of heavy vehicles passed daily through the bridge during a week is given in Table 2. A significant difference between working days and during weekends, and also before or after a holiday was detected. Seasonal changes can also be distinguished in each year of bridge monitoring.

Table 2 Average number of heavy vehicles (based on averaged 33 weeks)

Day	Monday	Tuesday	Wednesday	Thursday	Friday	Saturday	Sunday
No. of vehicles	5908	5313	4888	4729	3900	1664	1499
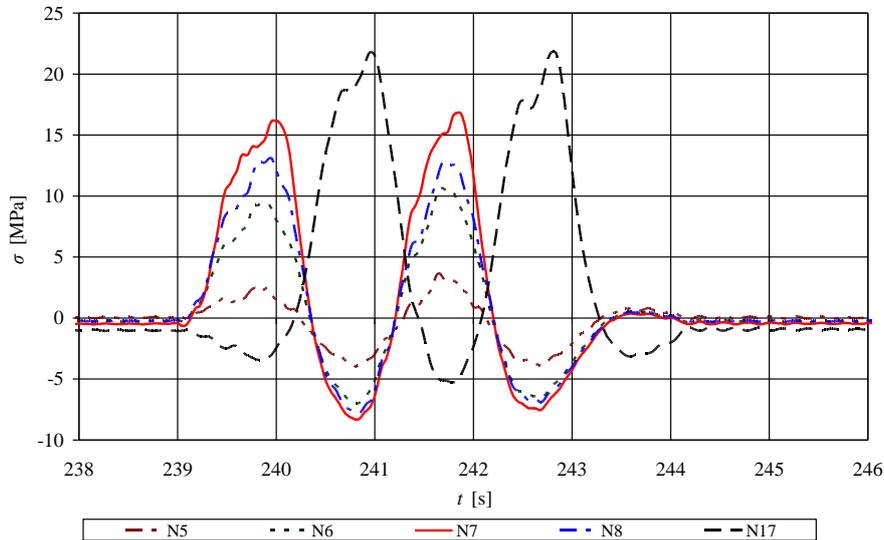
Figure 2: Example of time history of the axial stresses in bottom flanges of girders during the passage of heavy vehicles.

A number of vehicles with respect to their total weight in kN considering spring and summer of 2012 year is illustrated in Figure 3.
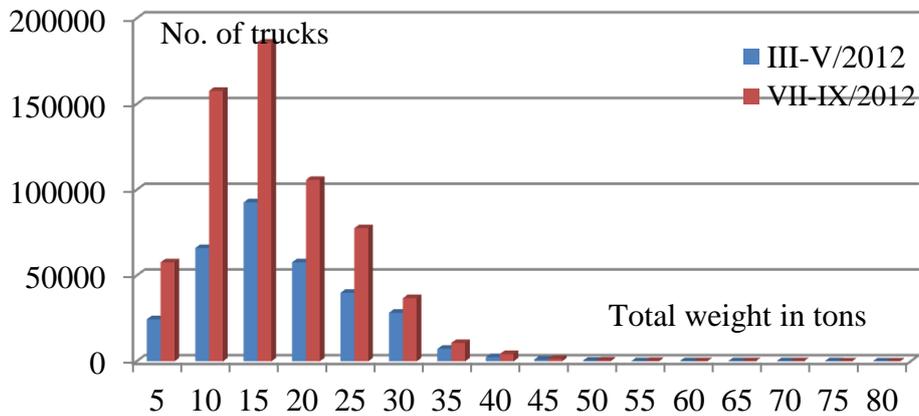
Figure 3. Number of vehicles with respect to their total weight in kN for spring and summer of 2012.

The histogram of a number of vehicles with respect to their total weight in kN is indicated in Figure 4 for selected days: Monday (1), Wednesday (3) and Sunday (7).
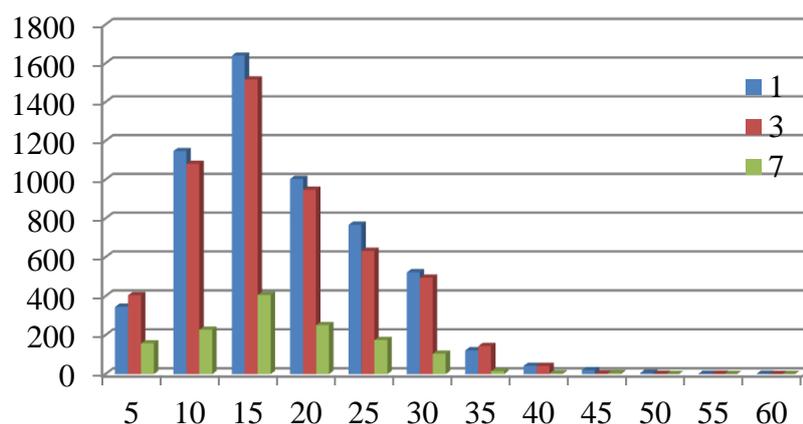
Figure 4. Histogram of a number of vehicles with respect to their total weight in kN.

3   Analysis of models LM1 and LM3

3.1 Adjustment factors and models of special vehicles

The adjustment factors of the model LM1 given in EN 1992-1 (2003) have been analysed on the basis of selected countries. Reports (2009, 2013) provide additional background information.

Nationally selected values of adjustment factors α_Q and α_q of the load model LM1 and decision on application of the model LM3 for highways and other types of main roads of some CEN Member States including the Czech Republic (before recalibrations) are given in Table 3.

Table 3. National decision on adjustment factors of LM1 in selected CEN countries.

Country	α_{Q1-3}	α_{q1}	α_{q2}	α_{qn}
Austria	1	1	1	1
Czech Rep.	0,8	0,8	0,8	0,8
France, Italy	1	1	1	1
Germany	1	1,33	2,4	1,2
Finland [1]	1	1	1	1
UK	1	0,61	2,2	2,2
Netherlands [2]	1	1,15	1,15	1,15

[1] uniformly distributed load 45 kN/m^2 in area (0 to 10 m) $\times$ 3 m considered as exclusive load, for private roads (not administrated by Finish transport agency) $\alpha_Q = 0,8$, the bridge clearness of 7 m is defined for specific routes

[2] for high intensity of heavy tracks and three or more traffic lanes $\alpha_{Q1} = 1,15$ and $\alpha_{q1} = \alpha_{q2} = 1,4$

In the Czech Republic, the roads are divided into Group 1 (highways, speedways and 1st to 3rd class roads), and Group 2 (special 3rd class roads specified by relevant authorities or other purpose roads). Table 3 indicates that the first Czech selection of adjustment factors in the nationally implemented EN 1991-2 (2003) based on a unique value of 0,8 for Group 1 roads (0,6 for Group 2) is rather low. Most of European countries have accepted recommended values of adjustment factors. It should be noted that Slovakia has decided to apply similar values of adjustment factors like the Czech Republic (slightly increased to 0,9 for Group 1 roads).

Analyses and calibrations resulted in recommendation of new, higher values of the adjustment factors for the Amendment of the Czech National Annex to EN 1991-2 (2003) as indicated in Table 4 for the roads of Groups 1 and 2.

Table 4. New adjustment factors of LM1 for roads of Groups 1 and 2

Road group	α_{Q1}	α_{Q2}	α_{Q3}	α_{q1}	α_{q2}	α_{qi}
1	1	1	1	1	2,4	1,2
2	0,8	0,8	0,8	0,45	1,6	1,6

4   Specification of Model LM3

A growing demand of industry and previous experience with special determined traffic routes revealed a need for specification of special vehicles of the model LM3. Two types of special vehicles (1800/200; 3000/240) were recommended for highways and speedways considering specific requirements for simultaneous traffic in other lanes. For 1st and 2nd class roads the special vehicle (1800/200) is recommended. No special vehicles were proposed for the roads of the Group 2.

The models of braking and acceleration forces in the National Annex to EN 1991-2 (2003) were improved. Newly the value of braking force depends on the weight of applied special vehicle located in the lane No. 1 and on potential other uniform load in the lane No. 2. Its maximal value is restricted to 600 kN.

5   Conluding remarks

Comparative studies, results of monitoring and probabilistic analyses of selected bridges in the Czech Republic revealed that reduced adjustment factors of the load model LM1 recommended in the first version of the National Annex to EN 1991-2 are lower than those used in the original Czech standards and should be increased. Furthermore, the special vehicles according to the load model LM3 should be taken into account.

The new set of adjustment factors is proposed for the Amendment of the National Annex to EN 1991-2. Moreover, two types of special vehicles (1800/200, 3000/240) were selected on the basis of the load model LM3. It is assumed that application of the model LM3 for bridge design will enable transport of heavy industrial devices and could also serve for military and other special purposes.

It is expected that the road traffic monitoring of selected bridges and their evaluation will continue, aimed at further analyses of load effects including overloaded heavy trucks.

In the framework of the COST Action TU1402 the database of traffic load effects and experience from experimental investigations could be utilized to provide information for monitoring of road bridges with respect to fatigue and loads due to heavy vehicles. Analysis of the database supplemented by appropriate structural verifications could lead to recommendations concerning the design of structural members and frequency of collecting data to be used for the development of fatigue models and for further improvement of load model LM3.

Contact information

Jana Markova

Assoc. Prof., Czech Technical University in Prague, Klokner Institute
+420 224353501
jana.markova@klok.cvut.cz

References

CSN 73 6203 (1987). Actions on bridges. UNMZ

CSN 73 6222 (2012). Load bearing capacity of road bridges. UNMZ

EN 1990 (2002). Basis of structural design - Applications for bridges. CEN

EN 1991-2 (2003). Eurocode 1 Actions on structures: Part 2 - Traffic loads on bridges.

Final Activity Report (2009). Assessment and rehabilitation of Central European Highway Structures. Arches - MG - DE 15

Final Research Report. (2013). Optimization of reliability and working life of existing bridges, TA01031314, CTU in Prague, KI. Czech Republic.

Markova, J. (2012). Probabilistic Assessment of Working Life for Bridges, In: Life-Cycle and Sustainability in Civil Infrastructure Systems. London: Taylor & Francis. pp. 2233-2238. ISBN 978-0-415-62126-7

Marková, J., Holický, et al. (2013). Probabilistic Analyses of Traffic Loads on Bridges. In: Safety, Reliability, Risk and Life-Cycle Performance of Structures and Infrastructures. Leiden: CRC Press/Balkema. p. 3749-3753. ISBN 978-1-138-00086-5.

Finding a link between measured indicators and structural performance of concrete arch bridges

Ana Mandić Ivanković, Faculty of Civil Engineering, University of Zagreb
Jure Radić, Faculty of Civil Engineering, University of Zagreb
Mladen Srbić, Faculty of Civil Engineering, University of Zagreb

Objectives, abstract and conclusions

Objective of this paper is to establish the relationship between the research on existing arch bridges in Croatia and objectives of the Working Group 2– SHM technologies and structural performance of the COST action TU 1402. Research on development of assessment procedures for existing arch bridges is developing through last few years in Croatia as a part of an extensive project to develop their appropriate maintenance strategy. We believe that this experience is a good basis to create a valuable link between a certain indicator measurement and corresponding structural performances of interest for arch bridges.

Figure 1: Flowchart of a proposed research activity
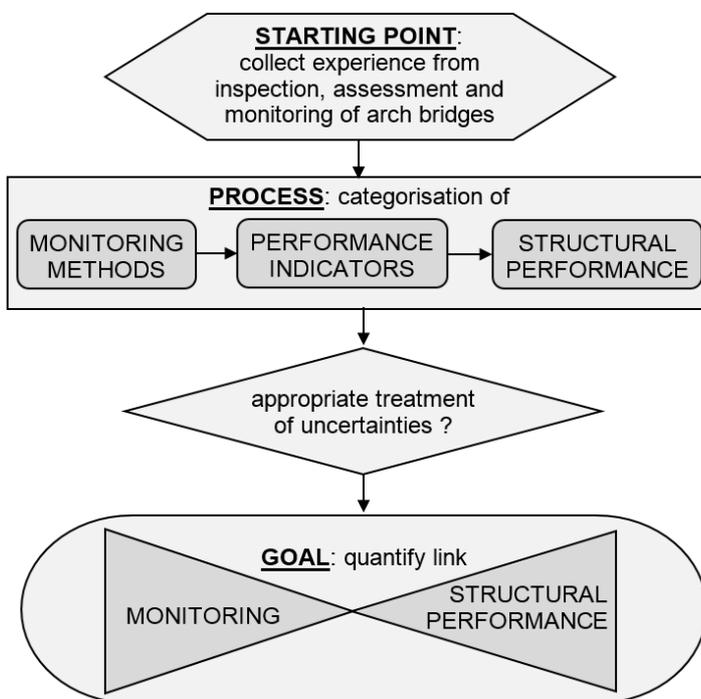
One of the causes for rapid structural degradation of the first generation of Croatian Adriatic arches was underestimation of maintenance role in the past, mainly due to lack of funding for regular maintenance activities. More recently constructed arch bridges of second generation are designed taking into account the experience from in-service performance of older arch bridges and are equipped with a range of sensors for long-term monitoring, but again due to lack of founding those are not exploited appropriately. To eliminate the errors of the past and ensure efficient and effective performance of existing but also the future concrete arch bridges, the appropriate monitoring and maintenance strategy should be further developed.

In this paper, the idea of the activity flow with particular steps of the process to establish this relationship between Croatian research and WG2 objectives is elaborated (Figure 1).

Upon collecting experience on Croatian arch bridges, the categorization of monitoring methods, performance indicators and structural performances are to be deliver. Uncertainties in measuring data, collecting data and combining appropriate performance indicators that affect certain structural performance should be appropriately treated within the theoretical framework of this COST Action.

An overview of inspections, repair, monitoring and assessment of large Adriatic arch bridges, as a starting point of the activity, will be presented in more detail in this paper.

1 Introduction

Numerous issues need to be considered in order to achieve efficient and effective performance of existing concrete arch bridge. To define a correct structural model of the existing structure and to perform adequate structural analysis in order to properly assess the existing bridge it is necessary to identify desired knowledge level of the existing structure based on the bridge importance. For the bridges of the average importance that are not critical for communications, lower knowledge level may be required together with a higher value of confidence factor to determine properties of existing materials. For bridges of critical importance for maintaining communications, especially in the immediate post-accidental period and for major bridges where longer design life is required the higher knowledge level would be necessary with a lower value of confidence factor.

In order to get a valuable link between a certain indicator measurement (performance indicator) and corresponding property of structure (structural performance) of interest at the desired knowledge level, it is of a great importance to establish adequate data collection using approporiate methods (SHM methods) for arch bridges.

Therefore the first step of a research is to identify monitoring methods in regard to the quantity that is indicated, the second step is to categorise performance indicators important for efficient and effective performance of arch bridges and the third step is to define all types of structural performances important for arch bridges (Figure 2).

The final goal of the research, in accordance with the WG2 intention, is to find adequate relations between each step with appropriate treatment of uncertainties. Between the first and the second step, where we need to establish which monitoring method (technique) is to be used for measure certain quantity in order to define adequate performance indicator, uncertainties in measured data and in collecting data may appear. Beetwen the second and the third step of a research process, while capturing all the indicators that affect certain structural performance, uncertainties in combining appropriate indicators should be appropriately treated.
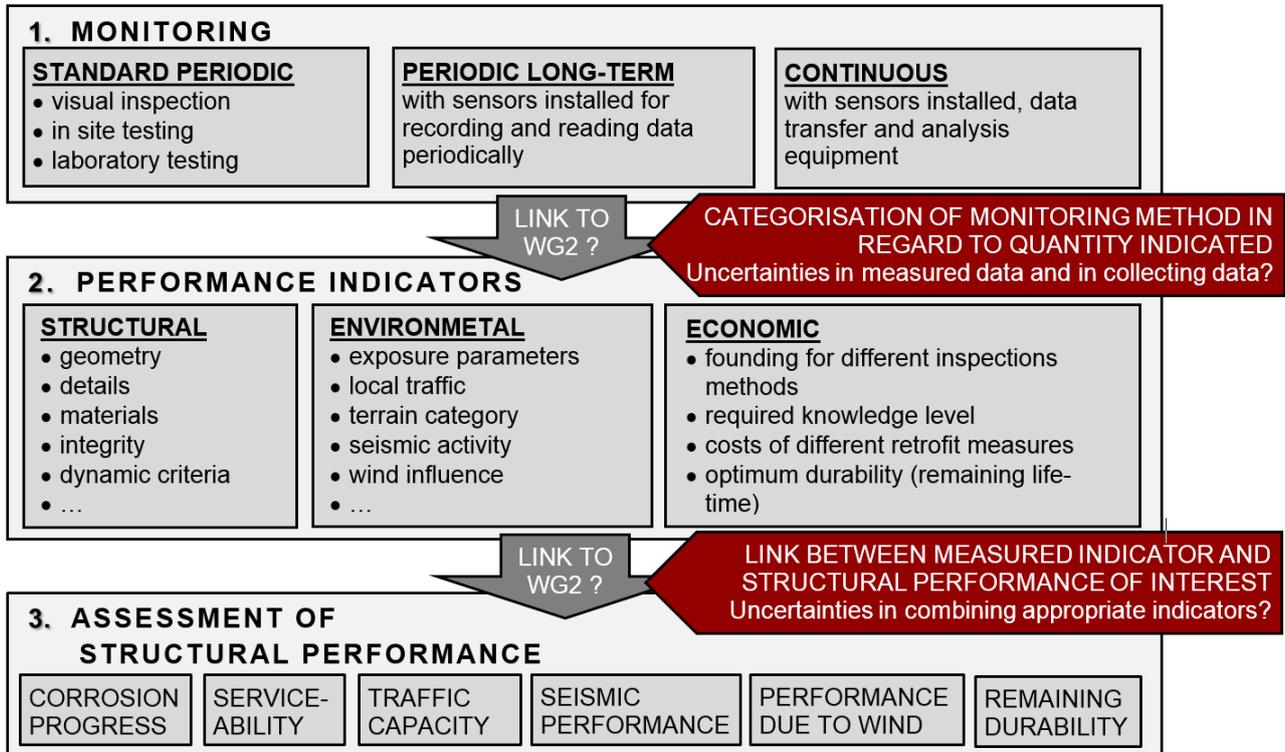
Figure 2: Research steps for quantifying the value of SHM of arch bridges

The experience with Adriatic arch bridges would be a solid base to prepare comprehensive guidelines for data collection on arch bridges to reach required knowledge level and to properly assess their performance abilities. Hopefully this paper, together with the paper submitted for the IABSE Conference 2015 (Mandić Ivanković et al. 2015), will present the start of this work plan to be further developed under the auspices of COST Actions TU 1402 and TU 1406.

2   Monitoring

According to COST 345 report (2008), monitoring can be defined as any periodic or continuous operation where the behaviour of a structure or structural components is quantified in some way so that its serviceability and stability can be evaluated. Reliability of a condition assessment of a structure will depend on the quality of the inspection. Two types of inspection can be considered:

- standard periodic inspections which will provide data on the structural condition in a particular time, but immediately after the inspection damage can be inflicted and deterioration processes can commence or accelerate which will require remedial works when the time between successive inspections is too long,
- continuous or long term monitoring with sensors installed at the structure, complete with data transfer and analysis equipment, to provide the data required to continuously and remotely track the condition of structure

In such sense SHM as a wider term, comprise standard inspection techniques performed periodically but following regular maintenance plan and continuous or periodic but long-term measurements of time variant measures.

Examples of standard inspection and investigation methods that are used in particular time at the Adriatic arch bridges are:

- geometrical surveying, visual inspection, loading tests,
- non-destructive methods such are: hammer sounding, rebound hammer, half-cell potentials, ultrasonic method, crack width measurements, …
- destructive test such are: pull of test, taking cores for laboratory testing for physical and mechanical properties, for permeability properties, for alkalinity properties and chloride content, for bond strength, ...

Additionally at the Skradin and Cetina bridge monitoring systems allows:

- periodic long-lasting displacement measurements with respect to the stabilized permanent datum marks
- periodic measurements with the help of anode-ladder sensors installed during construction to evaluate the corrosion progress.

Examples of measures that may be measured continuously are:

- strain, temperature and humidity on the structure of Skradin and Cetina bridge
- strain, acceleration, temperature, humidity, wind speed and direction and corrosion progress at Maslenica bridge and
- strain and temperature at two piers of the smaller Krk bridge.

3   Performance indicators

The performance indicators of arch bridges may be grouped as structural, environmental and economic. Structural indicators may be listed as:

- geometry (arch and pier axes, superstructure grade line, cross-section dimensions, …);
- details (built in reinforcement including amount and detailing of longitudinal and shear reinforcement and amount and detailing of confining reinforcement in critical regions, depth of concrete cover, connection between members (arch-pier, pier-superstructure, arch superstructure, continuous superstructure or the simply supported set of beams), support conditions, surface conditions,…;
- material properties (concrete strength, steel yield strength, modulus of elasticity, ..).

Additionally, dynamic criteria such are the required participation of effective modal masses, adequate stiffness distribution of spandrel columns and determination of reference point for forming capacity curves, need to be properly incorporated in seismic assessment (Franetović et al. 2014).

Environmental indicators include exposure parameters (of which most dangerous are sea-water splashing, tides, de-icing agents), local traffic, seismic activity, terrain category, wind influence.

Over the years, many deficiencies and advanced stage of deterioration processes were identified on older Adriatic Bridges. Chloride attack due to maritime exposure, followed by cracking, delamination, splitting and peeling off of concrete is identified as major deterioration mechanism (Radić et al. 2006).

Economic parameters will comprise, on one hand, founding for different inspections methods for establishing desired knowledge level of existing structure and, on the other hand, costs of different retrofit measures that may be offered based on the bridge assessment results.

4   Structural performances

Assessment of an existing reinforced concrete arch bridge comprises assessing bridge serviceability, its capacity for traffic, seismic performance and performance due to wind load (Mandić et al. 2010). Revealing corrosion progress is important to identify the effect of deterioration on the structural performance of each type. Based on those performance aspects, the prediction of service life (remaining lifetime) of the bridge in agreement with optimum durability request should be established.

Interaction of all types of indicators in assessing a performance of an existing arch bridge is inevitable. Some examples are as follows.

- Cross section dimensions might be changed due to deterioration processes from combined exposure to the sea and wind or on the other hand because of applied repair activities. This may result in reducing or improving a certain structural performance ability.
  Numerical model for realistically simulate the corrosion of reinforcement is currently under development. The structural health monitoring system installed on the Adriatic arch bridges could provide valuable data for verification and improvement of the model, but also for the more precise determination of relevant parameters (Radić et al. 2012)

- Recorded representative real traffic data need to be multiplied by a dynamic amplification factor that depends on the roughness and the quality of the pavement. At the first assessment level, for the realistic traffic simulation, data of the year average daily traffic at the location with the largest number of heavy vehicles in whole country may be enough. Only at the second level of assessment (when the first one failed) the traffic load may be even more localized by using data of traffic flow at the exact bridge location as elaborated in Mandić et al. 2010.

- To define design response spectrum representing seismic action, the behavior factor based on ductility capacities of the structure needs to be adopted and on the other hand, the distribution of load for different pushover methods will depend on significant mode shapes of the structure. Ductility capacities of the structure will depend on detailing of confining reinforcement in critical regions (Franetović et al. 2014) and mode shapes of the structure might be changed due to changes of stiffness or structural joints for example.

- Wind load on a bridge will depend on slenderness of elements (which might be changed due to deterioration or with repair as shown at the Krk bridge example in Mandić Ivanković et al. 2014), parapets types (due to adding windshields to provide better serviceability) and the angle between the dominant wind direction and the bridge axis.

Economic parameters are hidden in required knowledge level for a particular bridge in accordance with its importance and consequences of its failure. Higher knowledge level will require more extensive inspection works and comprehensive bridge monitoring. In general, Inspections of major bridges are more exhausting and require well-experienced personnel to identify the damage and determine its cause and consequences. However, we need to be aware that the extent of

inspections and test would greatly depend on the available costs provided by the investor so very often the engineer will need to assess the bridge condition based on a limited data collection. Therefore, it is of a great importance to establish the most significant locations of the arch bridge to be inspected, tested and monitored (Mandić Ivanković et al. 2015). Additionally the most critical structural cross sections are the ones evaluated as damaged in the visual inspection.

5 Collecting experience from Adriatic arch bridges

The Šibenik bridge spanning 246 m, built in 1966 was the first in the world to be constructed entirely by the free cantilevering method. The Pag bridge completed in 1968 with a span of 193 m is very similar in appearance and design. Three-cell box arches gradually increase depth from the springing towards the crown. They were constructed by suspended cantilever method with temporary stay cables and tie-backs anchored into the abutments of the superstructure at Šibenik bridge and directly into the rock at Pag bridge. Krk bridges, constructed in 1980 by an innovative procedure forming a trussed arch cantilevers, consists of two large reinforced concrete arches, of 390 m and 244 m span. Both arches are of three-cell box cross-section. To achieve exceptionally large spans it was necessary to reduce the dead load as much as possible. The structural members of minimum statically admissible dimensions were utilised, with very small concrete covers. The original superstructures of all those Adriatic bridges of first generation were designed as a series of simply supported grillages consisting of precast prestressed concrete girders joined by cast-in-place cross beams at supports and in the thirds of span.

More recently constructed Maslenica and Skradin bridges, serving two-lane carriageways, and Cetina bridge for a state road, are designed taking into account the experience from the in-service performance of older arch bridges and are equipped with a range of sensors for long-term control of stresses, strains and corrosion progress. The intention was to closely monitor both structural performance and durability related performance in order to facilitate the future maintenance activities by triggering timely adjustments and interventions (Radić et al. 2012).

5.1 Inspections and repairs of the first generation of Adriatic arches

The **Šibenik Bridge** is somewhat less exposed to aggressive maritime environment than other long span concrete arch bridges (Radić et al. 2003). The grade line of the Šibenik bridge was designed in one way slope with the convex camber of 5 cm. Already after 10 years of service, the grade line above the arch crown was 30 to 35 cm below the designed level (Figure 3 left). Namely deformations of arch due to the creep and shrinkage were much larger than anticipated in the design. The bridge was thoroughly inspected in 2005 (HIMK 2005). This was just third major inspection performed on this bridge over its 40 years history.

Following data were collected by geometrical surveying:
- arch (grade line of axis and top edge) at the distance of 5 m,
- roadway (grade line at the middle and at both edges of roadway next to curb, grade line of upper edges of both curbs and both cornices) in the cross-sections at abutments, piers, mid span and arch crown).

Visual inspection (Radić et al. 2008) comprised inspection of:
- traffic surface and adjacent bridge equipment: asphalt wearing course, sidewalks, railings, drainage system, expansion joints and bearings. They were checked for deterioration, cracking, water tightness and proper functioning (locking of expansion joints and bearings).
- massive structural concrete members were inspected for cracks, wetting, deficiencies in concrete cover, corrosion, honeycombs, splitting, scaling, spalling and delamination using special vehicle for inspection of hardly reachable parts of bridge.

Additionally,
- limited material testing comprising measurements of chloride ingress by rapid chloride test
- and measurements of concrete cover thickness

were performed at 20 locations of the bridge.

The most affected areas are at superstructure supports, designed as half-joints, where cracks opened in roadway slab above, allowing ingress of water as no waterproofing was installed.

Figure 3: Deflected vertical alignment of the Šibenik bridge built in 1966 (left) and deterioration of the superstructure (middle) and columns (right)

This is the main cause of deterioration of main griders and cross beams above pears (Figure 3 middle) showing poor condition of concrete (concrete cover spalling) and corroded steel reinforcement. Concrete sealing of cable ends are greatly damaged, and at few places even corroded cables are sticking out (Medak et al., 2006). Additionally, traces of wetting, cracks, corroded reinforcement and delaminations (Figure 3 right) were detected at most structural elements, but were not deemed to be critical for immediate repair. Measurements of concrete cover thickness fall into range of 4 to 80 mm, with the mean value of 37 mm. The chloride ions content testing showed that critical values were exceeded only at the location of arch springings.

Repair works on the **Pag Bridge** started already after a decade of its service, but did not prove efficient in terms of stopping the corrosion process. The detailed concrete arch inspection in the year 1998. showed severe cracking near the arch springings and peeleng off of the concrete cover at approximately 10 % of exposed surfaces due to the reinforcement corrosion. Arch deflections under test load were 25% larger than under the same loads in the first test performed prior to bridge opening. These disturbing results called for complete repair of the arch, comprising removal of the damaged concrete cover by a hydrodemolition device, grouting of all visible cracks, placing shotcrete minimum 4.0 cm thick strengthened by anchored reinforcement mesh and protected by special long-lasting elastic coating (Bleiziffer et al. 2011). These works were carried out in 1991. Both the superstructure and piers deteriorated even more inducing serious functional difficulties.
Major reconstruction commenced in 1999 when the original concrete superstructure was dismantled and replaced (Figure 4 left) by a completely new structure in steel (Šavor et al. 2008). The structural solution comprising steel provided reduction in the weight of the structure allowing for the increase in traffic design loads. It is important to notice that the dead load was already increased by 9.3% in 1991 with the measures applied for the repair of the arch. The bridge reconstruction solution comprising steel enabled that, after the new superstructure and column strengthening was executed, the dead load was 9.7% smaller than in the original bridge design. The new superstructure is lighter than the original one, but since the arch axis is designed as a thrust line for a certain permanent load, the distribution of lighter permanent load can be unfavourable and adversely affect the arch behaviour. The calculations revealed that the arch is capable of withstanding new loading within the designated threshold level only if the arch reinforcement contributes in the compressive zone and if the actual measured compressive concrete strength corresponding to Eurocode concrete class of C-50 is accounted for. The original design was based on the concrete grade C-35. Prior to the bridge re-opening to service the proof testing was carried out. The static and dynamic testing of the renovated bridge proved the

accuracy of the assumptions incorporated in the reconstruction design calculations, as the numerical and experimental results agree well. Columns were repaired by encasing in steel and concrete.

The latest inspection was carried out in 2009 (Bleiziffer et al. 2011) focusing on steel structure, but limited testing and visual inspection of the accessible parts of the arch were carried out as well. Inspection works included:

- visual inspection which revealed cracks, evidence of water penetration through cracks, seepage in from of calcification, corrosion stains, delamination, spalling of shotcrete and places with exposed corroded reinforcement ,
- hammer sounding which indicated delamination and cracks,
- rebound hammer to access concrete quality in-situ,
- half cell potential measurements at locations were visual inspection indicated active corrosion process revealed either medium or high risk of corrosion or parts where corrosion already propagates.
- laboratory testing of 19 concrete core samples
    - for physical and mechanical properties (concrete strength and modulus of elasticity),
    - for permeability properties (capillary absorption and gas permeability) indicating concrete quality,
    - for alkalinity properties and chloride content which at the reinforcement level is either below or above the critical value
    - for mortar/concrete adhesion
    - for shotcrete and coating thickness

These revealed substantial defects in the reinforced concrete arch protection system (Figure 4 right) and that further assessment works are necessary.

Figure 4: Pag bridge originally built in 1968 was repaired in 1999: new steel superstructure was installed by launching truss (left); delamination at the edge of the arch abutment as an example of defects in rc arch protection system (right, Bleiziffer et al. 2011)

Krk bridges are located in very aggressive marine environment including very high salinity (approximately 3,5%), very strong winds carying sea spray and winter drops of temperature below freezing point. They were designed with a too thin designed concrete cover of only 2.5 cm and althougt it had been planned to apply protective coating to the entire structure, only some parts were protected: some with epoxy coating and some with brittle polymer cement mortar (Ille et al. 2011). The former, as it is known, was not physically compatible with concrete and the latter as porous brittle coat even increased surface chloride concentration and penetration in concrete.

Maintenance works of the reinforced concrete structure of Krk Bridge started immediately after opening for traffic. (Beslać et al. 2010). The first general monitoring and restricted testing were performed in the years 1985 and 1986. Testing was restricted because the main part of the structure was not accessible. The conclusion was that the whole reinforced concrete structure

must be protected. Towards the end of 1980's more than 20 protective systems were tested on-site in order to find the best solution for the protection of the entire reinforced concrete structure. Only two or three of them were partly satisfactory. Some of them that have being forced for the application made the reinforcement protection even worse. The reinforcement corrosion was accelerated, what is understandable because 1 to 2 cm of very good concrete cover was removed and replaced with more porous mortar. At the time, there were no chloride impermeable coats. Some parts of the bridge near the sea level were protected with best of those systems but they did not solve the problem. They helped only by the absorption of chlorides in the added mortar and prolongation of their penetration in the concrete. Examination of the underwater foundation elements of the larger arch revealed that their surface was covered by sea flora and fauna and concrete cover was damaged by the sea shell dwellings.

The repair works on the Krk Bridge started several years after its completion focusing on superstructure supports. Stiff framed connections between columns and longitudinal girders with cross girders were greatly deformed and cracked, probably because of concrete shrinkage and temperature change (Beslać et al. 2008). The bearings were completely reconstructed on 20 of 31 columns. Affixed connections through cross girders were destroyed, elastomeric bearings were built in and new pretensioned cross girders executed. This was done on the big arch bridge before more than 20 years ago.

In the 1990's, when very complex multipurpose moveable scaffolding was constructed specifically for the Krk Bridge, the works were broadened to include the repair of columns (Figure 5). Different repair techniques had to be devised for spandrel and approach columns. In general on short columns and on high columns above 15 m above sea level, 2 cm of concrete cover was demolished and reconstructed with 2 cm of high quality repair mortar M45 and polymeric coating and in some parts with 5 cm of high strength micro-reinforced concrete MC60/75 and impregnation. It was considered that weakened cross section of short columns (about 15%) is compensated by the increase of compressive strength of concrete, from concrete grade C40/50 after bridge construction up to C60/75 which was estimated lately on a number of cores from the structures. On lower parts of high columns, up to 20 m above sea level, from which 3 cm or even more of concrete cover was demolished, reconstruction was made with 5 cm of high strength self-compacted concrete MC60/75 reinforced with 50 kg steel fibres per m3 of concrete volume (Beslać et al. 2008, IGH 2001). The concrete was designed to be of the same compressive strength and static modulus of elasticity as the concrete in columns (C60/75, E 40 to 45 GPa). Starting from the year 2004 the arch has been repaired by removal of 2 to 3 cm of the contaminated concrete, its subsequent replacement with shotcrete and adding protective coating. Nearly all columns and lower parts of the arches have been protected. The efficiency of the system has been tested after 7 years of use by comparing chloride ingress in the protective system with the threshold value for the Krk Bridge and assessed as satisfactory (Ille et al. 2011).

For the investigation and testing of composite cross sections of repaired columns under load, optical sensors were built in columns S20 (abutment pier towards St. Marko) and S26 (highest spandrel column towards Krk island), of the small arch (Mavar et al. 2007) with different repair technologies (Figure 5 right). Optical sensors are 2 m long and have the possibility of measuring the deformation of 1 micron on length of 1 m (2 microns on length of 2 m). Before the bearings reconstruction on column S26 and its unloading some mechanical properties of its 25 years old concrete under the load of 1.750 kN were measured by optical sensors (Beslać et al. 2008). Those are surface of column cross section, relative deformation, compressive stress in concrete, static modulus of elasticity and temperature coefficient.

Cathodic protection was envisaged for the submerged elements that support the larger arch of the Krk Bridge (Ille et al. 2011). During 2010 an investigation into the efficiency of 9 protective systems applied at 13 trial surfaces was carried out. This included laboratory and on-site testing. Six protective systems were assessed as inadequate, due to one or combination of the following deficiencies: cracking and delamination observed on site, low adhesion, low thickness, low resistance to freeze/thaw in chloride aggressive environment, low crack bridging ability, discoloration in UV resistance test. The remaining three protective systems were assessed as

provisionally adequate, as improvements are required to increase the adhesion to fully meet design specifications.

The works on the Krk Bridge initiated a further research into durability design of reinforced concrete structures in aggressive maritime environment, namely in developing further specifications for application of surface protection systems on damaged structures as well as integrating surface protection systems with concrete cover in the design of new structures in aggressive maritime environment.
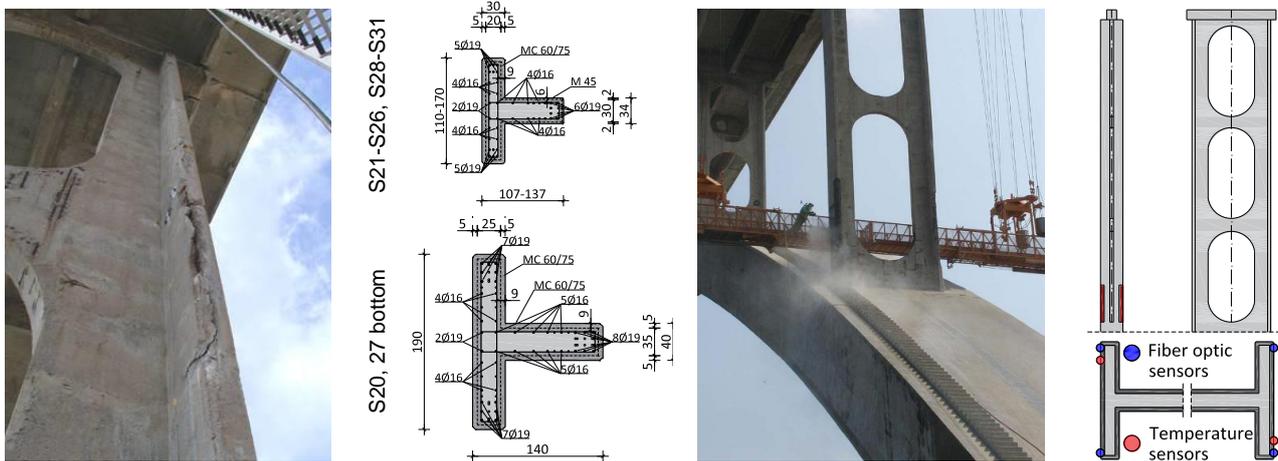
Figure 5: Deterioration (left) and repair (middle) of Krk bridge columns with the position of optical sensors embedded into columns during repair work (right, Mavar et al. 2007)

5.2 Monitoring of the second generation of Adriatic arches

The construction of the **Maslenica** highway **bridge** - a concrete arch of 200 meters span and rise of 65 metres (Čandrlić et al. 1999), started during war and was completed in 1997. It symbolizes the continuation of the tradition of building large concrete arches in Croatia. The cross section of the fixed arch is a double-cell box of constant depth. The bridge superstructure comprises eight simply-span precast prestressed girders made continuous over intermediate supports and interconnected by deck-plate cast in place, with cross-girders provided only at supports. The bridge design was strongly influenced by the severity of the marine environment and the seismicity of the site. Structural details and cross section were simplified to minimise execution problems. In order to avoid reinforcement congestion and increase durability all structural dimensions were increased, compared to previously built concrete arch bridges in the Adriatic coast area. The low permeability concrete has been designed which increased the bridge durability in marine exposures. The minimum concrete cover for all the bridge structural elements was set at 5.0 cm and for the arch foundations nearest to the sea at 10.0 cm. The number of structural joints has been reduced to a minimum, with most of the piers fixed to the superstructure and the expansion joints placed at the abutments only.

The monitoring system of Maslenica bridge (Šimunić et al. 1999), applied for the first time in Croatia, was used to record relative strains and accelerations (which serves to calculate stresses, velocities and displacements) at various construction stages and under load-testing prior to opening the bridge to the service. Monitoring of prestressed girders was used to investigate deflections, strains and stresses due to self weight and prestressing, natural frequencies of the girder after prestressing and strains and stresses in reinforcement due to creep and shrinkage. Strains and stresses of the arch during construction and dynamic properties before the construction of the superstructure were investigated as well (GF 2005). It appears that there was a considerable shrinkage of concrete in girders after their pouring because of a relatively small moisture level at summer time when the measurements were undertaken. This caused compression in the reinforcement. The stiffness of girders was determined by means of the

modulus of elasticity, by measuring their natural frequencies, and by means of concrete compression strength. By measuring stresses and displacements during construction and by comparing it with the values obtained by means of software which includes the material and geometrical non-linearity, a solid qualitative correspondence between theoretical and experimental research results has been established (Šimunić et al. 1999). Additionally, monitoring the environmental parameters such as air temperature, humidity, wind speed and direction was anticipated. Also the corrosion monitoring system was introduced which measures the strength of the corrosion current, electrochemical potential of the anode and the temperature and electrolytic resistance of concrete. Corrosion sensor contains electrodes made of reinforcing steel embedded at different distances from the concrete surface and at least one electrode made of stainless material that acts as a cathode. Using the conductor outside the concrete, the current between the electrodes and the electrical resistance of concrete, as an indicator of moisture content, are measured. As long as the electrodes are in carbonate and chloride free concrete, they are passively protected by the concrete alkalinity, so there is no flow of current between the electrodes. If the critical chloride concentration is exceeded, or alkaline protection disappeared due to the carbonation, reinforcement becomes exposed to the process of corrosion, as opposed to stainless material, and with the presence of oxygen and moisture the electrical circuit is formed.

The system consists of 92 strain-gauges as shown at Figure 7 top (18 on concrete and 74 on the reinforcement), 40 temperature sensors and 21 corrosion sensors (anode-ladder) mounted at carefully chosen spots on the arch and girders of the superstructure (Figure 8 top). They are connected by electrical wiring to a central unit, where recorded data is collected and processed by multi-channell measurement computer. These documented the initial condition of the structure needed as a reference for future measurements. Unfortunately, the monitoring project was stopped soon afterwards.

Thirteen years after the bridge was opened to traffic (Bleiziffer et al. 2011), in 2010, investigation works were carried out on Maslenica Bridge. They comprised:

- visual inspection of all structural members which was carried from mobile underbridge inspection unit and an arch inspection unit (Figure 6 middle), recording defect and registering cracks, together with identifying locations for taking specimens,
- chloride content measurements at 10 concrete samples taken at 2 positions of the arch abutments, 60 samples taken at 12 positions at the arch rib, 20 samples taken at the 4 positions of the column S3, 20 samples taken at the 4 positions of the column S10 and 10 samples taken at 2 positions of the superstructure (Figure 6 right).

Those investigation works revealed that the bridge is generally in good condition and in most structural members corrosion process is stil in the initiation stage. But there are some localized damage observed at the columns S3 and S10 (Figure 6 left) with the areas of exposed corroded reinforcement, and evidently concrete cover is at those locations less than 5 cm specified in the bridge design. This requires immediate repair and protection. Chloride measurements show that chloride penetration in concrete cover is uneven, and depends on location, with the higher content and deeper penetration in concrete members facing north. As there are locations where chloride content is reaching the threshold limit, it is suggested to apply a protective system to the entire bridge structure, in order to mitigate the future repair costs.

Figure 6: Maslenica bridge (Bleiziffer et al.2011): reinforcement corrosion on column S10 (Left); under bridge inspection unit (middle); taking dust samples for determination of chloride content and depth of chloride penetration into the concrete (right)

MASLENICA
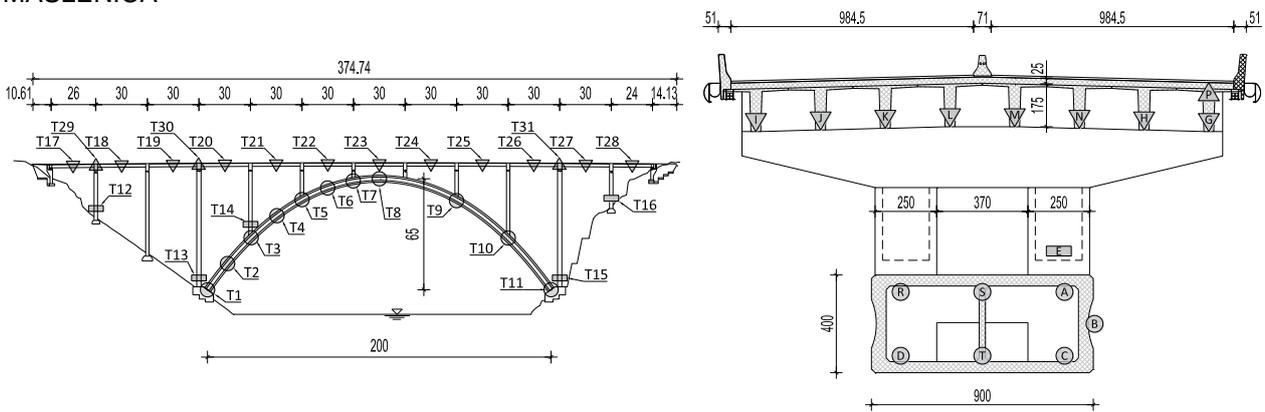
T1	T2	T3	T4	T5	T6	T7	T8	T9	T10	T11	T12	T13	T14	T15	T16	T17	T18	T19	T20	T21	T22	T23	T24	T25	T26	T27	T28	T29	T30	T31
A	A	A B	A	A	A	A	T S	A	A	A	E	E	E	E	E	G	G	I	I	I	G	I J	G	G	G	G	G	P	P	P
C	C	C D	C D	C	C	C	R D	C	C	C								H	G	H		K L								
D							C A			D									G		G		M N								
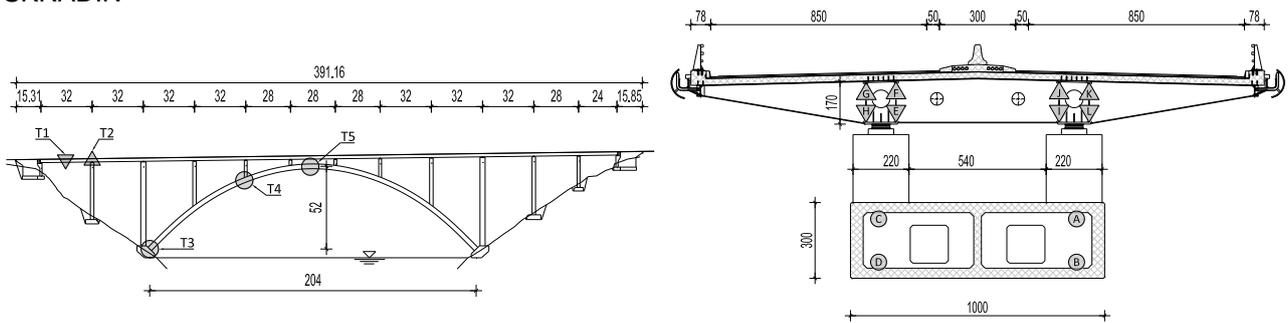
SKRADIN

	T1		T2		T3		T4		T5
	E F G H I J K L		E F G H I J K L		A B C D		A B C D		A B C D

CETINA
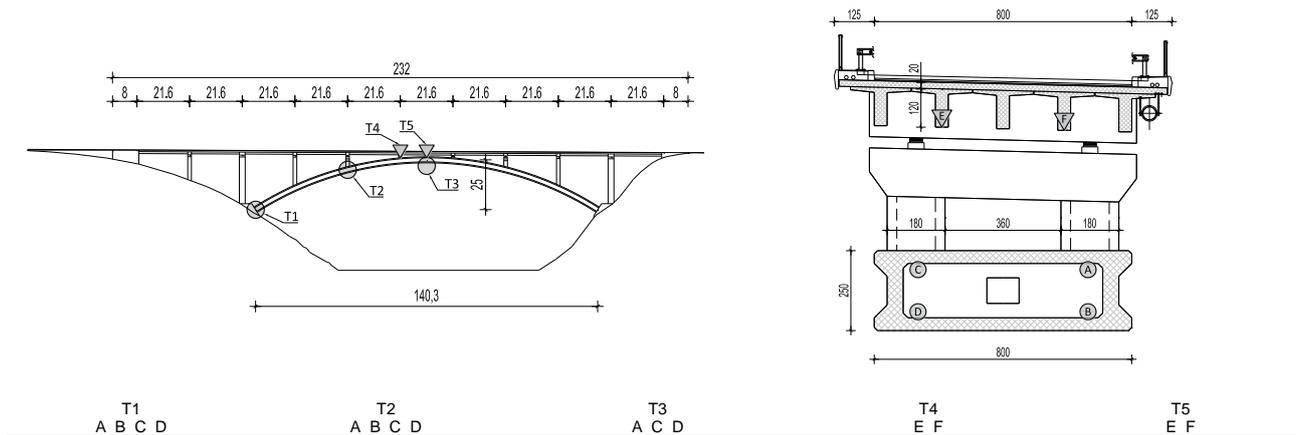
Figure 7: Location of strain gauges installed on Maslenica, Skradin and Cetina bridges

A concrete arch **Skradin Bridge** was constructed across the Krka River canyon (Radić et al. 2010) in the year 2005. Bridge spans 204 m with a rise of 52 m. It holds a unique position in the family of existing Croatian reinforced arch bridges because the bridge superstructure has been designed as a composite structure comprising steel girders and reinforces concrete deck plate, which resulted in substantial reduction of permanent actions. The arch itself is of considerably smaller dimensions than for the alternative solution with a prestressed concrete superstructure. The reduction of the total weight of the structure facilitated earthquake design as the bridge is located in the region of high seismicity. The arch was constructed by free cantilevering on traveling formwork carriages in 5.25 m long segments. The steel superstructure was erected by longitudinal launching in three phases. The concrete deck is formed by full depth precast slabs interconnected by on-site concreting of longitudinal and transverse joints above shear connectors. Steel corrosion protection has been adopted according to the latest standards for the most severe maritime environment.

Skradin bridge monitoring comprises structural and durability performance monitoring, with a smaller number of gauges than installed on the Maslenica bridge. The monitoring system (Rak et al. 2006) includes continuous monitoring of strain (Figure 7 middle), temperature and humidity on the structure, periodic displacement measurements, and periodic measurements to evaluate the corrosion progress (Figure 8 middle). The superstructure is instrumented with 16 strain gauges, 12 temperature sensors, and 1 humidity sensor. The arch is instrumented with 6 corrosion sensors (anode-ladder), 12 strain gauges, 9 temperature sensors, and 1 humidity sensor. Sensors were installed and some measurements were carried out even during the bridge construction phases.

The actual strain monitoring started during proof load testing in June 2005, before the start of bridge exploitation, and an initial report with measured values at all measurements locations is prepared. After that, the sensors are attached to loggers and strain, temperature and humidity data can be transferred via modem connection to the electronic computer, where they are read, stored and processed (Rak et al. 2010). Displacement control is performed twice a year at 13 spots in 4 lanes (each edge of each carriageway). Measuring points are located at abutments and over each pier. The displacement measurement is carried out with geodetic method with the use of precise geometric levelling (Rak et al. 2006). Reinforcing steel corrosion state measurements is carried out with the help of an instrument that measure following parameters: electric current, voltage, resistance of concrete and the temperature of the built-in sensors. Initial corrosion measurements were performed in May 2004. The expected frequency of the corrosion sensors readings is 2 to 4 times a year (Radić et al. 2008).

MASLENICA
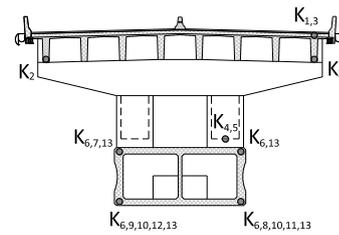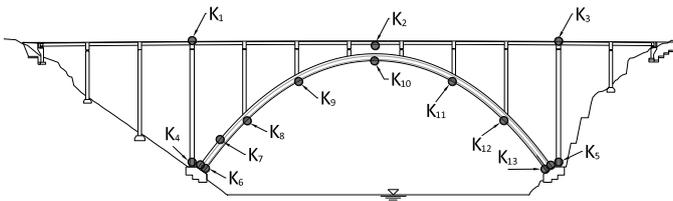
SKRADIN
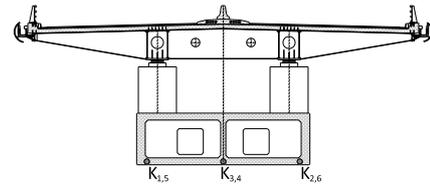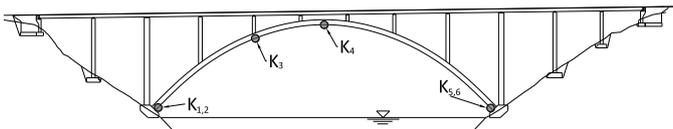
CETINA
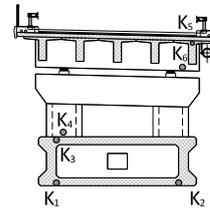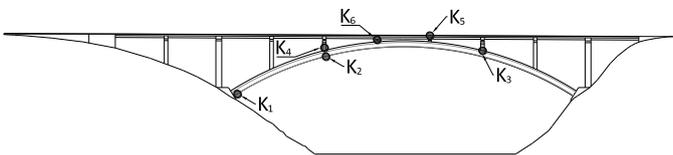
Figure 8: Location of corrosion sensors installed on Maslenica, Skradin and Cetina bridges

Concrete arch **Cetina bridge** spanning 140 m with a rise of 21.50 m was constructed across the Cetina River canyon that is an environmentally protected area. The arch is fixed of single-cell cross-section and the continuous bridge superstructure comprise five precast prestressed concrete girders, cast-in-site deck plate and cross-girders at supports only. The whole cross section of the arch was constructed by free cantilevering, on travelling formwork carriages, in segments 5.0 m long, symmetrically from arch springings. Every phase of the building process was monitored on site, thus providing necessary input for the adjustment of the structural analysis covering the bridge construction. The deviations of bridge geometry from the designed one were reduced to the minimum, amounting to about 2.0 cm for the arch axis (Žderić et al. 2008).

Cetina bridge monitoring system is similar to system installed on Skradin bridge but with less sensors (Rak et al. 2010). The monitoring system includes continuous monitoring of strain, temperature and humidity on the structure, periodic displacement measurements, and periodic measurements to evaluate the corrosion progress. The superstructure is instrumented with 4 strain gauges and 2 temperature sensors. The arch is instrumented with 6 corrosion sensors (anode-ladder), 11 strain gauges, 4 temperature sensors, and 1 combined humidity + temperature sensor. The expected frequency of the corrosion sensors reading is 2 to 4 times a year.

Unfortunately, once after the investor (Croatian Motorways Ltd. and Croatian Roads Ltd.) took over the facilities, they have not shown the interest in the maintenance of monitoring system. Both at the Skradin and Cetina bridges, monitoring system is installed based on the design request, but after releasing the system and collecting first results (in a year or a two years period) no one showed interest to finance costs of monitoring results and maintenance of the system. Nevertheless, a small investment could revive the monitoring project.

Contact information

Ana Mandić Ivanković
Associate professor, Faculty of Civil Engineering, Kačićeva 26, 10000 Zagreb
+385 1 46 39 424
mandicka@grad.hr

References

Mandić Ivanković, A., Srbić, M. and M. Franetović (2015): Performance of existing concrete arch bridges, Paper submited for IABSE Conference – Structural Engineering: Providing Solutions to Global Challenges. to be held September 23-25. Geneva. Switzerland.

COST 345 (2004) Procedures required for assessing highway structures, Joint Report of Working Groups 2 and 3: methods used in European States to inspect and assess the condition of highway structures.

Franetović M., Mandić Ivanković A. and J. Radić (2014). Seismic assessment of existing reinforced-concrete arch bridges, Građevinar (Civil Engineer) 66 (8): 691 – 703

Radić J., Bleiziffer J., and A. Mandić (2006) Maintenance strategy for large Adriatic bridges. Proceedings of the 10th International Conference on Inspection, Appraisal, Repairs & Maintenance of Structures. Hong Kong: 313-320.

Mandić A., Radić J. and Z. Šavor (2010). Limit states of existing bridges, Joint IABSE-fib Conference Dubrovnik. Cavtat: 1169-1176.

Radić, J., Kušter, M. and J. Bleiziffer (2012). Sustainable large arch bridge maintenance through inspections, assessments, monitoring, repairs and service life modelling. Proceedings of the 18th IABSE Congress: Innovative Infrastructures - Toward Human Urbanism. Seul: 1-8

Mandić Ivanković A., Gleđ N. and M. Franetović (2014). Balance of nature and engineering requirements on existing arch bridges, IABSE Symposium. Madrid: 26-27 +CD

Radić, J., Šavor, Z. and G. Puž (2003). Extreme wind and salt Influences on Adriatic bridges. Structural Engineering International13 (3): 242-245.

HIMK: Croatian Institute for Bridge and Structural Engineering (2005). Šibenik Bridge – Inspection Report. Vol. 1-4. Zagreb (*In Croatian*)

Radić, J. Šavor, Z., Bleiziffer J. and I. Kalafatić (2008) Šibenik bridge – design, construction and assessment of condition. Proceedings of the Chinese-Croatian Joint Colloquium: Long Arch Bridges. Brijuni. Croatia: 207-216

Medak, M., Radić, J., Veverka, R., Bleiziffer, J., Kučer, A. and I. Kalafatić (2006). Main inspection of Šibenik arch bridge. Proceedings of the International Conference on Bridges. Dubrovnik: 961-968.

Bleiziffer, J., Mavar, K. and A. Balagija (2011). Pag bridge-inspection and testing of the arch after 40 years of service. Proceedings of the 3rd Chinese-Croatian Joint Colloquium: Sustainable arch bridges. Zagreb: 317-324

Šavor, Z., Mujkanović, N., Hrelja, G. and J. Bleiziffer (2008). Reconstruction of the Pag bridge. Proceedings of the Chinese-Croatian Joint Colloquium: Long Arch Bridges. Brijuni: 241-251.

Ille, M., Bleiziffer, J and J. Beslać (2011). Continuation of repair and protection works on the Krk bridge. Proceedings of the 3rd Chinese-Croatian Joint Colloquium: Sustainable arch bridges. Zagreb: 301-308.

Beslać, J., Bleiziffer, J. and J. Radić (2008). An overview of Krk bridge repairs, Proceedings of the ARCH' 10, 6th International Conference on Arch bridges. Fuzhou. China: 824 – 829

Beslać, J., Tkalčić, D. and K. Štemberga (2008). Difficulties and successes in the maintenance of Krk bridge, Proceedings of the Chinese-Croatian Joint Colloquium: Long Arch Bridges. Brijuni, Croatia: 197-205.

IGH Institut d.d. (2001). Design of rehabilitation and protection of reinforced concrete bridge structure St. Marko – Krk (smaller arch bridge): Book 3 & Book 4: Technological solution for rehabilitation of piers & arch, superstructure and abutments. Zagreb. (*in Croatian*)

Mavar, K., Sekulić, D. and D. Würth (2007). Monitoring of Krk bridge colums with interferometric fibre optic sensors, Proceedings of the fib Symoposium Dubrovnik: Concrete Structures – Stimulators of Development. Dubrovnik: 709-716.

Čandrlić, V., Radić, J. and Z. Šavor, Z. (1999). Design and construction of the Maslenica highway bridge. Proceeding of the fib Symposium Structural Concrete – the Bridge Between People. Vol. II. Prague: 551-555.

Šimunić, Ž, Gašparac, I. and B. Pavlović (1999). Monitoring of Maslenica bridge during construction. Proceedings of IABSE Symposium Structures for the Future – The Search for Quality. Rio de Janeiro: 152-153 + CD-ROM.

GF: Faculty of Civil Engineering, University of Zagreb (2005). Guidelines for use and maintenance of Maslenica bridge. Zagreb. (*in Croatian*)

Bleiziffer, J., Mavar, K., Ille, M., Škarić Palić, S., Dimić Vuković, S. and A. Balagija (2011). Condition assessment of the Maslenica Highway bridge, Proceedings of the 3rd Chinese-Croatian Joint Colloquium: Sustainable arch bridges. Zagreb: 309-316.

Radić, J., Šavor, Z., Mandić A (2010). Two notable arch bridges on The Croatian Adriatic highway, Structural Engineering International. 20 (1): 36-40.

Rak, M., Bjegović, D., Kapović, Z., Stipanović, I. and D. Damjanović (2006). Durability monitoring system on the bridge over Krka river. Proceedings of the International Conference on Bridges. Dubrovnik: 1137-1146.

Rak, M., Krolo, J., Herceg, Lj., Čalogović, V. and Šimunić Ž. (2010). Monitoring for special civil engineering facilities, Građevinar (Civil Engineer) 62 (10): 897-904. (*in Croatian*)

Radić, J., Bleiziffer, J. and I. Kalafatić (2008). Structural health monitoring of large arch bridges in Croatia, Proceedings of the Chinese-Croatian Joint Colloquium: Long Arch Bridges. Brijuni, Croatia: 293-300.

Žderić, Ž., Runjić, A.and G. Hrelja (2008). Design and construction of Cetina arch bridge, Proceedings of the Chinese-Croatian Joint Colloquium: Long Arch Bridges. Brijuni, Croatia: 285-292.

SHM with fiber optic sensors at AIMEN technology center

Ander Zornoza, AIMEN technology center, Porriño – Pontevedra (SPAIN)
Tania Grandal, AIMEN technology center, Porriño – Pontevedra (SPAIN)
Ruben de la Mano, AIMEN technology center, Porriño – Pontevedra (SPAIN)
Lourdes Blanco, AIMEN technology center, Porriño – Pontevedra (SPAIN)
Francisco Rodriguez, AIMEN technology center, 36410 Porriño – Pontevedra (SPAIN)
Alberto Asensio, AIMEN technology center, Porriño – Pontevedra (SPAIN)
Pilar Rey, AIMEN technology center, Porriño – Pontevedra (SPAIN)
Elena Rodriguez, AIMEN technology center, Porriño – Pontevedra (SPAIN)

Objectives, abstract and conclusions

Recently AIMEN has been quite active in SHM, since it has been identified as an important working line for adding value to our research and development background and expertise. We have lead, regional, national and European R&D projects in the area of SHM. SHM is an Interdisciplinary field, where expertise from very different areas is needed. Being this the case, at AIMEN, the monitoring team has its core at the Robotics and Control unit. But depending on the projects needs, this team works together with experts from other units such as Advanced Materials, Environmental Technology or Advanced Manufacturing Processes. At Aimen we specifically focus on applying fiber optic sensors (FOS), mainly through fiber Bragg gratings (FBGs) as a monitoring tool in order to perform control, predictive maintenance or prevent failure and collapse. FOS's advantages are mainly their small size, light weight, their passive nature, the remote sensing and multiplexing possibilities they offer, their immunity to corrosive environment or electro-magnetic interferences and that they can operate in extreme temperatures (from -250ºC to >1200ºC). Therefore we have identified it as a strong technology for performing SHM in harsh conditions. In the following paragraphs five research lines under development at AIMEN are explained.
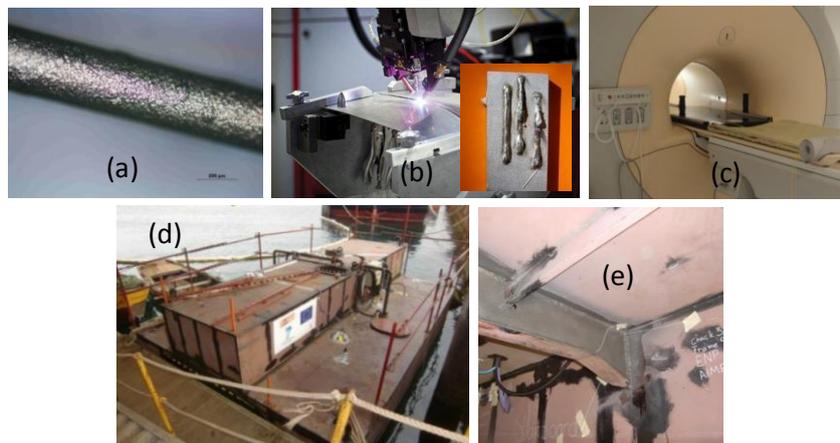
Figure 1: (a) metallic coated FOS. (b) Laser welding for FOS embedding. (c) Temperature monitoring of carbon fiber in MRI equipment from Galaria public company at Meixoeiro Hospital. (d) Catamaran for composite patch monitoring tests. (e) Detail of FOS monitored patch inside the catamaran.

FBG metallic coating, depicted in figure 1(a), has been developed by AIMEN to increase the thermal sensitivity of the sensor, add robustness to the sensor to protect the fiber and the grating in harsh environment processes like welding processes or to detect and measure corrosion.

Fiber optic embedding in metallic structures provides capabilities for controlling parameters of the structural health status, information about their own process of deterioration and to make smart

metallic tools and structures. It is an ongoing research taking advantage from our laser welding tools and expertise, as shown in figure 1(b).

In high magnetic/electric field environments, such as Magnetic Resonance Imaging (MRI) equipment, temperature monitoring can be a challenge. As depicted in figure 1(c), we have used FBG sensors to detect heating in carbon fiber fragments subjected to MRI.

Composite patch reparation for marine and civil engineering structures is a fast and reliable solution for cracks. At Aimen we have developed new polymer and adhesive solutions for these reparations, while developing FOS systems for monitoring their integrity. In figure 1(d) a catamaran used for test is shown, while in figure 1(e) an actual reparation with the monitoring system is shown.

Therefore FOS are a reliable solution when it comes to SHM in harsh conditions, where temperature monitoring phenomena, crack growth monitoring or embedding in metallic structures is needed.

Technical information

In designing a SHM system for a real world field application, ample consideration should be given to the robustness of the SHM sensors and algorithms to variable service conditions. The SHM system should be able to distinguish between signal changes due to damage events and changes in environmental conditions. It should also be able to compensate for these condition changes by the use of appropriate signal-processing methods. Furthermore, the physical SHM system components should be robust enough to anticipate to these changes. Fiber optic sensors are ideal for SHM applications for their properties and small size. Furthermore, they can be multiplexed and/or distributed and they can monitor a big structure with just a single fiber network. Fiber optic sensors have been used in SHM for more than two decades. At the beginning, these sensors were used to monitoring the strain and the temperature fluctuations of civil structures like bridges or tunnels, but in the last years that sensors are used to monitoring a lot of magnitudes and parameters and for all kind of structures. Furthermore, nowadays these sensors are used to make smart tools and materials. There are a lot of different technologies for fiber optic sensors but the most used in SHM are distributed monitoring Brillouin sensors and punctual monitoring fiber Bragg sensors. The latter is the sensors that AIMEN uses for monitoring and SHM applications and the ones discussed in this paper.

1   Fiber Bragg Grating Sensor Introduction

Fiber Bragg grating (FBG) sensors are the most widely used fiber optic sensor due to its versatility and its mechanical and thermal properties. FBG consist of a periodic refractive index perturbation in the core of a fiber optic, made usually by UV light laser. The UV beam passes through a phase mask which makes an interferometric pattern of light, after this, the fiber optic is exposed to this pattern and it modifies the refraction index of the core causing the grating. This grating usually has a length of 5 mm and it acts like a filter, reflecting one of the wavelengths which travel through the fiber optic and letting pass the rest of the wavelengths. The reflected wavelength is a very narrow peak (~0.2 nm) denominated Bragg wavelength (λ_B).
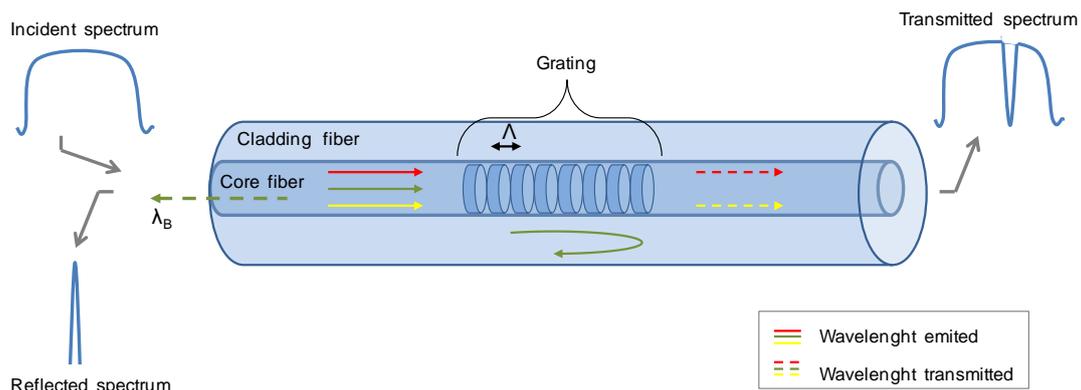
Figure 2: Fiber Bragg Grating structure, with refractive index profile and spectral response.

The Bragg wavelength depends on the effective index (n_{eff}) of the fiber optic and on the period of the grating (Λ). If either of them suffer any change the Bragg wavelength shifts proportionally, following the next equation:

$$\lambda_B = 2n_{eff}\Lambda$$

FBG based sensor measure the variation in the reflected wavelength as a sensing parameter. A tensile strain over the fiber changes the FBGs spatial frequency and therefore the wavelength of the reflected light. The optoelectronics required for the measurements are known as interrogators and include a light source and an optical spectrum analyzer (OSA) that determines the wavelength of the reflected light. It is possible implement sensing devices for strain, acceleration, vibration, tilt, pressure or any physical quantity by means of clever designs that translate the target parameter in strain. Furthermore, refractive index is also sensitive to changes of temperature so it is possible to implement temperature sensors in the same device.

2   Embedded FBG metallic coating

Embedding FBG sensors into structural materials give smartness to the structures and allow the monitoring in real time of critical locations where other sensors couldn't access. Embedding of the FBG sensors, also protect the sensor from possible damages and insulate it from adverse environmental conditions. This could be used for the monitoring of health or the integrity of a structure during manufacture. With this, the traditional visual inspections are no longer needed because the embedded sensors give information in real time of the state of the structure. The embedded process could be done during the manufacturing of the structure or tool, or when the process is completed. There are two well differentiated types of embedding according to the packaging material: embedded into composite material or into metal structure.

The embedded FBG sensor on metal material is made by melting the metal to make the union. For this process, high temperatures are needed (T>400ºC) which neither glues or the typical polymeric coating of the fiber support. Besides, in the case of embedding with a metal which has a high melting point (900ºC) the grating and/or the fiber could be damaged during the melting itself, due to the high temperatures reached. To make this type of embedding, it is necessary to take off the polymeric fiber coat and make a metal coating of the fiber, prior to the embedding, which will

protect the fiber during the later embedding process. Nowadays, fiber optics with metallic coatings are commercially available, but it is not the case of FBG sensors.

The metal coatings are the most widely used for their thermal properties: they have high thermal conductivity and high heat conductivity which favors an effective transfer of energy between coating-sensor and increases the sensor thermal sensitivity because it has higher sensitivity to thermal radiation than silica and therefore it transfers more thermal energy to the sensor. The metallic coating process of a FBG sensor is a process relatively recent, Xiao Chun Li et al. in 2001 were the first in embedding metal coating FBG sensor in a metal structure for monitoring the accumulated strain in stainless steel structures manufactured by laser-assisted manufacturing processes. The coating method that they used was a combination of sputtering of Ti and electroplating deposition of Ni. This setup was designed to work at temperatures above 500ºC, and the sensor sensitivity to temperature variations increased from 10 pm/ºC to 21 pm/ºC. In the last years there have been several studies where other techniques for metal coating and embedding were developed, among which dominates the developed by Li with some variations. Stefan Sandliu et al. embedded a FBG sensor by vacuum brazing of Inconel 600 between two sheets of two different Al for monitoring the high temperature of a metallic structure for a long spans of time. Wenbin Hu et al. made a Fe–C-coated FBG sensor for steel corrosion monitoring tested in different corrosion environments. Yulong Li et al. coated partially a FBG sensor with Ni and then he soldered the metalized part on a steel cantilever to monitoring the force and the temperature simultaneously with a resolution of 0.013N and 0.04ºC. See Yenn Chong et al. designed a copper/carbon-coated FBG acoustic sensor net for integrated health monitoring of nuclear power plants. Other interesting applications for embedding metal FBG coating is making smart tools, in this area H. Alemohammad et al. developed a smart tool with a metal FBG coating sensor embedded by laser cladding to monitor efforts of the tool during its operation.

In AIMEN we coated the FBGs sensors with various metals by different techniques for protecting them during the embedded processes and to increase their thermal sensitivity. The aim of this process is the SHM of several parameters like: temperature, strain, corrosion, pressure, acoustic emissions, etc. The techniques that we use to make the metallic coating are physical vapor deposition (PVD) of Ag, Electroless deposition of Ni and Electroplating deposition of Ni and/or Cu. We make coatings with Bi-material films to protect FBG sensors from high temperature damage and to improve the sensitivity of FBG sensors. The first layer of bi-material coating is thinner than the second, a few μm, this layer is used as a conductive layer and is made by PVD or Electroless deposition. Then, another thicker metallic film is deposited by Electroplating deposition techique. The second film is used for high temperature protection and sensitivity improvement. When the environment temperature increases, the metallic coating expands more than silica which results in the pitch length (Λ) shift more than that of the silica fiber without metallic coating, which makes coated fiber's thermal sensitivity higher. This metallic coating process is described more in detailed in previous works and depicted in Figure 3.

PVD of Ag	Electroless Ni Deposition	Electroplating Ni/Cu Deposition
(a)	(b)	(c)
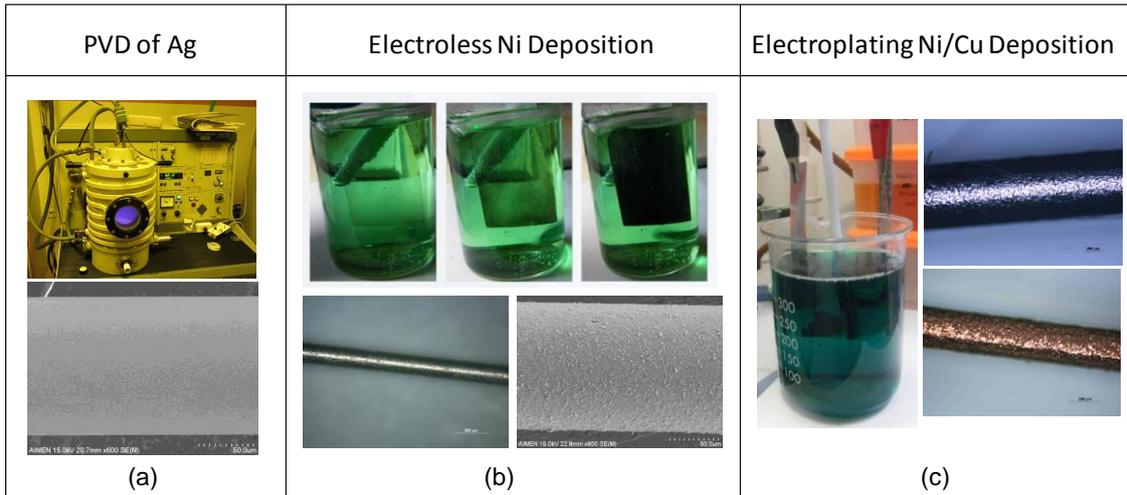
Figure 3: Metallic fiber coatings. a) PVD equipment and FBG coated with Ag by PVD, b) Electroless Niquel bath and FBG coated with Ni by Electroless deposition and c) Electroplating Ni process and two metallic coated FBGs, the first with Ni and the second with Cu.

Following, the thermal characterization of a metallic coated FBG sensor it is showed (figure 4). The sensor tested was coated with a thin film of Ag (0.9 µm) by PVD and a second film of Ni with a thickness of 474 µm which was made by Electroplating deposition. The thermal sensitivity of a commercial FBG sensor, coated with polymeric material, is 10 pm/ºC, while for this metallic FBG sensor was 22 pm/ºC. The sensitivity increased more than the double.
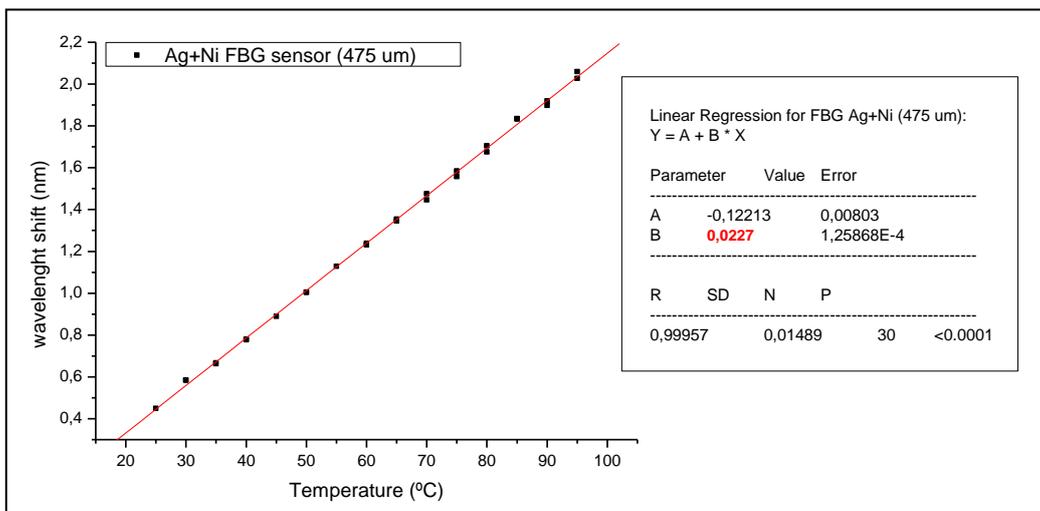
Figure 4: Thermal sensitivity characterization for a FBG sensor coated with 0.9µm of Ag by PVD and 474µm of Ni by Electroplating deposition.

Nowadays, we are working in the election of the best method for welding or embedding the metallic FBGs in metallic structures. We have tested with laser brazing and laser cladding, but we want to test more filler materials and even trying new techniques like microcladding laser or Selective Laser Melting (SLM).
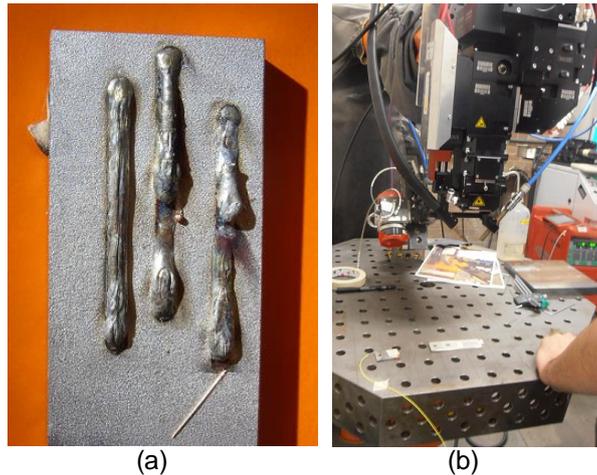
Figure 5: Test of embedded metallic coated FBG sensors by laser cladding. a) FBG sensors coated with Cu embedded by laser brazing, b) equipment of laser brazing.

3   FBG sensor for SHM in high electromagnetic field environments

Due to their dielectric nature, fiber optic sensors can support harsh environments without any impact in their functions. In AIMEN we have used FBG sensors to monitor the SHM of processes at high electromagnetic environments. FBG sensors were used to detect heating in carbon fiber fragments subjected to MRI.

3.1   FBG sensors subjected to MRI

Many radiotherapy accessories such couchs and immobilization devices are currently fabricated using carbon fibre composites. Carbon fibre composites are a tough tissue of carbon fibres immersed in an inert matrix material, usually, epoxy resin. They are used due to low density and high strength and stiffness. On the other hand, magnetic resonance imaging (MRI) becomes an important imaging modality in radiotherapy treatment planning, therefore, MRI compatible and safe accessories are required. Theoretically, Carbon fibres have a good compatibility with magnetic fields in MRI although their properties depend on the manufacturing process and on the matrix material. Carbon fibres are diamagnetic and highly anisotropic. However, carbon fibres are conductive, so, they are usually classified as "MR conditional". This is due to the possibility of induced voltages and RF-induced heating because of the materials'conductivity. For this reason, many companies are manufacturing MRI devices avoiding carbon composites but it is not well demonstrated in the literature that carbon fibre has problems in any MRI conditions.

In AIMEN we studied the effect of radiofrequency (RF) heating together with an electromagnetic field on carbon fibre composite samples during MRI tests by FBG sensors. We monitor the temperatures at several positions of CF samples. Different composite manufacturing processes were evaluated (hand layup, infusion and prepreg) trying to elucidate the effect of resin content on composite samples. On the other hand, different thicknesses for composite samples were also studied. All composite samples were made from epoxy resin carbon fibre composite skins (2 plain layers) and a PVC core. In adittion, a commercial carbon fibre couch top was evaluated using FBGs in the same MRI conditions for comparative purposes. The FBG sensors were glued on the surface of the carbon fibre composite samples forming a network of up to nine FBG sensors on a sample. This way, we monitor the entire surface temperature of the sample (figure 6).
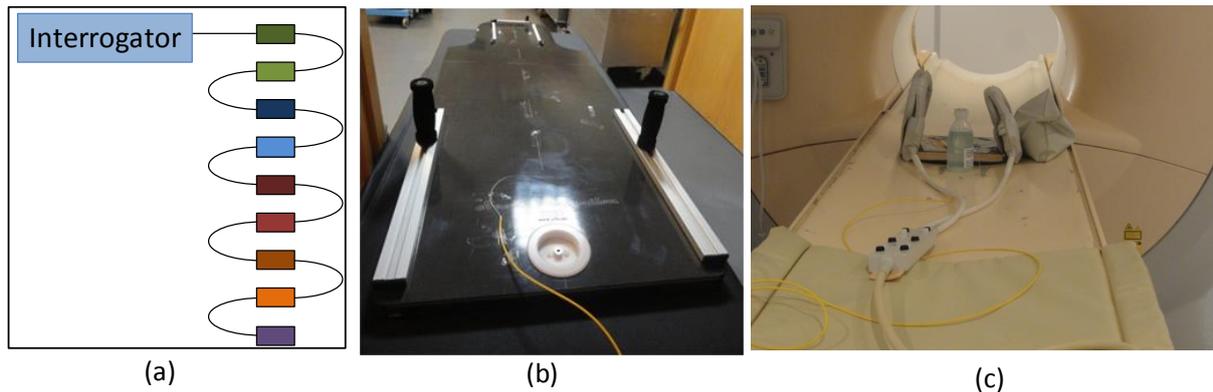
Figure 6: a) distribution of the FBG sensors in the CF samples, b) CF sample with the FBG sensors glued on the surface, c) MRI equipment.

Following, the results of these tests is showed (figure 7). The signal from the sensors is constant during all the test, the FBG sensors show that the CF samples weren't heated. Then, the CF samples aren't affected by the radiofrequency waves. Likewise, it is showing that the FBG sensors aren't affected by electromagnetic field, no matter how strong it is.
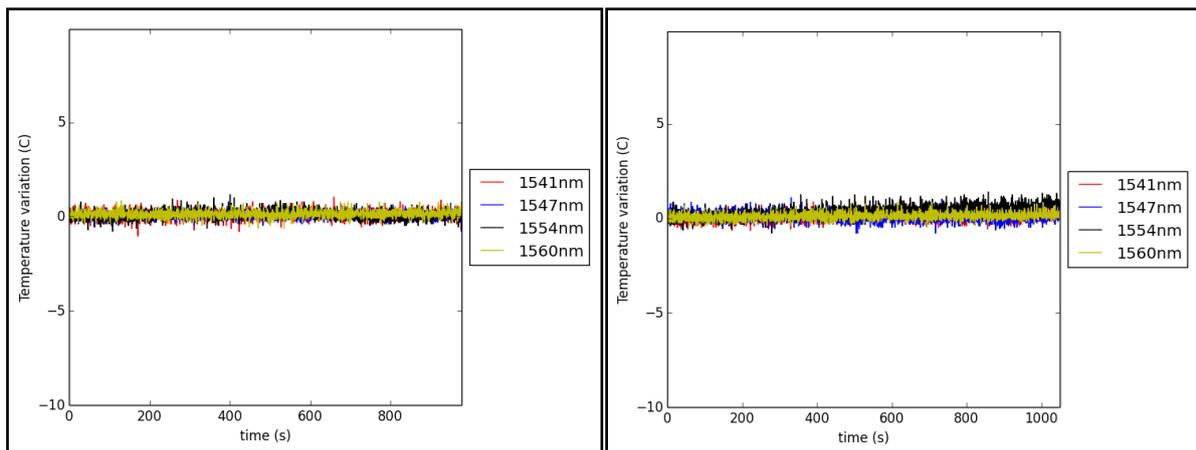
Figure 7: wavelength of the FBG sensors glued on the CF sample for two MRI process.

4 FBG sensors embedded into composites

Composites are materials made of a polymeric matrixes reinforced with fiber, which combines mechanic properties of the resins and the fiber separately, and the synergistic effect of their combination. The FBG sensors are embedded into these materials to be later installed into the structures to monitor, they are widely used in structural health monitoring and in processes to repair cracks for example on ships. It is possible to make the embedding process of FBG sensor into composite while manufacturing or later. While manufacturing, the sensor is inserted between the layers of composite material with the help of an epoxy resin or glue to fix them. This technique

is the most used for making embedded processes into polymeric materials, although the fragility and the difficulty of handling with the optical fibers during manufacturing makes this method difficult to integrate it in the automated manufacturing process. In case of installing the sensor is done after the manufacturing of composite is finished, the next task is gluing the sensor between the composite and the structure. The material of the bond must have some mechanic and thermal characteristics, similar to the composite in order to ensure a good transfer of information between sensor-composite. For a FBG sensor without embedding or coating the strain sensitivity is 1.2 pm/$\mu\varepsilon$ and the temperature sensitivity is 10 pm/$^{\circ}$C. These values are different for each composite, for thermoplastic composites is 1.08pm/$\mu\varepsilon$ and 14.1 pm/$^{\circ}$C while for thermostable composite is 0.26 pm/$\mu\varepsilon$ and 10.9 pm/$^{\circ}$C.

AIMEN was involved in the Co-Patch European project from FP7 (GA 233969). In this project it was developed a novel and effective repair and reinforcement method for large steel structures with composite materials. Two basic structural types were dealt with, namely marine structures (mainly steel ships) and iron/steel civil engineering structures (bridges). The aim of Co-Patch was to reduce quite significantly the maintenance costs of many large steel structures, and in the case of metallic bridges prolongs their design lifespan. It was the use of patches that reduced the maintenance costs and prolonged their design life, even they helped address the consequences of increasing live loads The developed technology created a new market and ended up giving the partners the capability of providing high technology and high added value services worldwide, thus improving Europe's competitiveness in specialized and advanced repair works. The work of AIMEN on the Co-Patch was to investigate the repair of cracks in the marine environment with composite materials and in mitigating the effects of corrosion and loss of section.

Structural defects on ships such as cracks are typically repaired by welding. Nevertheless, welding has many disadvantages: hot-work, long operational time and shutdown. This can cause very expensive production delays or even weight increases. On the other hand, repairs with composite patchs can be used as an alternative providing a safe and lightweight solution. The patches, which are placed over the defect, restore the integrity of the original structure. A smart repair was developed further, since if the crack tip and crack growth are a hazard: monitoring by FBG sensors, embedded in the patch.

Table 1 shows the properties after a full material characterization of the composites deployed for manufacturing the patches.

Composite	Properties
Vinylester Resin (Reichhold)	Viscosity: 1000 mPa.s
Carbon Fibber (Devold AMT) [O]$_2$	Density: 208 g/m^2 (each layer)
Composite (Hand Lay-up)	Modulus (tension$_{[0]}$): 74 Gpa
	Maximum stress (tension$_{[0]}$): 1000MPa
	w/w fibber: 50%
Steel	Properties
Naval Steel Grade A	Yield Strength: 315 Mpa
	Max Tensile Strength: 455 Mpa
	Elastic Modulus: 202 Gpa

Table 1: Material properties of composite patches and steel.

These patches were placed in a catamaran to repair and monitor 3 types of cracks (figure 8.a) in different frames of the ship, during a fatigue test (bending). Were used more FBG sensors glued on the surface of the crack (without patch) as reference placed to compare them with the patched cracks. To generate the fatigue cycle, a water tank, was placed on the catamaran (figure 8.b) and it was filling and emptying continuously (figure 8.c) during one year. The sensors were monitored each month for a year.

(a)

(b)

(c)
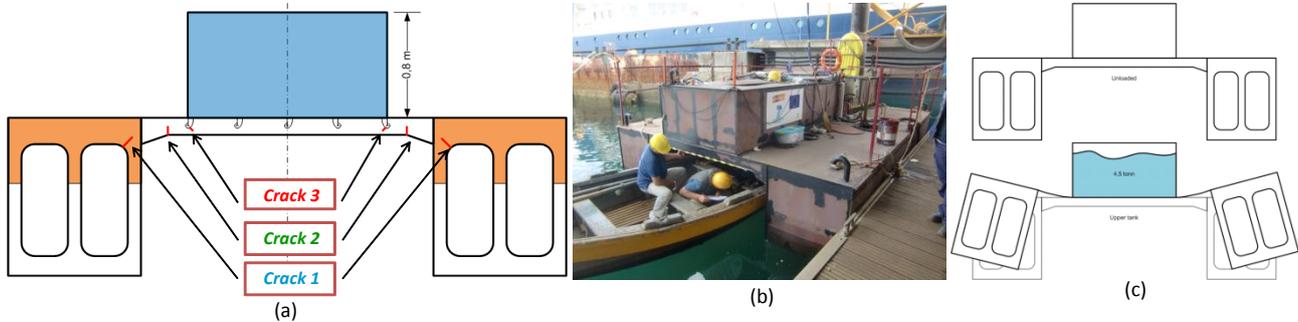
Figure 8: a) situation of the patches and the cracks of the catamaran, b) picture of the real catamaran. c) scheme of the fatigue cycles.

The sensors were monitored once a month during that year. In the figure 9 the response for the FBG sensors is showed. The first graph shows the respond of the sensors when the tank was empty and the bellow graph shows the response for the full tank. It is observed that the FBG glued on the unpatched crack suffer more strain than the patched cracks. Between the patched cracks the best response is for the patch placed on the top of the frame. The number of cycles at the end of the study was 10000 and neither of the patches were debonding and no crack growth has been observed.
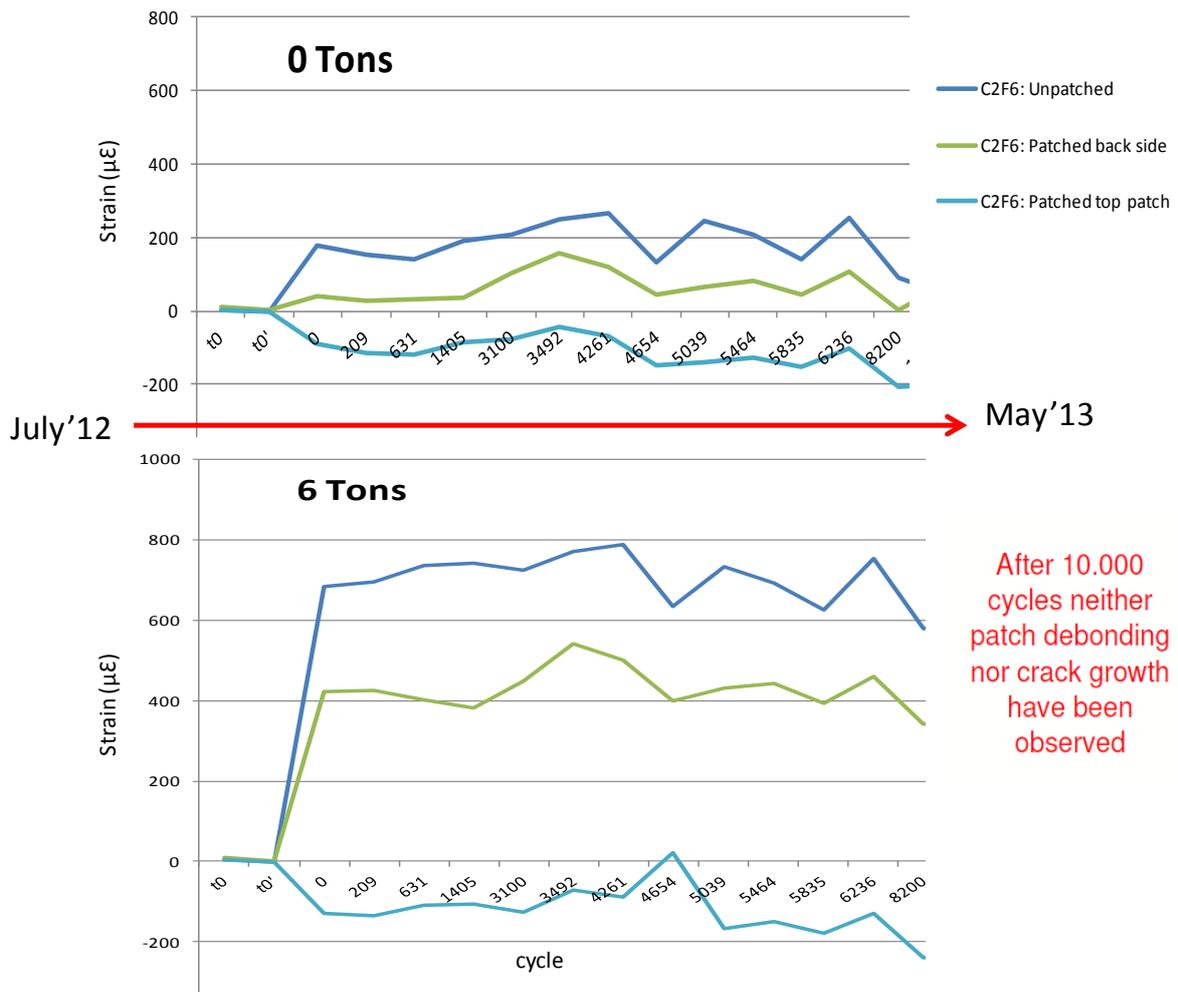
Figure 9: FBG sensors results during the one year test.

In conclusion we can said that the composite materials are good to repair and reinforce that kind of structures, likewise, they are robustness at the effects of corrosion of the marine environment. On the other hand, is demonstrated, that the FBG sensors are a good ally of composites materials to monitoring their behavior, the crack evolution and any fail in any of them.

Contact information

Ander Zornoza Indart, PhD.
Senior Researcher, Robotics and Control R&D Area
AIMEN technology center
C/Relva, 27 A - Torneiros
36410 Porriño - Pontevedra
Phone: 0034 697991236
Fax 00 34 986 337 302

References

Structural Monitoring with Fiber Optic Technology. Raymond M. Measures, Academic Press, 2001, ISBN-10: 0124874304

Hamidreza Alemohammad, Ehsan Toyserkani, Christ P. Paul (2007) Fabrication of smart cutting tools with embedded optical fiber sensors using combined laser solid freeform fabrication and moulding techniques; Optics and Lasers in Engineering 45 1010–1017

Xiaochun Li, Fritz Prinz; (2003), Metal Embedded Fiber Bragg Grating Sensors in Layered Manufacturing; Journal of Manufacturing Science and Engineering AUGUST, Vol. 125

Stefan Sandlin, Tuomo Kinnunen, Jaakko Rämö , Mika Sillanp; (2006) A simple method for metal re-coating of optical fibre Bragg gratings; Surface & Coatings Technology 201: 3061–3065

Wenbin Hu, Hanli Cai, Minghong Yang, Xinglin Tong, Ciming Zhou, Wei Chen. (2011); Fe–C-coated fibre Bragg grating sensor for steel corrosion monitoring; Corrosion Science 53: 1933–1938

Yulong Li, Yan Feng, Xingling Peng, Hua Zhang (2012); Simultaneous measurement of the temperature and force using a steel cantilever soldered with a partially nickel coated in-fibre Bragg grating; Optics Communications 285: 4275–4279

See Yenn Chong, Jung-Ryul Lee, Chang-Yong Yun, Hoon Sohn; (2011) .Design of copper/carbon-coated fiber Bragg grating acoustic sensor net for integrated health monitoring of nuclear power plant; Nuclear Engineering and Design 241: 1889–1898

E. Piñeiro, T. Grandal, A. Asensio, F. Rodriguez; (2014) Coating process of Fiber Bragg Grating sensors for SHM applications in metallic structures. 23rd International Conference on optical fibre sensors, June 2-6, Cantabria, Spain

T. Grandal, E. Piñeiro, A. Asensio, F. Rodriguez.(2013). Metallic coating techniques for Fiber Bragg Grating sensors; 8th Iberoamerican Optics Meeting / 11th Latinamerican Meeting on Optics, Lasers and Applications (RIAO/OPTILAS 2013)

Jeannot Frieden, Joël Cugnoni, John Botsis, Thomas Gmür. (2012). Low energy impact damage monitoring of composites using dynamic strain signals from FBG sensors – Part I: Impact detection and localization; Composite Structures 94: 438–445

H.C.H. Li, I. Herszberg, C.E. Davis, A.P. Mouritz, S.C. Galea. (2006) Health monitoring of marine composite structural joints using fibre optic sensors; Composite Structures 75: 321–327

R.P. BEUKEMA; (2012) Embedding Technologies of FBG Sensors in Composites: Technologies, Applications and Practical Use; 6th European Workshop on Structural Health Monitoring - Tu.4.C.4

M. S. Ferreira, J. C. Vieira, C. Frias, O. Frazão; (2011) STtrain and Temperature discrimination using FBG sensor embedded in hybrid composite laminates; 16th International Conference on Composite Structures, ICCS 16, FEUP, Porto,

http://www.co-patch.com

E. Rodríguez, R. de la Mano, L. Blanco; (2012). Crack repair of steel vessels with bonded composite Patches – Damage control with FBGs. *ECCM15 - 15TH EUROPEAN CONFERENCE ON COMPOSITE MATERIALS, Venice, Italy, 24-28 June 2012*

Selected aspects of structural health monitoring in the light of research carried out as part of the MONIT project

Wierzbicki, Stanisław, Faculty of Civil Engineering, Warsaw University of Technology, Poland
Giżejowski, Marian, Faculty of Civil Engineering, Warsaw University of Technology, Poland
Król, Paweł Artur, Faculty of Civil Engineering, Warsaw University of Technology, Poland

Objectives, abstract and conclusions

Building failures and collapses occur due to several factors that can be grouped into design, execution, and operation causes. Design and execution errors are usually related to the adoption of improper static schemes, incorrect connection solutions or acquired structural defects and defective fabrication procedures, whereas in the last cause, failures are sudden and Structural Health Monitoring systems are not able to provide sufficient time for an early warning of forthcoming disastrous events. Survey of building collapses in Poland proves that failure cases are mostly related to operation causes. This group of causes includes extreme loading events associated with climatic conditions that can exert severe impact on building structures leading to local damage that can trigger instant failure or progressive collapse. Extreme snowfall, snow-on-ice, rain-on-snow or rainfall ponding actions may lead to catastrophic roof failures.

Preventing such situations, which boils down in practice to the prevention of roof overload with excessive amount of snow or rainwater, falls within the scope of duties related to the building maintenance process, and therefore is the responsibility of the owner or manager of the building. Proper fulfilment of these obligations requires ongoing monitoring of the weight of elements covering the roof. As long as in the case of snow cover this is relatively simple, although quite tedious using conventional methods, then in the case of sudden and heavy rainfalls, it can pose certain difficulties. A suitable monitoring system that controls the structure response to the changing roof load may be one of the most effective solutions to improve safety of the building use and at the same time significantly facilitate these tasks.

The paper will discuss results of the MONIT Project, carried out in the years 2008-2012 by a consortium made of scientific and research units, led by the Warsaw University of Technology, entitled "Monitoring of the Structure Technical Condition and Assessment of its Service Life", one of the main areas of which involved research related to the monitoring of building structures. The project was co-financed from the European Regional Development Fund under the Operational Programme Innovative Economy 2007-2013. WND-POIG.01.01.02-00-013/08. As part of the work concerning enclosed buildings, a review of causes of disasters and failures of the existing buildings was carried out in view of the need of structural monitoring. The project also involved analysis of measurement methods of different magnitudes in terms of their suitability for building monitoring systems. Then, in collaboration with private companies, prototype systems of structural monitoring were developed, designed for two different applications and groups of interactions. The first prototype is a wireless system for displacement monitoring dedicated to typical single-storey hall buildings. The second one is a vibration monitoring system provided for buildings exposed to dynamic actions, mostly caused by the transport system (it will not be discussed in this article).

Considerations on issues related to the structural monitoring should be preceded by an analysis of failures and disasters, to better use advantages of the monitoring systems. MONIT database of reported structural failures and collapses indicate that lightweight large-span steel roofs, especially with different heights, are the most vulnerable systems to failures and collapses.

The WiSeNe^{MONIT} monitoring system is developed for typical single-storey buildings of steel lightweight roof structures and it facilitates assessment of safety criteria allowing suitable maintenance procedure.

Technical information

In recent years, we have seen intensively increasing interest in the issue of monitoring of building structures, however this particularly applies to large-space hall buildings. This interest stems from

significant benefits that the use of the monitoring system entails, namely support for ongoing safety inspections of structures and building maintenance cost optimisation. The need to develop methods to improve the safety of building structures and reduce costs of their operation is in turn linked to a general trend in the design of such buildings, involving the use of more and more economical design solutions. Modern design tools help create very lightweight structures, in the case of which climate actions form an essential part of all loads. At the same time, intensifying climate changes result in increasingly often anomalies and occurrence of extreme weather phenomena. If these aspects overlap, the structure overload becomes realistic and poses a threat to its safety, and thus also to the safety of persons residing in the building and property located therein.

The importance of the issues of structural monitoring is further emphasized by the introduction in 2009 to the Polish legislation of a requirement of constant monitoring of parameters relevant to the structural safety (displacements and deformations) in public buildings, such as: sports and entertainment venues, railway station halls, shopping centres, exhibition halls, etc.

12 Analysis of failures and collapses conducted within MONIT project

In the framework of the MONIT Project (see http://www.monit.pw.edu.pl/), a task of collecting information on building failures and collapse events in Poland in the years 1995-2010 has been completed. Building surveillance offices provided data on 443 officially submitted cases (out of which only 12 cases concerned large-span roof buildings). Activities were undertaken in order to bring this number closer to reality. Based on the data from the surveillance offices and from independent research (additional 48 cases of incidents reported for large-span roof buildings), conclusions regarding causes of the collapses were developed. This survey showed that failures and collapses of buildings with steel structural load bearing systems (SS) or with mixed reinforced concrete supports and steel roof structural systems (SS/RCS) were dominant - Figure 1.
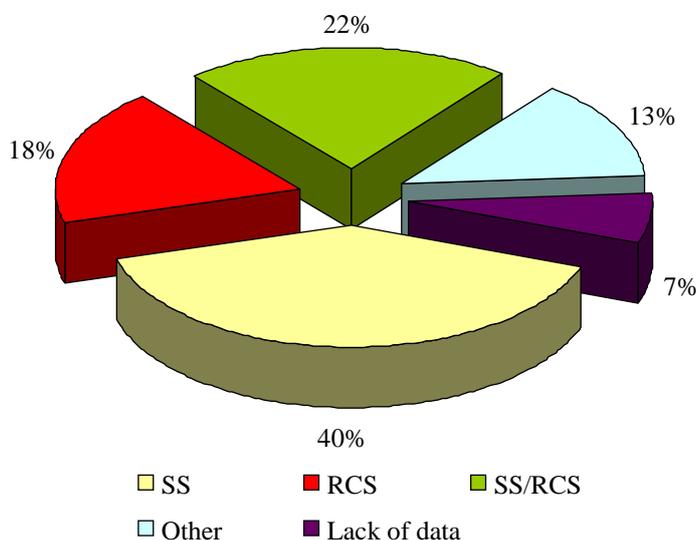
Figure 1. MONIT database incidents by construction type. [1]

Although the incidents reported as part of the MONIT project in majority related to climatic actions resulting from snow-ice overloading events, causes of failures and collapses were distributed into three groups of causes: design, execution and operation - Figure 2. The total number of reported cases for which factors causing incidents were provided is split almost equally between the three selected types of causes (design, execution and operation).
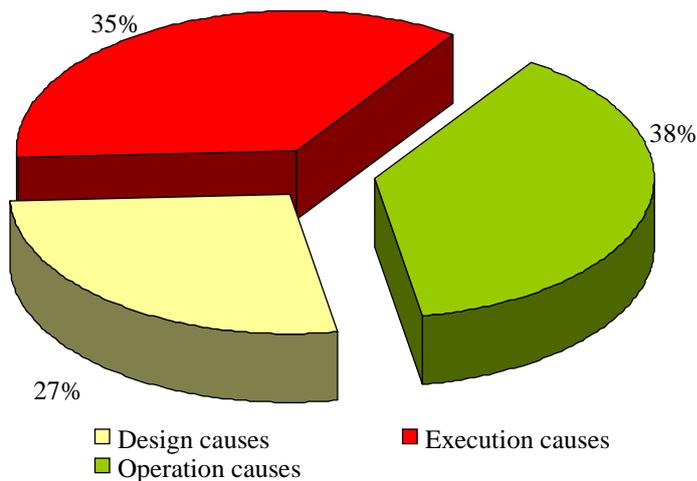
Figure 2. Groups of factors causing building incidents. [1]

The most dangerous factors relate to errors in the structure during the execution phase since they are difficult to detect after the construction has been finished and their existence usually manifests suddenly and frequently under climatic overloading. Figure 3 shows the factors affecting the execution causes of incidents of failure or collapse. As can be seen, low quality of site work and supervision are the dominant factors.
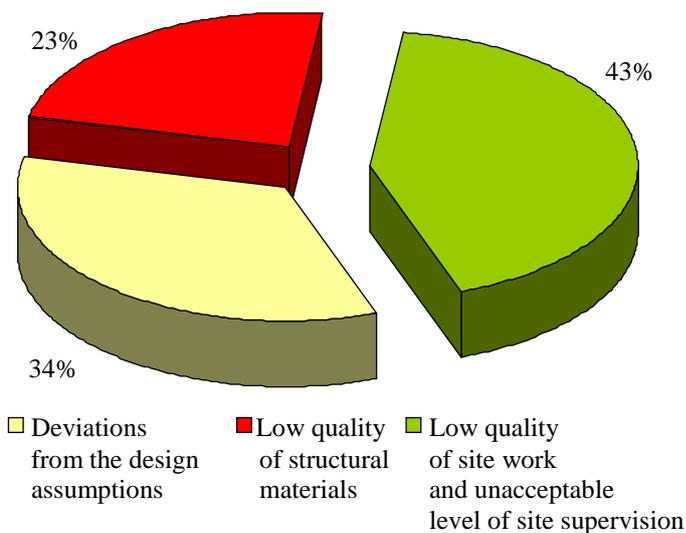
Figure 3. MONIT database factors affecting the execution causes. [1]

The following figure shows classification of operation causes of failures and collapses based on the MONIT data. Most of the causes in this group is linked with the climate loads, mainly snow but also torrential rains. They are associated with both extreme environmental loads as well as users' negligence in terms of roof snow removal and clearing the roof drainage system. In such cases, the application of monitoring systems is a very efficient tool ensuring their intended safe operation conditions.
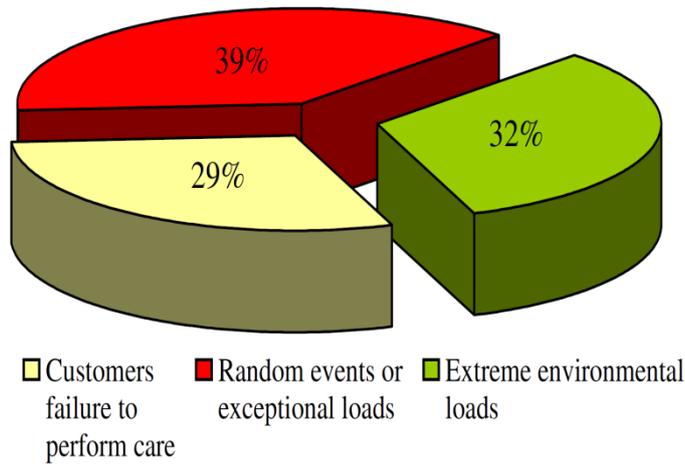
Figure 4. Classification of operation causes of failures and collapses. [2]

13 WiSeNe^{MONIT} structural health monitoring system

The key idea of the WiSeNe^{MONIT} system design was to improve safety of large-size buildings roofing and at the same time optimise costs associated with the building maintenance in winter conditions. The overall objective of the system is therefore to inform the user about an increasing roof load and, in the case of reaching certain specified load limits, to warn of the possibility of overloading the structure. A proper implementation of this task allows simultaneous planning and carrying out appropriate procedures, if needed, of roof snow removal in winter. The system has a hybrid structure and consists of two subsystems: *on-line*, including hardware part, which carries out measurements in the monitored building and *off-line* computing part, used to periodic, numerical global analysis of the structure taking into account the results of measurements transferred from the *on-line* subsystem. Figure 5 shows a block diagram of the system and Figure 6 shows a typical system design.
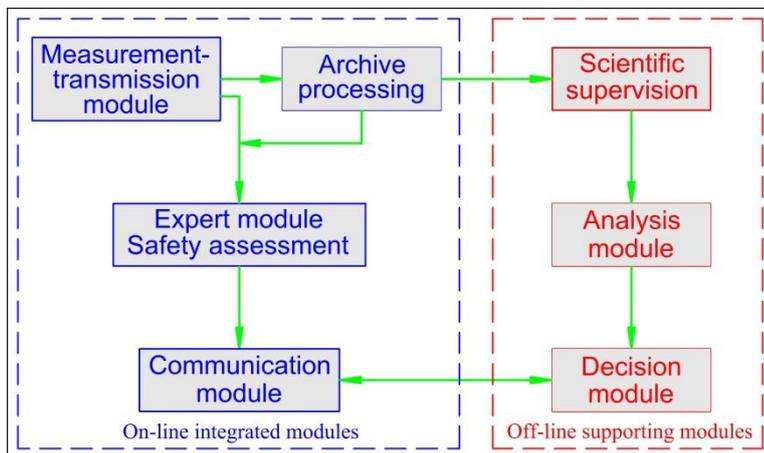
Figure 5. General diagram of the WiSeNe^{MONIT} system. [2]

The *on-line* subsystem uses laser measurement of deflections in a representative number of nodes and temperature in a representative number of structural members. Measuring devices are mounted to the structure without distributing any transmission system. The *on-line* subsystem, in addition to those devices, includes re-transmitters (optional, depending on the user's needs) and the central unit/controller with the transceiver. Both communication and power supply is wireless and the only element of the system that requires external power supply is the central unit.

Individual units of the system communicate with each other using wireless multi-step data transmission. The system systematically collects, processes and evaluates information on the structural behaviour in the form of deflection changes in representative members subjected to climatic actions.
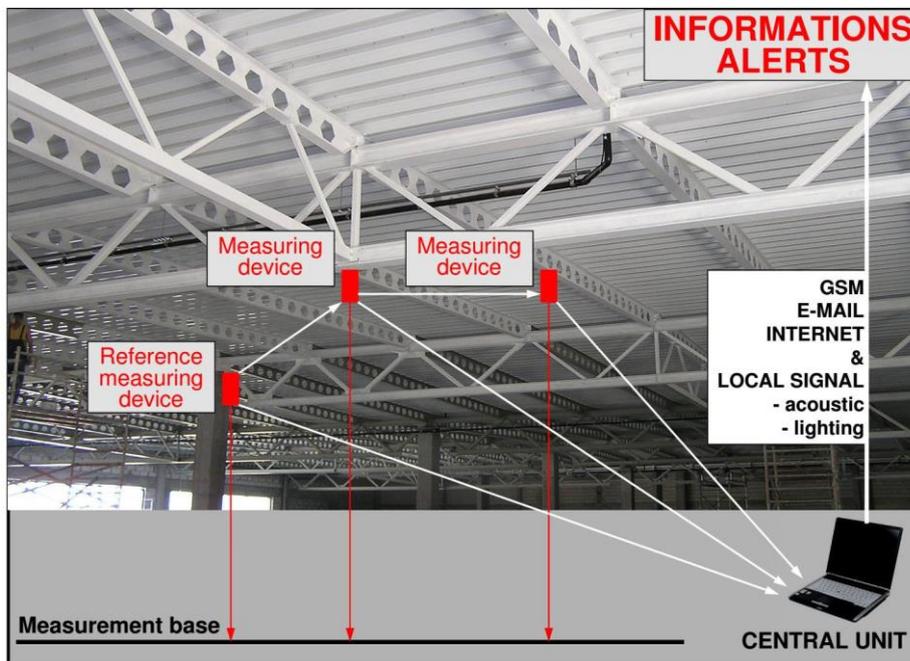
Figure 6. Typical installation scheme of the WiSeNe^{MONIT} system. [2]

The central unit manages operation of the *on-line* subsystem, it collects and processes measurement data and generates messages on the degree of the structure overloading risk and the system status. It is also responsible for communication between the system and users. Access is enabled via a standard web browser.

The *on-line* subsystem detects series of events of objective nature concerning the monitored structure as well as of systemic nature associated with the operation of the system itself, responding to them with relevant messages. These messages, depending on the expected response from the user, may be information (lack of required response), warnings (required inspection and possibly intervention) or alarms (absolute requirement for intervention). The most important event detected by the system is the crossing of successive levels (i.e. threshold levels) of deflection of structural elements in the sensor installation places. Based on a comparison of the measured value of the deflection changes with the threshold levels, the load bearing capacity utilisation of structural members is determined, and on the basis thereof - the type of message generated. Each measuring point in the building has a permitted LDP value assigned, namely load deflection changes that occur after the system is installed and four threshold levels of deflection changes with standard values equal to 30%, 50%, 70% and 100% of the LDP. Crossing of the subsequent threshold levels determines the type of messages generated by the system, the system response speed and desired user actions (Table 1). Standard time between successive measurements is T = 6 hours in summer (3 hours in winter) and can be individually adjusted.

Each measuring point also has a threshold level LD determined of step changes in displacement, understood as the maximum, real value of changes in displacement between successive measurements. It aims at eliminating erroneous measurements resulting from e.g. blocking the laser beam by a passing human or a bulky object. Exceeding the LD level is associated with the implementation by the system of special procedures for verification of the measurement result, generally consisting in ignoring the unrealistic measurement and repeating the measurement procedure, and finally informing the user about the disruption occurred.

Table 1. Reaction levels corresponding to threshold levels of structure health assessment [3]

Displacement state (due to climatic actions)	System state		End user state	
	Reaction type	Sampling frequency	Signal	Activity
δ≤L1	Normal	T	None	None
L1<δ≤L2	Raised	T/2	Alert	Observation
L2<δ≤L3	High	T/4	Warning	Inspection
L3<δ≤L4	Higher	T/8	Alarm	Intervention
δ>L4	Highest	T/8	Closure	Evacuation

The occurrence of certain events generates a relevant message, which is sent to selected users in the form of a SMS and/or e-mail. In addition, this message is properly signalled on the system website and some of the messages are also visualised by the indicator lamps on the front panel of the controller.

An important component of the WiSeNe[MONIT] system is the *off-line* subsystem serving as external analysis module. This module allows obtaining information on the state of strain/stress in structural elements, thereby complementing data on the deflection and temperature transmitted from the measuring and transmission module of the *on-line* subsystem. Thus, with the external support, comprehensive information is obtained about the stress strain level of all structural elements and, consequently, more accurate safety assessment. The *off-line* module is developed using standard engineering software, namely such as is used to structural analysis conducted in the building design process, and in more complex cases when it is necessary to obtain less typical information on the behaviour of the structure, adequate specialist software can be used, such as Abaqus or Ls-Dyna.

Pilot installation was carried out in a large-space commercial building. The *on-line* subsystem consists of a central unit with a transceiver, 18 measuring units and retransmission devices - Figure 7.
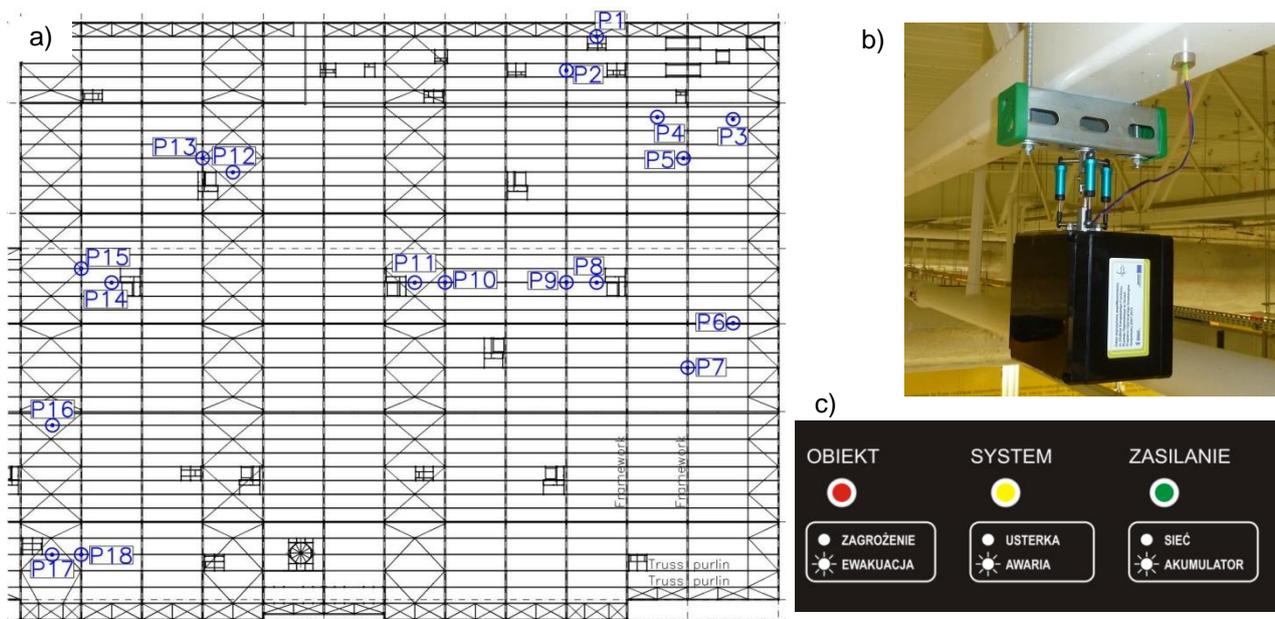
Figure 7. WiSeNe[MONIT] - o*n-line* subsystem: a) installation scheme, b) sample of the measuring device attached to the structure, c) the indicators on the front panel of the central unit [3], where the following Polish

words mean respectively: obiekt = building, zagrożenie = thread, ewakuacja = evacuation, system = system, usterka = faults, awaria = breakdown, zasilanie = power, sieć = network, akumulator = battery.

The numerical model of the *off-line* subsystem (Figure 8) was developed using Autodesk Robot Structural Analysis Professional 2013. The model includes all the main elements of the load-bearing structure, and thus the building frames, lattice purlins based thereon, bracings and secondary reinforced concrete structures. The results of measurements carried out throughout the period of the system installation to date were archived and interpreted on an ongoing basis. Figure 9 shows a chart of displacement/deformation in the sample measurement point. The analysis of the measurement results (also in other points) showed that only in two places (P7 and P5) the L2 threshold level was exceeded, which indicated the possibility of a situation requiring snow removal from the roof, not yet meaning the requirement to remove snow. At the same time, the history of changes in displacements measured shows significant declines in the values of the displacements measured recorded in a short time at certain points of measurement, which may indicate that roof snow removal operations were carried out even though the measurement results did not indicate such a need for (e.g. P7 point in December 2012) - Figure 10.
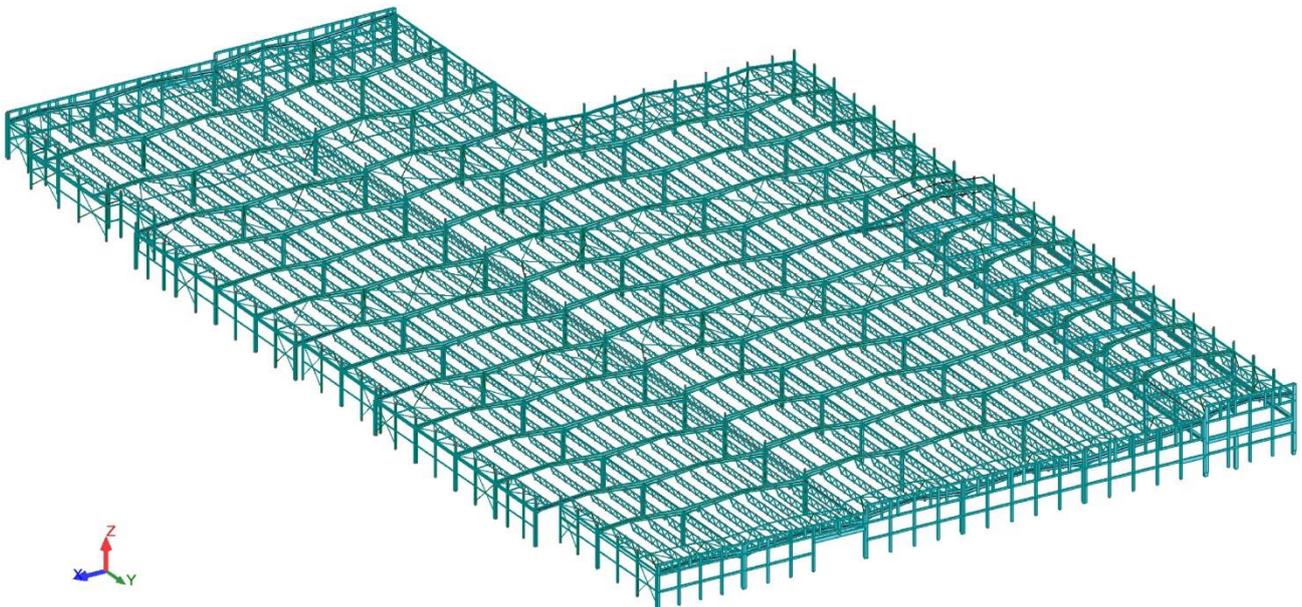
Figure 8. Printout of the numerical model of the off-line subsystem of WiSeNe[MONIT].[3]
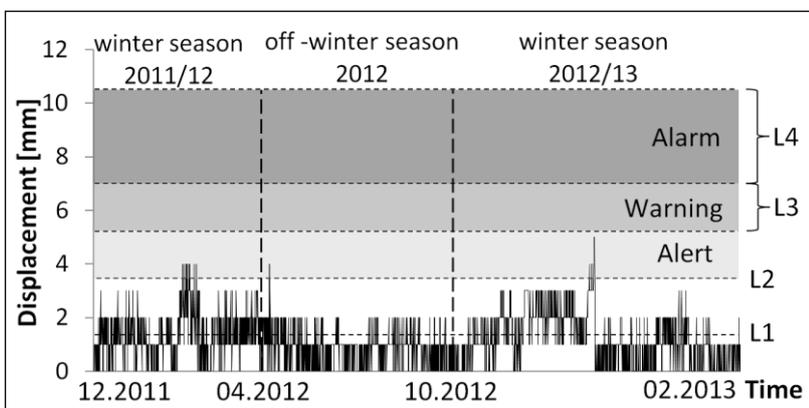
Figure 9. Displacement records from the measuring device P7. [3]
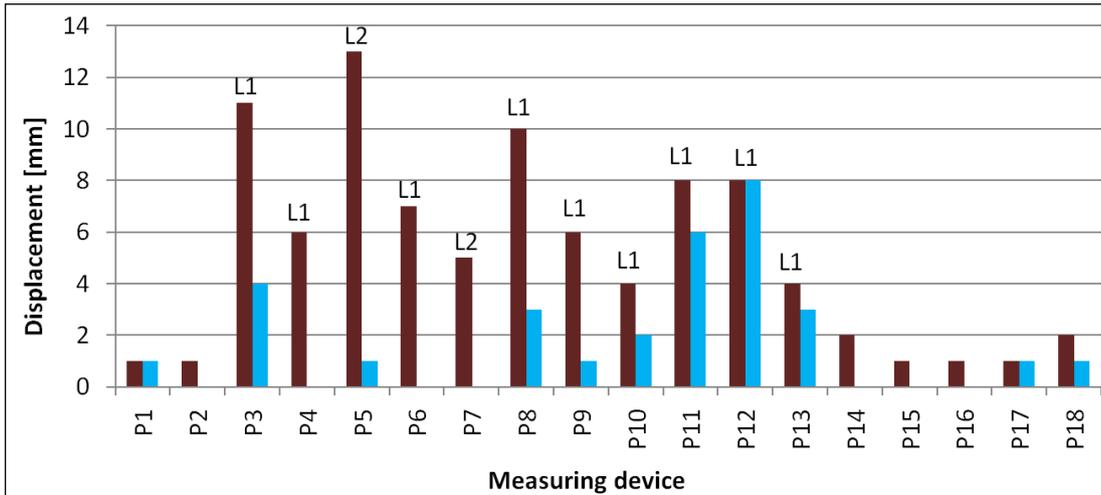
Figure 10. Displacement decrease caused by snow removal. [3]

Contact information

Wierzbicki Stanisław
Dr, Faculty of Civil Engineering, Warsaw University of Technology,
Al. Armii Ludowej 16, 00-637 Warsaw, Poland
+48 22 825 65 32
s.wierzbicki@il.pw.edu.pl

References

[1] Wierzbicki S., Giżejowski M., Stachura Z.: Structural failures and monitoring of structural health with use of WiSeNe[MONIT] system. Research and Applications in Structural Engineering, Mechanics and Computation (ed. A. Zingoni), CRC PRESS/BALKEMA-Proceedings and Monographs in Engineering, Water and Earth Sciences, Taylor and Francis Group, London 2013, 849-850 [full text in e-book, 2365-2370]

[2] Giżejowski M., Antoszkiewicz E., Wierzbicki S., Pioro Z., Wireless Sensor Network Systems for Structural Health Monitoring of Building Structures. Proceedings of the 5th International Conference on Structural Health Monitoring of Intelligence Infrastructure, Cancun, Mexico (SHMII-5), 11-15 December 2011, 34-34 [full length paper on a CD]

[3] Wierzbicki S., Monitoring of structure of industrial building on the example of the WiSeNe[MONIT] system, Structure and Environment, vol. 6, no. 4/2014, Kielce University of Technology, 17-23

[4] Wierzbicki S., Giżejowski M., Kwaśniewski L.: "Systemy "MONIT" technicznego monitorowania stanu bezpieczeństwa konstrukcji budowlanych", Aktualne Problemy Budownictwa Metalowego. Tom I, rozdz. XII Seria: Monografie Zespołu Konstrukcji Metalowych, Oficyna Wydawnicza Politechniki Warszawskiej (red. E. Szmigiera, S. Wierzbicki) ["MONIT" systems of technical monitoring of the building structures safety", Current Problems of Metal Construction. Volume I, Chapter XII, Series: Monographs of the Metal Structures Division, Warsaw University of Technology Publishing House(eds. E. Szmigiera, S. Wierzbicki)], Warsaw 2014, p. 201-220, ISBN 978-83-7814-251-5

[5] Giżejowski M., Wierzbicki S., Stachura Z., Structural Health Monitoring as a Tool Assisting the Structural Robustness Assessment (keynote paper). Proceedings of Twin International Conferences: 5th I.C. on New Dimensions in Bridges, Flyovers, Overpasses & Elevated Structures & 13th I.C. on Inspection, Appraisal, Repairs & Maintenance of Structures ((eds. Y. Zhuang, B. Chen), 28-29 July, 2012, Wuyishan, China, 27-36

Risk reduction through monitoring of road bridges

Peter Tanner. Eduardo Torroja Institute for Construction Science – Spanish National Research Council, IETcc-CSIC, Madrid, Spain

Miguel Prieto. Eduardo Torroja Institute for Construction Science – Spanish National Research Council, IETcc-CSIC, Madrid, Spain

José Manuel Mata. Euroconsult S.A., Madrid, Spain

Objectives, abstract and conclusions

Different causes may lead to the non-compliance of a particular requirement related with an existing infrastructure. Often, they may be traced back to deviations from expected actions or resistances. The quantification of parameters related with such influences may provide evidence about the degree of compliance of a given structure with a particular serviceability or safety requirement. Such parameters may therefore be called indicators and associated threshold values can be established on a risk basis, as well as admissible average frequencies for outcrossing.

Indicators can be monitored comparing the measured values continuously to the previously established threshold values. Alarm systems may be installed which are activated in case of outcrossing. Safety measures can therefore be adopted depending on the consequences of the observed non-compliance. Based on such an approach and by using modern information technology, inspections of large infrastructures may be automated and optimised.

A series of indicators for use in road bridge inspection are proposed hereunder, together with their respective threshold values and allowable mean frequency of outcrossing. The paper also includes a practical application in which these criteria are applied to a road bridge with an unknown reliability level.

1 Introduction

Structural systems must be engineered, built, operated and maintained to ensure economically sound use throughout their service life, while meeting predefined serviceability and structural safety requirements. Such requirements must be fulfilled with an acceptable level of reliability that depends on a number of parameters, including the reference period considered and possible consequence of non-compliance or failure.

Different influences and circumstances may underlie the non-compliance of a requirement:
- deviations from the assumed values for actions or the effects of environmental influences;
- deviations from values established for other influences, such as construction execution inaccuracies;
- geotechnical actions;
- chemical, physical and biological actions;
- actions or influences not considered;
- dynamic effects such as resonance;
- deviations from the structural or soil strength values assumed;
- strength loss due to decay mechanisms such as corrosion, embrittlement or fatigue;
- structural overloads or strength losses induced by accidental actions.

A structure's compliance with predefined requirements can be determined by quantifying parameters associated with these influences or circumstances, which are consequently called indicators and, generally speaking, refer to system geometry, materials, actions or structural

behaviour. The parameters chosen for effective inspection and monitoring should be the ones whose variation has the greatest effect on the reliability of the system studied. Hence, parameter selection depends on the type of technical system involved, its purpose and operation, exposure conditions, constituent materials and the data acquisition resources available.

When inspection planning is based on the adoption of suitable indicators, its scope can be adapted to the condition of the system elements, which can be prioritised in keeping with their significance and the decay mechanisms observed. From this perspective, the use of indicators to define inspection strategy can be interpreted as a risk reduction measure.

The objective of this paper is to define the grounds for the early detection of possible damage or anomalies with a view to adopting risk mitigation measures before an undesired event such as structural collapse occurs. Inspection scope and intensity should be determined on the grounds of the characteristics and significance of the structure inspected, as well as of the allowable risk.

2   Inspection

Depending on the context in which inspection is conducted and the objectives and resources used, a distinction can be drawn among the following:

- observation;
- periodic inspection;
- control measurements;
- monitoring.

Observation is understood to mean the perception, at pre-defined intervals, of the condition of a structure and its performance. Observations may also be conducted on the occasion of the performance of other tasks, such as maintenance. The qualitative determination and appraisal of the condition of a structure during inspections conducted at pre-defined intervals in accordance with given priorities constitute what is known as *periodic inspection*. *Control measurements* may be taken to quantify certain parameters representative of the structure or its performance. Lastly, *monitoring* consists of determining the condition of a structure through frequent or continuous recording of certain parameters representative of the system or its performance and the comparison of the values recorded to the respective thresholds.

The thresholds to which the data acquired with appropriate techniques and instruments are to be compared must be established depending on the level of reliability associated with each requirement. Information on how to determine thresholds is furnished in section 3 below. The measures that should be adopted when the acquired values for a given indicator exceed one or several of the associated thresholds are also discussed.

The data acquisition instruments used to monitor bridges must be able to record their static (lasting geometric changes) and dynamic (instantaneous geometric changes) behaviour. Moreover, for the data recorded to be useful in the long run, the instruments used must be able, at any given time, to establish the ratio between the existing and initial values. Thanks to recent progress in data acquisition, transmission and processing technologies, most parameters relevant to structural performance, particularly geometric change, can be continuously monitored. The effectiveness of inspection and maintenance measures can be considerably enhanced by systematically and suitably installing modern measuring systems on large infrastructures. One example of such a system can be found in the optical fibre sensors used in this project, which deliver resolution on the order of thousandths of a millimetre and feature stability over time.

Data acquisition on the established indicators forms part of programmed bridge inspections and should not be confounded with data collection for structural assessment. The need to assess

structural reliability may be the outcome of inspection findings, where, for instance, the indicators quantified exceed the respective thresholds (section 3).

3 Determination of threshold values

3.1 General

As in the determination of action effects in serviceability or structural safety calculations, the threshold values for the parameters quantified during road bridge inspections, known as reliability indicators, are normally established by structural analysis. Such analyses are based on the principles laid down in a consistent set of standards and recommendations such as IAP-11 (2011), EHE-08 (2008), EAE-11 (2011) and RPX-95 (1996) or the respective Eurocodes. Where existing bridges are involved, the updated values for the relevant variables should be used for the analysis, and where no updated information is available, the nominal values can normally be applied.

Structural analysis should deploy parameters able to predict a bearing structure's performance sufficiently accurately for the control situations studied. The methods used to these ends must be backed by substantiated theory. The analytical model must integrate actions and other influences, geometric data and the properties of the materials constituting the structure and the terrain.

3.2 Requirements

3.2.1 Principles

Tables 1 and 2 list the requirements for road bridges, irrespective of the constituent materials, in increasing order of the consequences of possible non-compliance. Indicators are established and the respective threshold values are also given, along with the allowable mean frequency of exceedance of the associated requirements. The measures to be adopted in the event of non-compliance of any of these requirements are mentioned in item 3.3 below.

The choice of indicators is conditioned by the availability of suitable data acquisition or measuring facilities. In the SEGUSTRUC project (Tanner and Prieto (2013a), Tanner and Prieto (2013b)), monitoring was usually, but not exclusively, conducted with fibre optic sensors. As a general rule, when threshold values are determined on the grounds of structural analysis, monitoring can only detect the effects of actions applied after a new or existing bridge is instrumented.

Table 1: Requirements, indicators and thresholds values associated with road bridge serviceability (SLS).

Demand		Consequences	Requirement	Indicator	Threshold	
					Value $E_{ser,lim}$; $C_{ser,lim}$	Mean frequency ω_{ser}
SLS	Appearance	Reversible	Deformations	Deflection	L/700 [1]	50 % of time
	Appearance	Reversible	Deformations	Strain	$E_{ser,lim,2}$	50 % of time
	Comfort	Reversible	Deformations	Deflection	L/1000 [2]	Weekly
	Comfort	Reversible	Deformations	Strain	$E_{ser,lim,1}$	Weekly
	Comfort – Maximum – Medium – Minimum	Reversible	Vibrations	Acceleration	a_v[3] a_h[3] 0,5 0,1 1,0 0,3 2,5 0,8	- - -

L: span length
[1] Deflection after subtracting possible precamber, bearing in mind long-term effects due to creep, shrinkage and relaxation
[2] Deflection due to traffic loads; higher values, up to L/500, acceptable for existing bridges on low traffic capacity roads
[3] a_v: vertical acceleration [m/s^2] ; a_h: horizontal acceleration [m/s^2]

Table 2: Requirements, indicators and thresholds values associated with road bridge structural safety (ULS).

Demand		Consequences	Requirement	Indicator	Threshold	
					Value $E_{d,lim}$	Mean fr. ω_d
ULS	Structural reliability	Reversible	Safety of structure and facilities	Traffic loads[1]	$E_{d,lim,1}$	Weekly
	Structural reliability	Reversible	Safety of structure and facilities	Strain	$E_{d,lim,1}$	Weekly
	Structural reliability	Irreversible	Safety of people	Traffic loads[1]	$E_{d,lim,0}$	Yearly
	Structural reliability	Irreversible	Safety of people	Strain	$E_{d,lim,0}$	Yearly

[1] Support reactions are recorded using the bridge as a weighing scale

3.2.2 Threshold values associated with structural safety

A bridge is regarded as structurally safe if the values of the parameters measured during inspection are non-compliant with condition (1) less often than the allowable frequency, ω_d, associated with the respective threshold value:

$$E_{mon} \le E_{d,lim} \tag{1}$$

E_{mon} measured value of a given indicator
$E_{d,lim}$ threshold value for the same indicator, associated with structural safety

The threshold value for action effects associated with the relevant control situations that should not be exceeded more than once a year can be determined from the following expression, in which the symbols are defined as in standard IAP-11 (2011):

$$E_{d,\lim,0} = E\left(\sum_{j\geq 1}\gamma_{G,j}\cdot G_{k,j} \,"+"\,\gamma_P\cdot P\,"+"\,\gamma_{Q,1}\cdot\psi_{0,1}\cdot Q_{k,1}\,"+"\,\sum_{i>1}\gamma_{Q,i}\cdot\psi_{1,i}\cdot Q_{k,i}\right) \tag{2}$$

The threshold value for action effects associated with the relevant control situations that should not be exceeded more than once a week can be determined from the following expression (symbols defined as in standard IAP-11 (2011)):

$$E_{d,\lim,1} = E\left(\sum_{j\geq 1}\gamma_{G,j}\cdot G_{k,j} \,"+"\,\gamma_P\cdot P\,"+"\,\gamma_{Q,1}\cdot\psi_{1,1}\cdot Q_{k,1}\,"+"\,\sum_{i>1}\gamma_{Q,i}\cdot\psi_{2,i}\cdot Q_{k,i}\right) \tag{3}$$

In case that the investigated bridge is correctly designed to consistent code specifications, and in the absence of more detailed analysis, the values of the partial factors for actions γ_G, γ_P and γ_Q as well as of the factors for combination values of actions ψ_0, ψ_1 and ψ_2 can be taken from standard IAP-11 (2011) or the respective Eurocodes, EN 1990 (2002), EN 1990:2002/A1:2005 (2005).

3.2.3   Threshold values associated with serviceability

A bridge is regarded as serviceably sound if the values of the parameters measured during inspection are non-compliant with condition (4) less often than the allowable frequency, ω_{ser}, associated with the respective threshold value:

$$E_{mon} \leq E_{ser,\lim} \tag{4}$$

E_{mon} measured value of a given indicator
$E_{ser,\lim}$ threshold value for the same indicator, associated with serviceability

For some indicators associated with serviceability requirements such as deflection due to traffic loads or acceleration induced by dynamic actions in bridges with pedestrian access, standard IAP-11 (2011) lists indicative thresholds for in-service structural performance parameters. Given that these values may be adopted as serviceability thresholds ($C_{ser,\lim}$) with no need to conduct structural analysis, bridge performance may be regarded as suitable where the values measured for the respective parameter are non-compliant with condition (5) less often than the allowable frequency, ω_{ser}:

$$E_{mon} \leq C_{ser,\lim} \tag{5}$$

The threshold value for action effects associated with the relevant control situations that should not be exceeded more than once a week can be determined from the following expression (symbols defined as in standard IAP-11 (2011)):

$$E_{ser,\lim,1} = E\left(\sum_{j\geq 1}G_{k,j} \,"+"\,P\,"+"\,\psi_{1,1}\cdot Q_{k,1}\,"+"\,\sum_{i>1}\psi_{2,i}\cdot Q_{k,i}\right) \tag{6}$$

The threshold value for action effects associated with the relevant control situations that should not be exceeded more than 50% of the time can be determined from the following expression (symbols defined as in standard IAP-11 (2011)):

$$E_{\text{ser,lim,2}} = E\left(\sum_{j \geq 1} G_{k,j} \,"+"\, P \,"+"\, \sum_{i \geq 1} \psi_{2,i} \cdot Q_{k,i} \right) \tag{7}$$

In the absence of more detailed analysis, the values of the factors for combination values of actions ψ_1 and ψ_2 can be taken from standard IAP-11 (2011) or the respective Eurocode EN 1990:2002/A1:2005 (2005).

3.3 Planning and adoption of measures

If any of the requirements set out in Tables 1 and 2 is not met, suitable corrective measures must be taken to mitigate the possibility of personal harm or environmental or economic damage. Such measures must be carefully planned, which necessarily entails an analysis of both, the cause or causes of the non-compliance observed and of structural reliability. In certain cases, such as where fluctuations in the mean or extreme values of a given indicator are observed to accelerate or follow a trend, it may be advisable to analyse the values recorded even where no non-conformity has been formally established.

4 Practical application

4.1 Introduction

The methodology proposed in the SEGUSTRUC project (Tanner and Prieto (2013a), Tanner and Prieto (2013b)) was applied to two bridges of unknown reliability located in the province of Seville, Spain. Only one of the two trials is discussed hereunder. The bridge chosen runs in the east-west direction and crosses the River Guadalquivir on ring road SE-30. This five-span (40 + 68 + 100 + 68 + 40 m), 316 m long composite bridge features a variable depth. Its approach viaduct consists of a six-span (4 x 27 + 30 + 22 m), 160 m long continuous, post-tensioned slab which lies outside of the scope of the study.

The bridge deck is 30,1 m wide. Its triple-cell composite box girder varies in plan and elevation view dimensions. The width of the bottom flange of the steel box ranges from 9,2 to 15,4 m while its depth gradually rises from 2,25 at the mid-point in the 100 m span to 4,55 m over piers P-2 and P-3. It is fitted with longitudinal and transverse stiffeners, as well as diaphragms placed at 4 m intervals, in addition to the support diaphragms. The concrete slab is 0,22 m thick with passive (two layers Φ20 at 0,15) and active (48 tendons 7 Φ0.6" in the sections on piers P-1 and P-4 and 96 tendons in the ones on piers P-2 and P-3) reinforcements. It has pile foundations, confined (Pot-type) neoprene bearings at abutment 1 (E-1), P-1, P-2, P-3 and P-5 and hooped neoprene bearings at P-4.
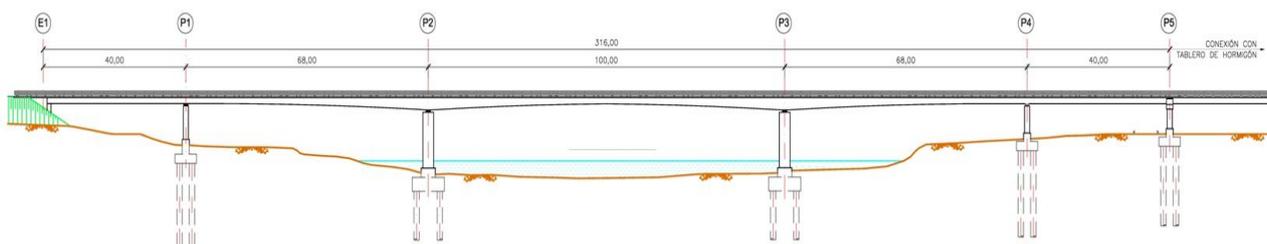
Figure 1: Longitudinal elevation view of bridge monitored

4.2 Instruments used and analytical model

The indicator used to monitor the bridge was unit strain. Given bridge symmetry and taking into account the resolution of the data acquisition system used, only one half of the structure was instrumented. The system chosen to monitor unit strain consisted of 2 m long fibre optic sensors inside steel protective sheaths. These sensors were able to log changes in shape and position to a precision of 0,01 mm for static readings (1 every 10 minutes) and 0,001 mm for dynamic readings (50 per second). The static values logged were the mean of the readings taken in each 10 minute interval.

Three sections were chosen to measure unit strain in the longitudinal direction of the bridge: the two sections with maximum hogging moments over piers P-1 and P-2, which, moreover, concurred with the sections actively reinforced, and the one with maximum sagging moments (mid-point in the 100 m span). Two optical sensors were positioned in the steel cross-section over pier P-2, one on the lower flange and the other on the upper flange. Pier P-1 and the centre of the 100 m span were instrumented only on the upper face of the lower flange. The temperature inside the box was recorded in the central cross-section of the main span.

Structural calculations were performed with Civilcad2000 (2000) software. Since the structure rests on deep foundations consisting of piles, analysis of the composite deck alone, i.e., separate from the under-structure, was deemed sufficient. The construction stages addressed in the analysis of the composite structure included positioning of the steel structure, concrete casting in 5 stages and subsequent cable prestressing in the upper slab, concrete casting on five non-prestressed stretches of the upper slab, concrete casting of the lower slab and prestressing of external post-tensioning. Taking into account that the bridge has been in service for several years when the aforementioned data acquisition system has been installed, the actions studied to assess the structure were self-weight, traffic loads, pedestrians, wind, as well as imposed deformations due to settlement and temperature.

From the stress values obtained in the extreme fibres of the sections studied with the numerical model for the relevant combinations of actions, unit strains were found assuming elastic structural behaviour. As the structure's self-weight and dead loads existed prior to when it was instrumented, the threshold values did not include the respective unit strain (item 3.2.1).

4.3 Comparisons of the findings to threshold values

Data acquisition started in December 2013. Figure 2 compares the data logged by the sensor positioned on the upper face of the bottom flange in the cross-section over pier P-1 to the respective thresholds. The convention used here was to show compression as negative and tensile strains as positive. Serviceability threshold $E_{ser,lim,1}$ was not exceeded and $E_{ser,lim,2}$ was exceeded less than 50% of the time. The readings were also well within structural safety thresholds $E_{d,lim,1}$ and $E_{d,lim,0}$, for while the bridge was designed to bear traffic loads characteristic of expressway bridges, its traffic is primarily urban.
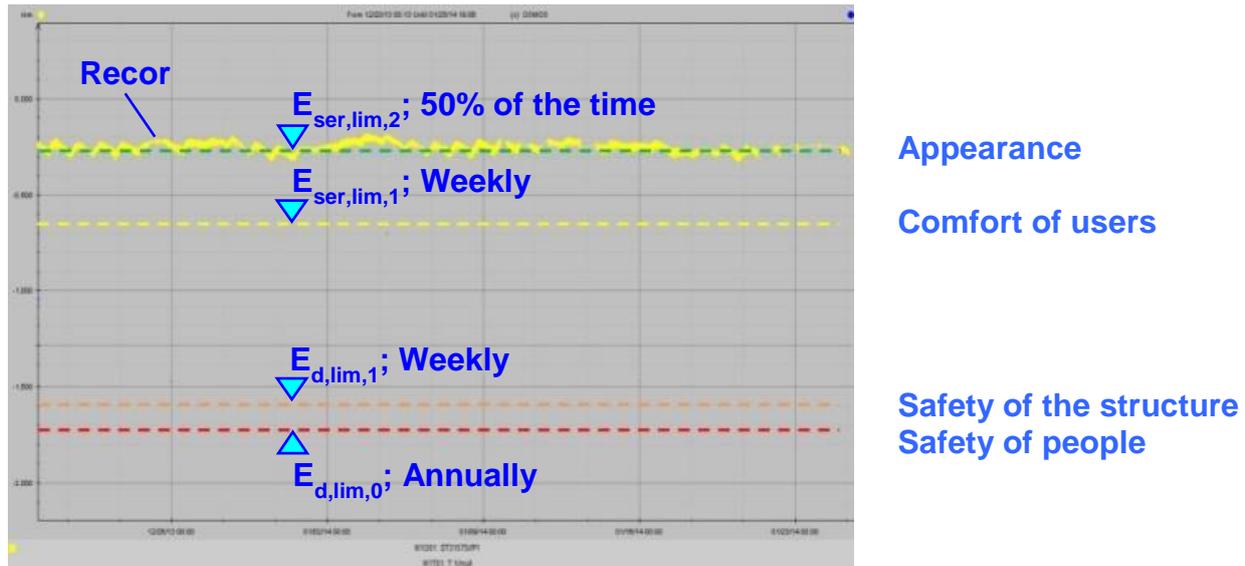
Figure 2: Results from monitoring with fiber optic sensors on bottom flange of the cross-section over pier P-1 and comparison with threshold values associated with serviceability and structural safety requirements

5   Final remarks

This paper defines a procedure for monitoring road bridges with a view to early detection of possible damage or anomalies to be able to adopt suitable measures before an undesired event such as structural collapse occurs. It contains proposals for indicators or quantifiable parameters that can provide information on the degree of compliance with serviceability and structural safety requirements. It also discusses recommended threshold values and the mean frequency with which they may be exceeded before risk mitigation measures are required.

The procedure proposed was applied to a road bridge with an unknown reliability level. While monitoring has been in place for a relatively short time, the findings suggest that long-term analysis of the data so acquired will improve the effectiveness of road bridge inspection and maintenance.

6   Acknowledgements

References

Civilcad2000 (2000), CivilCAD Consultores S.L.

EAE (2011). Structural steel standard (Written in Spanish). Madrid. Ministerio de Fomento.

EHE-08 (2008). Structural concrete standard (Written in Spanish). Madrid, Ministerio de Fomento.

IAP-11 (2011). Actions for the design of road bridges (Written in Spanish). Madrid. Ministerio de Fomento.

Tanner and Prieto (2013a). Theoretical basis for the inspection and maintenance project of road bridges. Technical Report nº 19.884-I (Written in Spanish). Madrid. Instituto de Ciencias de la Construcción Eduardo Torroja. IETcc-CSIC.

Tanner and Prieto (2013b). Recommendations for the inspection and maintenance project of road bridges. Technical Report nº 19.884-II (Written in Spanish). Madrid. Instituto de Ciencias de la Construcción Eduardo Torroja. IETcc-CSIC.

RPX-95 (1996). Design recommendations for composite road bridges (Written in Spanish). Madrid. Ministerio de Fomento.

EN 1990 (2002). Eurocode. Basis of structural design. Brussels. CEN.

EN 1990:2002/A1:2005 (2005). Basis of structural design. Annex A2: Application for Bridges. Brussels. CEN.

Contact information

Peter Tanner
MSc Bau-Ing. ETH Zürich. Eduardo Torroja Institute for Construction Science – Spanish National Research Council, IETcc-CSIC, Serrano Galvache, 4, 28033, Madrid, Spain
+34913020440 (extension 870228)
tannerp@ietcc.csic.es

Miguel Prieto
PhD in Civil Engineering. Eduardo Torroja Institute for Construction Science – Spanish National Research Council, IETcc-CSIC, Serrano Galvache, 4, 28033, Madrid, Spain
+34913020440 (extension 870375)
mprietor@ietcc.csic.es

ANALYSIS OF DEGRADATION PROCESSES ON SLOVENIAN BRIDGES

Matej Kušar, Faculty of Civil and Geodetic Engineering, University of Ljubljana, Slovenia
Jana Šelih, Faculty of Civil and Geodetic Engineering, University of Ljubljana, Slovenia

Objectives

The main purpose of the analysis is to determine the most important parameters influencing the degradation processes of bridges. Bridges are daily exposed to various external influences and as such, they are very suitable for analyzing the relationship between degradation processes and various parameters of influences.

The second purpose of the analysis is to assess the quality of analyzed data. Current condition assessment system for Slovenian regular and main bridge inspections has no quality control/assurance system. Although the assessors are trained to detect, classify and judge the observed damages in a unified manner, there can be significant discrepancies in recorded condition ratings. The assessment will show the necessity of quality control for structural health monitoring of bridges.

Technical information

Condition rating data, provided by the state road network manager, were analysed for the time period from 1993 to 2011 for a total of 1271 bridges. Condition assessments were performed by using the currently officially valid methodology that yields, as the final result, overall condition rating for the structure, accompanied by the list of partial ratings for separate structural parts. A total of 50.000 data was analysed.

Average yearly deterioration rates for all bridges and their parts (substructure, superstructure and deck) were estimated by using linear regression. For the purpose of the analysis, time required to achieve a pre-defined condition rating level was taken as a dependent variable of the condition rating, and defined by the piecewise linear relation. The assessment of data quality was determined using the standard error.

Summary

Results of the performed analysis show that climate impact is the most important parameter influencing the degradation processes of bridges (on the whole structure level). Further, the obtained results show that exposure to water flowing underneath the bridge influences only the substructure elements. The construction material of the bridge and traffic load have little or no influence upon the condition of the bridge.

The results obtained on the sample of bridges and passes on Slovenian state roads also show that raw data collected (using the current monitoring system with no quality control) is of low quality, as almost 50% of analysed datasets were considered unreliable due to their inconsistent variations with time. As a consequence, a special procedure for data processing was developed, with the purpose of creating meaningful datasets after using the processing procedure.

1 Introduction

During its operation and use, performance of all roadway structures is decreasing due to various deterioration processes: inherent ageing and deterioration phenomena triggered by environmental influences, increased traffic load, and eventual natural hazards, such as earthquakes, floods and landslides (Šelih et al. (2008), Frangopol (2011)). Structural design carried out in the initial design stage, even when carried out by state-of-the-art standards and guidelines, cannot protect the structure from deterioration during the operation stage (Frangopol (2011)). Appropriate maintenance and rehabilitation actions need to be planned and carried out throughout the life cycle of the structure in order to maintain its adequate performance (Ellingwood (2005)).

Most developed countries have prescribed regular routine condition monitoring for bridges within predefined time intervals by using adequate methodologies. The majority of the existing bridge maintenance systems (BMSs) are based primarily on information obtained through visual inspections (Gattulli and Chiaramonte (2005)). Documented ongoing experience reveals this type of inspection is often unreliable; however, it should remain the main aid collecting data due to its simplicity and cost effectiveness (Tenžera et al. (2012)).

The purpose of the present research is to identify parameters that influence the deterioration rate of bridges, and to structure the existing Slovenian bridge network database according to these parameters. Available data describing the condition state of structures within the selected bridge network (measured by the bridge condition rating coefficient) for the past 20 years will therefore be analysed. Three levels of road networks, highways, state roads and community roads are distinguished by the legislature within the territory of Slovenia. The subject of present research is limited to structures within the state road network.

2 Parameters of influence

The first step in management of bridges within the road network under consideration is creating their comprehensive inventory that contains relevant data associated with every individual bridge. Within this context, it has to be acknowledged that state road bridges in Slovenia differ in construction material, bearing structure type, length, number of lanes and traffic load, and are located in different climate zones. Deterioration mechanisms of the materials that influence the performance of structures are strongly dependent on environmental factors, in particular ambient temperature, relative humidity and presence of aggressive elements in air and water (Žarnić (2005). The existing inventory of bridges was structured with respect to the identified parameters of influence.

From the structural material point of view, the superstructures are constructed of reinforced concrete, steel, stone or pre-stressed concrete. As only eleven bridges within state road network are constructed of either wood or as composite bridges, they are not taken into the account in the analysis. The substructure load bearing material is predominantly reinforced concrete, except in the case of stone bridges, where the substructure is made of stone as well. Consequently, the indicator that defines the structural material of bridges has the following values;

$$M_i \in (RC, PC, Sto, Ste) \tag{1}$$

Where *RC, PC, Sto* and *Ste* denote reinforced concrete, pre-stressed concrete, stone and steel bridge superstructures.

Three significantly different climate zones can be observed in Slovenia: Alpine, Mediterranean and Continental zone. They result in the appearance of a different set of deterioration processes in structural materials (Moncmanova (2007)), therefore climate is considered to be a relevant parameter of influence, namely:

$$Cl_i \in (Me, Co, Al) \tag{2}$$

Where *Me, Co* and *Al* denote Mediterranean, Continental and Alpine climate.

Traffic load, as one of the key load types for road bridges, is identified as the third parameter of influence. Slovenian technical standard addressing traffic load (TSC 06.511 (2014)) distinguishes 6 categories of traffic load as a function of nominal vehicle axial load of 100kN, transmitted by double wheels (4x25kN) to the pavement surface. For the purpose of the present study, these 6 categories were aggregated into 3: light (L), medium (M) and heavy (H) traffic load, depending on number of passes of nominal axial load of 100 kN, namely:

$$T_i \in (L, M, H) \tag{3}$$

Values limiting the intervals defining *L, M* and *H* are presented in Table 1.

Table 1. Traffic load categories

Traffic load	Number of passes nominal axial load of 100 kN	
	daily	in 20 years
heavy (H)	over 300	over 2 x 106
medium (M)	80 to 300	6 x 105 to 2 x 106
light (L)	under 80	under 6 x 105

Identification of the last parameter of influence on the structure level concerns deterioration processes related to the presence of water. From the viewpoint of their function, the bridges can span over water, valley or road (overpasses). The main difference among these structures stems from the fact that foundations, abutments and wing walls of bridges are exposed to deterioration phenomena associated with the presence of water: abrasion, erosion, freezing and thawing, or permanent high relative humidity. Substructures of overpasses and underpasses are not in direct contact with water and consequently, they are not exposed to these deterioration processes. Structural type (F_i) is therefore added to the list of parameters of influence;

$$F_i \in (B, P) \tag{4}$$

Where *B* and *P* indicate a bridge (B) and overpass/underpass (P), respectively.

Deterioration rate of the structures (b_i) under consideration can be expressed as a function of above-identified parameters of influence;

$$b_i = b_i(M_i, Cl_i, T_i, F_i) \tag{5}$$

Where, as already mentioned, M_i indicates the structural material, Cl_i the climate type of the geographic area where the structure *i* is located, T_i traffic load over the structure, and F_i the type of the structure *i*.

For the purpose of the analysis, the bridge structure is divided into structural parts: substructure, superstructure and bridge deck. These parts may be subjected to different environmental factors: bridge deck is subjected to traffic load as well as various environmental loads causing material

deterioration; substructure can be, in case of a bridge, exposed to direct contact with water; and various environmental loads that depend on the bridge location (e.g. wind carrying salt particles for a bridge in the coastal area). Deterioration of these bridge elements may progress at different rates; therefore, they have to be assessed and analysed separately. In this way, the bridge structural part (Be_i) is identified as an additional parameter of influence, as follows:

$$Be_i = (S_{sub}, S_{sup}, D) \tag{6}$$

Where S_{sub}, S_{sup}, and D refer to substructure, superstructure and deck, respectively. The complete list of parameters of influence and possible range of values for each of them is presented in Table 2.

Table 2. Identified parameters of influence and range of assigned values for each parameter

PARAMETER OF INFLUENCE	NO. OF VALUES	VALUE
struct. material, M	4	RC (reinforced concrete), PC (pre-stressed concrete), Sto (stone), Ste (steel)
climate zone, Cl	3	Me (Mediterranean), Co (Continental), Al (Alpine)
traffic load, T	3	L (light), M (medium), H (heavy)
structural type, F	2	B (bridge over water), P (bridge over valley or road)
structural part, Be	3	S_{sub} (substructure), S_{sup} (superstructure), D (deck)

The present bridge inventory of the Slovenian state road network consists of 1282 bridges. Due to their small number, as already mentioned, 11 bridges made either of wood or composite material were not included in the analysis. A total of 1271 bridges were therefore taken into the account in the present analysis. Table 3 shows that a vast majority of bridges are made of reinforced concrete and are located within Continental climate type. Only a small number of bridges are located in Alpine climate region, due to large proportion of the mountainous terrain having low density of population and accompanying scarce road infrastructure.

Table 3. Number of bridges under consideration, structured with respect to the identified parameters of influence

MATERIAL (superstructure)	STR: TYPE	NO. [n]	TRAFFIC LOAD			CLIMATE TYPE		
			L	M	H	Me	Co	Al
RC	B	899	538	202	159	81	754	64
	P	150	62	29	59	35	104	11
Sto	B	97	58	30	9	37	58	2
PC	B	75	29	20	26	1	74	0
Ste	B	50	42	6	2	6	40	4
TOTAL		1271	729	287	255	160	1030	81
			1271			1271		

3 Analysis of data

3.1 Assessment methodology

The assessment methodology is presented in (Kusar and Selih (2014)).

3.2 Assessment of data quality

One of the major deficiencies of the current condition assessment system identified by scrutinizing the procedures being employed is the absence of a quality control/ assurance system applied to the data acquired by the inspection. The comparative assessments that were carried out on the same structure simultaneously by several assessors in some cases showed significant discrepancies in recorded condition ratings. This occurrence, which leads to several inconsistencies in the collected data, was also studied by other researchers (Tenžera et al. (2012), Gattulli and Chiaramonte (2005)). Consequently, the damage ratings data and their changes with time were scrutinized prior to initiating the analysis. The complete database along with individual Investigation Reports, were checked. For the data sets that exhibited inconsistent trends of ratings with time, the relevant individual Investigation Reports were scrutinized. If repair activities were recorded in the Investigation Report, the data sets were kept and handled in the manner that will be described.

For the bridges that were repaired during the time interval under consideration, two partial data strings are distinguished, the first describing the behavior of the structure prior to refurbishment, and the second representing the changes of rating with time after the refurbishment. Out of these two data strings, the longer partial data string (i.e. containing more data points) was taken into the account for further analysis. Complete time interval was analysed for bridges that have not been repaired during the observed time interval.

The deterioration rates (defined as change of the condition rating per time unit) for all structures and their parts (substructure, superstructure and deck) were estimated by using linear regression for the complete time period under observation. Attempts were also made to use the exponential regression curve, however the obtained results have revealed that the linear relationship can represent well the available data, due to the data variability (Kusar (2013)). For an individual structure j, rating $y_{j,lin}$ was determined as follows;

$$y_{j,lin} = a + b \cdot x_j \tag{7}$$

Where b is average deterioration rate for the interval under consideration, and x_j represents time. Coefficients a and b were determined by applying least square method to the available datasets as follows;

$$b = \frac{\sum_{j=1}^{p}(x_j - \bar{x}) \cdot (y_j - \bar{y})}{\sum_{j=1}^{p}(x_j - \bar{x})^2} \tag{8}$$

$$a = \bar{y} - b \cdot \bar{x} \tag{9}$$

$$\bar{x} = \frac{1}{n} \cdot \sum_{j=1}^{p} x_j \tag{10}$$

$$\bar{y} = \frac{1}{n} \cdot \sum_{j=1}^{p} y_j \tag{11}$$

j indicates the year under consideration, p the final year of the analysis and n dataset size.

The actual values of the ratings in the year under consideration, j, differ from the values determined by the regression line, $y_{j,lin}$, that presents the course of deterioration. In order to determine the magnitude of discrepancy between the actual and the calculated rating values, standard error of these two values was calculated. The calculation was carried out for structures as

a whole as well as for their individual structural parts. Standard error, SE, of the linear regression line defined by Eq. (7), $y_{j,lin}$, was calculated as;

$$SE = \sqrt{\frac{1}{(n-2)} \cdot \left[\sum_{j=1}^{p}(y_j - \bar{y})^2 - \frac{\left[\sum_{j=1}^{p}(x_j - \bar{x}) \cdot (y_j - \bar{y}) \right]^2}{\sum_{j=1}^{p}(x_j - x)^2} \right]} \qquad (12)$$

Where $\bar{x}$ and $\bar{y}$ are the mean values of the dataset and x_j and y_j are the independent and dependent data, respectively. The dataset is considered consistent if standard error, SE, conforms to the condition;

$$\frac{SE}{\bar{y}} \le 0,3 \qquad (13)$$

Conversely, if, for a given dataset, standard error SE does not meet the criterion Eq. (13), the data point for which the standard error is the largest is eliminated from the dataset, as it is considered to be unreliable (Figure 1). To ensure that a) there is not more than one extremely unreliable data point and b) the elimination of the selected data point results in significant (at least 30%) reduction of the initial standard error, the following criterion needs to be met for the dataset after being processed, namely;

$$1,3 \cdot (SE_1 / \bar{y}) \le (SE_0 / \bar{y}) \qquad (14)$$

Where SE_1 indicates standard error of the processed set (after the elimination of the data point with the largest standard error), and SE_0 the standard error of the original data set. If Eq. (14) cannot be satisfied for the dataset under consideration, the dataset as a whole is considered unreliable and is excluded for further examination.
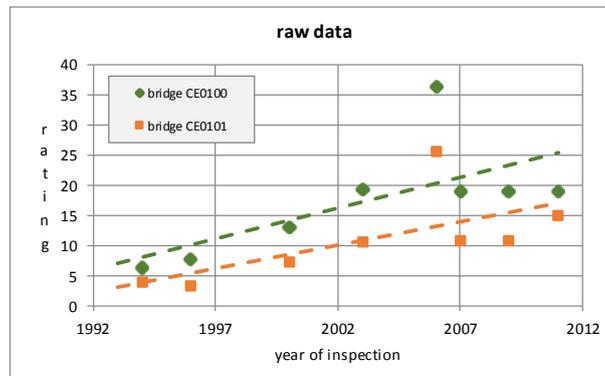
Figure 1: Condition rating changes with time for two individual bridges in the period from 1994 to 2011 and their linear trend line (the 2006 data is clearly not in line with the trend and was eliminated)

Analysis of complete data describing the condition of state road bridges shows that only 2599 out of the 4956 datasets (approx. 52%) datasets conformed to the condition in Eq. (13). After eliminating the single most unreliable data set in the string that did not meet the condition in Eq. (13), another 41% of the total datasets under consideration became suitable for further analysis. Of the remaining datasets, 4% did not meet any of the conditions in Eq. (13) and (14) and 3% contained data strings too short (with less than 3 data points) to be used in further analysis.

After processing the raw data, the average deterioration rate, b, was determined for all structures and its structural parts within the network, for all combinations of the parameters of influence

(Table 2) by linear regression. Details of the procedure and the results can be found in Kusar (2014).

The above-described procedure shows that absence of quality control during bridge inspections (data gathering) results in unreliable raw data as almost 50% of datasets had SE higher than 0,3. After processing, the raw data can later be improved to a certain extent, but its reliability could be much higher with implementation of quality control.

3.3 Determination of the average deterioration rate

The main goal of the study was to determine average deterioration rate for structures and structural parts subjected to the selected combinations of parameters of influence. In order to analyse the bridge behaviour, condition rating ranges for bridge decks, sub- and super-structures were structured into 4 intervals that define the deterioration levels (excellent, good, satisfactory, sufficient). Deterioration rate, b, is then calculated for each dataset, k (defined for each individual condition rating interval) as;

$$b_k = \frac{\sum_{j=1}^{p}(x_{k,j} - \overline{x_k}) \cdot (y_{k,j} - \overline{y}_k)}{\sum_{j=1}^{p}(x_{k,j} - \overline{x}_k)^2}$$

(15)

For each combination of parameters of influence, the average deterioration rate $\overline{b}$ is determined as:

$$\overline{b}(M,Cl,T,F,Be,R) = \frac{\sum_{k=1}^{r} b_k}{r}$$

(16)

$$r = r(M,Cl,T,F,Be,R)$$

(17)

Where R denotes the condition rating level and r number of data sets with the same combination of parameters of influence within the condition rating interval.

For all combinations of influence defined in Table 3, the values of average deterioration rates $\overline{b}$ for the structures under consideration were determined. For the purpose of the analysis, time required to achieve a pre-defined condition rating level was taken as a dependent variable of the condition rating, and defined by the piecewise linear relation. For substructure and superstructure, time is determined by Eq. (18). The value of time for bridge deck is determined with expressions similar to Eq. (18), where condition rating interval size is taken as 2.

$$t(R) = \begin{cases} \dfrac{R}{\overline{b}_{[0,3)}} \; ; R \in [0,3) \\[2ex] \dfrac{3}{\overline{b}_{[0,3)}} + \dfrac{R-3}{\overline{b}_{[3,6)}} \; ; R \in [3,6) \\[2ex] \dfrac{3}{\overline{b}_{[0,3)}} + \dfrac{3}{\overline{b}_{[3,6)}} + \dfrac{R-6}{\overline{b}_{[6,9)}} \; ; R \in [6,9) \\[2ex] \dfrac{3}{\overline{b}_{[0,3)}} + \dfrac{3}{\overline{b}_{[3,6)}} + \dfrac{3}{\overline{b}_{[6,9)}} + \dfrac{R-9}{\overline{b}_{[9,12]}} \; ; R \in [9,12] \end{cases}$$

(18)

3.4 Impact of selected parameters of influence upon the deterioration

3.4.1 Traffic load

The influence of the traffic load upon the deterioration rate of structures under consideration was analysed for bridges constructed of all structural materials. Results of the whole bridge as well as results of the bridge deck alone were obtained. There are only a few structures subjected to medium or heavy traffic load in the Alpine climate region, therefore the traffic load influence was analysed only for Continental and Mediterranean climate regions. For reinforced concrete bridges it can be observed, that the structures subjected to heavy traffic load deteriorate with practically the same rate as those loaded by medium/light traffic load when located in the same climate region (Figure 2). The only minor discrepancy from the observed rating trend can be noticed for structures subjected to medium traffic load located in Mediterranean climate region.

The influence of traffic load upon the behaviour of structures was also analysed for the individual structural parts of which bridge decks are the most exposed. Results show that deterioration of structures as well as their individual structural parts does not depend upon traffic load. Data analysis of stone, prestressed and steel bridges yield similar results as obtained for reinforced concrete structures, shown in Figure 2.
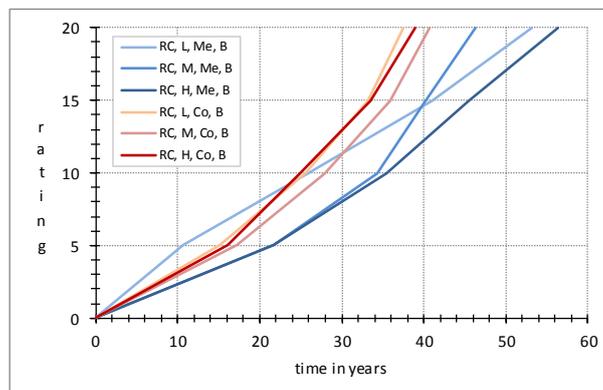
Figure 2: Temporal deterioration development for reinforced concrete bridges, as a function of traffic load

Taking into account scatter of recorded condition rating values, we can conclude, that the deterioration rate for the structure as a whole, as well as its structural parts, does not depend on the traffic load. We attribute this behaviour to the fact that the structures under consideration were designed and constructed according to the national structural codes that demand the structure to be mechanically resistant to appropriate design traffic and other loads. As a consequence, other parameters of influence are analysed without taking into account the traffic load.

3.4.2 Climate type

In Slovenia, only reinforced concrete structures are present in all three climate zones while steel and stone bridges are located in Continental and Mediterranean climate and prestressed bridges were built exclusively in areas with Continental climate. Therefore, the influence of the climate type upon deterioration could only be studied for reinforced concrete structures. Analysis of the available data shows that the climate type has noticeable influence upon deterioration of all structural elements of bridges (substructure, superstructure and bridge deck, Figure 3).
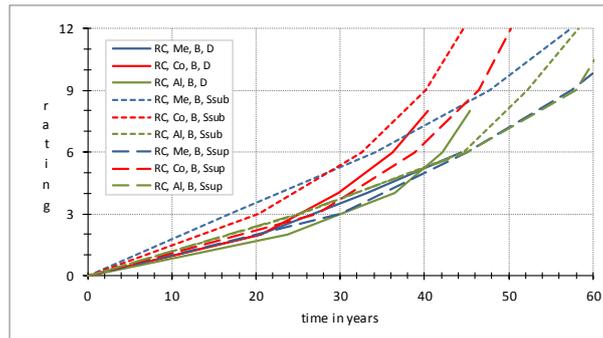
Figure 3: Temporal deterioration development for reinforced concrete bridge structural parts, as a function of climate type

3.4.3 Structural material

The deterioration rate of structures was studied with respect to the structural material type. For the inventory under consideration, four different structural materials are encountered in superstructure. Substructure, however, is constructed of reinforced concrete regardless of the type of the superstructure, except for stone bridges that represent a minor portion of the inventory. Consequently, only the deterioration rates of structures as a whole and superstructures were compared.
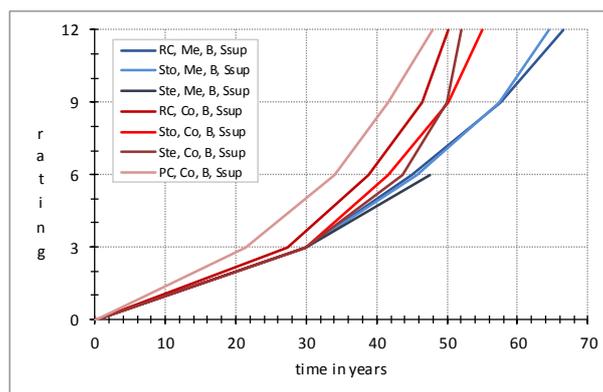
Figure 4: Temporal deterioration development for bridge superstructures, as a function of material type

Bridges are designed according to the needs of the expected traffic and are only indirectly related to the structural material of the bridge. The deterioration development is therefore expected to be independent of the structural material type of the bridge. Results presented in Figure 4 show almost identical deterioration rates of superstructures regardless of structural material of the bridge, for Continental and Mediterranean climate. Similar results were obtained for bridge decks (Kusar, 2014).

3.4.4 Structural type

The analysis of the influence of the structural type upon observed deterioration rates of the bridges under consideration was carried out in the final step. In Slovenia, bridges are constructed of all structural materials and combinations. On the other hand, overpasses and underpasses are constructed almost exclusively of reinforced concrete (Table 3). Their majority is located in Continental and Mediterranean climate; and mere 11 are located in the Alpine climate zone. The relationship between the structural type and exhibited deterioration rate of the structures was

therefore determined only for reinforced concrete structures located in Mediterranean and Continental climate zone.

The analysis of data shows that substructures of passes deteriorate at a visibly slower rate (approximately 25%) than the substructures of bridges. This observation can be explained by the permanent exposure of structural elements to river water that can be further augmented by floods or changing water level with or without simultaneous occurrence of sub-zero temperatures. Furthermore, it can be observed that superstructures of bridges and passes deteriorate at almost the same rate. Fig. 5 presents results for behaviour of substructures and superstructures for reinforced concrete structures located in Continental climate.
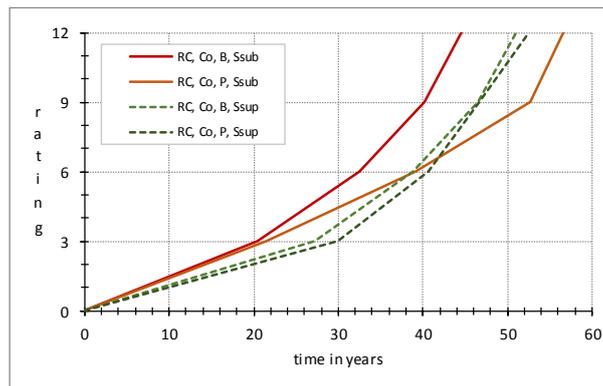
Figure 5: Temporal deterioration development for substructures and superstructures of reinforced concrete structures as a function of structural type in the Continental climate

4   Results and discussion

Based on the analyses carried out for the available bridge rating data, the relationships between parameters of influence and bridge deterioration rate were determined. It can be observed that climate has the largest impact upon bridge deterioration rate (for all considered parameters of influence). The progress of decay of all structural parts of bridges is the slowest in the Mediterranean climate and significantly faster in the Continental climate (where a large number of freeze/thaw cycles occurs during winter). The deterioration of structural parts in the Alpine climate is almost as slow as in the Mediterranean climate, which occurs most likely due to a small number of annual freeze-thaw cycles, as temperatures in the winter months are constantly below freezing. The deterioration process in Alpine climate was analysed for reinforced concrete structures only, as the number of other bridge types is very small. Since even the number of reinforced concrete structures in Alpine climate zone is relatively small (when compared to the number of these structures in other climate zones), the results obtained for these structures may be associated with a higher level of uncertainty as well.

The structural type, as already stated, affects only the rate of deterioration of substructural elements. This parameter of influence could only be analysed for reinforced concrete. Exposure to running water can cause soil erosion at or below foundations, and abrasion of wing walls and abutments. During floods, mechanical damage can occur due to large pieces of material floating in the stream at high speeds. These events cannot occur under overpasses or viaducts, making their substructure deterioration slower than those of bridges, as clearly seen in Figure 5.

The influence of material type upon deterioration progress is relatively small. Furthermore, the analysis of the data shows (Kusar, 2014), that the deterioration of sub- and superstructures is almost independent of the structural material employed. Visible differences in deterioration rates when various structural materials are used can be noticed only when the structure is already considerably damaged. Accelerated deterioration of steel structures in later years is attributed to fast corrosion progression when anti-corrosion coating no longer adequately protects the steel elements. Stone bridges, according to field experience, begin to deteriorate faster after the failure of the first stone block, as appearance of the first gap between blocks in a stone structural element typically results in progression of damage and accelerated loss of material.

Traffic load analysis shows that there is no correlation between bridge elements deterioration rate and traffic load magnitude. This observation can be explained by appropriate design of structures in relation to the expected traffic load, but could also be the result of over sizing of structural elements during design.

Currently employed monitoring system has no quality control. Gathered data is therefore considered unreliable and assessment of its quality before using data for any analysis is therefore essential. Performed assessment showed significant discrepancies in almost 50% of datasets which indicates the necessity of quality control during data gathering.

Contact information

Matej Kušar, Ph. D.
Faculty of Civil and Geodetic Engineering
University of Ljubljana
Jamova 2
1000 Ljubljana
Slovenia
mobile: +386 31 653 561
email: matej.kusar@fgg.uni-lj.si

References

Ellingwood, B.R. (2005): Risk-benefit-based design decisions for low-probability/high consequence earthquake events in mid-America. Progress in Structural Engineering and Materials. Vol. 7: 56-70.

Frangopol, D.M. (2011): Life-cycle performance, management, and optimisation of structural systems under uncertainty: accomplishments and challenges. Structure and infrastructure engineering: Maintenance, Management. Life-Cycle Design and Performance. Vol. 7: 389-413.

Gattulli, V., Chiaramonte, L. (2005). Condition assessment by visual inspection for a Bridge Management System, Computer-Aided Civil and Infrastructure Engineering. Vol. 20: 95-107.

Kušar. M. (2014). Development of bridge management system for roads and highways. Doctoral dissertation. Faculty of Civil and Geodetic Engineering. University of Ljubljana: 150 (in Slovenian).

Kušar, M., Šelih, J. (2014). Analysis of the state network bridge condition in Slovenia. Građevinar. Vol. 66: 811-822.

Moncmanova, A. (2007). Environmental deterioration of materials, WIT Press, Southampton, UK: 312.

Šelih, J., Kne, A., Srdič, A., Žura, M. (2008). Multiple-criteria decision support system in highway infrastructure management. Transport. Vol. 23: 299-305.

Tenžera, D., Puž, G., Radić, J. (2012). Visual inspection in evaluation of bridge condition. Građevinar. Vol. 64: 717-726.

TSC06.511 (2014). http://www.dc.gov.si/fileadmin/dc.gov.si/pageuploads/pdf_datoteke/TSC/TSC-06-511-2009.pdf

Žarnić, R. (2005). Lastnosti gradiv. Univerza v Ljubljani, Fakulteta za gradbeništvo in geodezijo: 350 (in Slovenian).

Thirty years of structural monitoring of São João Bridge

Luís Oliveira Santos, National Laboratory for Civil Engineering (LNEC)
Xu Min, National Laboratory for Civil Engineering (LNEC)

Objectives, abstract and conclusions

This document intends to present briefly the work done under the monitoring of an important railway bridge and thus characterize the general procedure that has been used over the last thirty years in more than twenty bridges monitored by LNEC.

The paper presents the evolution of the structural health monitoring system of São João Bridge, covering three different stages over about 30 years. The first stage was the bridge instrumentation during construction, including several mechanical devices, and the monitoring of its structural behaviour based on measurements carried out in periodic campaigns. The second stage was an important update in order to introduce automatic data acquisition with remote access, as well as dynamic monitoring. For this purpose several new sensors were installed. Finally, the third step was the use of an integrated system for the management of the experimental information collected on the bridge, which includes the automated data uploading, the data processing and a Web portal to provide secure access to the data.

An updated structural health monitoring system gives a very complete and reliable information about a bridge structural behaviour, allowing to acquire and process huge amount of data in real time, store it in safety and present it through a Web portal. This way is possible to anticipate the detection of both equipment and structural problems.

Future challenges are the development of monitoring systems to assess the corrosion of reinforcement in concrete and chemical attacks on concrete structures, the monitoring and assessment of concrete structures affected by alkali-aggregate reactions and the detection of damage from SHM data.

Technical information

1 Introduction

LNEC has a large background in the experimental study of bridges structural behaviour, leading to the current involvement in the monitoring of twenty bridges, in four different countries.

Despite some problems with existing bridges have motivated a different approach, the usual procedure implies the instrumentation during construction, the final load testing and the bridge structural monitoring in service.

São João Bridge is a good example of the application of this methodology. Designed by Edgar Cardoso, this railway bridge crossing the River Douro, in Oporto, Portugal, is open to traffic since 1991.

This bridge was instrumented during the construction and its structural behaviour has been experimentally followed since then. The original observation plan includes the measurement of strains and temperatures in concrete, horizontal displacements at expansion joints in abutments, vertical displacements in the deck and rotations at the bottom and top of the piers. However, the observation of the bridge was based only on periodical measurements.

Ten years ago, this system was updated in order to introduce automatic data acquisition with remote access, as well as dynamic monitoring.

More recently, after a period of interruption, this monitoring system was connected to a database application for the management of the experimental information, which includes the automatic data uploading, the data processing and a Web portal to provide secure access to the data being collected on the bridge.

After a brief description of the bridge, this paper presents the evolution of its structural health monitoring system, as well as some experimental results measured since bridge construction which are compared with the numerical values predicted by a finite element model.

2 Description of the bridge

São João Bridge is a prestressed concrete bridge, with a total length of 1028 m, including a main span of 250 metres, two 125 m side spans and approaching viaducts from both sides of the river banks (Fig. 1).
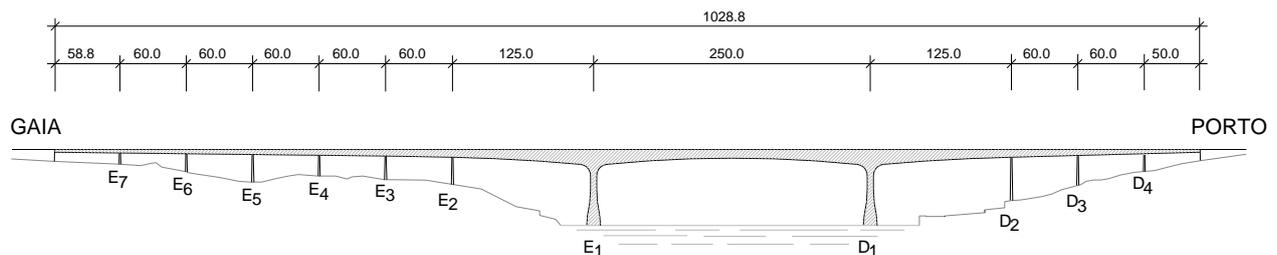
Figure 1: São João Bridge general layout

The twin-cell box-girder, built by the cantilever method, has a trapezoidal cross-section with a variable height of 12 m near the main piers decreasing to 7 m at mid-span. The bottom slab thickness decreases from 2.45 m near the main piers to 0.30 m at mid-span.

The main piers, 50 m high, have a circular cross section becoming rectangular at the top of the piers.

To prevent the long-term deflection due to creep effects in concrete and losses in prestressing steel, the bridge has external prestressing in the three major spans. For this purpose fourteen cables of 5000 kN were used, and it is possible to increase the number of cables to twenty (Bastos,1993).

3 The structural health monitoring system

3.1 The original observation plan

The original observation plan includes the measurement of strains in 14 sections (Figure 2), the measurement of temperatures in 6 sections (S1, S6, S7, S9, S11 and S12), vertical displacements, rotations and horizontal displacements at expansion joints in both abutments.
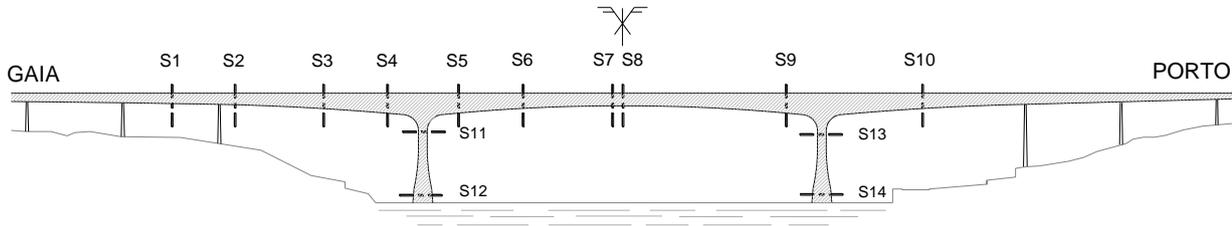
Figure 2: General observation plan of the bridge

The measurement of concrete strains was made using 124 vibrating-wire strain gauges. In the highest sections, near the main piers, besides the strain gauges placed in the top slab, some devices were positioned in the webs and in two different levels in the bottom slab, due to the huge thickness of this slab. Figure 3 shows the distribution of strain gauges in sections S5 and S8.
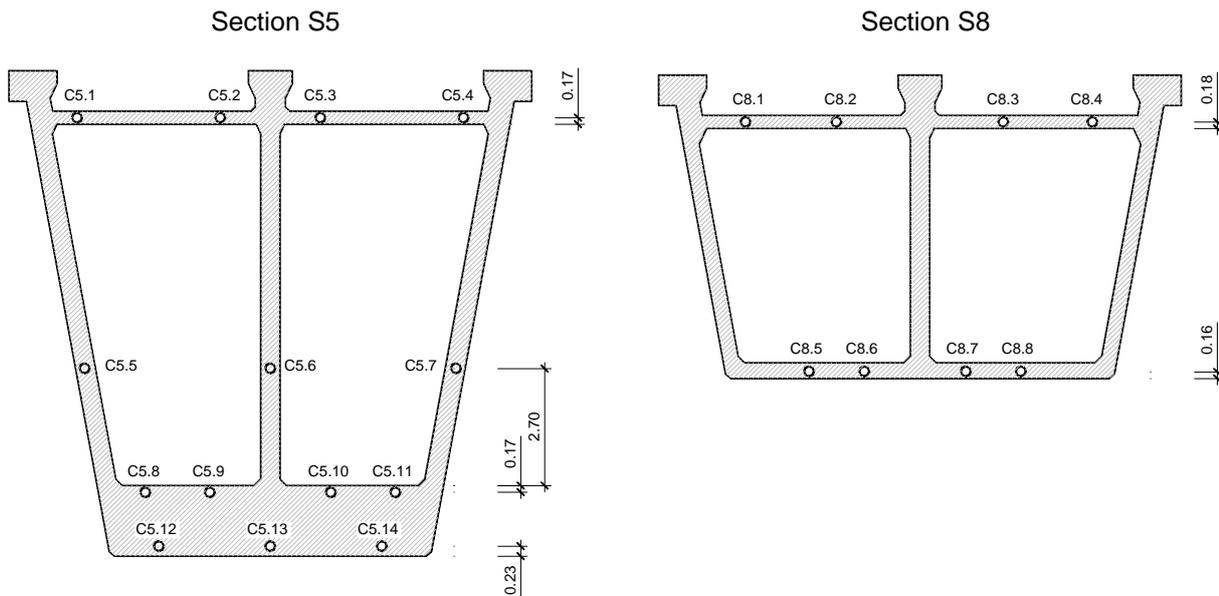
Figure 3: Instrumented cross sections S5 and S8

In order to measure thermal gradients in concrete, 97 thermocouples were placed across the thickness of the elements of the six different sections.

The original observation plan of this bridge also includes the use of air bubble clinometers to evaluate rotations in the top and bottom of the main piers and mechanical strain gauges to measure the horizontal displacements in both abutments. The measurement of deck vertical displacements was made by means of geometric levelling.

Besides measurements in the structure, an *in situ* study of the creep and shrinkage of concrete was carried out using specimens made with the same concrete of the bridge. These specimens were kept inside an experimental segment, built in the river bank .The shrinkage specimens were not loaded, subjected only to environmental conditions. The creep specimens were subject to a constant axial load imposed by hydraulic jacks, which maintained the pressure level. Taking into account the different thickness of slabs and webs of the box-girder, specimens were made in different thicknesses (300 mm, 350 mm and 500 mm).

A detailed description of the experimental procedure followed in this study and the methodology developed for the processing of the data measured in these specimens is presented in Santos *et al* (2001). This methodology includes the identification of the specimen's deformation due to temperature variations, the statistical evaluation of the experimental data (assuming a normal distribution) and the use of a non-linear regression to fit prediction models to the experimental data.

Figure 4 presents the experimental creep coefficients obtained from six specimens with notional size (h_0) of 300 mm.
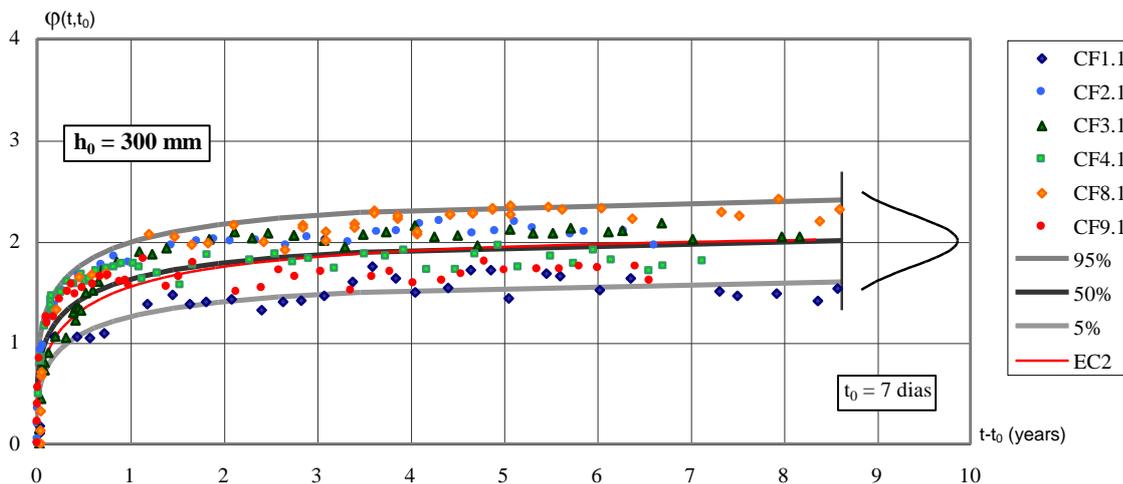
Figure 4: Creep coefficients from specimens with notional size of 300 mm

Even with the extensive instrumentation presented, until 2006 the observation of this bridge was based only on periodical measurements.

3.2 The upgrade of the SHM system

The importance of this bridge, the large investment in its initial instrumentation and the posterior advances in the field of structural health monitoring were the main reasons for the decision of upgrading the monitoring system. The main purpose of this upgrade was to install an automatic data acquisition with remote access. Another target was the monitoring of the bridge's dynamic characteristics.

In the definition of the upgraded SHM system, the first step was the integration of all the original sensors allowing automatic acquisition, as vibrating-wire strain gauges and thermocouples. For the measurement of deck vertical displacements, expansion joints movements and rotations new sensors were installed.

The use of hydrostatic levelling systems associated with pressure cells was the solution chosen for the measurement of deck vertical displacements. A system was installed in each box girder cell in order to measure the displacements in both upstream and downstream sides. Pressure cells were installed in the mid-span section of the three main spans, in the quarter span of the main span and at the top of the main piers (Figure 5a).

The measurement of expansion joints movements is provided by four magnetostrictive position sensors (Figure 5b). In each expansion joint, two sensors were installed, one in the upstream side and the other in the downstream side.

Gravity-referenced inclinometers were installed to measure rotations at the top and bottom of both main piers (Figure 5c).

The automatic acquisition of all presented sensors has been carried out by nine loggers *DataTaker DT515*. These data acquisition units are connected to a fibre optic based backbone LAN.

| Hydrostatic levelling: pressure cell | Magnetrostrictive position sensors | Gravity-referenced inclinometer |

Figure 5: Sensors installed in the SHM system upgrade

The monitoring of dynamic properties is based on the measurement of accelerations in the main span: transverse accelerations are measured at mid-span and at the top of both main piers; vertical accelerations are measured in mid-span and quarter span. Dynamic acquisition is carried out by Gantner e.series, as presented in Figure 6.

Figure 6: Structural dynamic monitoring: accelerometer and data acquisition system

The local management of the measured data is assured by an industrial computer installed in the bridge for that purpose. This includes data acquisition, data processing and data transfer.

3.3 The integrated system for the management of the experimental information

A third stage of the structural health monitoring of this bridge was the introduction of an integrated system for the management of the experimental data. Originally developed for the monitoring of dams, this system allows the automatic data uploading and processing, including also a Web portal providing secure access to the data being collected on the bridge. This system has the usual capabilities of a high-performance database management system, as retrieve data from the database for queries and reports, provide comprehensive data security and perform complex data manipulation tasks based on queries. Figure 7 shows the general appearance of the web portal.
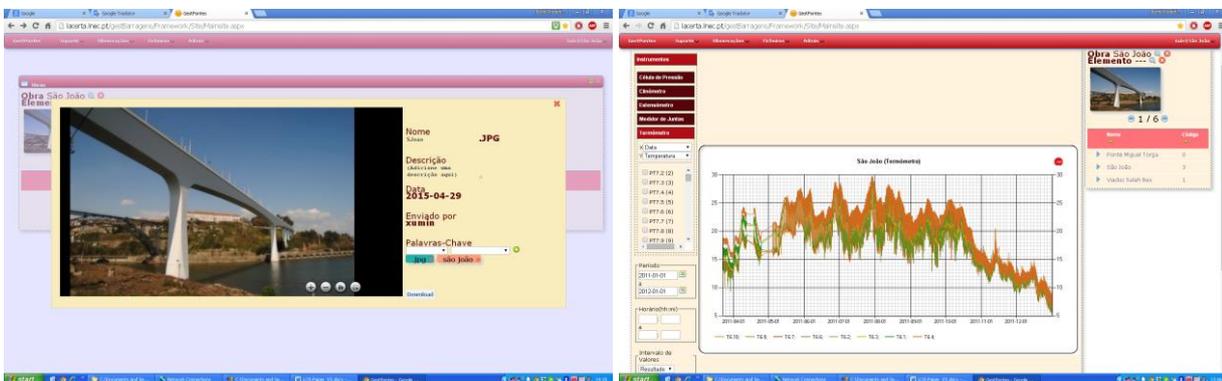
Figure 7: Layout of the integrated system for management of experimental information

4   Structural analysis

The prediction of concrete creep and shrinkage is deeply associated with a great uncertainty due to the variability of many parameters, namely those related with environmental conditions. For this reason, in structural analysis of the bridge time dependent behaviour this uncertainty should be taken into account in the modelling of creep and shrinkage.

To take this uncertainty into account, a probabilistic-based analysis was carried out, considering concrete creep and shrinkage as random variables (Santos, 2001). The characterization of these variables was based on the experimental values, achieved as previously described. In the analysis performed, creep and shrinkage variability was considered through the Monte Carlo simulation.

The time dependent behaviour of the bridge was analysed using a three-dimensional finite element model developed at LNEC (Santos, 2001). This numerical model has elements for modeling of concrete bars, reinforcement bars and prestressing bars, as well as external prestressed tendons. The segmental cantilevering process was modelled with phased structural analysis. The numerical simulation was the projection of the construction stages into calculation phases. The model takes into account the time-dependent effects including concrete hardening, creep and shrinkage and prestressing steel relaxation. The creep function was approximated by a finite number of terms in a Dirichlet series, which avoid the storage of entire stress history.

5   Experimental results

In order to illustrate the experimental data collected during almost thirty years of bridge monitoring, some experimental results are presented.

The values of the longitudinal rotation measured at top of main right pier are presented in Figure 8. The blue dots represent the values measured in observation campaigns, while the blue line results of the automatic measurements performed since 2006. The average value and the 90% confidence interval computed by the probabilistic analysis performed are also presented in this figure. Finally, the red line was obtained by a deterministic analysis carried out with the values of creep and shrinkage predicted by EC2.
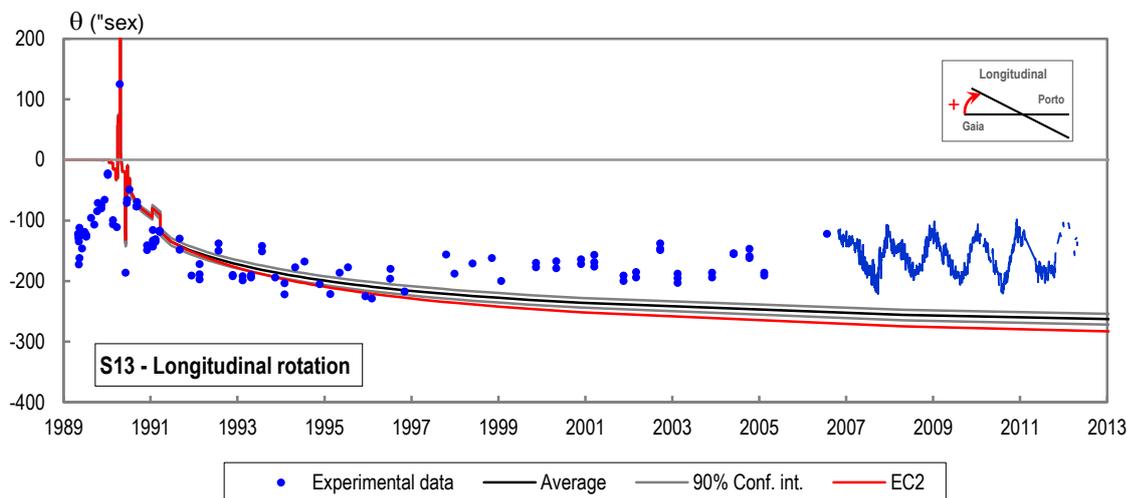
Figure 8: Longitudinal rotations at top of main right pier (PD1)

Figure 9 presents concrete strains measured at the upper and bottom slabs of section S5. The difference between the values measured before and after the upgrading is obvious.

In similar way, Figure 10 presents the evolution of the extensions measured in S8 section, located in the central mid-span.

In these figures the agreement between computed and measured values is satisfactory. Also the sazonal effects in the structural bridge behaviour are clear in these charts.
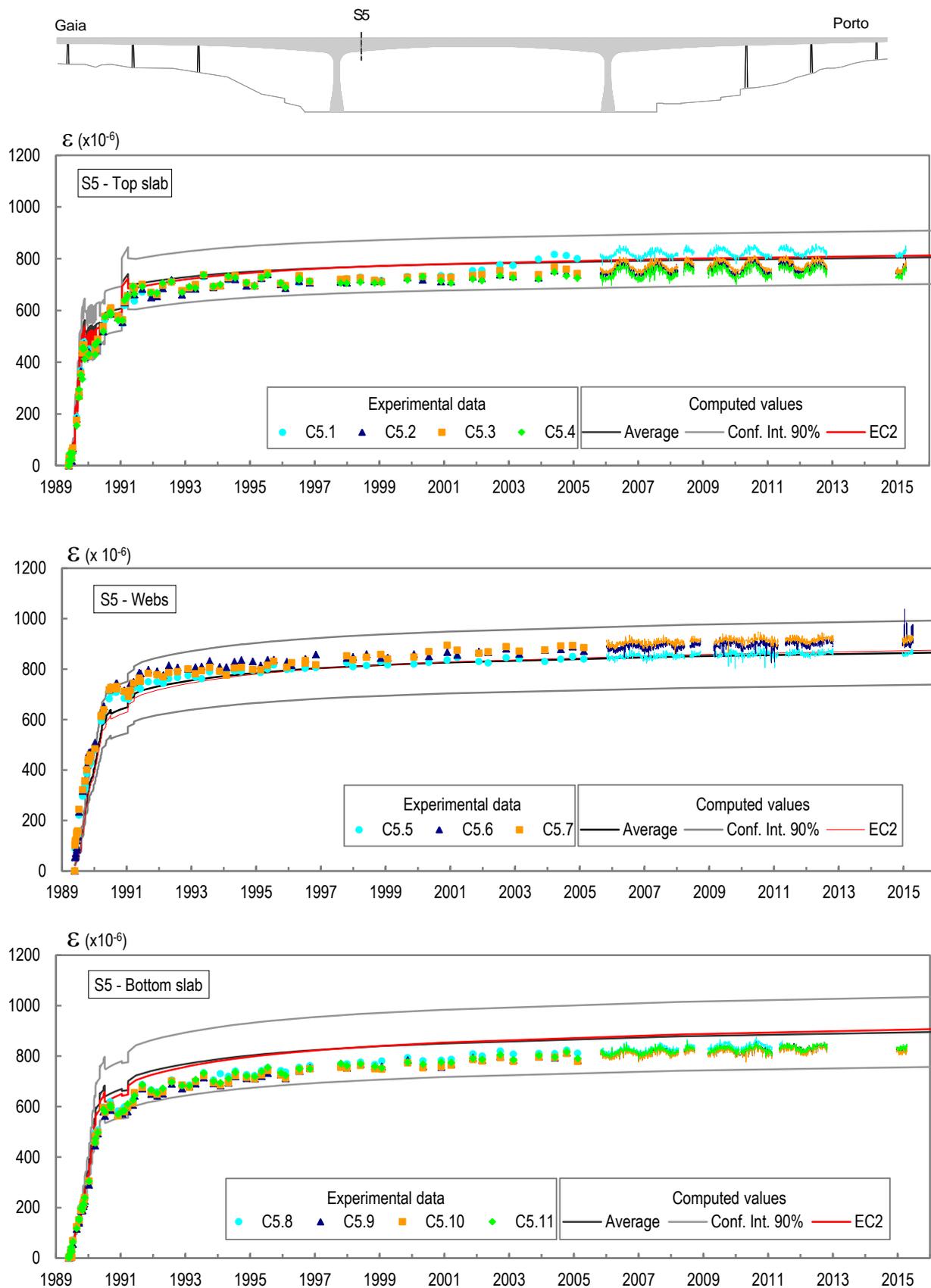
Figure 9: Concrete strains at section S5
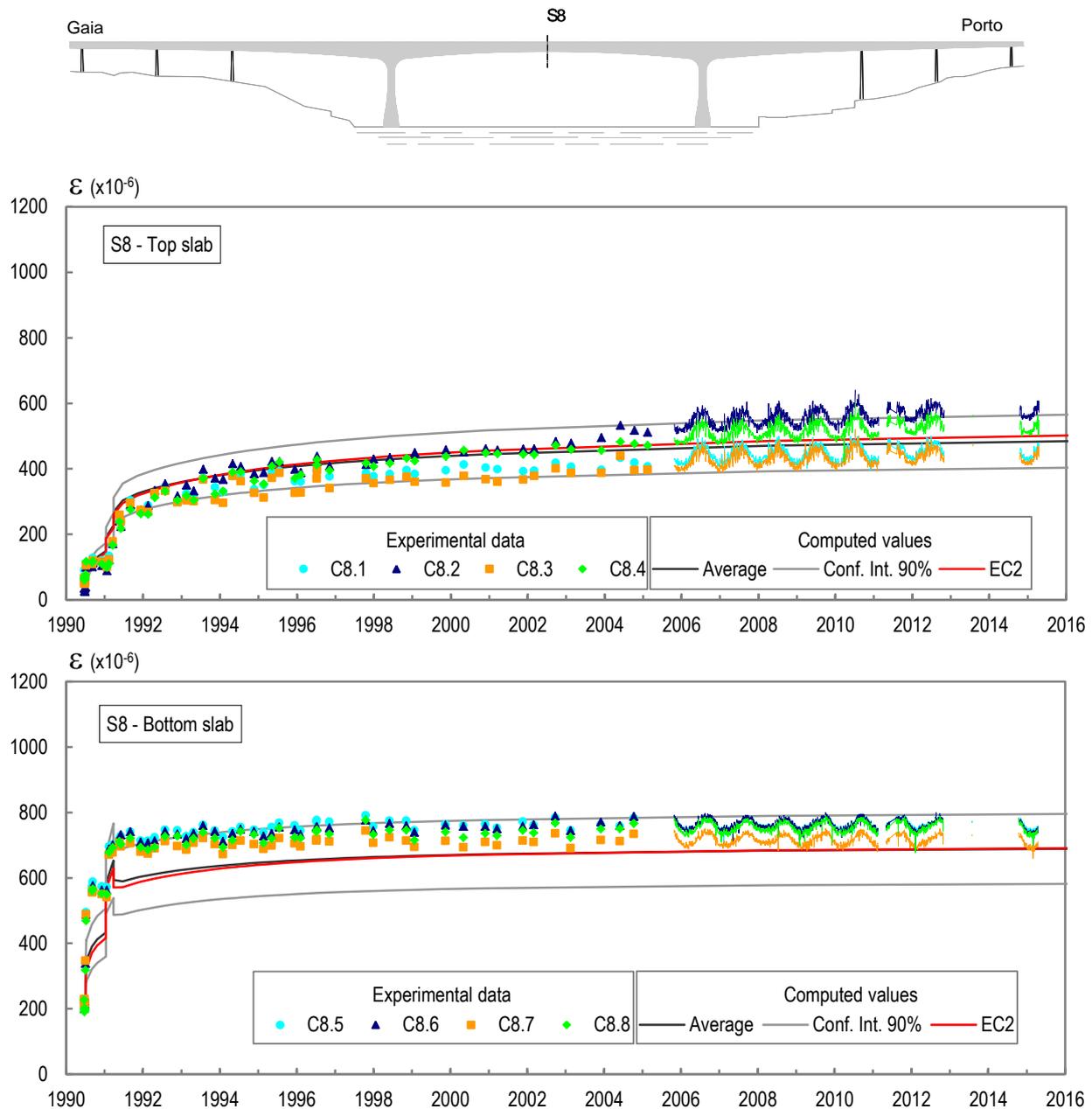
Figure 10: Concrete strains at section S8 (mid-span section)

6   Conclusions and futures challenges

This paper presents the evolution of the structural health monitoring system of São João Bridge, resulting of the interest of the bridge owner (REFER – Portuguese Rail Network) and of the continuous technological developments.

This evolution gives more complete and reliable information about the bridges structural behaviour, allowing to acquire and process huge amount of data, store it in safety and present it worldwide through a graphical or numerical interface. Indeed, the effective monitoring of the bridge, giving continuous information about its structural behaviour, as well the data processing in real time provides more reliable information, as the result of the detection and elimination of outliers, and, if necessary, the repetition of measurements. A better knowledge of the bridge's structural behaviour

is thus possible. It is also possible to anticipate the detection of both equipment and structural problems.

The usual procedure of LNEC for the structural health monitoring of bridges implies the instrumentation during construction, the final load testing and, then, the bridge structural monitoring in service. In all new concrete bridges instrumented, several concrete specimens were made in order to characterize the in situ time-dependent behaviour of concrete. A probabilistic-based analysis considering concrete creep and shrinkage as random variables is an adequate way to take into account the uncertainty of these phenomena, allowing a better comparison between the experimental and computed structural behaviour.

An important challenge is the development of monitoring systems to assess the corrosion of ordinary reinforcement in concrete. For this purpose LNEC developed an integrated corrosion monitoring system constituted by the following sensors appropriated to be embedded in concrete: galvanic current sensors, corrosion potential sensors, concrete resistivity sensors and thermometers (Pereira *et al*, 2015). The systems have been installed in several structures, new and existing, and data from permanent monitoring of corrosion of reinforcement have already been analysed for about some years.

The detection of damage from SHM data has been a one of the main topics of research at LNEC, and some very promising results have been already achieved by using static SHM data and by assuming that early damage produces dead load redistribution (Santos *et al*, 2013).

Contact information

Luís Oliveira Santos
Senior Research Officer, National Laboratory for Civil Engineering (LNEC)
Av. do Brasil, 101, 1700-066 Lisboa, Portugal
+351 218 443 305
luis.osantos@lnec.pt

References

Bastos J. (1993). "External Prestressing System in the New S. João Bridge", *in* External Prestressing in Structures, Workshop AFPC, Saint-Rémy-lès-Chevreuse, pp 397-404.

Marecos V., Santos L.O. and Branco F.(2004). "Data Processing for Safety Control of Bridges in Real Time", *in* Bridge Maintenance, Safety, Management and Cost, A. A. Balkema Pub.

Pereira E.V., Salta M.M., Fonseca I.T.E. (2015). On the measurement of the polarisation resistance of reinforcing steel with embedded sensors: A comparative study, Materials and Corrosion 01/2015; DOI:10.1002/maco.201407910.

Santos J.P., Orcesi A.D., Crémona C. & Silveira P. (2013). Multivariate statistical analysis for early damage detection, Engineering Structures 56, 273–285.

Santos, L.O. (2001). Observation and Analysis of Time Dependent Behavior of Concrete Bridges, PhD Thesis, Technical University of Lisbon (in portuguese).

Santos L.O., Virtuoso F. and Fernandes J.A. (2001). "In situ measured creep and shrinkage of concrete bridges", *in* Creep, Shrinkage and Durability Mechanics of Concrete and Other Quasi-Brittle Materials, Elsevier Science, pp. 367-372.

Santos L.O.(2009). "Upgrading of São João Bridge Structural Health Monitoring System" *in* IABSE International Symposium on Sustainable Infrastructure: Environment Friendly, Safe and Resource Efficient, Bangkok, Thailand.

Structural Health Monitoring in end-of-life prediction for steel bridges subjected to fatigue cracking

Thomas Attema*
Wim Courage*
Johan Maljaars*,+
Hendrik van Meerveld*
Joep Paulissen*
Richard Pijpers*
Arthur Slobbe*

*Netherlands Organization for Applied Scientific Research (TNO), Delft, the Netherlands
+Eindhoven University of Technology, Eindhoven, the Netherlands

Objectives, abstract and conclusions

This paper presents a monitoring and modelling methodology to assess the current and future conditions of steel bridges subjected to fatigue cracking. Steel bridges are subjected to fatigue cracking as a result of fluctuating stresses caused by the crossing of heavy vehicles. Specifically for orthotropic steel bridge decks, fatigue cracking is considered as one of the dominant failure mechanisms that drive maintenance interventions. These maintenance interventions, such as repairs, renovations or renewal, can have significant impact in terms of costs and traffic hindrance. Bridge owners would therefore benefit from clear indicators that enable sufficient reliable forecasts of the bridge conditions in terms of technical, functional and/or economic performance.

This paper describes a pilot project in which Structural Health Monitoring is applied on an orthotropic steel deck of a bridge in the Netherlands. The focus of the pilot project was on the detection and monitoring of crack propagation in the deck plate. Firstly, the applied monitoring system and its purpose are explained. Subsequently, the paper discusses the prediction of the future condition via a three-step procedure:
1. The crack growth rate and crack size are evaluated by using a physical fracture mechanics model;
2. The monitoring data is combined with predictions of the crack growth development from the physical model of the monitored section of the bridge by using an updating procedure;
3. The end-of-life is predicted for the entire bridge (including the non-monitored part) by using a non-parametric belief net.

The results of the three-step procedure demonstrate the value of combining monitoring techniques with modelling approaches by an increase of reliability in bridge performance predictions. Such an increased reliability can support bridge owners in their asset management decision making process.

Technical information

1 Introduction

Bridges are often critical assets within road or rail networks. Unavailability of bridges will immediately result in decreasing network performance. To prevent unforeseen failures and subsequent unavailability, asset owners aim to take maintenance actions. According to the Institute of Asset Management (IAM), a planned approach is often appropriate for critical assets. In this regard, the key question in managing assets changes from 'what is the condition of the asset?' to 'when will the condition of the asset become unacceptable?' (IAM, 2012).

The aforementioned challenge also applies to steel bridges with an orthotropic deck. These bridges are subjected to fatigue cracking as a result of fluctuating stresses caused by the crossing of heavy vehicles. Fatigue cracking in orthotropic steel bridge decks is currently considered as one of the dominant failure mechanisms that drive maintenance interventions. These maintenance interventions, such as repairs, renovations or renewal can have a large impact in terms of costs and traffic hindrance, and need to be well prepared . Bridge owners would therefore benefit from clear indicators that enable sufficient reliable forecasts of the bridge conditions in terms of technical, functional and/or economic performance. Hence, forecasting techniques become a key component in the development of an effective strategy for ageing assets (IAM, 2012).

This paper briefly presents a monitoring and modelling methodology to assess the current and future condition of an orthotropic steel bridge deck in the Netherlands subjected to fatigue cracking. By means of the application on such a large scale structure, it is aimed to illustrate how monitoring techniques combined with modelling approaches can increase the reliability of bridge performance predictions. More details of the proposed methodology are given in another work of the authors (Attema, et al).

The content of the paper is as follows. Section 2 describes the monitored bridge deck and the monitoring system that has been applied. Section 3 explains the modelling approach to assess the future condition of the entire bridge deck and presents some results. Section 4 treats some remaining aspects of the proposed methodology that are relevant to consider when the proposed Structural Health Monitoring (SHM) methodology will be applied in the future. Finally, conclusions are drawn in Section 5.

2   APPLICATION OF SHM TO AN ORTHOTROPIC STEEL BRIDGE DECK

In a recent pilot project, SHM was applied on an orthotropic steel deck of a bridge in the Netherlands. The pilot project focused on detection and monitoring of fatigue cracks. So-called hot spots (potential crack locations) can be found at every crossbeam and trough intersection (see Figure 1). For each intersection, two hot spots can be defined, which leads to numerous potential crack locations in the heavily loaded lanes. It should be noticed that other types of cracks might also occur in the deck structure, such as cracks in the longitudinal weld of the trough walls and the deck plate, cracks in the trough splice joints and cracks in the trough to crossbeam joints. The primary focus of the current research is on deck plate cracks, as this type of crack is known to be one of the most severe fatigue cracks in orthotropic bridge decks (De Jong, 2004). Furthermore, this crack type is potentially dangerous and the detectability is generally low unless dedicated (and expensive) inspection techniques are used. These cracks typically grow from the weld root on the inside of the trough stiffener.
Note that only a part of the bridge deck was monitored, since the bridge is quite large (see Figure 2). The monitored area was located underneath the heavy traffic lane, adjacent to one of the expansion joints of a large steel bridge.
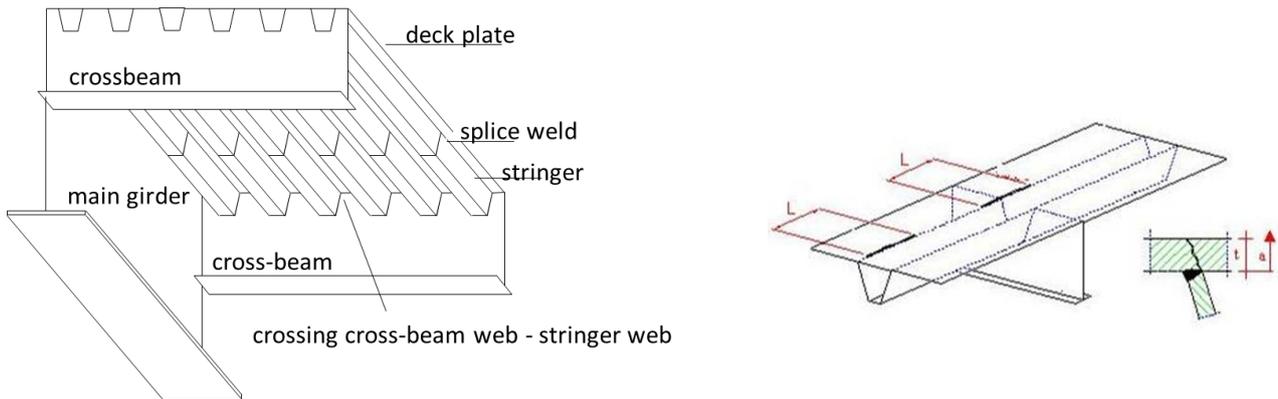
Figure 1: Orthotropic bridge deck with deck plate cracks.
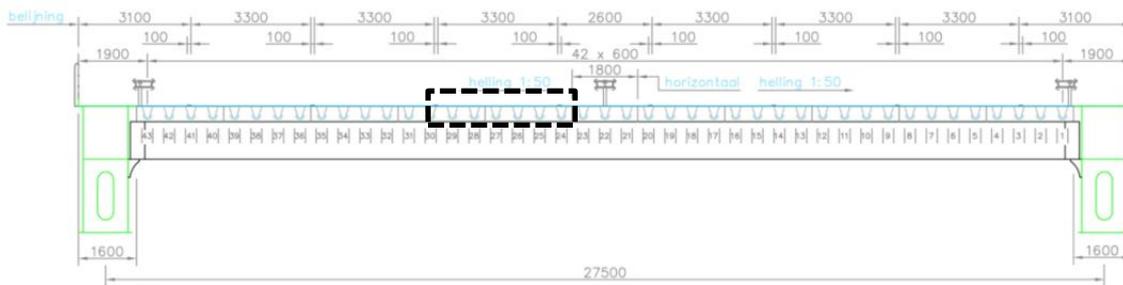
Figure 2: Cross section of bridge with monitoring area.

The purpose of the monitoring system in the pilot project is twofold. Firstly, the monitoring system should gain information about the fatigue condition of the monitored area in the bridge deck. This provides insight in the actual condition of a part of the bridge deck and provides model input to predict the future condition of the entire bridge deck. Secondly, the monitoring system should gather information about the fatigue loading on the bridge. Compared to (generalized) code based fatigue load models, bridge specific information regarding the fatigue loading is valuable information for more accurate fatigue life predictions.

The applied monitoring system consisted of two main components:

(i)   A commercially available acoustic emission (AE) system to monitor the crack activity in the bridge deck. This is done by recording ultrasonic sound waves emitted by actively growing fatigue cracks. Once an emitted signal is recorded by multiple sensors, its origin can be identified with source localization techniques

(ii)   A strain gauge measurement system to measure the fluctuating strains at various locations in the orthotropic bridge deck, measuring both in longitudinal and transverse direction.

The AE system was able to detect and localize actively growing fatigue cracks in orthotropic bridge decks. Figure 3 gives an example of the output of the AE monitoring system. The AE system identified three locations with a potential deck plate crack during the monitoring period.
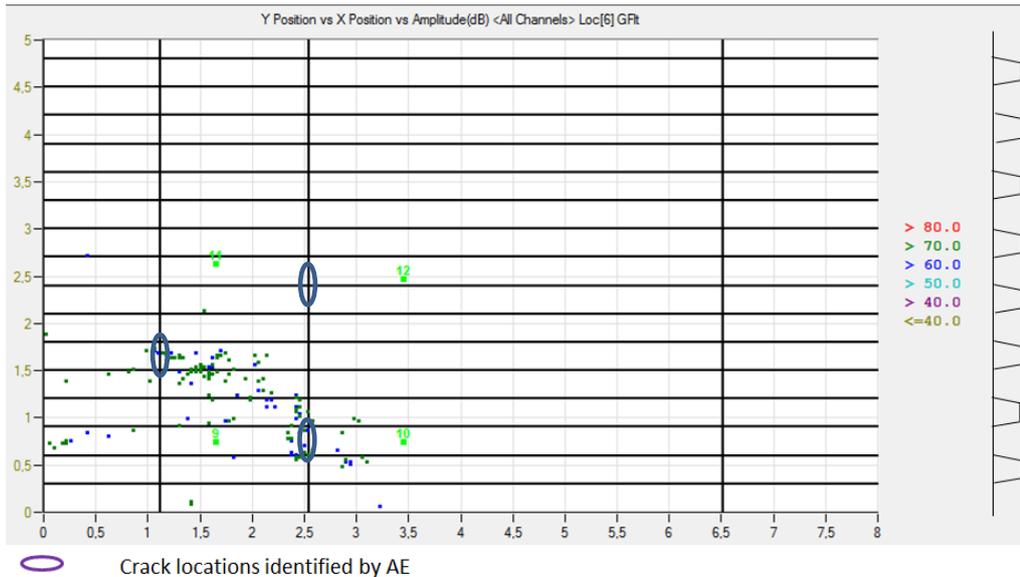
Figure 3: Example of monitoring output from the AE system and the potential deck plate crack locations identified by the AE system.

The strain gauge measurement system recorded the minimum and maximum strain level of heavy traffic passages at 24 locations underneath the bridge deck. These measurement locations differ from the hot spot locations for the deck plate crack, since it was difficult to reach the considered hot spots with strain gauges. As the stress ranges cannot be directly measured at the hot spots of interest, a finite element model (FEM) of the bridge structure is used to relate the stress spectra at the measurement locations to the calculated spectra at the hot spots (see Figure 4). In this way, an indirect quantification of the vehicle loading is derived through the comparison of the measured and calculated spectra at the measurement locations, by making use of influence lines. With the quantification of the vehicle loading, the stress spectra are then calculated at the "hot spot" locations, which are the intersections of the deck plate, crossbeams and trapezoidal stiffeners directly below the wheel tracks. These stress spectra are direct input for the crack growth calculations.
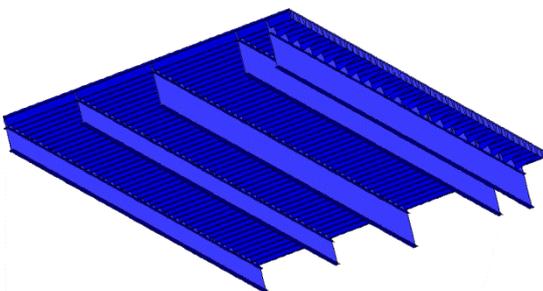
Figure 4: Graphical representation of bridge deck in FEM model.

3   END-OF-LIFE PREDICTION

This section discusses the procedure to obtain an end-of-life prediction of the bridge, by combining the aforementioned monitoring data with models. Three steps are distinguished:

1. The crack growth rate and crack size are evaluated by using a physical fracture mechanics model;
2. The monitoring data is combined with predictions of the crack growth development from the physical model of the monitored section of the bridge by using an updating procedure;
3. The end-of-life is predicted for the entire bridge (including the non-monitored part) by using a non-parametric belief net.

3.1   Predictions on fatigue degradation and crack growth for the monitored area of the bridge

A probabilistic fatigue crack growth simulation model has been developed with which the propagation of a crack can be predicted and the (remaining) fatigue life of a welded detail can be determined (Maljaars and Vrouwenverlder, 2014; Attema, et al). The crack growth model has also been extended for through-thickness cracks, meaning that the remaining fatigue life can be determined for cracks that have already grown through the thickness of the deck plate. The simulation model is written in Fortran code.

The basis of the model is the theory of linear elastic fracture mechanics (LEFM). The main parameter of LEFM is the stress intensity factor which is a measure for the amount of stress in the direct vicinity of the crack. The stress intensity factor depends on various variables, such as the geometry of the joint, the crack shape and the type of loading. The finite element method and tests carried out at Delft University of Technology have been used to determine the relation between these variables and the stress intensity factor.

Crack growth is determined by 31 variables in the proposed model. Important variables are for example the deck plate thickness, the number of heavy vehicles passing the bridge, the size of a critical crack and the stress spectra. Each of these variables is subjected to uncertainty and scatter. Based on test data and in some cases expert judgment, a-priori distributions are defined for each of these 31 variables. Obviously, the resulting crack growth and fatigue life prediction are subjected to uncertainty and scatter too. To determine the crack growth, a Monte Carlo simulation is applied. From the distributions of each variable a value is taken, which forms a set of variables that is subsequently used in the fatigue crack growth analysis. Repeating this thousands of times, gives us an equal number of crack growth curves. The end of each crack growth curve represents the attainment of a critical crack.

The grey curves in the left-hand graph of Figure 5 show the simulated crack growth developments for the considered steel bridge in the pilot project. From each of the curves, the year of attainment of a critical crack is selected. Plotting the probability density function of these failure years provide us the fatigue end-of-life distribution of the considered section of the bridge, see the grey curve of the right hand graph in Figure 5. It can be observed that this so-called a-priori distribution, i.e. the obtained distribution without the result of the monitoring data, shows a significant uncertainty and scatter.

The next step is to include the monitoring data in the fatigue life prediction. The acoustic emission (AE) results provide an estimation of the crack size in the monitored section of the bridge. In our pilot project the monitoring results indicate an estimated crack size between 3 and 6 mm in the year 2014, see the red line in the left-hand graph of Figure 5. Subsequently, we solely select the simulations that match the AE results in the monitored section (blue curves). Now, the fatigue end-of-life distribution is estimated for those simulations that satisfy the AE results. This posteriori distribution, i.e. the updated distribution based on the monitoring data, is shown by the blue curve of the right hand graph in Figure 5. It can be observed that the variation of the fatigue end-of-life

distribution is significantly reduced, indicating increased accuracy and reduced uncertainty in the crack growth development predictions of the considered section of the bridge.
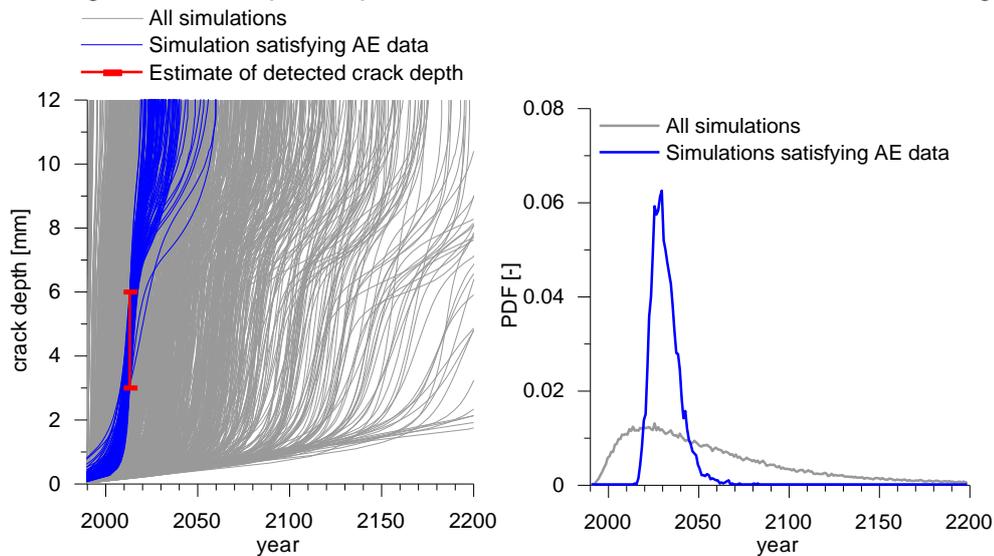
Figure 5: Graphs showing Monte Carlo simulations of crack growth (single location). Indicated in blue are simulations that comply with the measuring results of the acoustic emission sensors.

3.2   Extrapolation of the results to the entire bridge

The previous section showed how monitoring data can be used in updating the prediction of crack growth for cracks within the monitored section of the bridge. These crack growth predictions are a measure of the condition of one section of the bridge. However, we are interested in the condition of the entire bridge. Therefore, the crack growth development is simulated for every heavily loaded section in the bridge. Depending on the length of the bridge the number of heavily loaded sections is between tens to hundreds. As was observed in the previous section, non-monitored parts of the bridge leave us with high uncertainty and inaccurate crack growth predictions. For this reason an extrapolation model was developed. The extrapolation model is used to model crack growth predictions for the non-monitored locations and to update these predictions based on measurement data in the monitored location. The main contribution of this model is that it takes into account the spatial correlation between the different locations.

For both the monitored and non-monitored locations the crack-growth model of the previous section is used. However, the crack growths of defects in different sections of the bridge are not independent. For example, vehicles pass the complete bridge, so the vehicle load on different sections of the bridge is highly correlated. Another (weak) correlation is caused by the fact that all welds are created by the same company, using the same procedure and the same materials. Hence, multiple variables influencing the crack growth are correlated amongst the different sections of the bridge. The dependence structure of these variables is modelled using a non-parametric Bayesian network (BN) (Kurowicka and Cooke, 2005). The correlations in this BN were quantified using field data, literature study and expert opinion.

Under some assumptions the BN enables us to determine the multivariate distribution of all variables in all locations. In order to predict the crack growth on all sections of the bridge, Monte Carlo simulations are used. Instead of sampling from the univariate marginal distributions we now sample from the multivariate distribution taking the dependence structure into account. Each Monte Carlo sample contains a value for each variable in each simulated section of the bridge, which results in a crack growth curve for all these sections. Again, the Monte Carlo simulations are selected for which the crack growth development of the monitored section agrees with the

monitoring results. Conditioning on these simulations will not only influence the results of the monitored section but, via the dependence structure, also influence the results of all other sections. By this procedure we can reduce the uncertainty and the scatter in the crack growth predictions of not only the monitored section, but also of the non-monitored sections of the bridge.

Simulating the crack growth developments of all heavily loaded sections of the bridge enables to assess the condition of the bridge. A measure that indicates the condition of the bridge is, for example, the number of critical cracks in these heavily loaded sections. Figure 6 shows the expected number of critical cracks in the non-monitored sections of the bridge, conditioned on the monitoring results, from year 2000 till 2200. The right-hand graph shows a more detailed plot of the curves for the period 2000 till 2050.
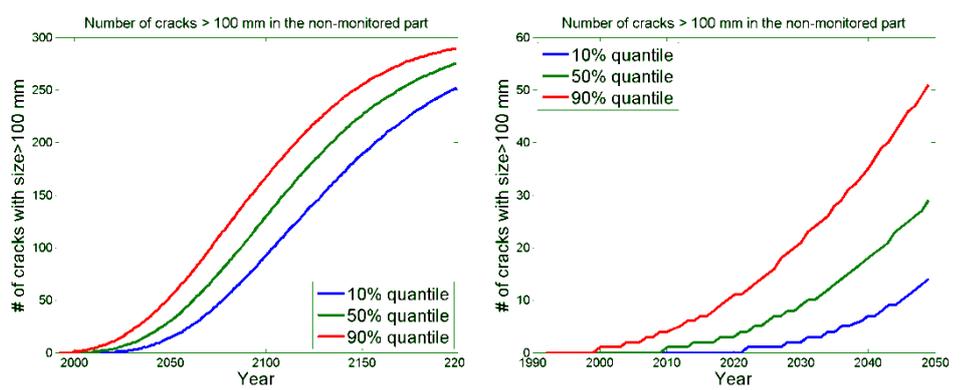
Figure 6: The expected number of defects reaching a crack size of at least 100 mm in the non-monitored section, conditioned on a crack size of 3-6 mm in 2014 in the monitored section.

3.3 Potential value of the results

The previous sections have shown how the expected number of cracks over time can be predicted using the monitoring and modelling approach. Such information can help bridge owners in multiple ways. Firstly, the probability of emerging cracks provides information to determine appropriate inspection regimes. According to the new ISO norm on asset management, the asset management organization should consider potential deterioration rates in determining the frequency of condition or performance monitoring (ISO, 2014). Secondly, the expected number of cracks provides insight in the number of required repairs and when the technical 'end-of-life' state is likely reached or when renovation is likely required. Such information can also be represented in direct costs (e.g. repair costs) and or indirect costs (e.g. costs related to traffic hindrance).

It is further shown that the predictions become more reliable when using monitoring data, which makes the predictions more valuable to bridges owners. More accurate predictions allows better assessment of the condition of a bridge and required maintenance actions can be foreseen earlier in time and scheduled more appropriately. This in turn allows for longer preparation periods which may result in a more effective and efficient maintenance approach.

4 Discussion

This section treats some remaining aspects of the proposed methodology, which are important to consider for future applications of the proposed Structural Health Monitoring (SHM) methodology.

4.1 The monitoring system

The AE monitoring data in the pilot project was compared to results of a TOFD inspection (Time of Flight Diffraction). From this comparison it was found that the AE system was able to successfully

detect and localize relatively small deck plate cracks in orthotropic bridge decks. Regarding the size of the cracks the results of the AE system were less useful, due to the asphalt surface on the bridge deck. Since the crack size is essential information to update the remaining fatigue life prediction, it is currently investigated whether alternative NDT techniques, like Phased Array and Guided Wave, can provide reliable crack sizes without disturbing the traffic flow.

From a practical point of view, it was found that the applied AE system in the pilot project could detect deck plate cracks from a depth of approximately 3mm. However, the detection limit is dependent on a number of aspects, i.e. the sensor coverage area, the sensor layout and the type of surfacing. For the bridge (with asphalt surfacing) in this pilot project, the coverage area of one AE sensor was in the order of a radius of 3m around the sensor. The exact coverage area of AE sensors for asphalt and other types of surfacing needs to be investigated.

System robustness and redundancy of the sensor system is an important aspect for, especially, long term monitoring campaigns.

The sensor system described focussed on specific types of cracks in the deck plate. It will be worthwhile to further develop the system such that other types of cracks can also be detected and quantified.

In this pilot project, still considerable human interaction was needed to go from data to information and to lifetime predictions. It is expected that most of these actions can be automatized.

4.2   End-of-life prediction

A straightforward updating procedure was applied in this pilot case in which pre-calculated curves that matched the observed crack size interval were accepted and other rejected. A more extended Bayesian approach taking proper likelihood distributions into account could be elaborated on further. In this context also Markov Chain Monte Carlo Sampling will be worthwhile looking at. Computational efficiency has to be sought for, as individual simulations with the crack growth model are time consuming.

In this context, so far only the position with largest crack size was taken into account in the updating process. Proper Bayesian updating should allow to process data from multiple locations. The same holds for measurement data gained over multiple points in time.

Extrapolating the impact of the monitoring information from only a few locations towards other hot spots, i.e. the whole bridge, is an aspect where much is to be gained. Value of Information methods assessing the number and positions of sensors should in future be developed and looked at in more detail.

4.3   Asset management

An asset management organization should evaluate its asset management activity in order to ensure their continuing suitability, adequacy and effectiveness (ISO, 2014). This pilot project can be evaluated from a similar perspective and leads to three considerations.

The first consideration is related to the efforts and costs involved in a monitoring project. In any case, the costs of the monitoring should be proportional to its potential benefits (e.g. reduction of costs and risks). The pilot project showed that potentially valuable information can be gained, but also that such an approach can be costly. Further steps are required to find suitable application

areas, to reduce the costs and efforts and to further increase the value of the proposed SHM methodology.

The second consideration is related to data management. Monitoring systems can provide abundant amounts of data. However, these data need to be properly combined with other data sources to make correct interpretations possible. For example, in the pilot project it was also important to know the information of the bridge characteristics (e.g. type, dimensions, structure type) and traffic loads.

Finally, in this pilot project the focus was on fatigue cracks in one specific fatigue sensitive detail. Although that type is currently considered as one of the dominant degrading mechanisms, many others can play a role in the asset or stock of assets.

5   Conclusion

This paper presents a monitoring and modelling methodology to assess the current and future conditions of steel bridges subjected to fatigue cracking. The application of the proposed SHM methodology provides a good example of the potential value of monitoring data, when combined with end-of-life prediction models and extrapolation models.

In the considered pilot project this combination leads to a more accurate understanding of the current condition of the bridge, a more reliable prediction of fatigue crack growth developments and a reduction in uncertainty regarding the fatigue end-of-life distribution. Furthermore, this combination enables to assess the condition of the entire bridge rather than the condition of only that part of the bridge where the monitoring system is installed.

The increase of reliability in bridge performance predictions can support bridge owners in their asset management decision making process.

Contact information

Wim Courage
Research Scientist
Netherlands Organization for Applied Scientific Research (TNO), Delft, the Netherlands
wim.courage@tno.nl

References

Attema, T., Kosgodagan Acharige, A., Morales-Napoles, O. and J. Maljaars (IN PREPARATION). Maintenance decision model for steel bridges: a case in the Netherlands.

Institute of Asset Management (IAM) (2012). Asset-Management – an anatomy. Bristol, United Kingdom: The institute of Asset Management.

Jong, F.P.B. de (2004). Overview fatigue phenomenon in orthotropic bridge decks in the Netherlands. Orthotropic Bridge Conference, Sacramento, California, USA.

Kurowicka, D. and Cooke, R.M., (2005). Distribution-free continuous Bayesian belief nets. Modern Statistical and Mathematical Methods in Reliability, p. 309-323.

Maljaars, J. and A.C.W.M. Vrouwenvelder (2014). Probabilistic fatigue life updating accounting for inspections of multiple critical locations. International Journal of Fatigue, Vol. 68, pp. 24-37

The International Organization for Standardization (ISO) (2014). ISO 55002:2014 (E) Asset management – Management systems – Guidelines for the application of ISO 55001. Geneva, Switzerland: The International Organization for Standardization.

Service life prediction by monitoring of three bridges in Sweden

John Leander, Division of Structural Engineering and Bridges, KTH Royal Institute of Technology Raid Karoumi, Division of Structural Engineering and Bridges, KTH Royal Institute of Technology

Objectives, abstract and conclusions

Three existing bridges in Sweden all exposed to unexpected deterioration are presented. Each one is of crucial importance in their local infrastructural system. To secure their operation and safety, the bridge owners have requested long term monitoring campaigns and service life assessments.

The objectives of the paper are: (a) to present the bridges and the monitoring campaigns as possible case studies in future research projects, (b) summarize the theoretical investigations based on the measurements, and (c) show specific examples on the merit of using measured response in assessment of existing bridges.

The bridges presented are the High Coast Bridge – a suspension bridge for highway traffic completed 1997, the Söderström Bridge – a continuous steel beam bridge for railway traffic completed 1950, and the Götaälv Bridge – a continuous steel beam bridge including a bascule span completed in 1939. The three bridges are different in many aspects such as age, design and loading. What they have in common is the time dependent deterioration mechanisms that limit their service lives. The monitoring campaigns were initiated to investigate the true behavior of the bridges during service and to measure the load effect caused by the actual traffic. In the cases of damage, the monitoring results have provided a foundation for mitigation proposals.

This paper is divided between the three bridges. Each bridge is described together with a brief description of the monitoring campaigns. Some measured data is presented and the research activities performed are summarized. For the High Coast Bridge, the concern has been on the wear of the bearings. A long term performance measurement has been conducted to establish the behavior of the bridge during service and to investigate the reason for the wear. For the other two bridges, fatigue is the main concern. Cracks have been found and repaired repeatedly over the years. The monitoring campaigns have been designed to produce accurate estimations of the load effect in terms of stress at fatigue prone details. The purpose has been to extend the service lives of the bridges until replacement bridges are in service.

A selection of results from the three projects is shown. The focus has been to show how the monitoring campaigns have contributed to the improved understanding of the structural behavior or specific benefits of using measured response. For the High Coast Bridge, a plausible explanation to the unexpected wear of the bearing is presented. For the Söderström Bridge, a significant increase in the fatigue life is reached using measured stresses and reliability-based methods. For the ongoing project, the Götaälv Bridge, the measurements are expected to provide information whether there is any composite action of the superstructure and, furthermore to increase the accuracy of fatigue life predictions.

Technical information

1   Introduction

Monitoring is typically requested when theoretical investigations are not sufficient to explain or resolve a specific issue. It is not an obvious measure in a conventional bridge assessment. The use of measurements is a choice of the bridge owner which can be a question of opinion and resources. The Swedish code for assessment of existing bridges (Trafikverket, 2011) allows the use of

measured stresses for fatigue assessment. The support on the use of measurements is otherwise sparse in today's codes for bridges. Practical examples as given in this paper and more applied research are expected to facilitate the choice to use monitoring in the future.

In research, monitoring is an established tool and several international projects have addressed the challenges and opportunities of monitoring bridges. Guidelines and recommendations can be found in, e.g., Feltrin (2007) and Sedlacek et al. (2007). In the latter, the concept of monitoring has been divided between the following categories:

- Action monitoring,
- Performance monitoring,
- Stress monitoring and
- Health monitoring.

Action monitoring is described as the assessment of the response in time and space due to a known load. Performance monitoring allows an assessment whether a structural component meets the performance requirements under a known or any load. Stress monitoring allows an assessment of the state of stress in a structure or a structural component. Health monitoring provides real time information for assessment of the safety and serviceability of a structure or structural component.

The monitoring campaigns treated in this paper cannot be classified into a single category. The final projects have become more complex and comprise more than one single aim. The scope of the projects is described in subsequent sections.

2   The High Coast Bridge

The High Coast Bridge is located on the east cost of Sweden. It is a road bridge carrying the traffic on the main route E4 over the Ångerman River (Ångermanälven). The bridge opened 1997 is a suspension bridge with a main span of 1210 meters and a total length of 1867 meters. The pylons made of concrete have a height of 182 meters. The stiffening girder is a multiple-cell steel box-girder, continuously suspended without any direct supports at the pylons. The girder rests on sliding bearings at both ends with a sliding surface of PTFE/Teflon. The bridge is shown with a schematic sketch in Fig. 1 and with a photo in Fig. 2.
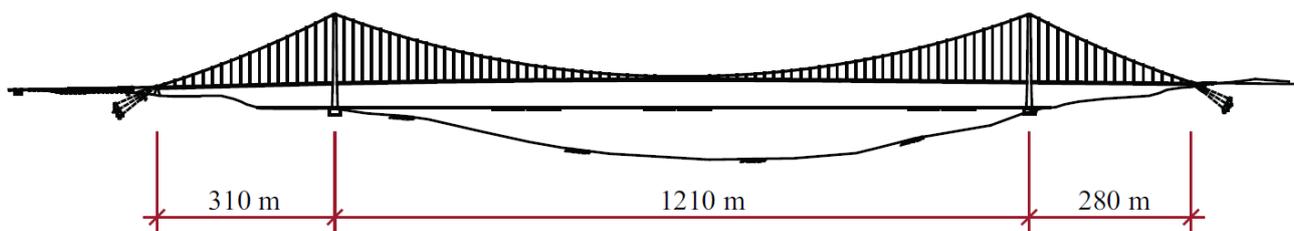
Figure 1. A schematic sketch of the High Coast Bridge.

Figure 2. A photo of the High Coast Bridge.

Shortly after the opening, unexpected wear of the bearings was discovered. Flakes of the teflon layer was found at the abutment. The actual traffic loads on the bridge in combination with dynamic effects was suspected to create much larger bearing forces than predicted in the theoretical calculations. One theory was that misalignments in the expansion joints were the cause of impact like loading in the Teflon bearings, leading to the exaggerated deterioration. To clarify the cause of the problem, a monitoring campaign was initiated in 2005 by the former Swedish Road Administration, now Swedish Transport Administration (Trafikverket). The main aim of the project was to measure the loads in the first hangers as well as to monitor the vertical loads acting on the bearings. A brief summary of the monitoring system and the outcome will be given in the following. More information about the bridge and the monitoring campaign can be found in Karoumi et al. (2009) and González and Karoumi (2014).

2.1 Instrumentation and monitoring

To determine the total vertical force in the bearing, the effect of both permanent and live loads were required. The permanent action was attained by a calibration process where the bridge deck was lifted with six hydraulic jacks (three at each bearing) and the pressure in the lifting device was registered. During that process readings from strain gauges mounted on the crossbeam above the bearings were recorded giving a zero strain level for the unloaded bearings. With the known force from the lifting device and the measured strains for the loaded and unloaded condition, the gauge setup could be used as a load cell to measure the bearing forces.

After the calibration, a monitoring program was started for continuous measurements of the bearing forces with real time data collection, processing and storage. The results from the first period of measurements are presented in Karoumi et al. (2009). These measurements showed no extreme loads on the bearings. The values where well within the design limits, despite some overloaded trucks captured in the response.

To further investigate the cause of the wear, the instrumentation was expanded in 2010 with a camera for traffic monitoring, two accelerometers mounted to the hangers closest to the instrumented bearings, a displacement sensor to monitor the longitudinal movement of the girder, and a thermocouple registering the temperature at the soffit of the girder. A second calibration was performed using a moving truck with a known weight of 25.7 tons. The truck was driven in different speeds to enable a study on the influence of dynamics.

2.2 Results

The results shown in the following is a selection of results previously presented in González and Karoumi (2014). The calibration of the strain readings at the crossbeam made it possible to use the bridge as a scale, a so-called Bridge Weigh in Motion (B-WIM) system. The maximum allowed gross weight in Sweden is limited to 60 tons. Several vehicles heavier than that have been registered during the monitoring. One example, shown in Figure 3(a), is a heavy vehicle with a permit to pass the bridge. Figure 3(b) shows the bearing force for the same vehicle exceeding the maximum allowed value of 590 kN.

(a) Photo of a special transport with permit.
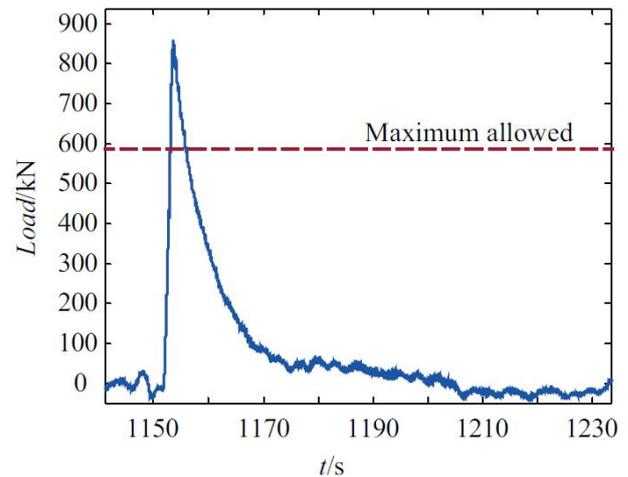
(b) Bearing force during the passage of the vehicle.

Figure 3. Results from the traffic monitoring system of the High Coast Bridge.

Despite several overloaded trucks, the measured bearing forces never exceed the capacity of the bearing. The wear of the Teflon layer is believed to be caused by a combination of temperature changes and vehicle loads. The measured longitudinal displacement of the stiffening girder shows that large displacements occur when thermal stresses build up as temperature changes rapidly and the sliding bearing is locked by friction. When a truck crosses the bridge the friction is released and the displacement jumps into a next level, giving the displacement curve a staircase appearance, with jumps in the displacement up to 5 mm. This phenomenon could contribute to the wear observed in the bearings. Fig. 4 shows an example of measured displacement of the stiffening girder. Every jump in the curve corresponds to a vehicle crossing.
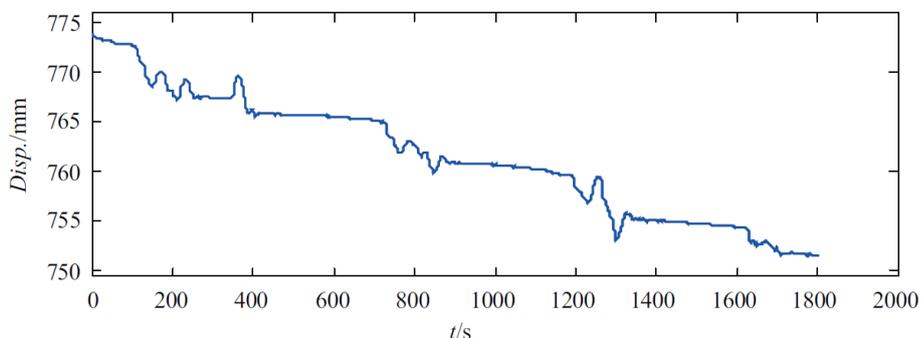
Figure 4. Measured longitudinal displacement of the stiffening beam of the High Coast Bridge. Temperature changes are believed to build up friction forces in the bearing which are released by vehicle passages, causing a staircase appearance.

3 The Söderström Bridge

The railway line from Stockholm and southwards passes through the so-called wasp waist. Ten tracks at the Stockholm Central Station are merged into two tracks passing the island of Riddarholmen. The Söderström Bridge carries the two tracks over the stream between Riddarholmen and the island of Södermalm. These two tracks have the highest traffic intensity in Sweden with about 520 trains passing every day.

The Söderström Bridge, completed 1954, is a continuous steel beam bridge built up by a grid of main beams, crossbeams and stringer beams. The bridge has an extensive system of bracing for horizontal forces and for local stability. The track with wooden sleepers is resting directly on the stringers. The bridge type is sometimes called open deck bridge due to the lack of a covering surface. The total length of the bridge is about 190 meters divided in six spans. A schematic sketch of the bridge is shown in Fig. 5 and a photo in Fig. 6.
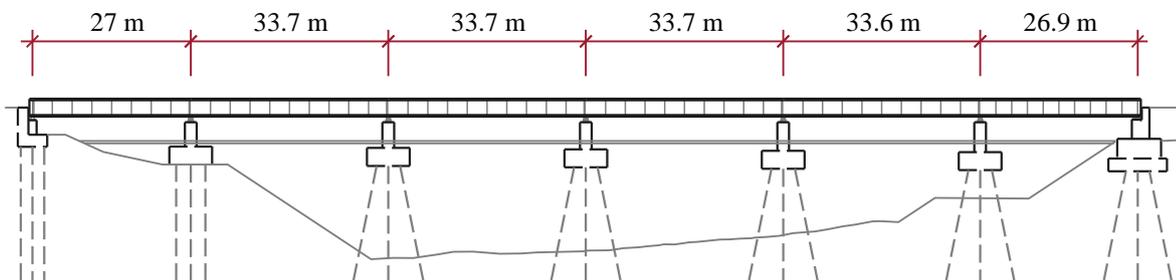
Figure 5. A schematic sketch of the Söderström Bridge.

Figure 6. A photo of the Söderström Bridge.

During routine inspections, cracks have been found in the webs of the main beams at the connections between the vertical stiffeners and the webs, see Fig. 7. Until 2008, a total of 90 similar cracks have been found. The cracks have been repaired successively by welding and grinding. The cracks are caused by out-of-plane bending of the web. The behaviour called web gap cracking is common for this kind of bridges, see e.g. Fisher (1984).

The discovery of the cracks initiated extensive efforts in securing the safety of the bridge until a replacement is arranged. In addition to the web gaps, theoretical assessments have shown an exhausted fatigue life for other connections as well. A monitoring campaign was started 2008 to determine the true behaviour of the bridge and to reduce the uncertainties of the theoretical load models. The monitoring has been ongoing in periods until 2011. More information about the bridge can be found in Leander et al. (2010) and Leander (2010).
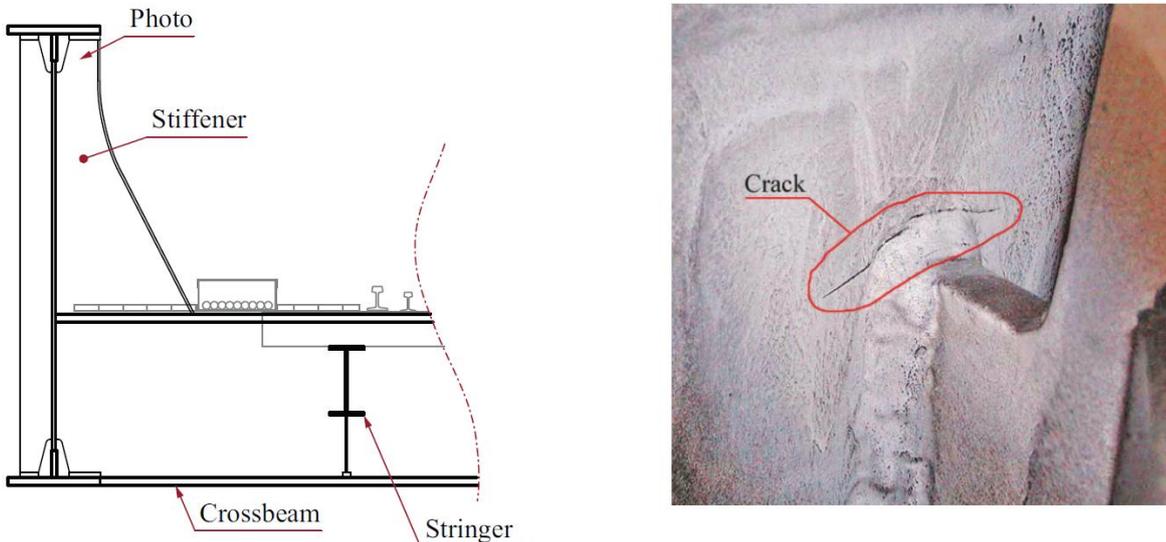
(a) A section of the superstructure and the location of the photo in (b).

(b) A crack in the web of the main beam.

Figure 7. Cracks have been found in the webs of the main beams on the Söderström Bridge.

3.1 Instrumentation and monitoring

The main concern about the Söderström Bridge is the fatigue resistance. One of the most crucial variables in a fatigue assessment is the stress range. To reduce the uncertainties related to the response of the traffic load, strain gauges were mounted close to a selection of fatigue prone details. A total of 56 strain gauges were used in the initial setup. Most of the gauges were positioned to measure nominal strains, away from abrupt geometry changes. The measured strains could by Hooke's law and rainflow cycle counting be presented as stress range spectra representative for the actual load conditions.

The monitoring campaign started with a calibration measurement using an Rc6 locomotive with a total weight of 78 tons and known axle distances. Several crossings were performed in different speeds enabling a study on the influence of the dynamic behaviour. After the calibration, continuous measurements were recorded 24 hours a day for an initial period of 43 days in August and September 2008. Additional monitoring has been performed 2010 and 2011 with minor revisions of the gauge setup. Strain gauges were mounted to measure hot spot stresses at some identified critical connections. During the latter monitoring period, local stresses were measured to verify improvement actions for some of these connections. More information about the monitoring can be found in Leander et al. (2010) and Andersson et al. (2013).

3.2 Results

The monitoring has shown that the response is dominated by the commuter trains. The most frequent train on the bridge is the X60 train shown in Fig. 8(a). The stress ranges are relatively low but the number of cycles is large, especially for the beams with short influence length where every bogie

creates a cycle. A stress range spectrum for one of the gauges on a stringer beam is shown in Fig. 8(b).

(a) A Swedish X60 commuter train.
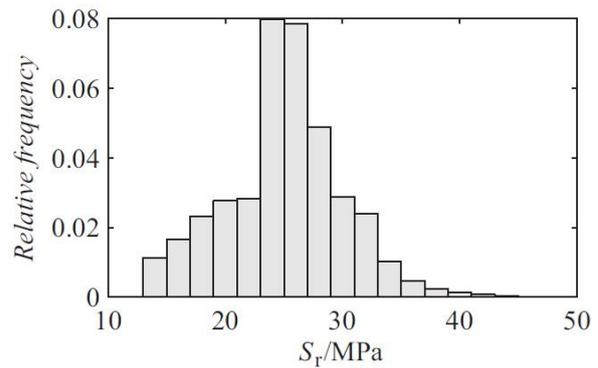
(b) Stress range spectrum for gauge 35 on one of the stringer beams.

Figure 8. The stress range spectra based on the measurements on the Söderström Bridge is dominated by the response of the commuter trains.

In the doctoral thesis Leander (2013), a numerical example is presented for the fatigue assessment based on measured response. Results for a deterministic assessment based on theoretical calculations and measurements are compared to the result of reliability-based calculations. The studied connection is a gusset plate welded to the flange of a stringer beam, see Fig. 9. The result of the assessments is summarized in Table 1.
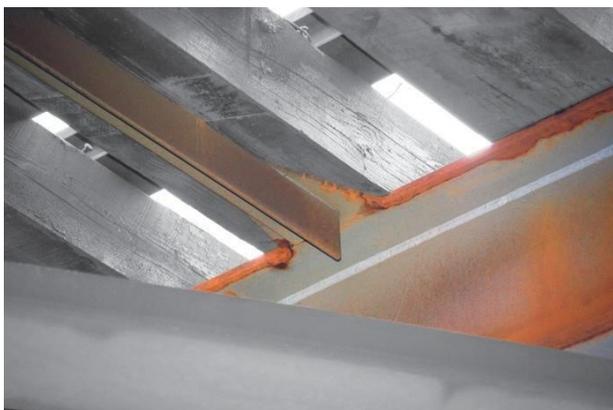
(a) A photo of the connection.
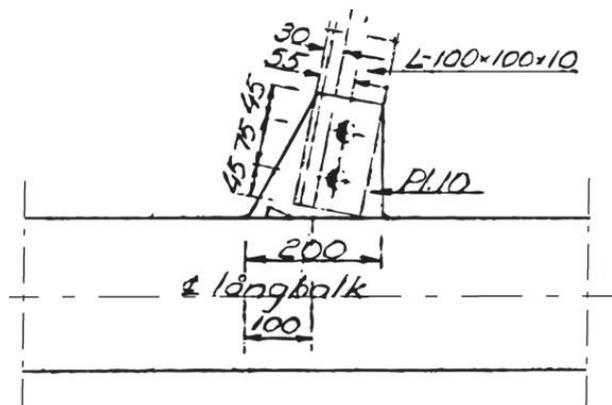
(b) A cutting from the original

drawings. Figure 9. The connection of the bracing to the mid span of the stringer.

Table 1. Predicted fatigue life for the detail in Fig. 9 based on simulated and measured response.

Method	Traffic	Fatigue strength S_C/MPa	Safety factors	Fatigue life / years
Deterministic	Simulated quasi static	40	$\gamma_{Ff}\gamma_{Mf} = 1.35$	1.3
	Measured	40	$\gamma_{Ff}\gamma_{Mf} = 1.35$	2.7
		47	$\gamma_{Ff}\gamma_{Mf} = 1.35$	4.5
Reliability-based	Measured	40	$\beta = 3.1$	3
		40	$\beta = 2.3$	5.2
		47	$\beta = 3.1$	5.7
		47	$\beta = 2.3$	10.5

The result presented in Table 1 shows a severely limited fatigue life. This is an outcome reached already in early theoretical assessments of the bridge, see e.g. Leander et al. (2010). Adeterministic fatigue assessment following the Eurocodes EN 1991-2 and EN 1993-1-9 gives a fatigue life of merely 1.3 years. The same verification format but considering the measured stress range spectra gives a fatigue life of 2.7 years. A deterministic assessment is performed also for the fatigue strength increased from 40 MPa to 47 MPa based on Leander et al. (2013). It increases the fatigue life further to 4.5 years.

The reliability-based assessments have been performed using the first order reliability method (FORM) with a limit state equation formulated on accumulated damage. The target reliabilities suggested in ISO 13822 (2010) have been adopted. The values $\beta = 2.3$ and $\beta = 3.1$ are suggested for details possible to inspect and not possible to inspect, respectively. For a characteristic fatigue strength of 40 MPa and a target reliability of $\beta = 3.1$ a fatigue life of 3 years is reached. With a target reliability of $\beta = 2.3$ the fatigue life increases to 5.2 years. With an increased fatigue strength, the fatigue life increases to 5.7 years and 10.5 years for $\beta = 3.1$ and $\beta = 2.3$, respectively.

With all considered measures, the fatigue life is increased from 1.3 years to 10.5 years which is a considerable increase but, still a severely limited fatigue life. To secure the resistance of the Söderström Bridge, recurrent inspections are required until it can be replaced. The consideration of measurements provides a significant contribution to the increase in service life, especially when a reliability-based assessment is conducted where the reduction in uncertainty of the loads can be utilized.

4   The Götaälv Bridge

The Götaälv Bridge is one of the first welded steel bridges in Sweden. It was completed in 1939 and connects the City of Gothenburg with the island of Hisingen. It is considered momentous for the local traffic system in the city, for one thing because it provides the only tram connection to Hisingen.

The bridge has three major parts: the south viaduct, the elevated part over the river containing a bascule span, and a north viaduct. The total length is about 950 meters divided in 24 + 9 + 14 spans. The load carrying structure is built up by a concrete slab resting on continuous steel beams, steel columns and concrete foundations. There are no conventional shear connectors between the concrete slab and the steel beams which makes any composite action uncertain. The concrete deck is about 20.5 meters wide and carries six lanes of traffic. The two lanes in the centre are devoted to buses and tram. In 1958, two additional lanes for pedestrian traffic were built alongside the main deck. These lanes are carried by their own steel structure linked to the main structure by hinged bars. A schematic sketch of the structure is shown in Fig. 10 and a photo in Fig. 11.
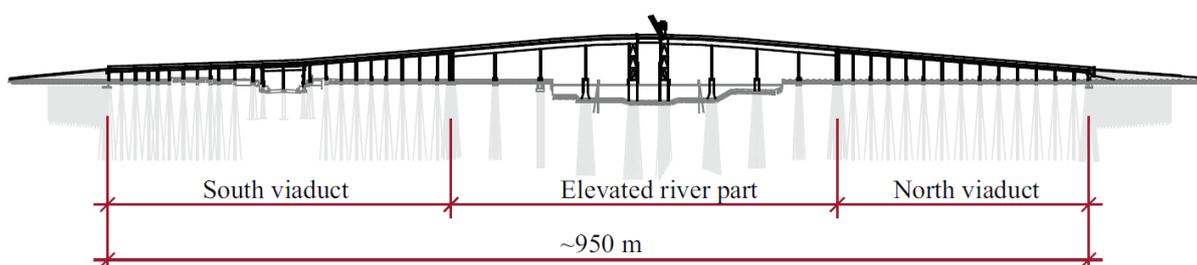
Figure 10. A schematic sketch of the Götaälv Bridge.

Figure 11. A photo of the Götaälv Bridge.

The bridge was built in the infancy of the welding technique, before the detrimental influence of welds on the fatigue resistance was widely known. Several joints have an inappropriate design considering fatigue, with welds in areas with high stresses. The steel material, Thomas steel, is another unfortunate circumstance causing a high risk of brittle failure at low temperatures.

Several fatigue damages have been revealed over the years. One example is the connection between the main longitudinal beams and the crossbeams at the supports. Cracks have initiated at the splice of the top flange and propagated through the whole width as shown in Fig. 12(a). To prevent a sudden collapse all similar joints have been secured with a preloaded bar as shown in Fig. 12(b).

(a) The top flange of a main beam cracked through the whole width.

(b) Safety measures to prevent collapse in case of a propagating crack.

Figure 12. A fatigue critical connection in the Götaälv Bridge.

Due to its critical position in the infrastructural network, the Götaälv Bridge cannot be taken out of service until a replacement bridge is built. The owner, the City of Gothenburg, is planning for the new Hisings Bridge to be completed 2020. Until then, the safety of the old bridge has to be secured. As a measure to increase the accuracy of theoretical models and assessments, the owner has requested

a monitoring campaign. At the writing of this paper, the project has just started and the monitoring is ongoing.

4.1 Instrumentation and monitoring

The main concern is the fatigue resistance. The bridge is loaded with a large variety of vehicles, from light cars to public buses and heavy trucks, spread among six lanes. To reach a more realistic estimation of the load effect, in comparison to code based load models, strain gauges have been mounted on the main beams. The system comprises a total of 22 gauges divided between two areas, one at the south viaduct and one at the elevated river part.

A specific issue is the composite action of the superstructure. Whether the concrete deck interacts with the longitudinal beams or not has a significant influence on the stresses in the steel beams. By measuring on the top and bottom flanges in the same section the location of the neutral axis can be studied.

The campaign was started with a calibration monitoring using two trucks with known weight and axle distributions. Measurements have been recorded for fixed load positions and for moving load response. A long term monitoring will also be conducted but has not been initiated yet. The calibration can be classified as an action monitoring and will be used mainly for updating of theoretical models. The long term monitoring will be used to determine realistic stress histories for improved fatigue life predictions.

4.2 Results

So far, only some preliminary measurements have been analysed. Fig. 13(b) shows the crossing of a series of unidentified vehicles recorded as strains at one of the main beams of the south viaduct. The measured strains are recalculated to stresses by Hooke's law.
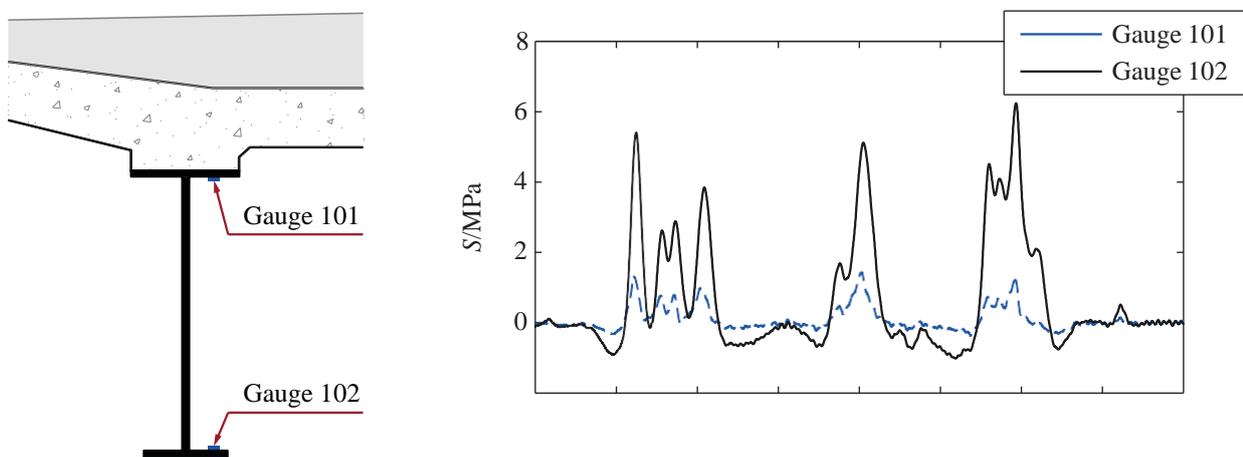
(a) The locations of the strain gauges vehicles.

(b) Measured stresses for the crossing of a series of unknown vehicles.

Figure 13. Preliminary results from the monitoring of the Götaälv Bridge.

A strain gauge mounted to an existing structure does not provide any information about the stress due to existing permanent loads. Only the change in strain over time can be measured. The zero levels for the stresses shown in Fig. 13(b) at the top and bottom flange are determined as the stress when no vehicle is present. It is apparent that a vehicle crossing causes a positive increase of the stresses at both flanges. It indicates that the neutral axis is situated above the top flange in the concrete deck. These preliminary results imply that there is a composite action between the concrete

deck and the steel beams. However, the question at issue needs further investigation. The monitoring campaign has not yet rendered enough data for any fatigue assessment.

5   Conclusions

The three bridges presented in this paper suffer from unexpected deterioration mechanisms. The bearings at the High Cost Bridge are exposed to exaggerated wear leading to increased costs in maintenance and replacement of the bearings. The Söderstöm Bridge and the Götaälv Bridge suffer from inappropriate design of the joints causing fatigue cracks.

The monitoring campaigns have and will be used to clarify the behaviour of the bridges and the response due to known loads. All three campaigns have started with calibration measurements which is a typical example of action monitoring.

Stress monitoring has been or will be performed for all three bridges. For the High Coast Bridge, the measured strains have been used to determine the bearing forces. For the other two bridges, measured strains recalculated to stresses can be directly incorporated in fatigue assessments.

All three projects have been initiated due to specific problems revealed. None of them have started as true structural health monitoring projects. However, the measured data could together with models for damage accumulation be used to quantify the health of the structures. When it comes to fatigue, stress range spectra determined by monitoring can be incorporated in crack growth predictions to estimate the residual life.

The benefits of monitoring have been shown with three specific examples. For the High Coast Bridge, a plausible explanation to the unexpected wear of the bearing is presented. For the Söderström Bridge, a significant increase in the fatigue life is reached using measured stresses and reliability-based methods. For the ongoing project, the Götaälv Bridge, the measurements is expected to provide information whether there is any composite action of the superstructure and, furthermore, to increase the accuracy of fatigue life predictions.

Contact information

John Leander

Researcher, Division of Structural Engineering and Bridges, KTH Royal Institute of Technology, 100 44 Stockholm, Sweden

Phone: +46 8 790 6493

Email: john.leander@byv.kth.se

References

Andersson A, Leander J, Kraoumi R, 2013. Extending the Fatigue Service Life of a Railway Bridge by Local Approaches. IABSE Symposium Report, Vol. 99(11),

Feltrin G (Ed.), 2007. Monitoring Guidelines for Railway Bridges. Sustainable Bridges – Assessment for Future Traffic Demands and Longer Lives, Report D5.2.

Fisher JW, 1984. Fatigue and fracture in steel bridges – Case studies. John Wiley & Sons, Inc.

González I, Karoumi R, 2014. Continous monitoring of bearing forces and displacements in the High Coast Bridge. Bridge Maintenance, Safety, Management and Life Extension. May 2014 , pp. 566 -572.

Karoumi R, Svedjetun K, Gilliusson S, 2009. Monitoring Vertical Loads on the Bearings of the High Coast Suspension Bridge. Key Engineering Materials, Vols 413-414, pp. 401-405.

Leander J, 2010. Improving a bridge fatigue life prediction by monitoring. Licentiate thesis, KTH Royal Institute of Technology, TRITA-BKN, Bulletin 106.

Leander J, Andersson A, Karoumi R, 2010. Monitoring and enhanced fatigue evaluation of a steel railway bridge. Engineering Structures, Vol 32(3), pp. 854-863.

Leander J, Aygül M, Norlin B, 2013. Refined fatigue assessment of joints with welded in-plane attachments by LEFM. International Journal of Fatigue, Vol 56, pp. 25-32.

Sedlacek G, Hechler O, Lösche A, Kühn B, 2007. Guidelines for monitoring of steel railway bridges. Sustainable Bridges – Assessment for Future Traffic Demands and Longer Lives, Background document D5.2.S1.

Trafikverket, 2014. Bärighetsberäkning av broar (in Swedish). TDOK 2013:0267. The Swedish Traffic Administration (Trafikverket).